Carbohydrate Auxiliaries for the Asymmetric Synthesis of α-Amino Acids and γ-oxo-α-amino acids

by

Marion Earle

A thesis
submitted to the Faculty of Graduate Studies
in partial fulfillment of the requirements
for the degree of

Doctor of Philosophy

Department of Chemistry
University of Manitoba
Winnipeg, MB, Canada
2002

THE UNIVERSITY OF MANITOBA

FACULTY OF GRADUATE STUDIES

*****

COPYRIGHT PERMISSION PAGE

CARBOHYDRATE AUXILIARIES FOR THE ASYMMETRIC SYNTHESIS OF α-AMINO ACIDS AND γ-oxo-α-amino ACIDS

BY

Marion Earle

A Thesis/Practicum submitted to the Faculty of Graduate Studies of The University of Manitoba in partial fulfillment of the requirements of the degree of

DOCTOR OF PHILOSOPHY

Abstract

The synthesis of two carbohydrate-based auxiliary systems has been accomplished and these systems have been studied in alkylation and aldol or Mannich type reactions.

Previous work had established that a bicyclic oxazinone ring system could give excellent diastereoselectivity in alkylation reactions. This earlier work has been extended using a modified version of the original template. Excellent diastereofacial selectivity was observed with each electrophile, however yields were lower with the poorer electrophiles. A non-aggregating base was found to significantly improve the yields for these electrophiles. Mild conditions were found to remove the amino acid product from the auxiliary. The carbohydrate-based template possessed many properties of a good auxiliary system.

The second study focused on the synthesis of γ-oxo-α-amino acids. This less common approach involved reaction of a glyoxylimine and a ketone (or silyl enol ether) in an aldol or Mannich type reaction. An achiral glyoxylimine and a diacetone D-glucose based glyoxylimine were synthesized. Reactions of the achiral imine showed generally low diastereoselectivity for the *syn* products in Mukaiyama type reactions but higher selectivity for the *anti* products with bulky titanium enolates. Higher diastereofacial selectivity for addition to the chiral imine was achieved by inverting the order of reagent addition. Highest yields were achieved when a cerium enolate was employed. An intramolecular decomposition was implicated as the cause of the generally modest yields. Difficulties arose in removing the auxiliary from the products. The molecules proved to be sensitive to conditions used in various cleavage attempts. Relative stereochemistries were assigned by x-ray crystallographic techniques.

Acknowedgments

I would like to express my sincerest thanks to my supervisor Dr. Philip G. Hultin for his help and advice during the course of this research. His expertise and enthusiasm has been much appreciated. I also wish to thank Kirk Marat, Terry Wolowiec, and Tad Foniok for their help with the NMR spectra and Wayne Buchannon for the mass spectra. Also thanks to Dr. Robert McDonald (University of Alberta) and Angela Toms (University of Manitoba) for acquiring the X-ray structures. I thank the members of my advisory committee, Dr. J. Charlton, Dr. N. Hunter and Dr. B. Hasinoff for their advice and comments regarding the thesis research. I am also grateful for the help of the secretaries, Barbara, Cheryl and Trisha and storeroom guys Wayne and Curtis for all the little things they did. Big thanks to the graduate members of our group; Mikaela, Manjula, Jeff, Wen and Jason, as well as all the other undergraduate students for making the lab an enjoyable and interesting place to work. Finally thanks to my family and friends who have supported me and given me encouragement along the way. Finally I acknowledge the University of Manitoba and the Natural Sciences and Engineering Research Council of Canada for their financial assistance.

List of Abbreviations

[α]	specific rotation
Ac	acetyl
aq	aqueous
ALL	1,2:5,6-Di-*O*-isopropylidene-D-allofuranosyl
Ar	aryl
BINAP	2,2′-bis(diphenylphosphino)-1,1′-binaphthyl
Bu	butyl
*t*Bu	*tert*-butyl
Boc	*tert*-butoxycarbonyl
Bzl	benzoyl
c	concentration in g/100 mL
CAN	ceric ammonium nitrate
Cbz	benzyloxycarbonyl
CD	circular dichroism
CE	cotton effect
CSA	camphorsulfonic acid
δ	chemical shift in ppm
DAG	1,2:5,6-Di-*O*-isopropylidene-D-glucofuranosyl
DBA	dibenzylideneacetone
DCC	1,3-dicyclohexylcarbodiimide

de	diastereomeric excess
DMAP	4-dimethylaminopyridine
DMF	*N*,*N*-dimethylformamide
ee	enantiomeric excess
Et	ethyl
FDA	food and drug administration (USA)
fod	6,6,7,7,8,8,8-heptafluoro-2,2-dimethyl-3,5-octanedionate
h	hour
hfc	tris [3-(heptafluoropropylhydroxymethylene)-(+)-camphorate]
HMDS	1,1,1,3,3,3-hexamethyldisilazane
HMPA	hexamethylphosphoramide
Im	imidazole
J	coupling constant (in NMR)
LDA	lithium diisopropylamide
LICA	lithium cyclohexylisopropyl amide
Me	methyl
MPA	α-methoxyphenylacetic acid
MTPA	α-methoxy-α-trifluoromethylphenylacetic acid (Mosher's acid)
NMR	nuclear magnetic resonance
nOe	nuclear Overhauser effect
*i*OPr	*iso*-propoxy
OTf	trifluoromethanesulfonate
PDC	pyridinium dichromate

PET	positron emission tomography
Ph	phenyl
Piv	pivaloyl
*i*Pr	*iso*-propyl
pmp	*p*-methoxyphenyl
TBDMS	*tert*-butyldimethylsilyl
TBPS	*tert*-butyldiphenylsilyl
TFA	trifluoroacetic acid
THF	tetrahydrofuran
TMEDA	*N*,*N*,*N*′,*N*′-tetramethyl-1,2-ethylenediamine
TMS	trimethylsilyl
Ts	tosyl, *p*-toluenesulfonyl

Table of Contents

CHAPTER 1

Introduction

There are many challenges to the synthesis of organic compounds. One of the more difficult aspects is the synthesis of pure enantiomers or diastereomers. This thesis will focus on research using carbohydrate chiral auxiliaries to synthesize both enantiomerically and diastereomerically pure amino acids. Two key approaches have been undertaken. The first involves a 'chiral glycine' approach using a bicyclic template (Section 2.1); the second, a glyoxylimine-aldol approach to the synthesis of γ-oxo-α-amino acids (Section 2.2). Various methodologies for chiral synthesis will be reviewed. Some of the advantages and disadvantages of carbohydrate auxiliaries will also be discussed. The key reaction used in the synthesis of the γ-oxo-α-amino acids is an imine-aldol or Mannich type reaction. Pertinent background on the aldol and the Mannich reactions will be reviewed.

1.1 Asymmetric Synthesis

All organic molecules possess a three-dimensional structure. The term *stereochemistry* has been introduced to address this issue. Organic substances which contain the same number and type of atoms (i.e. have the same constitution) but which differ in various physical properties are referred to as isomers. Isomeric compounds, which differ in the connectivity of their atoms, are referred to as *structural* or

constitutional isomers. Isomeric compounds in which the atoms are bonded in the same sequence but which differ in the spatial arrangement of these atoms are referred to as *stereoisomers*. Stereoisomers can be further subdivided into *enantiomers*, *diastereomers* and conformational isomers. Conformational isomers are those that can be interconverted by rotation about a single bond

An enantiomer is one of a pair of molecules that are nonsuperimposable mirror images of each other. Enantiomers have identical physical and chemical properties except in their interaction with a chiral environment or with plane or circularly polarized light. To illustrate this, (2*R*,3*R*)- and (2*S*,3*S*)-threonine are examples of mirror images or enantiomeric compounds (Figure 1.1). The compounds (2*R*,3*S*)- and (2*S*,3*R*)-threonine are another pair of enantiomers. However although, (2*R*,3*R*)-threonine is a stereoisomer of (2*R*,3*S*)-threonine, it is not its mirror image and cannot be superimposed on it. These compounds are therefore referred to as diastereomers.

Figure 1.1

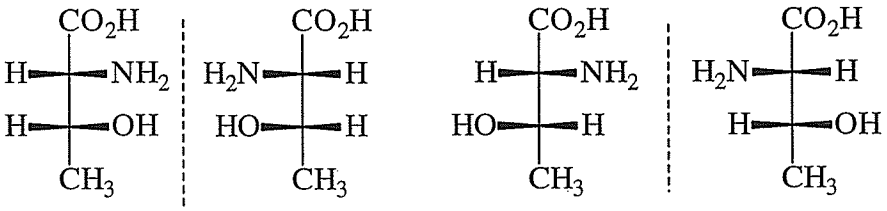

2R, 3R 2S, 3S 2R, 3S 2S, 3R

The first documentation of the existence of stereoisomerism can be traced to French scientist Jean Baptiste Biot's work with plane polarized light.[1] In 1815, Biot observed that when a beam of plane polarized light was passed through a solution of

certain organic compounds (e.g. camphor, sugar), the plane of polarization was rotated. He recognized what is now termed as optical activity as being an inherent property of the molecule. It was not until 1848 that the cause of this optical activity was correctly postulated by Louis Pasteur. Pasteur discovered that two distinct types of crystal precipitated from a solution of sodium ammonium tartrate. Although the original salt mixture was optically inactive, the separated crystals were optically active. Pasteur correctly explained his results by describing a nonsuperimposable asymmetric arrangement of atoms within each crystal. It was not until 25 years later that the idea of an asymmetric carbon atom was proposed.

Why are some compounds optically active while others are not? A compound that is nonsuperimposable on its mirror image is referred to as chiral (from the Greek word *cheir* meaning hand). The criterion for optical activity is then chirality. A broader definition is that chiral compounds lack certain symmetry elements. A chiral compound cannot contain a plane (σ), center (i) or alternating axis (S_n) of symmetry. A compound, which contains one asymmetric carbon atom (a *stereogenic* center), is always chiral due to the lack of any symmetry elements. However, the presence of more than one stereogenic center does not mean that a compound is chiral, as symmetry elements may be present. Compounds which contain stereogenic centers but which themselves are achiral are referred to as *meso* compounds.

Chiral organic compounds generally, but not always, contain asymmetric carbon atoms. Other quadrivalent atoms such as Sn, Si or tervalent atoms such as N can also act as chiral centers. For amines, this is usually restricted to compounds where the nitrogen cannot undergo pyramidal inversion (Figure 1.2). Molecules in which restricted rotation

about single bonds is present can also exist as enantiomers. This is referred to as atropisomerism. Allenes and spiranes may also be chiral if unsymmetrically substituted.

Figure 1.2

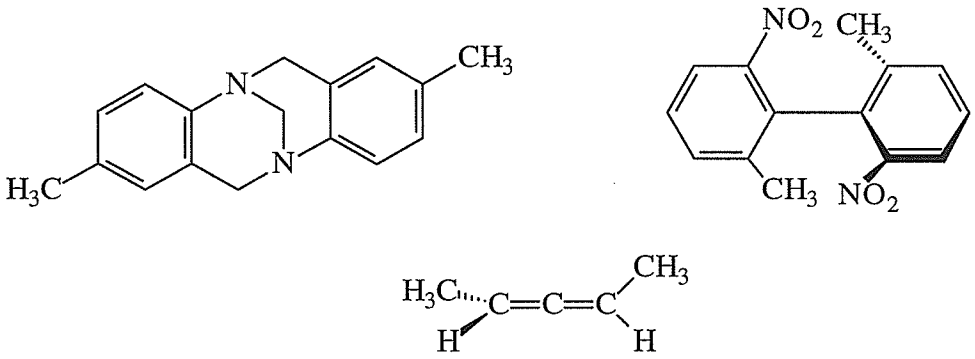

The spatial identification of the stereogenic centers must lastly be addressed. The assignment of a chiral compound as +/- based on the direction in which it rotates plane polarized light, says nothing about the configuration of the stereogenic centers. Adoption of a standard compound was proposed and its configuration arbitrarily assigned.[2] Glyceraldehyde was chosen because of its relationship to the sugars. The (+)- or D-isomer was given the configuration shown in Figure 1.3.

Figure 1.3

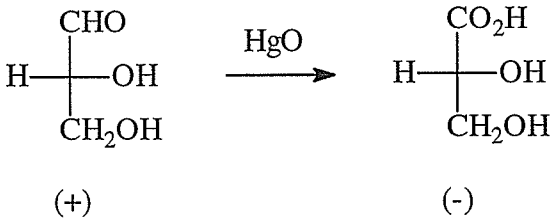

Configurations of other compounds could then be referred to this standard, for example by chemical manipulations that did not affect this center, as in the oxidation of

D-glyceraldehyde to give D-glyceric acid.[2] A limitation in this system of nomenclature became apparent. In some instances a compound could be related to both the D and the L isomer of glyceraldehyde by a similar number of chemical transformations.

The Cahn-Ingold-Prelog system,[3] which is explained in most undergraduate texts, has replaced the D/L nomenclature. In this system the substituents around a chiral center are ranked according to a set of rules based on decreasing atomic number (Figure 1.4). Once sequenced the molecule is oriented such that the lowest priority group is facing away from the observer. If the remaining substituents decrease in rank clockwise they are assigned the *R* (Latin *rectus*, right) configuration. If they decrease counterclockwise they are assigned the *S* (Latin *sinister*, left) configuration. The configuration of any chiral center can then be unambiguously assigned. However in carbohydrates and amino acids, the D/L nomenclature is still commonly used.

Figure 1.4

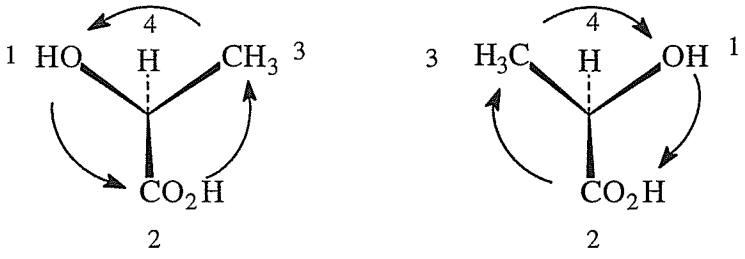

S Configuration *R* Configuration

1.1.1 Rationale for Asymmetric Synthesis

In recent years there has been an increase in attempts to synthesize compounds in enantiomerically and diastereomerically pure form.[4,5] While the synthesis of diastereomers is complex, there has been greater attention to the more difficult task of synthesizing pure enantiomers.[6-11] This has involved exploration of enzymatic systems, chiral catalysts, reagents, auxiliaries and polymeric supports, to name a few. A significant driving force behind this research is the pharmaceutical industry. Recently there has been an increased awareness of the biological implications of using racemic compounds. In 1992 the FDA had issued statements on the development of chiral drugs as single isomers.[12] Although they did not mandate the development of single isomers and they stated that racemic compounds are appropriate in some instances, many companies started to take notice of the trend. It is estimated that the annual sale of single enantiomer drugs worldwide will have surpassed the $100 billion US mark in the year 2000.[13]

There are two chirality issues facing the drug industry, the development of chiral compounds as single isomers and *racemic switching*. Development of a single isomer can be synthetically challenging and expensive. Various approaches will be discussed in Section 1.1.2. An advantage to this method is that only one end product is tested (which can decrease the cost to the company) unlike racemic drugs where both enantiomers must be proven to be clinically effective, or at least not harmful. A *racemic switch* is the redevelopment of a single isomer of a drug to replace an existing marketable racemate. It is estimated that the average drug takes approximately 12 years and $500 million US to

come to market.[14] The patent period (20 years) gives the manufacturers the exclusive right to sell the drug and recoup their investment. Through racemic switching, new information on the active single isomer can increase the life of the patent after the patent on the racemate expires. The amount of annual sales protected by racemic switching is estimated to be approaching $9 billion US.

The fact that enantiomeric compounds can have very different pharmacological behaviors is most often the driving force for developing enantiopure drugs. In some instances only one enantiomer of a drug is biologically active as in the two examples shown in Figure 1.5. *Threo*-methylphenidate (Ritalin®) is a racemic drug used to treat attention deficit hyperactivity disorder. Radiolabeling and PET imaging studies have shown that it is the D-enantiomer that is active.[15] With α-methyldopa, it is the L-enantiomer which acts as an effective antihypertensive agent.[16]

Figure 1.5

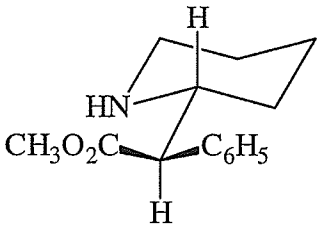

D-*threo*-methylphenidate

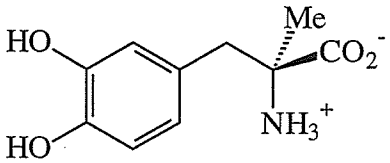

L-α-methyldopa

In some situations each enantiomer can elicit a different, but not harmful response. For example the sense of taste and smell can be influenced differently be individual enantiomers because each enantiomer interacts differently with sensory molecules. A classic case is the natural product carvone. (*S*)-Carvone has a faint caraway

odor, while (*R*)-carvone has a strong spearmint odor (Figure 1.6).[17] Several amino acids also exhibit this type of enantiomeric variation. The L-enantiomers of leucine, phenylalanine, tryosine and tryptophan are bitter tasting, while the D-enantiomers are sweet. Combining L-aspartic acid, which has little taste, with the bitter tasting L-phenylalanine gives the dipeptide aspartame, which is 160 times sweeter then sucrose. If instead D-phenylalanine is used, the resulting dipeptide is bitter.[18]

Figure 1.6

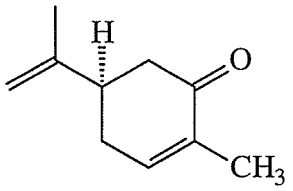

(*R*)-Carvone

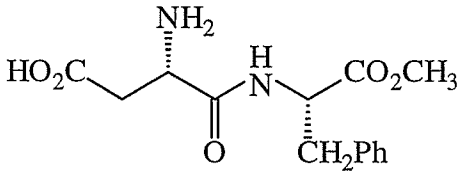

Aspartame®

In other situations one enantiomer can give rise to serious toxic or other harmful effects. D-Penicillamine (Figure 1.7) is a chelating agent, which is used to remove heavy metals such as Cu, Pb, Au, or Hg from the body. This isomer is seldom toxic. In contrast, administration of L-penicillamine can lead to blindness due to atrophy of the optical nerve.

Figure 1.7

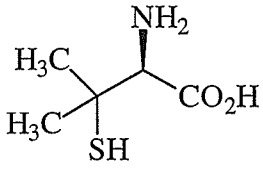

D-penicillamine

In some instances production of a single isomer is not advantageous. This is usually the case when interconversion of the enantiomers is possible. The glitazones are a family of compounds used to treat Type II diabetes by restoring sensitivity of cells to insulin in cases where the body is still producing it. The glitazones are known to racemize readily in solution. Thus pioglitazone (Eli Lilly and Takeda Pharm. America) and rosiglitazone (SmithKline Beecham) (Figure 1.8) have both been approved by the FDA for marketing as racemates.[13]

Figure 1.8

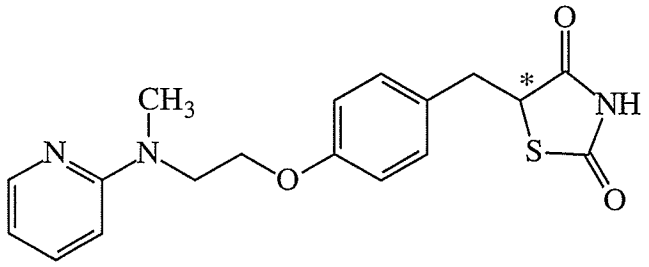

rosiglitazone (Avendia®)

1.1.2 Methods for obtaining single enantiomers

Chiral compounds can be prepared or isolated in several manners. Single enantiomers can be isolated through resolution of enantiomers, deracemization, the use of chiral pool reagents, or by stereoselective synthesis.[19]

1.1.2.1 Resolution of enantiomers

Enantiomers may be resolved (that is, the two component enantiomers may be separated) by the following four general methods. The compounds can be separated

mechanically, as in the manner Pasteur separated (+) and (-)-tartaric acid. In this situation, molecules of (+)-tartaric acid crystallized separately from molecules of (-)-tartaric acid when a hot saturated solution of the racemic tartaric acid was cooled. The crystals themselves were visibly asymmetric and could be mechanically separated using tweezers. This technique is rarely used as too few compounds crystallize in this manner.

Enantiomers may also be separated through 'chiral chromatography'. If the column is packed with a chiral isomerically pure adsorbent, in principle, the two enantiomers will interact differently with the adsorbent and move through the column at different rates. How much material needs to be separated and the cost of the chiral packing material will determine the usefulness of this method for a given application.

Enantiomers may be separated by temporary conversion to diastereomers. The racemic mixture is derivatized with another compound, which is a pure enantiomer. The product diastereomers are then separated by a suitable method. Removal of the derivatizing agent results in separation of the enantiomers.

The final process is kinetic resolution. Enantiomers will react with chiral non-racemic reagents or catalysts at different rates due to the diastereotopic nature of the transition states for their reactions. It is therefore possible to increase the enantiomeric excess (ee) of the product relative to that of the starting mixture by stopping the reaction before completion.

The drawback to each of these processes is the loss of half the material, unless the undesired enantiomer can be racemized and recycled or used in some other manner.

1.1.2.2 Deracemization

Deracemization is the conversion of one isomer in a racemic mix to its enantiomeric form. The racemic mixture is thereby enriched in one enantiomer. This is not the same as kinetic resolution, though a chiral additive is still required. For deracemization to occur, each enantiomer must coordinate to the added chiral reagent in a different manner. The enantiomers must also interconvert under the conditions of the experiment. For example, P. Reider et al.[20] found that addition of a catalytic amount of an aromatic aldehyde to a racemic solution of **1** resulted in an equilibrium mixture of imines **2** being formed (Scheme 1.1).

Scheme 1.1

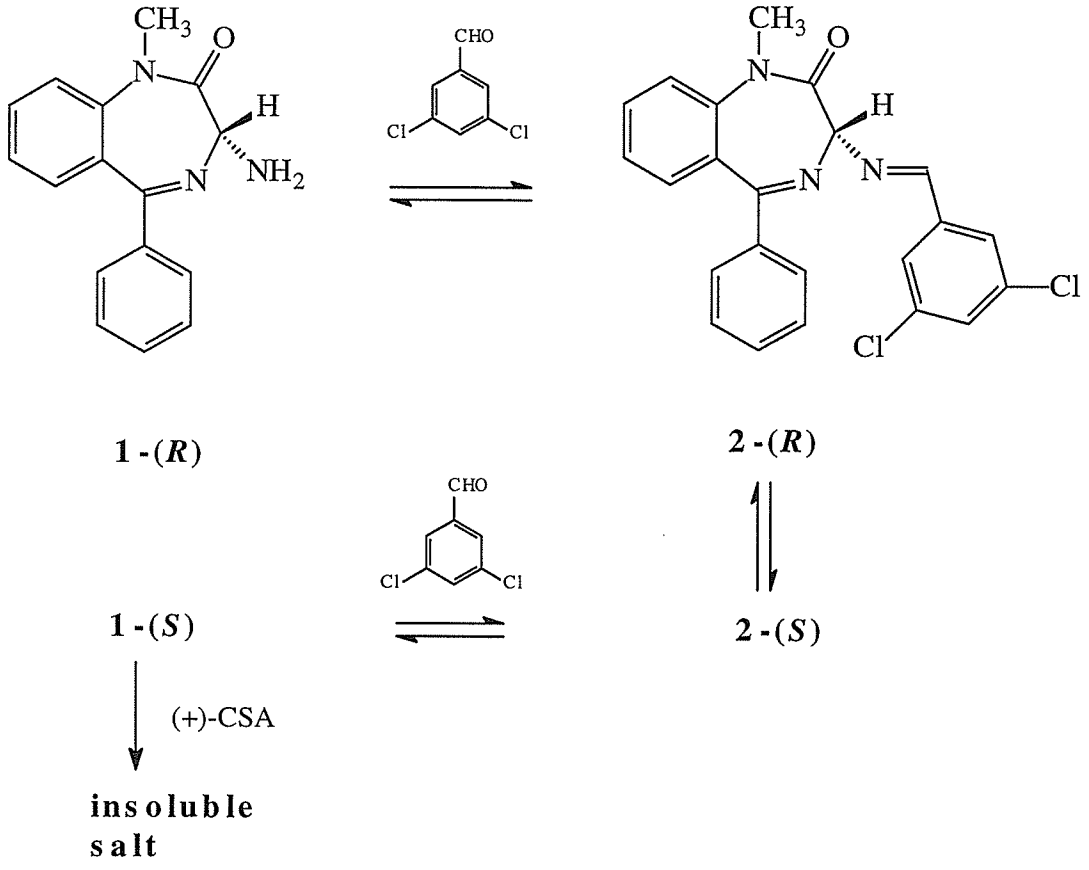

Enantiomeric interconversion of the imines **2**, presumably caused by the residual amine, can occur. In the presence of the chiral additive (+)-camphorsulfonic acid (CSA), the *S* amine forms a salt preferentially, driving the equilibrium towards producing more of *S* amine. The result is a 91% yield of the optically pure CSA-(*S*)-amine salt. By contrast, addition of (+)-CSA to a racemic solution of **1** gives the CSA-(*S*)-amine salt with a 99.5% ee but only a 40 – 42% yield.

When deracemization is combined with kinetic resolution, theoretically all of the starting racemate may be utilized. Because of the chiral nature of enzymes they often preferentially catalyze the reaction of one enantiomer during the reaction. Isomerization of the unreactive isomer to its enantiomer under the reaction conditions allows complete consumption of the starting material. The reductions of racemic ethyl 2-cyclohexanone and -cyclopentanone carboxylate using various strains of yeast or mold gives the alcohol products in high yields with both good diastereoselectivity and good enantioselectivity.[21]

1.1.2.3 Chiral pool reagents

Single enantiomers (and diastereomers) may be prepared by employing chiral pool reagents.[22,23] These are naturally occurring chiral molecules which are generally inexpensive and readily available as pure isomers such as carbohydrates[24-26] and amino acids.[18] The stereochemistry of these compounds is incorporated into the final product. For example the nine member dilactone ring of the naturally occurring antifungal agent (+)-antimycin A_3 (blastmycin) is based on an L-threonine (boxed area) residue (Figure 1.9).[27]

Figure 1.9

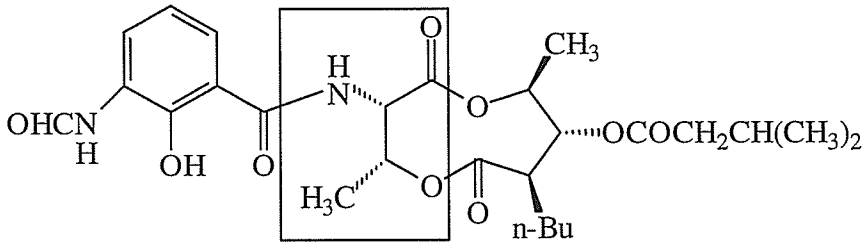

(+)-antimycin A_3

If further chirality is introduced with selective configuration, this can also be considered as a stereoselective synthesis.

1.1.2.4 Stereoselective synthesis

The most versatile method of synthesizing single stereoisomers of chiral compounds is called stereoselective synthesis. A stereoselective synthesis involves the introduction of one or more stereogenic centers such that when there is the possibility of forming more then one stereoisomer, one is formed in preference. Reactions of this type can be either enantioselective or diastereoselective.

Enantioselective syntheses involve the generation of one enantiomer preferentially from an achiral reactant. An enantioselective synthesis can be accomplished using a chiral catalyst, a chiral reagent, a chiral template or a chiral solvent. In a diastereoselective synthesis, the reactants are not necessarily achiral and one of several diastereomers is preferentially formed. For both enantioselective and diastereoselective reactions, interaction of the reactant with the chiral reagent or chiral catalyst results in the formation of diastereomeric intermediates or transition states. The free energy changes

on formation of these diastereomeric intermediates ($\Delta G°$) or transition states ($\Delta G^{‡}$) will be different. Unequal product ratios can result from the difference between transition state energies ($\Delta\Delta G^{‡}$) leading to faster formation of one isomer (kinetic control). The greater the energy difference between these states the more likely only one isomer will be formed selectively. Diastereoselectivity can also be a result of thermodynamic control if the ground state energies ($\Delta G°$) of the products or key intermediates differ and the reaction occurs via an equilibrium process.

The use of a chiral catalyst is one method of performing an enantioselective synthesis. Chiral ruthenium complex **3**, enantioselectively (and regioselectively) catalyzes the hydrogenation of geraniol and homogeraniol (Scheme 1.2).[28]

Scheme 1.2

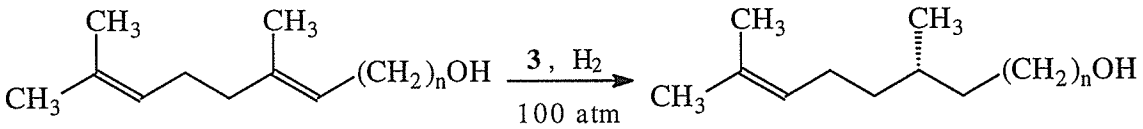

n = 1, geraniol — ee = 96%
n = 2, homogeraniol — ee = 92%

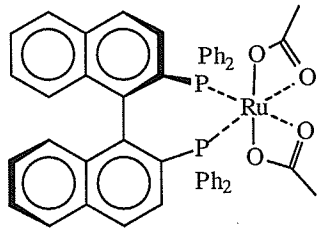

3

Another classic example is the epoxidation of allylic alcohols using the Sharpless epoxidation reagent, which is catalyzed by a titanium/diethyl tartrate complex.[29] The

stereochemistry of the resultant epoxide is determined by the tartrate isomer used in the complex.

Figure 1.10

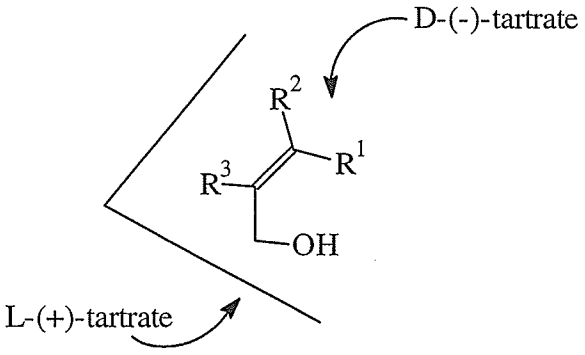

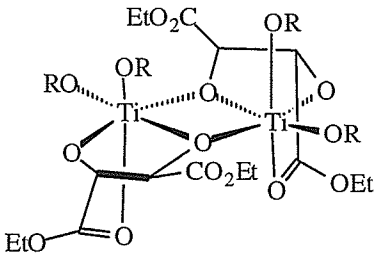

Proposed titanium complex

Enzymes are natures' chiral catalysts, the availability of which has increased over the last few years, making their use more feasible for routine synthesis. Enzymes are classified into six main groups:[30] oxidoreductases, transferases, hydrolases, lyases, isomerases and synthetases. Enzyme catalyzed reactions may be enantioselective and/or diastereoselective.

Enantioselective reactions can also be done using chiral reagents. These are similar to catalysts except that, stoichiometric amounts of the reagent are necessary. Reaction of allylmagnesium chloride with a diacetone D-glucose derived titanium complex gives compound **4**. Reaction of **4** with aldehydes at –78 °C affords homoallylic alcohols in good yields (50 – 88%) and enantioselectivities (86 – 94% ee) (Scheme 1.3).[31]

Scheme 1.3

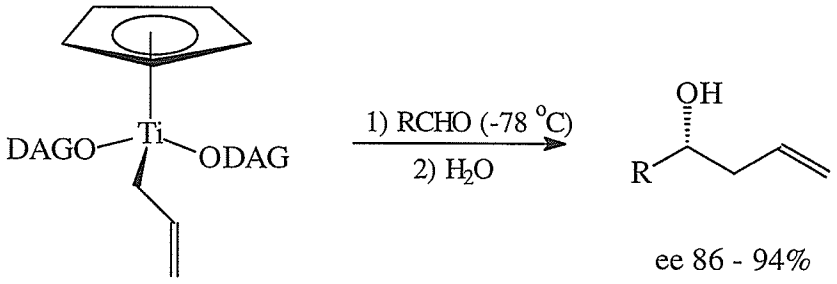

ee 86 - 94%

4

Formation of a polymeric material in the presence of a chiral molecule (template) is referred to as 'chiral templating'. The enantiomer used as the template will then have a better 'fit' into this active site.[32] Lemaire et al.[33] used this technique in designing a rhodium based complex catalyst for hydride transfer reductions (Scheme 1.4). The catalyst was polymerized in the presence of optically pure 1-(*R*)-phenylpropanol and the template was then removed. The reduction of propiophenone was carried out in the presence of this polymer and the results compared to those obtained using the non-polymerized version of the catalyst. The template increased the enantioselectivity by about 19% to give a 66% ee.

Scheme 1.4

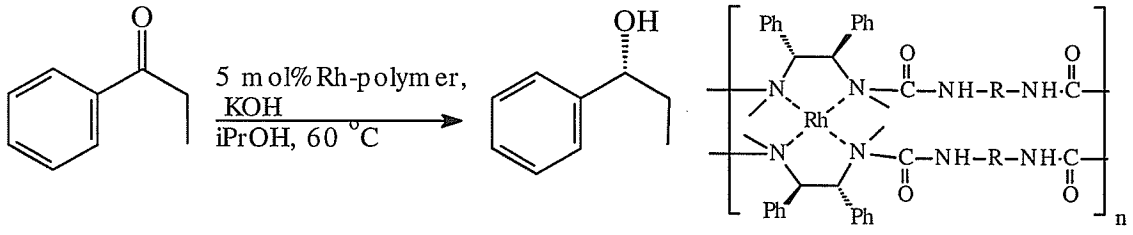

Rh-polymer

A chiral solvent or circularly polarized light can also induce chirality, however these methods have not been as widely pursued.[28] For example, chiral solvents having opposite (+ or –) optical rotations have been shown to give diastereomeric products in Grignard reactions.[34] The diastereoselectivities for these reactions were usually small however (~5%). Circularly polarized light has been studied in photochemical reactions. The light can induce asymmetric destruction, partial photoresolution or asymmetric synthesis. Earlier results showed only small levels of enantioselectivity. It has been shown that the use of right or of left circularly polarized light can lead to production of enantiomeric products.

A diastereoselective reaction forms one diastereomer in preference to the other possibilities. This occurs due to the energy differences between the transition states or of the products. For example, assume only two diastereomeric products may be formed from a single starting reagent. The free energy profile for the reaction passes from the starting reagent, through diastereomeric transition states to the final products. If the reaction is not reversible, the product formed through the pathway having the lowest activation energy ($\Delta G^{\ddagger}$) will dominate because it is formed faster. The reaction is then said to be under kinetic control. However, if the reaction is reversible, over time, more of the thermodynamically stable product (lowest $\Delta G°$) will be formed and the reaction is said to be under thermodynamic control. There are many reactions that can be considered as diastereoselective. Two general classes of transformations relevant to this thesis are the generation of one new chiral center from a chiral reactant or reagent and the generation of more than one chiral center from two prochiral compounds. Examples of each of these are shown in Scheme 1.5.[35,36]

Scheme 1.5

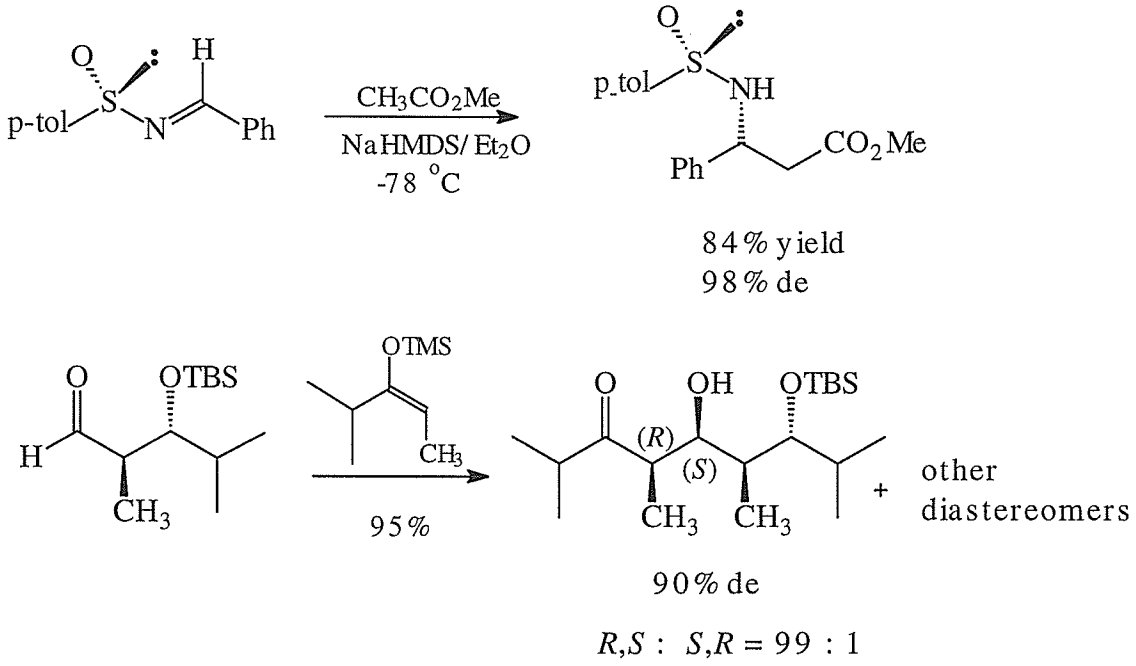

One method of performing a diastereoselective synthesis is the use of a chiral auxiliary. Depending on the reaction, the overall process can also be considered as enantioselective once the auxiliary is removed. In this approach a chiral compound is attached to a substrate, reactions are then carried out and the auxiliary is removed. The first reaction in Scheme 1.5 is an example of an auxiliary-based synthesis. Removal of the *N*-sulfinyl auxiliary with TFA gave the β-amino acid in 92% yield with >98% ee. The use of carbohydrates as chiral auxiliaries will be reviewed in the next section.

A final topic to be addressed is the concept of double stereodifferentiation, which can occur when both reaction partners are chiral.[36-38] With chiral compounds, the configuration of new stereocenters is established relative to existing stereocenters. The original stereocenter influences how the chiral species approaches another reagent (that is,

which face is attacked) by, for example, minimizing steric interactions. When both the reagent and substrate are chiral these species can ideally work together and increase the overall diastereoselectivity (matched case) of the reaction. Alternatively, they can work against each other lowering the overall diastereoselectivity (mis-matched case) of the reaction. For example, allylation of aldehyde **5** with achiral allyl borane **6a** gives the Felkin product* with 60% ee (Scheme 1.6). Chiral borane **6b** gives the same major

Scheme 1.6

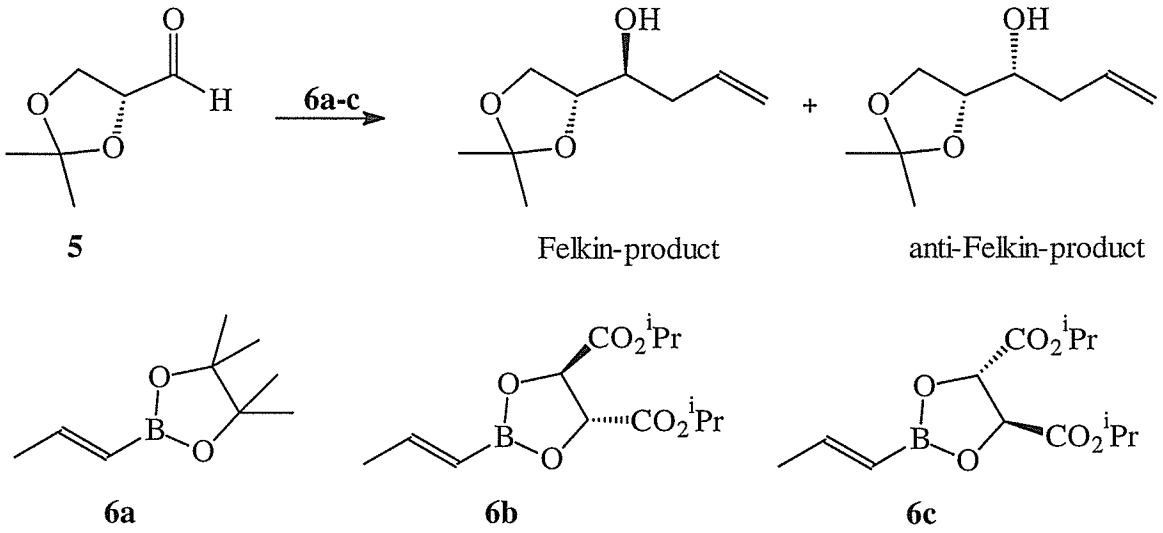

product with an 86% ee (matched case) while **6c** gives only a 28% ee (mismatched) in favor of the anti-Felkin product. The mismatched example was also found to be more dependent on the reaction conditions used (e.g. temperature and solvent) while the matched case gave excellent results in all cases.[39,40]

* The major or 'Felkin' product is assigned based on the Felkin model.[38]

1.2 Carbohydrate Auxiliaries

One method of performing an enantioselective reaction is to attach a chiral auxiliary to one of the reactants. Any compound that is available as a pure enantiomer may, in theory, be used as a chiral auxiliary. For a compound to be considered as a good chiral auxiliary, the usual criteria are that the material should be inexpensive, readily available, stable to the reaction conditions and easily removed after the reaction. Some materials that have been used as auxiliaries include camphor,[41] menthol, substituted cyclohexanols[7,42] amino acids,[18] and carbohydrates.[43]

Carbohydrates have several potential advantages for use as chiral auxiliaries. One advantage is the availability of a large number of monosaccharides with different configurations. Carbohydrates in nature exist primarily in the D-form, which often makes the L-form expensive. For some sugars both enantiomers are available at reasonable cost allowing possible access to enantiomeric products. In some instances another D-sugar can behave as a "pseudo-enantiomer".

The orientations of the various hydroxyl groups of each sugar, gives numerous environments in which ligands may be attached. The remaining hydroxyl groups also provide positions for the incorporation of protecting groups, which can provide steric barriers or stereoelectronic interactions around the ligand. The stereoelectronic nature of the protecting groups can also influence the reactivity of the system. For example, aromatic groups may influence the stereochemical outcome through π-stacking. The use of bicyclic acetal or ketal derivatives can be advantageous by restricting the flexibility of the system. Finally, the presence of other oxygens on the ring also provides modes for metal complexation during the reaction.

The choice of sugar to use as an auxiliary may have a large effect on the reaction outcome. Which reaction partner is attached to the auxiliary will also have an effect. Reactions that give poor results can, in some instances, be improved by either changing the sugar or changing which reactant partner is attached to the auxiliary. Examples where some of these effects play a role will be reviewed.

Carbohydrate auxiliaries have been applied to a wide variety of reactions and are the subject of several reviews.[44-46] They have been used in various types of cycloadditions, aldol reactions, alkylations, and oxidation/reduction reactions to name a few. In some of these reactions the carbohydrate auxiliary may be incorporated into either of the reactants. It may be attached to the diene or the dieneophile in the Diels-Alder reaction or to the electrophile/nucleophile in other reactions. Several of these will be discussed along with pertinent observations by the researchers as to how the carbohydrate auxiliary behaved.

Some of the earliest work in this area was done by Kunz et al., who applied carbohydrates as chiral auxiliaries in the Ugi and Strecker reactions. 2,3,4,6-Tetra-*O*-pivaloyl-β-D-galactopyranosylamine (**7**) undergoes an Ugi reaction in a one-pot procedure in the presence of a Lewis acid to give the (*R*) amino acids (on cleavage from the auxiliary) with good diastereoselectivity (de, 82 – 94%) (Scheme 1.7).[47,48] In a related process, the amine **7** was used in a Strecker reaction (Scheme 1.8) to synthesize α-amino nitriles which can also be turned into amino acids on removal from the auxiliary.[49,50]

For the Strecker reaction, aldimines were prepared *in situ* from **7** and reacted with NaCN or TMSCN, a process that took several days to weeks. By preparing the imine **8**

first and using the more active TMSCN reagent along with a Lewis acid, the process was accelerated to give the D-amino nitriles in almost quantitative yields with good selectivity (de, 72 – 86%) in a matter of minutes to hours. The amino acid could be effectively removed from the auxiliary by acidic hydrolysis.

Scheme 1.7

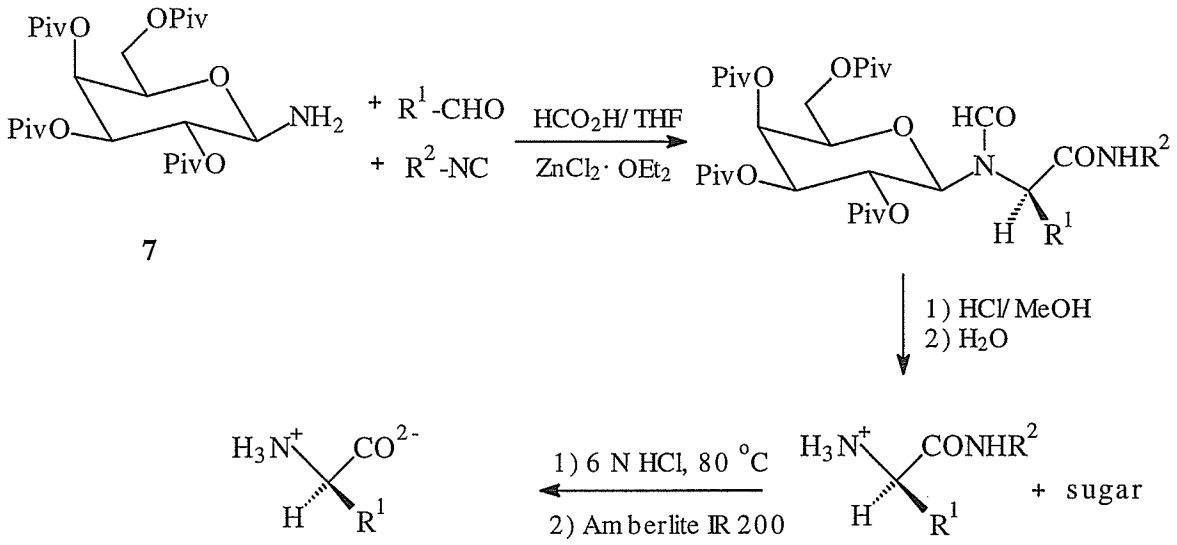

Scheme 1.8

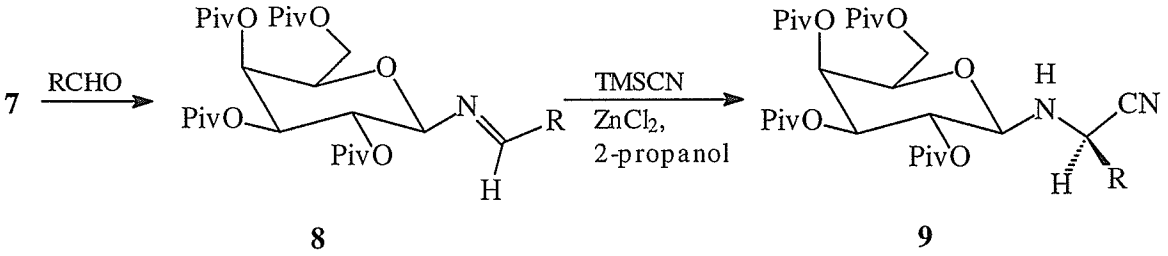

The diastereoselectivity observed for both of these reactions was explained, in part, by nuclear Overhauser effect (nOe) experiments. Both reactions go through an intermediate aldimine, which was shown to have the preferred conformation depicted in Figure 1.11, with the imine proton in close proximity to the anomeric proton.

Complexation of the Lewis acid with the bulky C-2 protecting group blocks the *re* face such that attack preferentially occurs to the *si* face of the aldimine. Use of the less sterically hindered acetyl group in the Ugi reaction resulted in slightly lower selectivities.

Figure 1.11

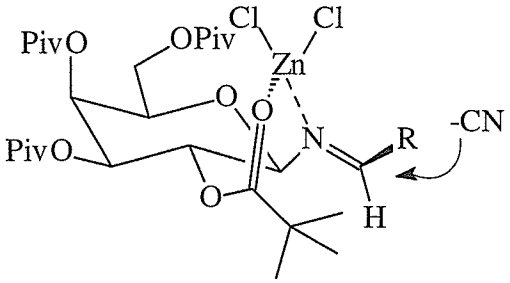

In polar solvents

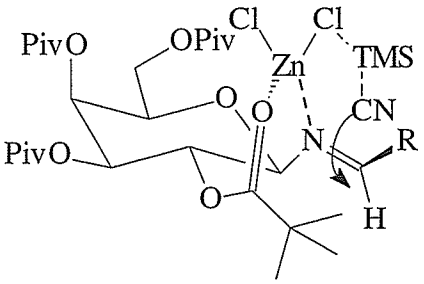

In non-polar solvents

The direction of asymmetric induction for the Strecker synthesis was reversed by changing the solvent from 2-propanol to chloroform.[51] This reversal was attributed to the need for complexation of TMSCN in the non-polar solvent. In polar solvents CN^- reacts in its free form attacking the less hindered *si* face of the imine as in Figure 1.11. In non-polar solvents the cyanide must be liberated from the TMS presumably by complexation to a ligand of the zinc catalyst. The cyanide is thus delivered to the opposite face of the aldimine.

The Ugi reaction did not show this interesting solvent effect. In order to gain access to the enantiomeric series of amino acids for this reaction, the D-arabinosylamine compound **10** was prepared.[52] Although it belongs to the stereochemical D-series of sugars, it is almost the mirror image of **7** as can be seen in Figure 1.12. This is a good example of how two different sugars can behave as "pseudo-enantiomers".

Figure 1.12

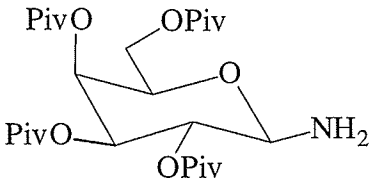

7

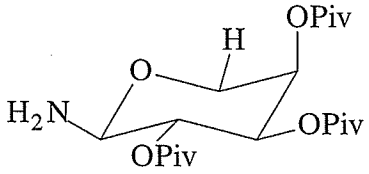

10

Diastereoselectivities of 7 – 10:1 in favor of the L-diastereomer were attainable using **10** in the Strecker synthesis. Ratios of 22 – 30:1 were obtained for the Ugi reaction where arabinosylamine **10** also showed enhanced reactivity over galactosylamine **7**.

Stoodley et al.[53,54] have studied the Diels-Alder reaction by attaching a carbohydrate auxiliary to either the diene or the dienophile. The glucosyl analog of Danishefsky's diene (**11**) underwent reaction with *p*-nitrobenzaldehyde in dichloromethane in the presence of Eu(III) catalysts to give the 2,3-dihydropyran-4-ones **12** – **15** (Scheme 1.9).[53] The diastereoselectivity for this reaction was influenced by the catalyst used. When chiral catalysts were used, the reaction showed a double diastereodifferentiating[37] pairing. (+)-Eu(hfc)$_3$ afforded a 1.2:1 ratio of the cis products **12** and **13** resulting from the expected endo addition. (-)-Eu(hfc)$_3$ gave an 8:1:1 ratio of **12**, **13** and **14** from which **12** was isolated in 39% yield. Therefore (-)-Eu(hfc)$_3$ represents a 'matched' catalyst while (+)-Eu(hfc)$_3$ a 'mismatched' catalyst.

Scheme 1.9

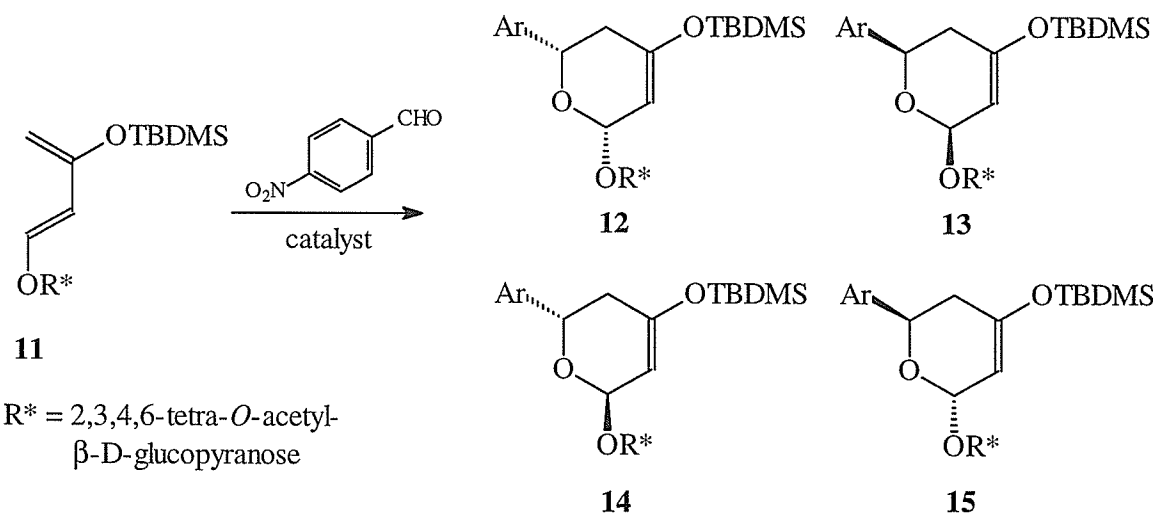

R* = 2,3,4,6-tetra-*O*-acetyl-β-D-glucopyranose

The achiral catalyst $Eu(fod)_3$ gave a slight preference for product **14** (which is formally an exo cycloadduct). The stereochemical outcome for this catalyst was found to be both solvent and time dependent. After 24 h compound **14** accounted for only 39% of the isomeric products, but after 96 h the amount increased to 72%. Stoodley postulated that the cycloaddition initially gave the expected endo products **12** and **13** in a 9:1 ratio regardless of the solvent used. Epimerization induced by the catalyst then occurred to give the thermodynamically more stable trans counterparts in a time and solvent dependent manner.

Stoodley also studied a related system in which the glucose auxiliary was attached to the aldehyde partner to determine if any remote chiral induction could be observed.[54] In this system the carbohydrate was located further away from the reactive center on the dienophile. Reaction of the glucose-linked benzaldehyde derivative with Danishefsky's diene under $BF_3{\cdot}OEt_2$ catalysis in THF gave products **16** and **17** in a 9:1 ratio after acidic

work up (Figure 1.13). The major product **16** in this case could be isolated in 70% yield by crystallization, a substantial improvement over the previous experiments.

Figure 1.13

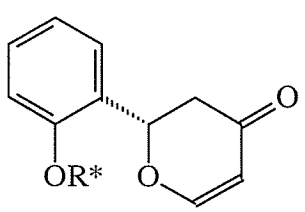

16

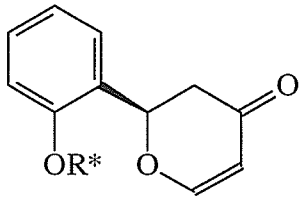

17

The selectivity again depended on the catalyst used. With $Eu(fod)_3$ in toluene, product **17** was the major isomer in a 3:1 ratio after acidic work-up. The authors suggested this change in diastereoselectivity was a result of different reaction mechanisms for the reactions catalyzed by the two different Lewis acids. Acyclic intermediates isolated in the $BF_3 \cdot OEt_2$ promoted process suggested that an aldol mechanism, rather then the expected Diels-Alder mechanism, was occurring in this instance.

Other researchers observed only low diastereoselectivities in reactions involving remote auxiliaries.[55] Reaction of the iminoglycinate **18** (Scheme 1.10), prepared from diacetone D-glucose, with tetradecanal under solid-liquid or liquid-liquid phase transfer conditions gave only modest results. Preparation of the enolate in THF using LDA gave only a 16% de and a 45% ee. When the enolate was prepared using $ClTi(OiPr)_3$ only one diastereomer was isolated, however the enantioselectivity dropped to only 6% and the yield to 11%.

Scheme 1.10

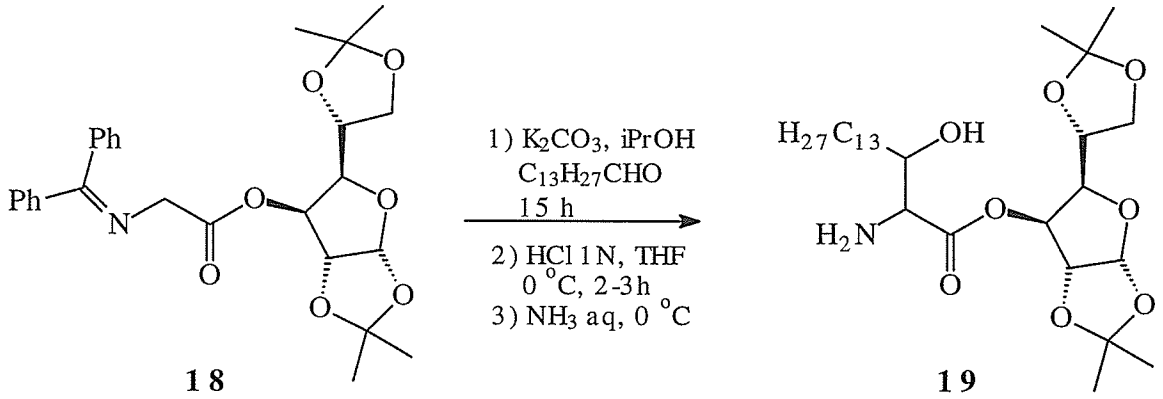

18 **19**

Many chemists up to the mid 1980's regarded carbohydrates as too complex and too polyfunctional to be used for directed diastereoselection. Initial work (1981) by Heathcock et al.[56] reinforced this opinion. Aldol reaction of the propionate **20**, derived from D-fructose, with benzaldehyde gave only a small *anti/syn* preference for aldol adducts **21** (Scheme 1.11). Little diastereofacial selectivity was also observed. Reaction of this and other similar sugar derived esters gave complex reaction mixtures, many components of which could not be separated.

Scheme 1.11

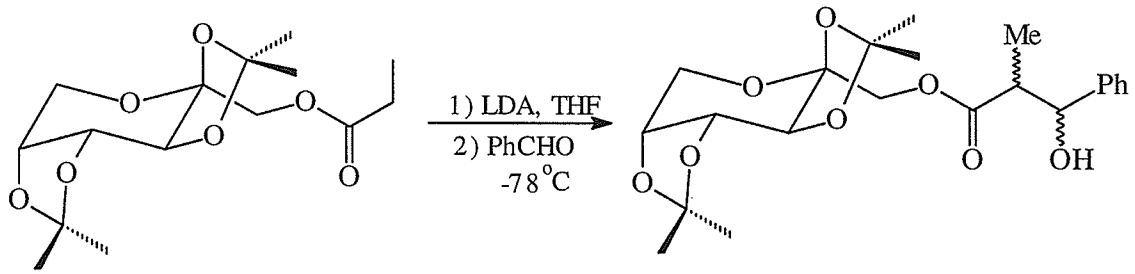

20 **21**

The complications induced by the cation complex-forming ability of carbohydrates started to become more understood by researchers in the late 1980's.

Reaction of 3-*O*-propionyl diacetone D-glucose **22** with ethyl iodide at –70 °C gave **24** with only low selectivity and yield (Scheme 1.12).[57] Product **25** which arose from an apparent Claisen condensation was also formed in 50% yield. These results were attributed to the slow decomposition of the enolate **23**, which was proven by trapping both the alcoholate and the ketene byproducts. The enolate **23** decomposes via a reversible ketene elimination process, a reaction that is not normally observed for ester

Scheme 1.12

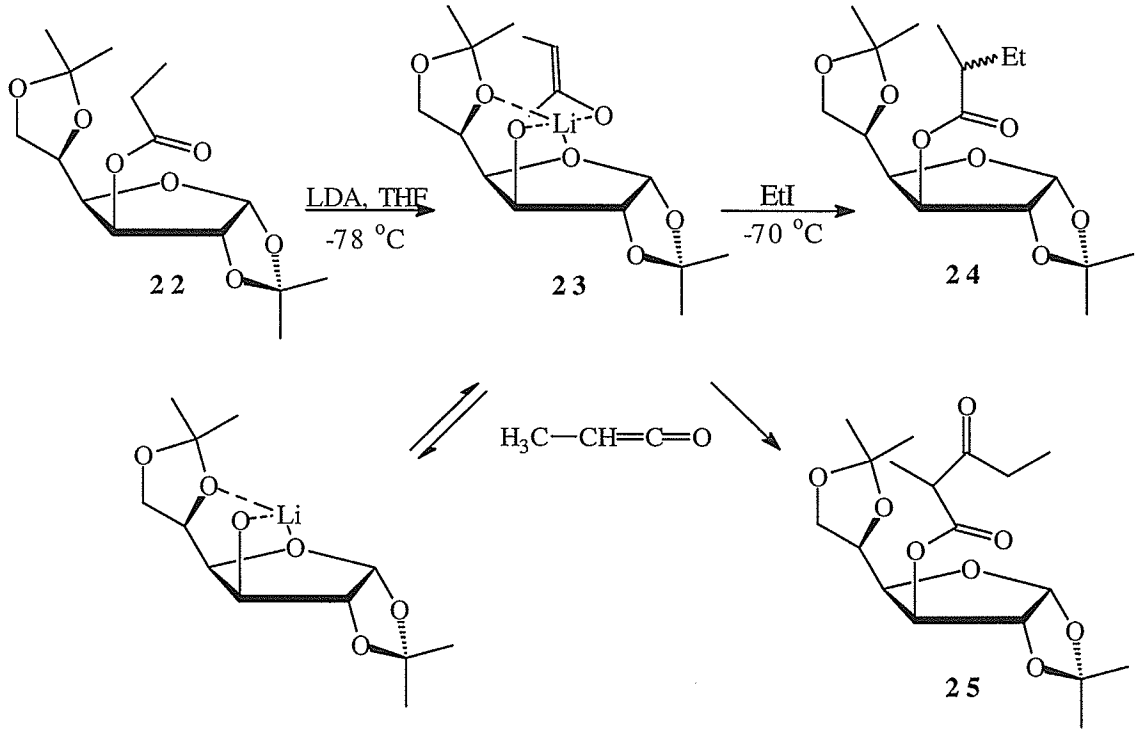

enolates at such a low temperature. The ability of the carbohydrate to form a strong intramolecular complex with the lithium cation increases its tendency towards acting as a leaving group. Both the *E* and the *Z* enolate can then be formed in the re-association of ketene. This scrambling of the enolate stereochemistry reduces the observed

stereoselectivity of the reaction. The ketene also undergoes reaction with **23** to give the observed byproduct **25**.

The epimeric D-allofuranose (Figure 1.14) compound **26** did not show this tight cation complexing ability and could be alkylated at –90 °C with LDA and various alkyl iodides giving improved yields and diastereoselectivities.

Following Kunz' idea that a tight polydentate cation complex was responsible for an increased tendency towards ketene elimination, Mulzer et al.[58] proposed that the gulose compound **27** would form a similar complex that would readily undergo ketene elimination. The results unexpectedly showed no evidence of ketene elimination occurring. Instead, the yields appeared to be affected only by the amide base used in generating the enolate, with the bulkier bases giving poorer results.

Figure 1.14

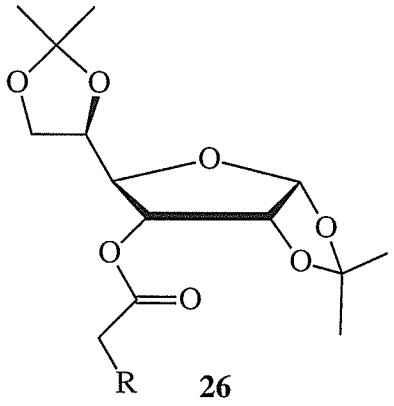

26

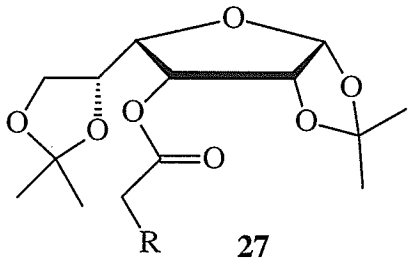

27

The different results obtained by Mulzer and Kunz illustrate the difficulty in generalizing and planning experiments with carbohydrate auxiliaries based on related literature. Kunz' result, which clearly pointed towards a ketene elimination process,

could not be reproduced in Mulzer's system that he had purposely designed to be susceptible to ketene elimination.

A common functional group used as an enolate synthon is the chiral *N*-acylated oxazolidin-2-one pioneered by D. A. Evans.[59] These systems have often delivered high levels of diastereoselection in aldol and alkylation reactions. They are readily prepared and the products can be hydrolized from the auxiliary under mild conditions. P. Köll,[60] M. R. Banks[61] and H. Kunz[45] have all developed carbohydrate-based oxazolidin-2-ones and applied them to a variety of reactions.

Köll prepared an oxazolidin-2-one compound in a simple two-step synthesis from D-xylose. *N*-Acylation with a variety of acyl chlorides then gave the starting compounds **28** (Scheme 1.13). Alkylation reactions of the lithium derived enolates of **28** required active alkyl halides. The yields were generally moderate and the diastereoselectivities were typically in the 5 – 10:1 range. An interesting observation was the reversal of product stereochemistry obtained when the acyl substituent R was changed from alkyl to aryl reflecting a change in enolate geometry. Aliphatic imides formed chelated (*Z*)-enolates **29**, which exposed the *si* face to attack giving adducts **30**. The aryl substituted compounds formed the (*E*)-enolates **31**, which exposed the *re* face giving **32**. Köll postulated that the short distance between the furanoid ring oxygen and the aromatic ring may have generated a stereoelectronic interaction that caused a change in the preferred enolate geometry.

Scheme 1.13

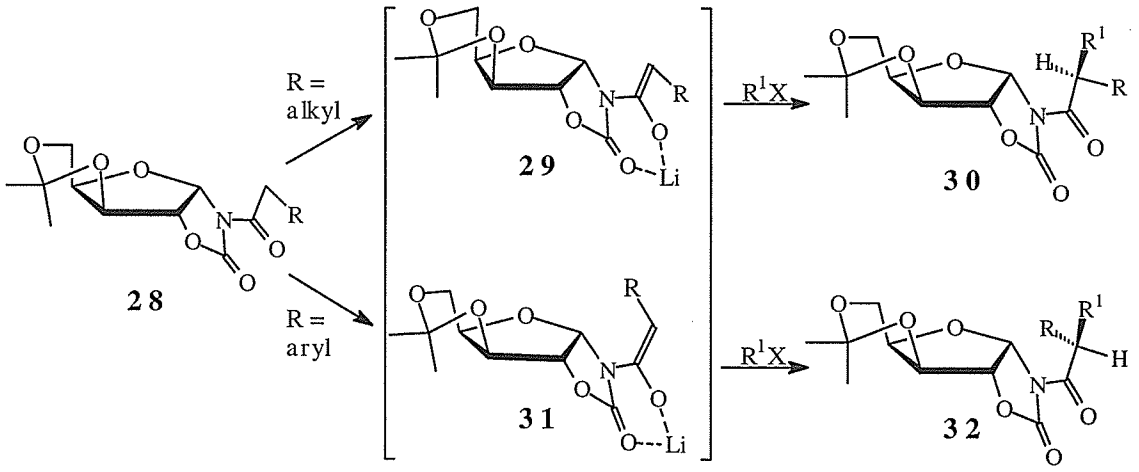

Köll also used **28** in aldol condensations generating enolates **29** and **31** using LiHMDS. For alkyl imides, reaction with simple aliphatic aldehydes gave the *syn* (2′*R*,3′*S*) product while aryl imides gave the diastereomeric *syn* (2′*S*,3′*R*) product. In each case, the major product was obtained with a 5 – 15:1 selectivity with respect to the other three possible products. The yields in all cases were low.

Figure 1.15

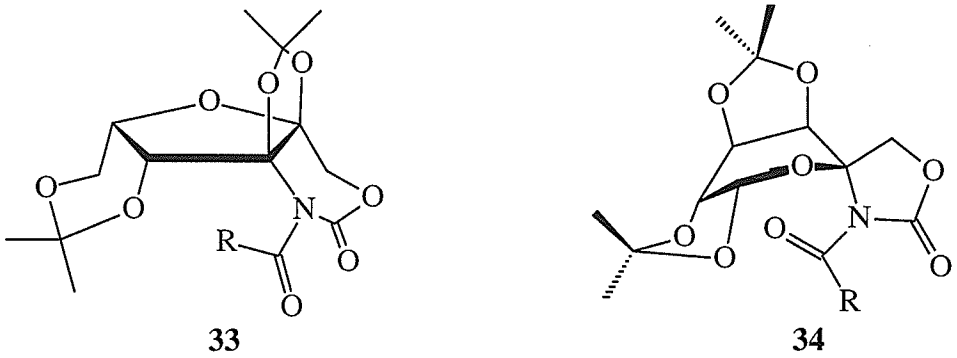

33 **34**

Banks and coworkers prepared the oxazinone **33**, a less frequently used template structure, and the spirooxazolidin-2-one **34** (Figure 1.15).[61,62] Compound **33** was

prepared in four steps from the appropriately protected L-gulonic acid while compound **34** was prepared from D-galactose. Both were applied to Diels-Alder and enolate/aldol reactions. While compound **34** (R = $CHCH_2$) gave excellent selectivity in the Diels-Alder reaction (endo:exo, 98:2; endo de, 80 – 92%) and high yields, it performed poorly in enolate reactions (R = CH_2CH_3). The lithium and sodium enolates failed to react with active alkyl halides and decomposition occurred at elevated temperatures, presumably via a ketene elimination process. Reaction with acyl chlorides led exclusively to *O*-alkylated products. Only when methylcyanoformate was used as an acylating agent was highly selective *C*-alkylation observed.[63] The auxiliary was also prone to epimerization around the spiro carbon on cleavage of the adducts, thus reducing its recoverability and usefulness.

Compound **33** (R = $CHCH_2$) fared equally well in the Diels-Alder reactions and better in aldol reactions (R = CH_2CH_3) using LDA and benzaldehyde at –78 °C (Scheme 1.14). Of the four possible products, only the two *syn* isomers were formed, in a 91: 9 ratio. The absolute stereochemistry was confirmed by reductive cleavage of the major adduct from the auxiliary using $LiBH_4$ from which the *syn* diol **35** was isolated (78% yield). Significantly, in this situation, the cleavage occurred without any isomerization of the auxiliary.

Scheme 1.14

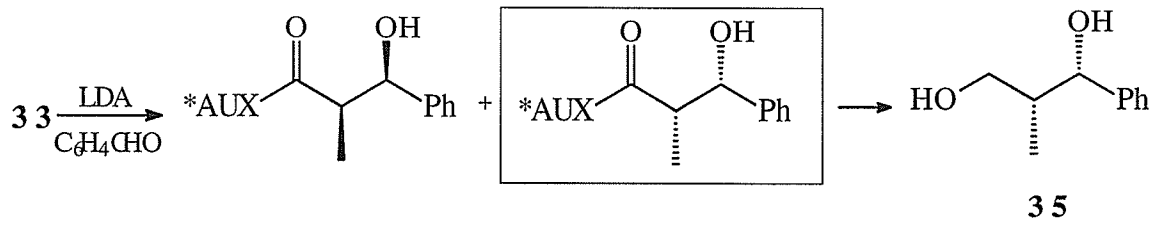

35

1.3 α-Amino Acids

The α-amino acids are an important class of natural products. The class is typically subdivided into the 20 proteinogenic and the other non-proteinogenic categories. The number of naturally occurring, non-proteinogenic α-amino acids is constantly increasing, as new compounds are isolated from natural sources. The naturally occurring amino acids have important biological functions as they can be found in proteins, peptides, and peptidoglycans. Except for the simplest, glycine, these amino acids are chiral compounds.

The proteinogenic compounds are produced on an industrial scale using extraction, fermentation, enzymatic or synthetic methods.[64] If an amino acid in a protein hydrolyzate has a significantly different solubility from the others present, then the amino acid can be isolated by extraction. For example, cystine and tyrosine can be separated from other water soluble, amino acids in a protein hydrolyzate, as both are only sparingly soluble. Fermentation methods have become a more viable method for the preparation of amino acids with the advances in biotechnology and the use of wild-type or mutant microorganisms. For example, the raw carbon and nitrogen sources and any other necessary feed stock are added to the chosen microorganism. The amino acid is then isolated from the culture broth. Enzymatic methods for amino acid synthesis are slightly different from fermentation methods because isolated enzymes are used instead of the entire microorganism. For example, the enzyme aspartase has been used for the industrial synthesis of L-aspartic acid from fumaric acid. Non-biological synthetic methods use a wider variety of starting materials and are useful in synthesizing phenylalanine and

tryptophan, amino acids for which no practical biotransformation methods have been developed.

The naturally occurring non-proteinogenic compounds are initially identified by isolation from a natural source. However unless this source is abundant chemists usually seek methods of preparing these compounds synthetically. This approach also allows for modification of the initial structure at various positions to alter the compounds' biological activity. A number of these amino acids have been applied in the pharmaceutical industry. Several different synthetic methods have been utilized in preparing α-amino acids. Some approaches produce racemic mixtures of compounds, but isolation of pure enantiomers then requires separation and incurs significant material loss as mentioned earlier. Asymmetric synthesis is therefore more desirable for the preparation of pure enantiomers. Appropriate synthetic methods may include the use of carbohydrate auxiliaries, chiral pool reagents, and the 'chiral glycine' approach to name a few.

Figure 1.16

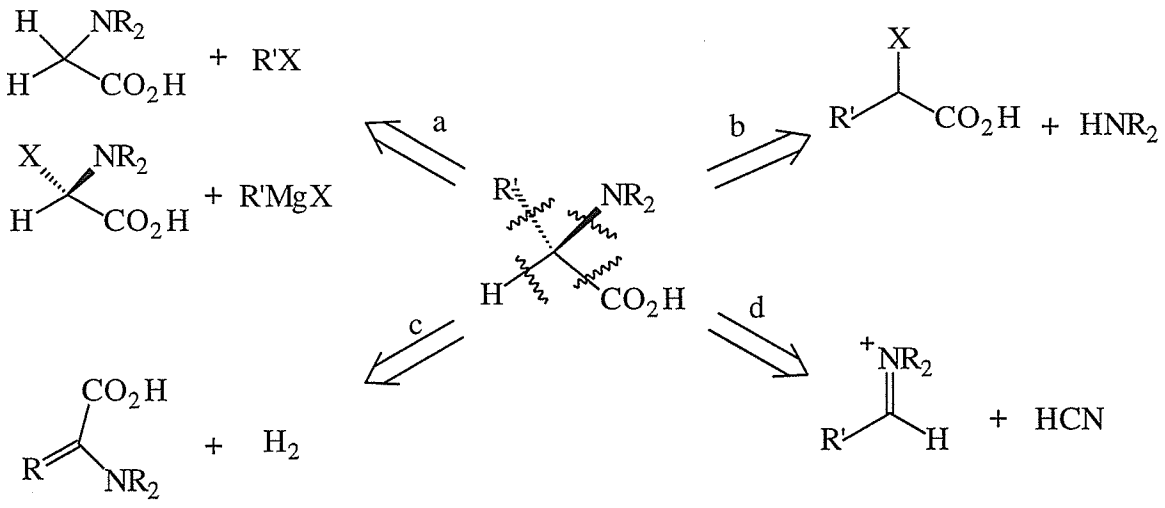

If an α-amino acid is studied by a retrosynthetic approach, it can be seen that disconnections can be made at any of the four substituents at the stereogenic α-carbon.

Some common synthetic approaches are shown in Figure 1.16. Path (a) is simply the alkylation of a glycine fragment. The *asymmetric* chiral glycine methods developed for this route will be discussed in the next section.

Disconnection (b) generates the α-amino acid by introducing the -NR_2 fragment. The reaction is generally based on an S_N2 displacement reaction. Therefore, the chirality is usually introduced into the molecule prior to this step. Epoxides[10] and halides[65] are both amenable to displacement. For example, 2,3-epoxy alcohol **36** was readily obtained with high enantioselectivity via a Sharpless asymmetric epoxidation. Oxidation of the alcohol **36** to the carboxylic acid **37** followed by stereoselective amination gave the amino acid product (Scheme 1.15). Aminating agents such as ammonia, amines and hydrazine all attack preferentially at C(2), except with unsubstituted or phenyl derived epoxides.

Scheme 1.15

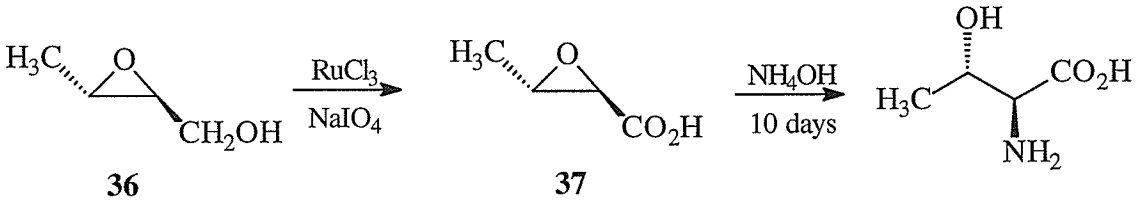

36 **37**

Electrophilic amination is the other option for path (b) (not shown). One of the earliest electrophilic reagents used was di-*t*-butyl azodicarboxylate which, converts lithium enolates into α-hydrazido acids. Due to the harsh conditions necessary to cleave

the N-N bond, this method has limited application. A more promising agent is the trisyl azide **39**, introduced by Evans in reactions with **38** (Scheme 1.16).[65] The potassium

Scheme 1.16

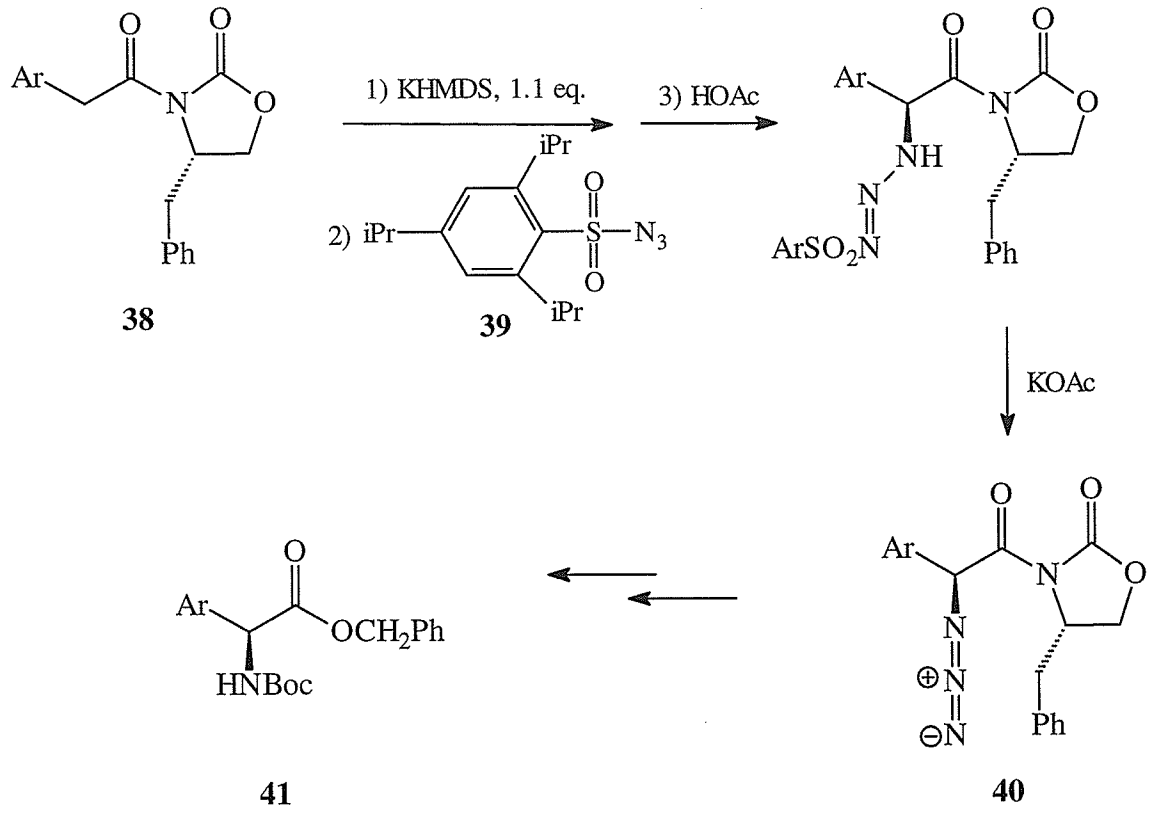

enolate of **38** was treated with azide **39** for a short time, then quenched with 4 – 6 equivalents of glacial AcOH at low temperature. After warming, the adduct was fragmented using KOAc/HOAc to give the azide **40** with good diastereoselectivity (82%) and yield (82%). Further high yielding transformations gave the amino acid product **41**.

Disconnection (c) encompasses methods to introduce the α hydrogen. Hydrogenations, asymmetric protonation of enolates, or reductive aminations are possible approaches for introducing the α hydrogen. For example, enantioselective hydrogenation

of **42** by a chirally modified Wilkinson catalyst gives phenylalanine derivative **43** (Scheme 1.17).[66] This efficient process has been applied to the industrial production of optically active amino acids.

Scheme 1.17

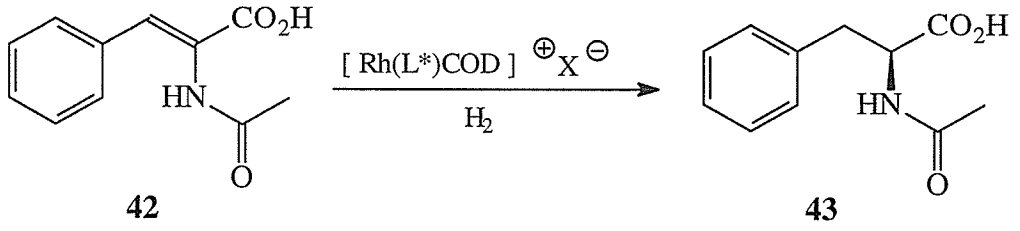

42 **43**

L* = Chiral diphosphine
X = ClO_4, BF_4, PF_6, CF_3SO_3

One possible set of synthetic equivalents for path (d) is an imine/iminium ion and a cyanide source. Strecker, in 1850, inadvertently discovered this pathway (Scheme 1.18). Following an attempt to synthesize lactic acid, Strecker found racemic alanine had been produced instead.[67] When ammonia and acetaldehyde were mixed, an *N,O*-acetal (**44**) was formed. Subsequent addition of HCN gave amino nitrile **45**, which was converted to racemic alanine following hydrolysis with aqueous acid. However, the toxicity of HCN and the low overall yields (10%) obtained made this method inefficient.

Scheme 1.18

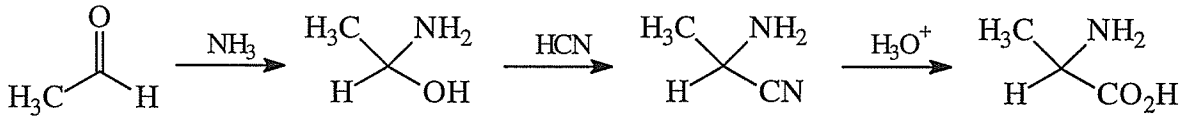

44 **45**

Various modifications, such as using KCN and NH_4Cl that gives HCN *in situ*, have improved the yield (70%) for this process.[68] The Strecker synthesis is still an important method for the industrial synthesis of α-amino acids. Kunz and coworkers (section 1.2) have successfully developed an asymmetric version of this reaction, using carbohydrate auxiliaries.

1.3.1 Chiral glycine approach

Glycine has been employed in several asymmetric methods for synthesizing more complex α-amino acids. A chiral glycine is synthesized using a glycine residue and a chiral auxiliary. After asymmetric substitution at the α-center of the glycine fragment, the auxiliary is removed. Carbon-carbon bond construction can be achieved at the α position through nucleophilic, electrophilic, or radical reactions. While there are many approaches to chiral glycines,[69,70] three major research groups (Williams, Seebach, and Schöllkopf) have developed chiral glycinates, some of which are now commercially available, based on a cyclic framework.[71] In each of these methods the chiral template is destroyed on removal of the amino acid fragment after the stereoselective reaction.

Schöllkopf and coworkers developed a chiral glycine based on a bis-lactim ether (**48**) (Scheme 1.19).[72] The bis-lactim ether was prepared by peptide coupling of two amino acids. Many bis-lactim ethers are possible using different pairs of amino acids, however **48**, prepared from glycine and L-valine, is the most popular. The *N*-carboxyanhydride derivative of L-valine **46** was used as the precursor. Condensation with glycine, followed by heating gave the dipeptide **47**, which was converted to **48** using

trimethyloxonium tetrafluoroborate. Enolate formation, followed by alkylation, gives adduct **49** with generally excellent yields (80 – 92%) and selectivities (85 – 95%). Hydrolytic cleavage using dilute HCl or trifluoroacetic acid releases the new amino acid ester **50**, from which the valine ester byproduct can usually be removed by distillation.

Scheme 1.19

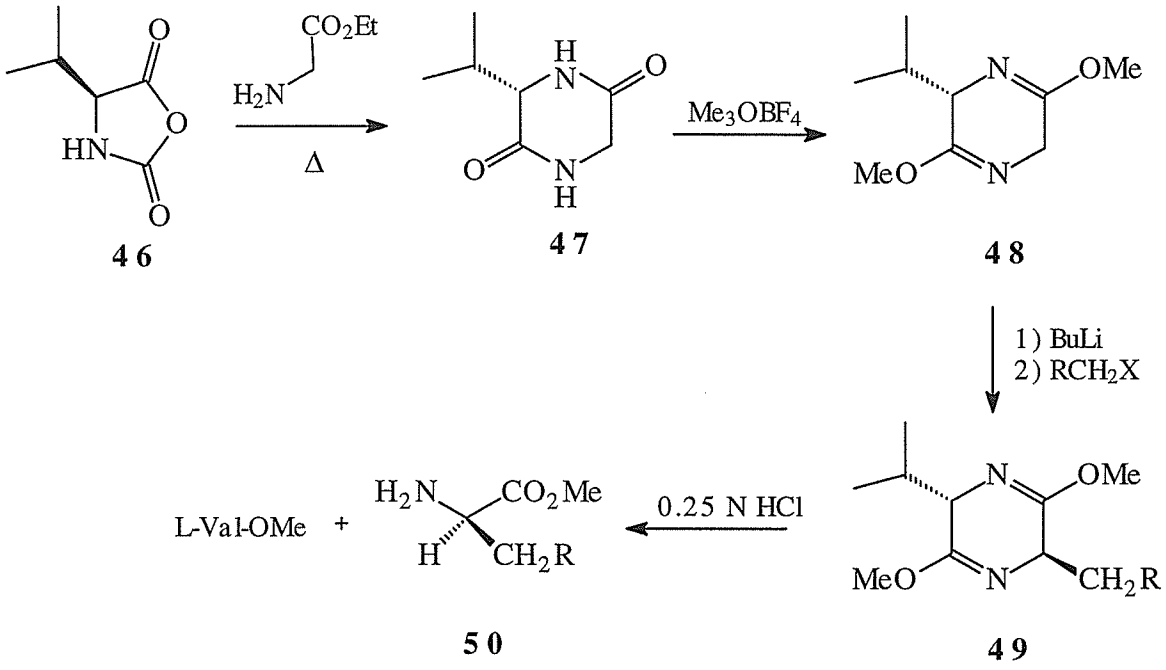

Figure 1.17

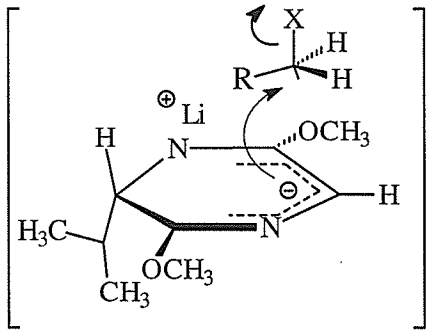

Alkylation occurs *trans* to the C-6 (isopropyl) substituent. Schöllkopf rationalized the asymmetric induction observed using a planar transition state (Figure 1.17). The diastereotopic faces of the enolate are shielded differently (H vs. *i*Pr) with the top face, as shown, being more open to approach of the electrophile.

Another family of chiral glycines is the imidazolidinones prepared by Seebach.[71,73] The general synthetic approach to these compounds is shown in Scheme 1.20. Glycine methyl ester **51** was treated with concentrated methylamine to form the *N*-methyl amide. The Schiff base was formed on addition of pivalaldehyde (with azeotropic removal of water), which then cyclized under the reaction conditions giving racemic **52.** The racemate was resolved using (*S*)-(-)-mandelic acid, and each enantiomer treated with benzoyl chloride to give **53** and **54**. Treatment of **53** with LDA followed by an alkylating agent gave the *trans* product **55** with >95% diastereoselectivity (Scheme 1.21). Hydrolysis released the α-amino acid in high yield.

Scheme 1.20

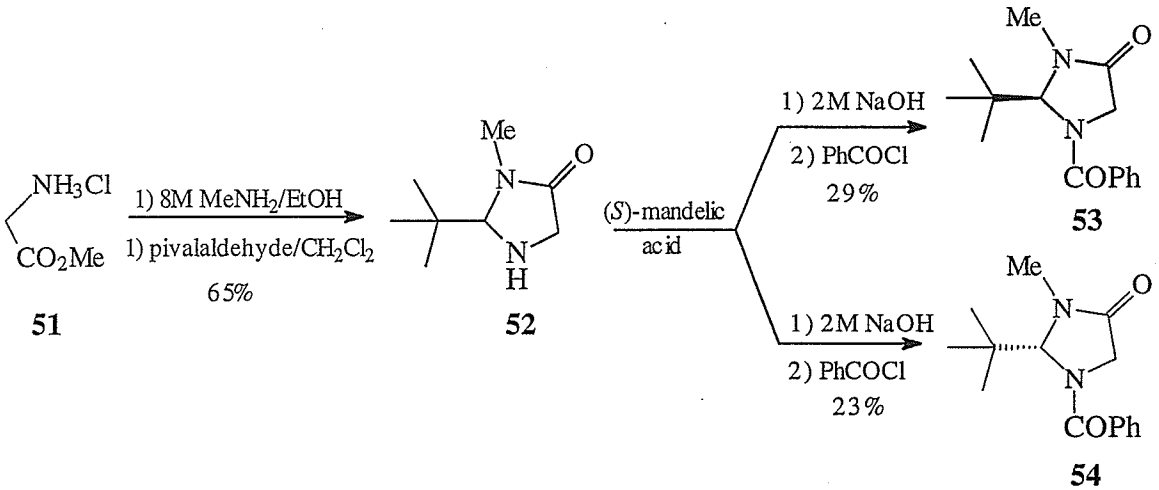

The rationale for this high selectivity was hypothesized to be two fold. The enolate adopts conformation **56** in which the *t*-butyl group lies in a pseudoequatorial position. This forces both nitrogens to be pyramidalized so that the nitrogens' lone pairs are pseudoaxial. The steric effect of the *t*-butyl group and the donating effect of the enamine nitrogen both favor attack of the electrophile *trans* to the existing stereocenter.

Scheme 1.21

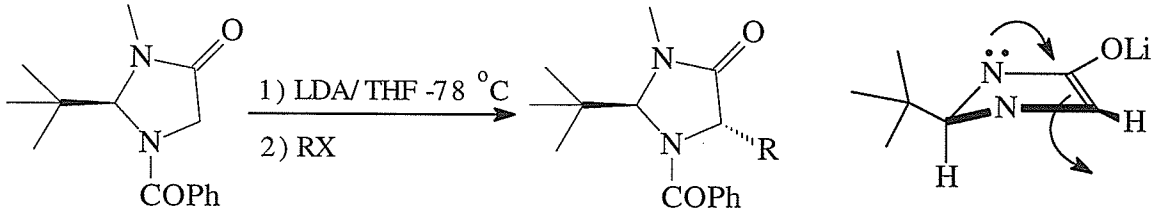

53 **55** **56**

The last cyclic chiral glycine is that of Williams which is based on an oxazinone structure.[71,74] Benzoin was converted to the oxime **57** and stereoselectively hydrogenated to the racemic *syn*-amino alcohol **58**. This mixture was then resolved by crystallization of its L-glutamate salt (Scheme 1.22). The oxazinone provided access to either amino acid enantiomer depending on which antipode was used. Alkylation with bromoacetate, *N*-protection, and lactonization gave the resulting chiral glycine **59**.

Scheme 1.22

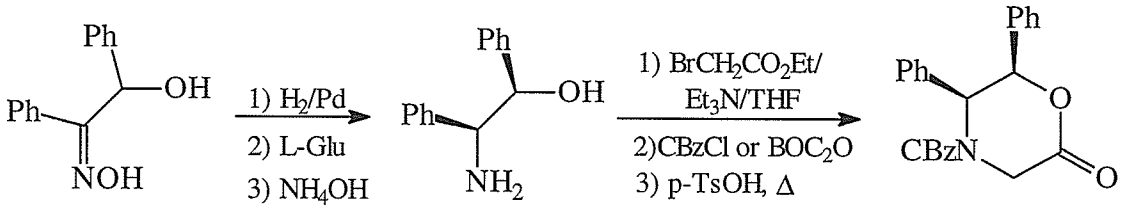

57 **58** (+ enantiomer) **59**

Compound **59** has been utilized in both electrophilic and nucleophilic alkylation reactions.[75,76] Nucleophilic alkylation occurred through a two step process, halogenation, which occurred exclusively *trans* to the phenyl groups, followed by alkylation with retention of configuration (Scheme 1.23). The authors speculate that the retention of configuration was a result of the zinc (II) salt coordinating to the halogen, providing the iminium species, which was followed by attack of the nucleophile from the less hindered face. [74]

Scheme 1.23

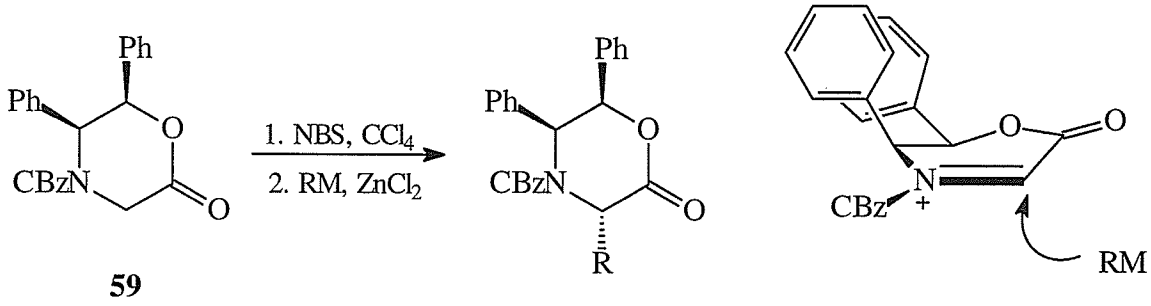

59

Electrophilic addition occurred by a one step procedure. The enolate of **59** was generated using a strong base, and reacted with an alkyl halide. Again, alkylation occurred on the less hindered face. The selectivity of these reactions can be modest to excellent. Although no aldol reactions have been reported, the chiral glycine has been

used to synthesize several interesting amino acids such as clavalanine,[77] (*S*)-(-)-cucurbitine,[78] meta-tyrosine,[79] and several 1-aminocyclopropane-1-carboxylic acids.[80]

1.3.2 γ-Oxo and γ-hydroxy-α-amino acids

One particular family of non-proteinogenic α-amino acids is the γ-oxygenated series. There has been an increased interest in synthesizing these unique compounds. The γ-oxygenated, and particularly the γ-hydroxy, amino acid skeleton is relatively common (Figure 1.18). This structure can be found in many naturally occurring compounds, such as the nikkomycins (antifungal agents),[81] (-)-bulgecinine (a proline derivative)[82] and L-kyneurinine (an L-tryptophan metabolite).[83] There are several common approaches to the syntheses of these amino acids as well as a few uncommon methods.

Figure 1.18

Jackson and Salituro both used a metal coupling approach to form the γ-oxo compounds. Jackson[84] prepared iodide **60** in two steps from CBz-L-serine (Scheme 1.24). Treatment with zinc or zinc/copper using sonication gave the organometallic species, which was coupled *in situ* to an acyl chloride in the presence of a palladium catalyst. The resultant product was the β-unsubstituted amino acid **61**. Subsequent β-

methylation using LiHMDS/MeI gave predominately the *anti* material **62** (20:1) in good yield. The γ-hydroxy-α-amino acids could then be prepared by reduction. Reduction of the *anti* material with L-Selectride gave a mixture of alcohols, while Et_3SiH plus BF_3 resulted in stereoselective 1,2-*syn* reduction (40:1) and *in situ* lactone formation. By contrast, the *syn* isomer could be reduced with better selectivity using L-Selectride, which gave a single lactone (66%) after cyclization. The authors attributed the stereochemical outcome of the reductions primarily to steric interactions due to the adjacent methyl group and, to a lesser extent, by the α group.

Scheme 1.24

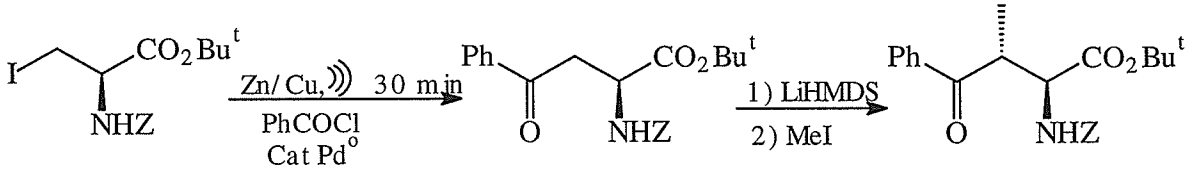

60 **61** **62**

However, this method was found to be unsuitable when using ortho-nitrogen substituted benzoyl chloride derivatives. Any nitrogen protecting group tested hindered the reaction by enhancing the acidity of the NH or increasing the steric bulk of the acylating agent. Nitrobenzoyl chlorides also gave unsatisfactory results. To overcome this limitation, Jackson et al.[83] devised a strategy based on a palladium catalyzed carbonylative cross coupling of an aryl iodide to their prepared organozinc compound (Scheme 1.25). Using this adaptation they were able to prepare several aryl substituted compounds in modest yields.

Scheme 1.25

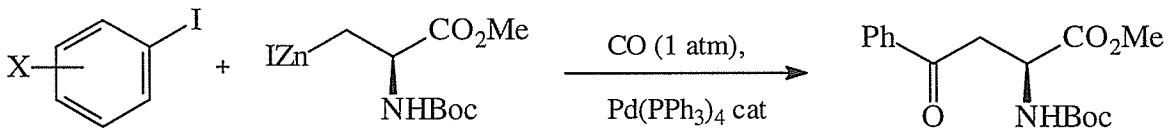

X = NH_2, NO_2, OCH_3

Salituro[85] was able to use *N*-substituted aromatics by employing tin (in place of Zn/Cu) in the metal coupling reaction (Scheme 1.26). Ortho metalation of Boc protected aniline followed by quenching with trimethylstannyl chloride gave **63**. This was coupled to the protected L-aspartyl acid chloride **64** giving **65** in 79% yield after chromatography.

Scheme 1.26

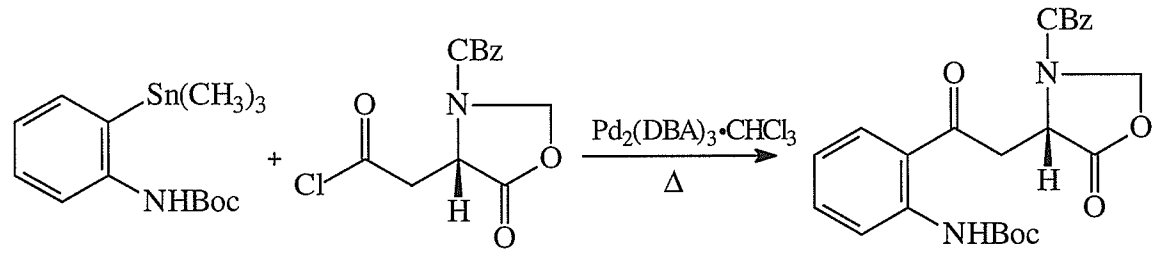

63 **64** **65**

A common synthetic approach to the γ-hydroxy series is through isoxazolines. In 1980 König reported the first nonstereoselective synthesis of the *N*-terminal amino acid residue of nikkomycin B and B_x via this method.[86] The key step in these reactions was a nitrile oxide cycloaddition (Scheme 1.27) which gave predominantly the *trans* product **68** (93:7). Since this early work several other researchers have explored this method.

Scheme 1.27

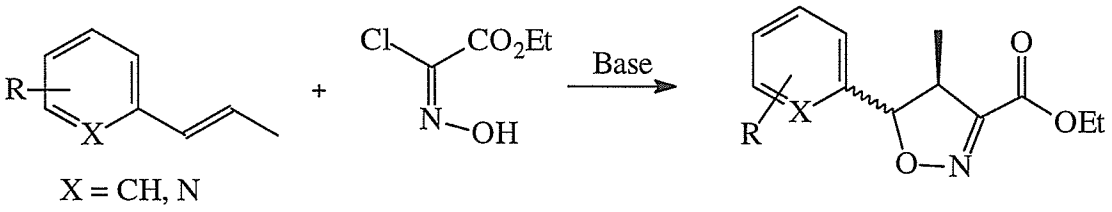

66 **67** **68**

Barrett et al.[87] used the α-oximino amide trianion **69** in the dipolar cycloaddition and got exclusively the *trans* isoxazoline **70**. Reduction using Red-Al led primarily to the 2,3-*syn*-3,4-*anti* product. Concurrent, or subsequent, cyclization to the lactone **71** occurred depending on the conditions used (Scheme 1.28). By changing the nature of the amide (i.e. changing the *t*Bu substitutent) by using (*R*)-α-methylbenzylamine, they were able to prepare the optically pure analog of **70**.

Scheme 1.28

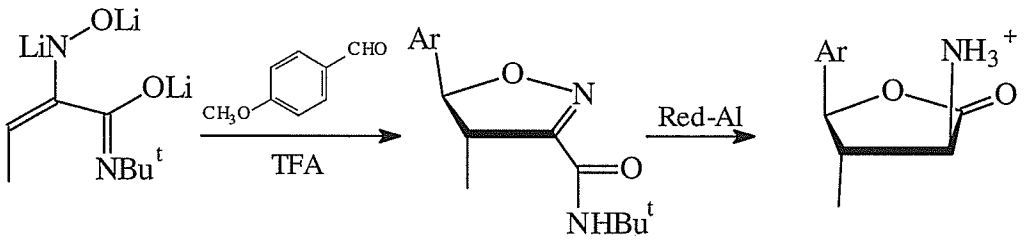

69 **70** **71**

Saksena et al.[88] used the isoxazoline method to prepare the pyridyl series of γ-hydroxy α-amino acids, which they wished to couple with uracil polyoxin C to give nikkomycin Z. Of key importance in their research was the observation that chemistry useful in the phenyl series generally failed when applied to the analogous pyridyl series of compounds. For example, compound **66** (X = N) was much less reactive then the phenyl

counterpart (X = CH). With the pyridyl series, it was necessary to carry out the reaction at high dilution with slow addition of the base to avoid self-condensation of the nitrile oxide. Reductive opening of **68** to form the γ-hydroxy compounds also produced erratic results and low yields which had some dependence on the ester group used. The *t*-butyl ester analog of **68** gave the best results in the reductive opening of the isoxazoline.

Several protecting group manipulations were also described in attempts to obtain a suitably protected derivative. For example although the *t*-butyl ester of **68** could be reductively opened with high yield (80%), any subsequent attempts to protect the hydroxy or amine groups directly led to lactonization. Several protection or deprotection steps also led to dead ends where the material lactonized and could not be activated towards intermolecular coupling. After several trials, the authors were able to synthesize a racemic amino acid (**72**), which would couple to the uracil residue to make nikkomycin Z. The final pathway is shown in Scheme 1.29.

Scheme 1.29

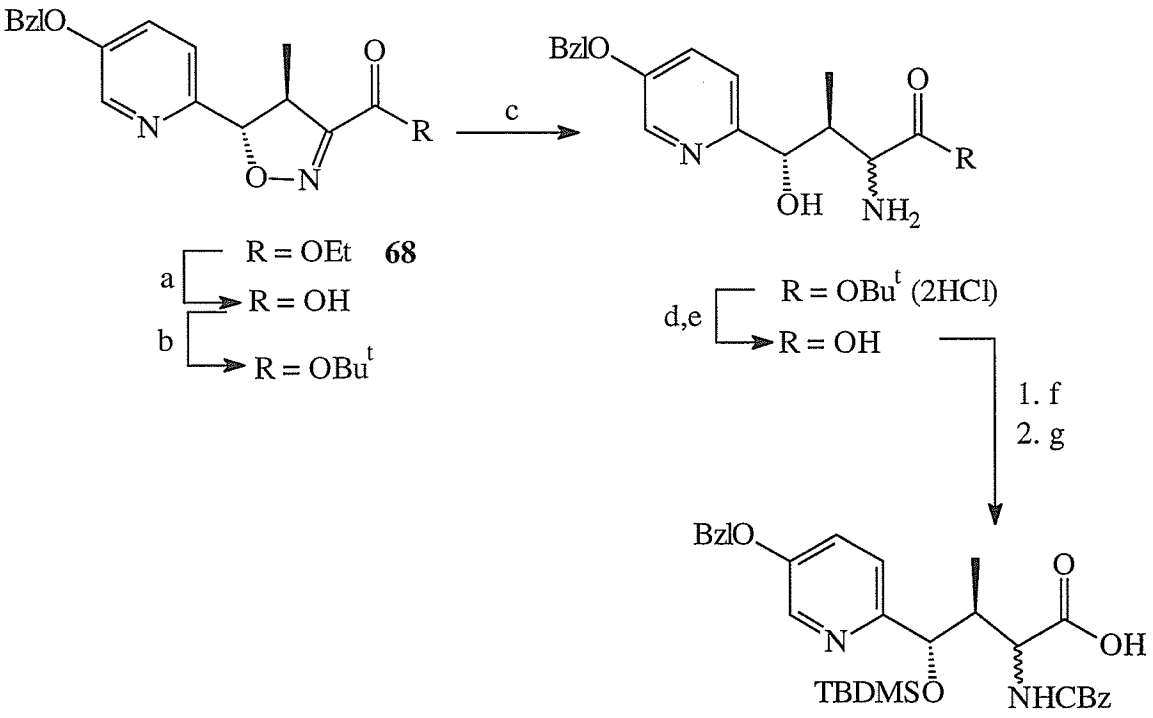

Reagents: **a**) KOH, THF-H_2O (95%). **b**) Im_2CO, DMF, *t*BuOK, *t*BuOH (90%). **c**) Zn-Cu, HOAc, 6 h; HCl (79%). **d**) KOH (3 eq), THF-H_2O (95%). **e**) H_3O^+, AG50W resin, 2N NH_4OH (84%). **f**) *N*-methyl-*N*-(*t*-butyldimethylsilyl)trifluoroacetamide. **g**) *N*-(benzyloxylcarbonyloxy)-succinimide

Barrett et al. encountered similar problems using the isoxazoline method to prepare nikkomycin B.[89] The products prepared as shown in Scheme 1.28 could not be suitably protected and activated for coupling to a uracil fragment. They decided to approach the synthesis in a completely different manner. Barrett's synthesis of the *N*-terminal amino acid segment is shown in Scheme 1.30. Reaction of 4-(pivaloyloxy)benzaldehyde **73** with (-)-(*E*)-crotyldiisopinocampheylborane gave homoallyl alcohol **74a** (R = H, X = CH_2) as a single diastereomer after work up and chromatography. The alcohol was next protected as a silyl ether. Ozonolysis to the

aldehyde **74b** followed by reaction with (1-ethoxyvinyl)lithium and a second treatment with ozone gave α-hydroxy ester **75**. The nitrogen functionality at C2 was introduced by conversion to the iodide and nucleophilic displacement with sodium azide in DMF to afford **76**. Changing the phenolic protecting group to a silyl ether and formation of an

Scheme 1.30

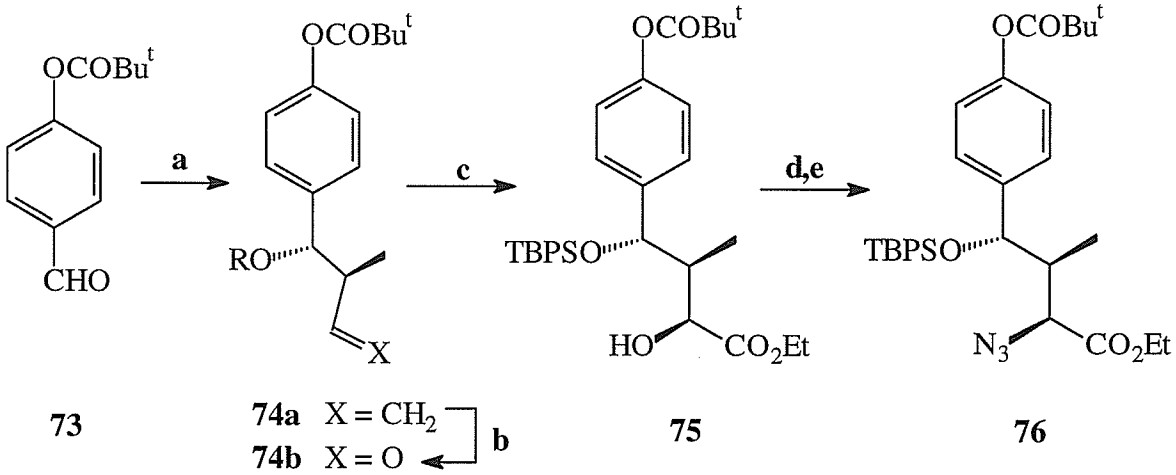

a) (i) (-)-(*E*)-crotyldiisopinocampheylborane, THF, Et_2O, –78 °C, H_2O_2, NaOH; (ii) TBPSCl, DMF, imidazole, DMAP. **b**) O_3, –78 °C, CH_2Cl_2; Me_2S. **c**) (i)$CH_2C(Li)OEt$, THF –100 °C. (ii) O_3, CH_2Cl_2 –78 °C; Me_2S. **d**) $(PhO)_3PMeI$, DMF. **e**) NaN_3, DMF, 60 °C.

active ester were accomplished in four more steps. The protecting groups were removed and the azide was reduced to give the amine after coupling to the uracil fragment (which they also prepared) resulting in the total synthesis of nikkomycin B.

Another popular approach to the γ-oxo compounds is through the functionalization of aspartic acid (Scheme 1.31).[90] The differentially protected aspartate **77**, readily prepared from aspartic acid, was first converted to the isoxazolidide **78** and

then to aryl ketone **79** in good yield (73 – 76%). Deprotection of the carboxylic acid gave the γ-oxo-α-amino acid, which the authors used in synthesizing tripeptides.

Scheme 1.31

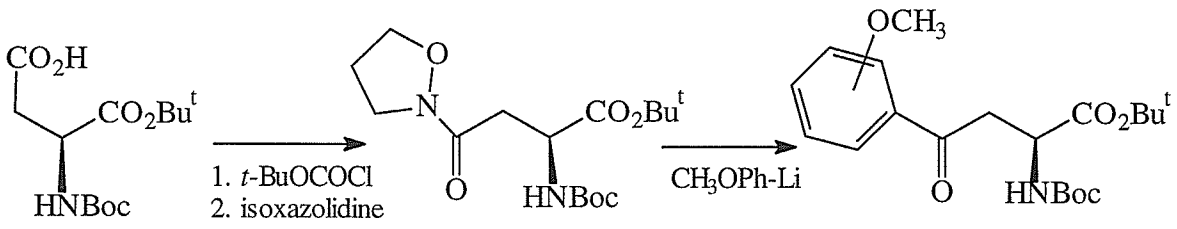

77 **78** **79**

An appealing approach to the synthesis of the γ-oxo series of α-amino acids is through reaction of an iminium ion and a silyl enol ether. This method can be considered as a chiral glycine approach (section 1.3.1). Hiemstra and Speckamp prepared racemic γ-oxo-α-amino acids using this method.[91,92] The iminium ion **81** was generated from precursor **80a** using tin tetrachloride at –78 °C (Scheme 1.32). The silyl enol ether was then added and the reaction was allowed to warm to room temperature to give **82**. Yields were modest to excellent depending on the type and amount of silyl enol ether used. The best results were obtained using two equivalents of the silyl enol ether. When the methoxyglycine precursor **80b** was used in the presence of $BF_3 \cdot OEt_2$ to generate iminium ion **81**, poorer yields were obtained. Also, in those cases where stereoisomers were formed, little diastereoselectivity was observed.

Scheme 1.32

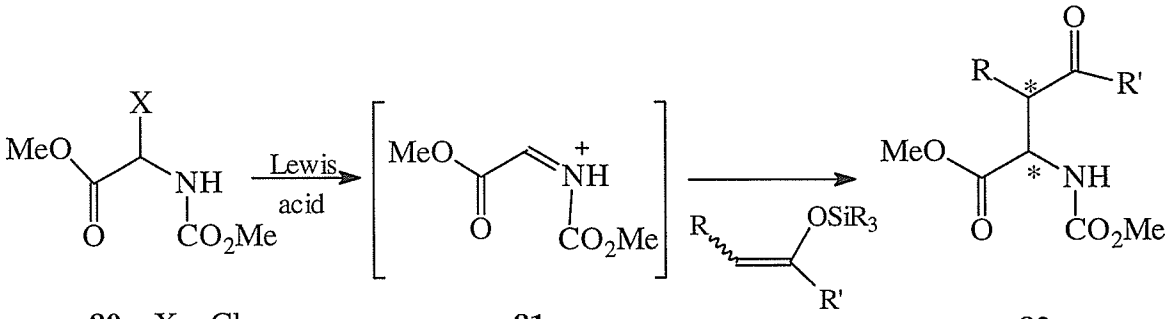

80a X = Cl
80b X = OMe

81

82

The authors successfully applied this method to the synthesis of racemic 5-hydroxy-4-oxonorvaline (HON). HON, a compound originally discovered in 1958 in the culture broth of *Streptomyces akiyoshienis novo sp.*, is known to possess antitubercular and antifungal properties. In later work,[92] the authors synthesized α,α-disubstituted γ-oxo-α-amino acids by using a suitably modified version of compound **80**.

Nikolaus Risch and coworkers[93] prepared their iminium ion by electrophilic attack of acetyl chloride on the aminal compounds **83** (Scheme 1.33). Reaction of **83a** with cyclohexanone or tetralone gave the *anti* products **84** and **85** respectively with high yields and excellent diastereoselectivities (≥99:1). The use of **83b/c** gave lower and more variable stereoselectivities in reactions with the two ketones.

Reduction of **84** with zinc borohydride in Et_2O at room temperature gave the 3,4-*anti* γ-hydroxy product which lactonized during purification on silica gel. L-Selectride gave the 3,4-*syn* lactone as a single diastereomer. Using the bulkier reagent L-Selectride, **85** was also reduced to the *syn* lactone with high diastereoselectivity. Both zinc and sodium borohydride gave inferior results with **85**.

Scheme 1.33

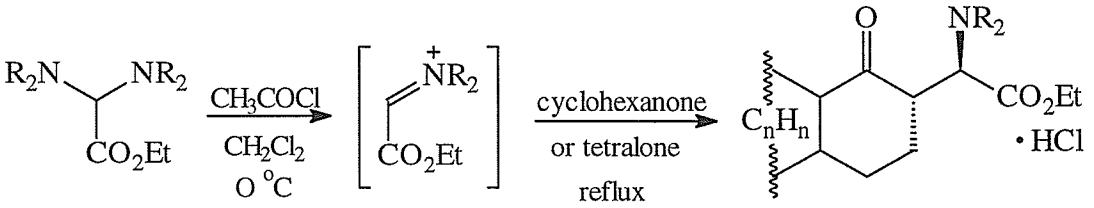

83a $R_2 = -(CH_2)_5-$
83b $R_2 = -(CH_2)_2O(CH_2)_2-$
83c R = Me

84 n = 0
85 n = 4

A mechanistically similar approach to γ-oxo-α-amino acids is through reaction of an imine with a ketone enolate (or silyl enol ether) in an aldol or Mannich like reaction. This approach has been undertaken by various researchers using non-stereoselective methods (one-pot, *in situ* generation of the imine) and asymmetric methods (asymmetric ketone equivalents, chiral catalysts).

Loh and Wei[94] prepared racemic **86** in a one-pot procedure. In the presence of indium trichloride (20 mol %), the aldehyde was treated with p-chloroaniline and then by the silyl enol ether, trimethyl-(1-phenyl-vinyl)-silane, giving **86** in 63% yield (Scheme 1.34). This is the only example the authors give for the synthesis of a γ-oxo-α-amino acid so the applicability of this method to more hindered or aliphatic silyl enol ethers is unknown.

Scheme 1.34

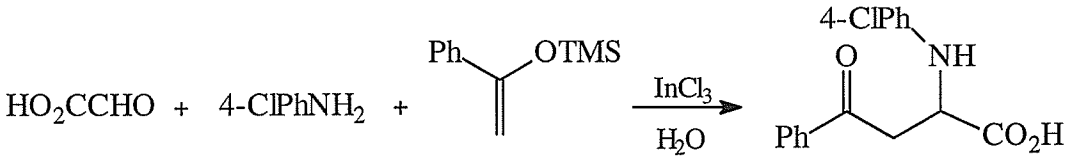

86

Steglich et al.[8,95] generated achiral *N*-acylimines **88** (R′ = Et, *t*-Bu) *in situ* from compounds **87** and Et_3N (Scheme 1.35). Reaction with various silyl enol ethers in the presence of $TiCl_4$ gave the desired products **89** in modest to good yields (58 – 80%) but with little diastereoselectivity.

Scheme 1.35

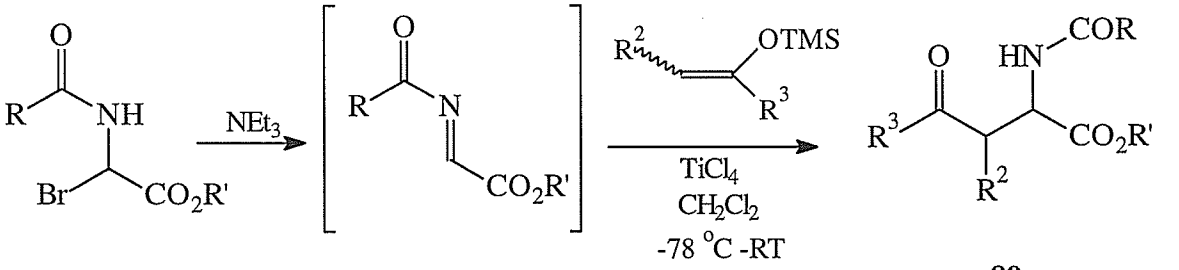

87

R = Ph, Me, OtBu

88

89

R^2 = H, R^3 = CH_3, Ph

$R^2 + R^3 = (CH_2)_4$

Reactions of the amines **90a-d** with the morpholino enamine of cyclohexanone (**91**) (Scheme 1.36) gave better *anti* diastereoselectivity (de, 75 – 98%) and yields than did the TMS derivative used in Scheme 1.35. The results were somewhat temperature dependent, with the higher diastereoselectivities and yields occurring at –100 °C. Steglich attributed the improved diastereoselectivity to a Diels-Alder like transition state (Figure 1.19) instead of the expected aldol transition state, a proposal that was supported by the isolation of a cyclic compound in one instance.

Scheme 1.36

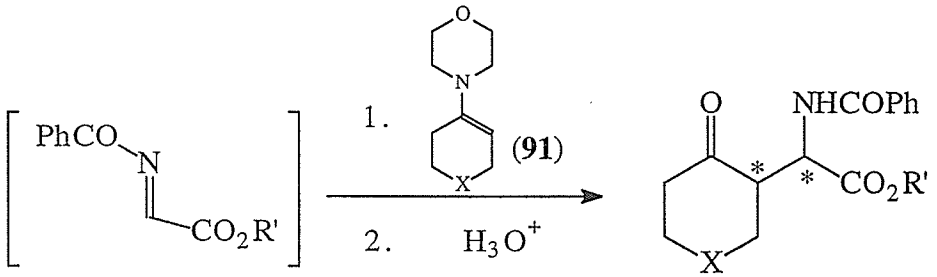

90a R' = Me
90b R' = (-)-menthyl
90c R' = (+)-menthyl
90d R' = (-)-8-phenylmenthyl

92 a - d

Figure 1.19

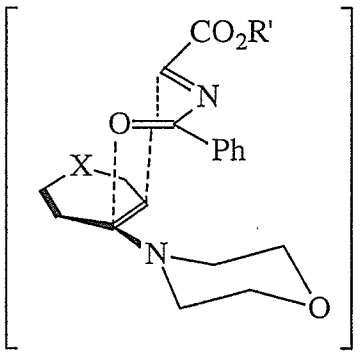

The authors also prepared chiral versions of *N*-benzoyl **90** (R′ = (+) or (-)-menthyl, (-)-8-phenylmenthyl) which were reacted with enamines **91** (X = CH_2, S). This is one of the few examples in the literature where the chiral auxiliary was attached to the α carbon of the imine. Each reaction gave excellent *anti* diastereoselectivity (≥96%), however only the (-)-8-phenylmenthyl ester gave even moderate enantioselectivity (67%) (**92d**). Reactions of **90b** and **90c** with chiral enamines showed the system to undergo a double diastereodifferentiating effect.

One approach, which has given very good results, is the use of chiral BINAP catalysts for Mukaiyama reactions. Sodeoka and Lectka are the principal researchers in this area. Sodeoka[96,97] found that aldol reactions of simple silyl enol ethers **93** with glyoxylimines **94** could be promoted using Pd (II)-BINAP catalysts **95** and **96** (Scheme 1.37).

Scheme 1.37

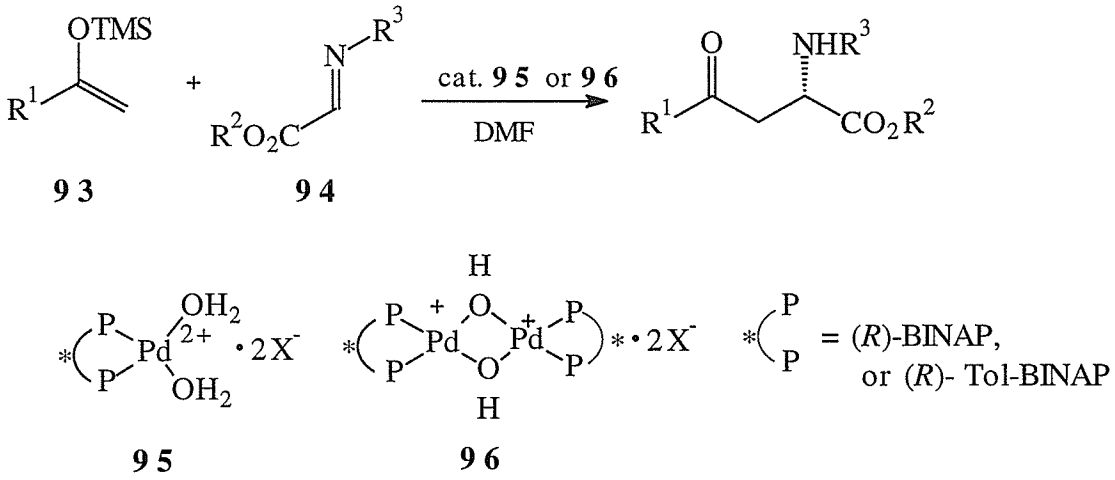

Interestingly, simple addition of the glyoxylimine **94** to a mixture of the silyl enol ether **93** and the catalyst **95** gave a reasonable yield, but the product was racemic. In order to obtain an enantioselectivity of 67% and an improved yield (85%), a complicated procedure was developed involving slow addition of the imine over a four hour period. The enantioselectivity also improved on raising the reaction temperature. The authors suggested that the unusual temperature dependence and sensitivity were the result of an undesired proton-promoted competitive pathway (Scheme 1.38). Upon generation of the palladium enolate **97**, an equivalent amount of tetrafluoroboric acid is generated. This acid could catalyze the unselective aldol reaction. In order to prepare a catalyst that would give a similar enolate yet suppress the undesired formation of HBF_4, binuclear μ-

hydroxo palladium complex **96** was prepared. Using catalyst **96**, Sodeoka et al. were able to increase the enantioselectivity of the reaction to as much as 90% and at the same time avoid the complicated reaction procedure required for catalyst **95**.

Scheme 1.38

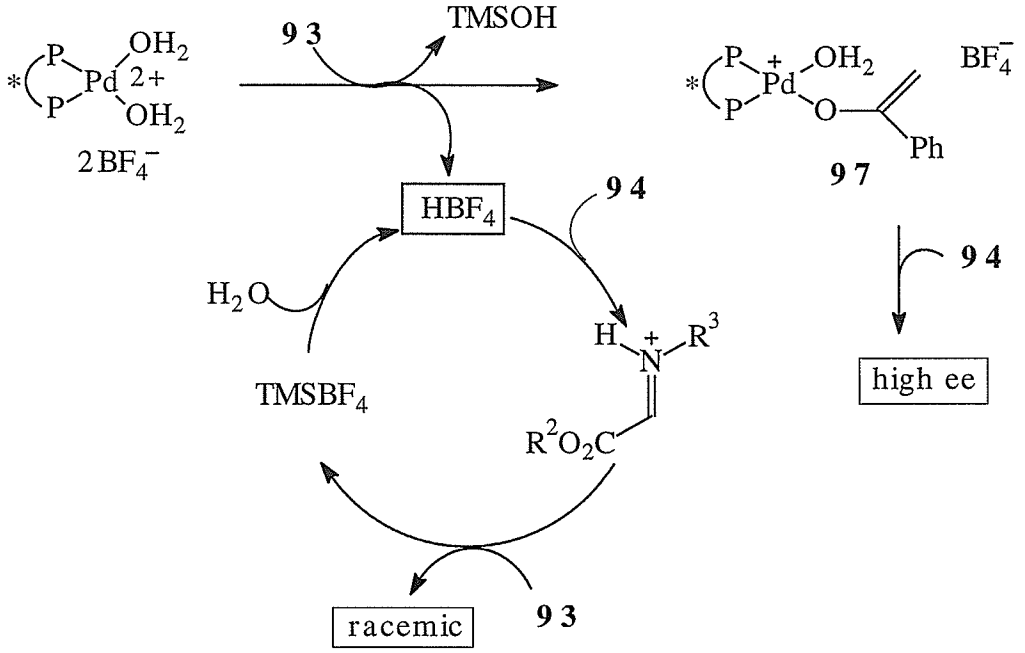

Leckta et al.[98,99] have looked at the same reaction but have explored the effect of changing the transition metal. They examine BINAP or Tol-BINAP complexes of Ag(I), Cu(I), Ni(II) and Pd(II). High yields were obtained in most instances when the reaction was carried out at –80 °C. (*R*)-BINAP-$AgSbF_6$ gave the product amino acid in 95% yield and 90% ee (*S* isomer) but only 67% ee was obtained when the reaction was carried out at –40 °C. (*R*)-BINAP-$Pd(ClO_4)_2$ was slightly less effective and (*R*)-BINAP-$Ni(SbF_6)_2$ performed the worst, giving only a 30% ee at the lower temperature. The catalyst (*R*)-

Tol-BINAP-$CuClO_4$ performed the best giving excellent yields (91%) and selectivities (98% ee) even at 0 °C.

The copper catalyst was then further explored to include diastereoselective variants on the reaction. In most instances the catalyst gave good *anti* diastereoselectivity (7 – 25:1), regardless of the silyl enol ether geometry. Based on reports by Sodeoka[96] and Carreira[100] that intermediate Pd(II)- and Cu(II)-based enolates were involved in imine additions and aldol reactions, Leckta examined whether the Cu(II) species might be involved in their system. Earlier studies by IR had demonstrated that a chelate interaction between the imine and the catalyst was occurring. Treatment of the silyl enol ether with the Cu(I) catalyst produced no discernible change in the ^{1}H or ^{13}C NMR spectra over 48 h. They concluded from these studies that their catalyst was behaving as a Lewis acid only.

Finally, there are also some less common approaches to the synthesis of γ-oxo and γ-hydroxy-α-amino acids (Scheme 1.39). Barluenga et al.[11,101] prepared β-amino ketones from 4-amino-1-aza dienes **98**. Reaction of **98** with a chiral aldehyde allowed for subsequent stereoselective reduction at C-6. Hydrolysis then gave the corresponding β-amino ketones as a mixture of isomers (*anti*:*syn*, 3:2), which could be separated by chromatography. The 2-furyl group used in this synthesis has been shown to be an effective carboxylic acid equivalent.[102] Crossley[103] used oxidative denitration of **99** to prepare the γ-oxo α-amino acid product. A third method developed by Panek[104] involved Lewis acid catalyzed addition of an (*E*)-crotylsilane to an acetal (generated in situ) followed by allylic azide isomerization giving **100**. Compound **100** is a precursor to the

γ-hydroxy-α-amino acids, however the researchers did not report any attempts to oxidatively cleave the double bond or reduce the azide.

Scheme 1.39

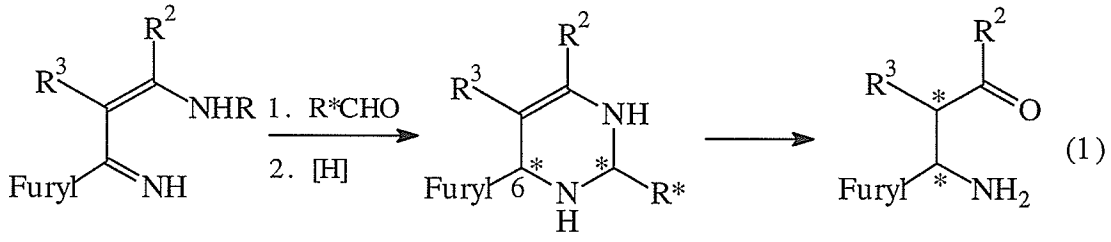

98 (1)

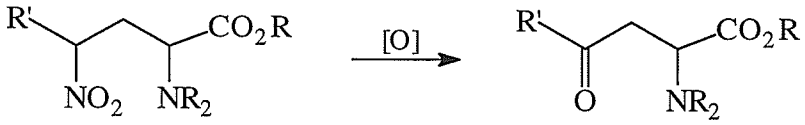

99 (2)

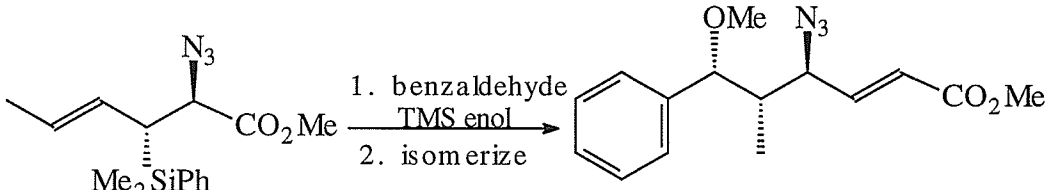

100 (3)

1.4 Mannich and aldol reactions

The synthesis of the γ-oxo-α-amino acids to be discussed in section 2.2 involves the reaction of an imine with an enol (or silyl enol) ether. These reactions can be viewed as Mannich[105-107] or aldol-like reactions.

The importance of the aminoalkylation reaction of CH-acidic compounds was first recognized by Carl Mannich in the early 1900's.[108] Mannich systematically studied this

reaction and developed the methodology. In the classic Mannich reaction, a carbonyl component is heated in the presence of formaldehyde and an amine hydrochloride (Scheme 1.40) giving a β-amino ketone (Mannich base) as the product. The classic reaction, however, has some serious disadvantages.

Scheme 1.40

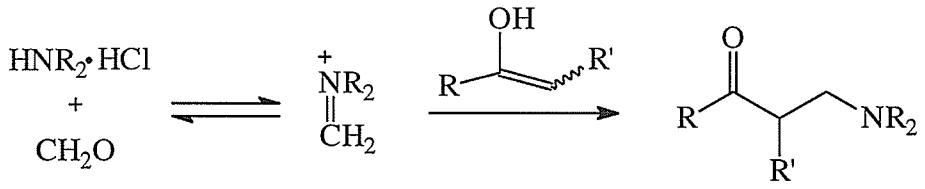

The drastic reaction conditions and long reaction times can result in unwanted side reactions such as deamination, and the formation of bisketones. Also, monosubstitution of the amine occurs only when secondary amines are used. Since the enol is generated only in small amounts *in situ*, there is no control over the regioselectivity of the reaction with unsymmetrical ketones. In addition, with few exceptions, only formaldehyde can be used in generating the iminium ion.

Modern variants have helped to overcome most of these shortfalls. In the classic Mannich, the iminium ion is generated only in small amounts through a series of equilibrium reactions. By pre-forming this electrophilic partner it can be employed at higher concentration, thus reducing the reaction temperatures and times required. The reaction also is no longer restricted to aminomethylation, aminoalkylation can also be achieved by using other carbonyl partners besides formaldehyde in the form of the iminium ion. The electrophilic Mannich reagent may be pre-formed as imines (**101**), N,O-acetals (**102**), aminals (**103**) or as iminium ions (**104**) (Figure 1.20).[105]

Figure 1.20

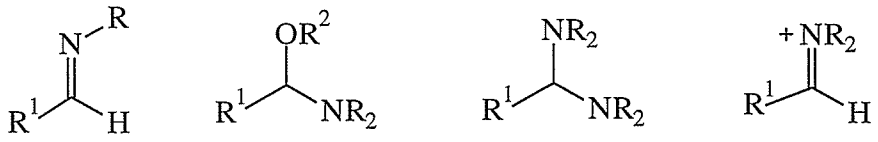

101 **102** **103** **104**

Imines (**101**) are typically generated from an aldehyde and a primary amine. They are generally less electrophilic than the corresponding aldehyde, and for this reason examples of condensation reactions using electrophilic imines are less common. However imines are also more versatile than iminium salts as they possess an additional site on the nitrogen for further elaboration and they are usually more stable. One possible reason for their limited use as Mannich reagents is that the *catalytic* Lewis acids that are often used in these reactions can be deactivated by the nitrogen on the imine starting material. The reactivity of imines can be improved to some degree, by changing the nature of the *N*-substituent or by activation with an *excess* of Lewis acid, during the reaction.

N,O-acetals (**102**) and aminals (**103**) resemble imines in their reactivity. They are usually activated by Lewis acids and are postulated, in some instances, to react through iminium intermediates. The synthesis of these compounds is limited to formation from non-enolizable aldehydes (R^1 = H, aryl).

Iminium salts (**104**) may be formed from a variety of starting materials including aminals, N,O-acetals, or directly from a carbonyl compound and a secondary amine. These reagents are more extensively used in Mannich reactions, as they are the most electrophilic. These salts are normally hygroscopic but can often be stored for long

periods of time with exclusion of moisture. It is often more convenient to prepare these reagents *in situ*.

1.4.1 Ketone enolates

Control of how the ketone partner reacts has also improved due to advances in the understanding of enol and enolate chemistry. The ability to regioselectively generate the desired enols *in situ* or to trap them as their silyl derivatives means that unsymmetrical ketones can now be routinely used in these reactions. Many of these techniques were developed during studies of the aldol and Claisen reactions. Many advances have also been made in the regioselective generation of enolates.

The term enolate was first used to describe the C=C–O$^-$ species in 1920.[109] However, it was not until 1950 that Levine[110] reported the use of the strong base LDA to prepare enolates by deprotonating carbonyl compounds. The ease of preparing LDA and its generality with a wide range of carbonyl compounds marked the beginning of the usefulness of this species. One consequence of using strong bases such as LDA was the ability to deprotonate weakly acidic carbonyl compounds regioselectively (Scheme 1.41). Bulky bases such as LDA or LICA deprotonate ketones under low temperature conditions at whichever α-center is less hindered. The enolate formed in this situation is referred to as the 'kinetic enolate'. When the deprotonation is carried out under equilibrium conditions such as with the *t*BuOK/*t*BuOH, the more stable 'thermodynamic enolate' will dominate.[111] The ability to control which enolate is generated allows for regioselective control of the ketone moiety in a variety of reactions including the aldol and Mannich.

Scheme 1.41

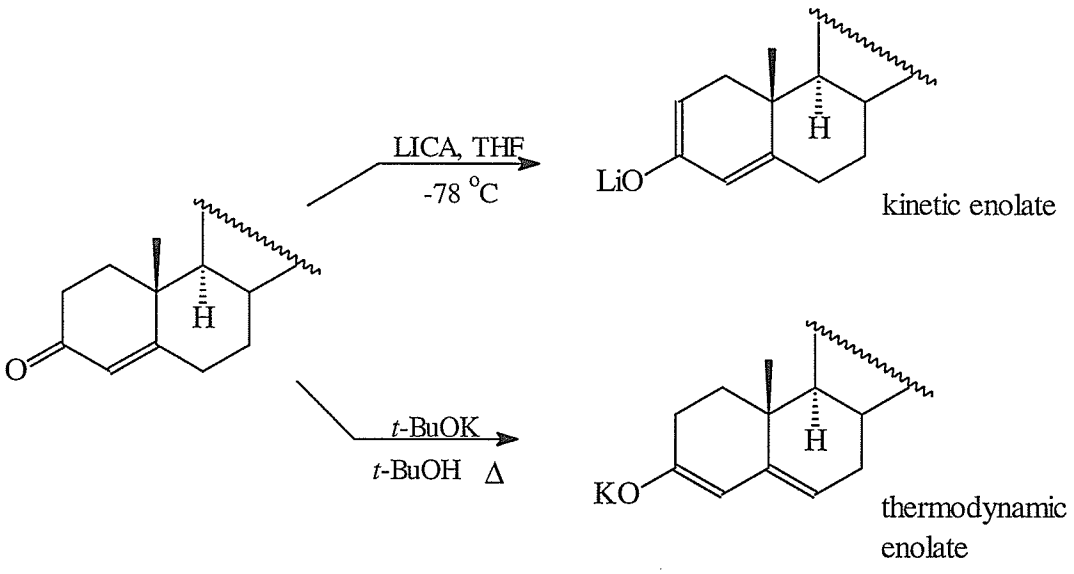

Dubois reported the first systematic investigation of the relationship between enolate geometry and the stereochemical outcome of reactions in 1967.[112] These studies suggested that the stereochemistry of the product could possibly be controlled by controlling the geometry of enolate formation. In the mid 1970's Ireland and Willard[113,114] reported that the *E*/*Z* stereochemistry of ester enolate formation was influenced by solvent polarity. Although they had no direct way of confirming the configuration of the enolates generated, they deduced them indirectly based on the stereochemistry of the products. Ireland proposed that the enolates were generated through chair like transition states. Two different reaction conditions, THF and THF-HMPA were used to demonstrate this hypothesis (Scheme 1.42).

In THF, the lithium cation coordinates to the carbonyl oxygen and the proton transfer takes place intramolecularly through the more stable transition state giving the *E* enolate. HMPA disrupts this by coordination/solvation of the lithium cation giving an open transition state instead. The more stable transition state in this instance leads to the

Z enolate being generated. Since this earlier research, the selectivity of enolate formation using various ketones/esters with different bases and solvents has become well documented.[111,115]

Scheme 1.42

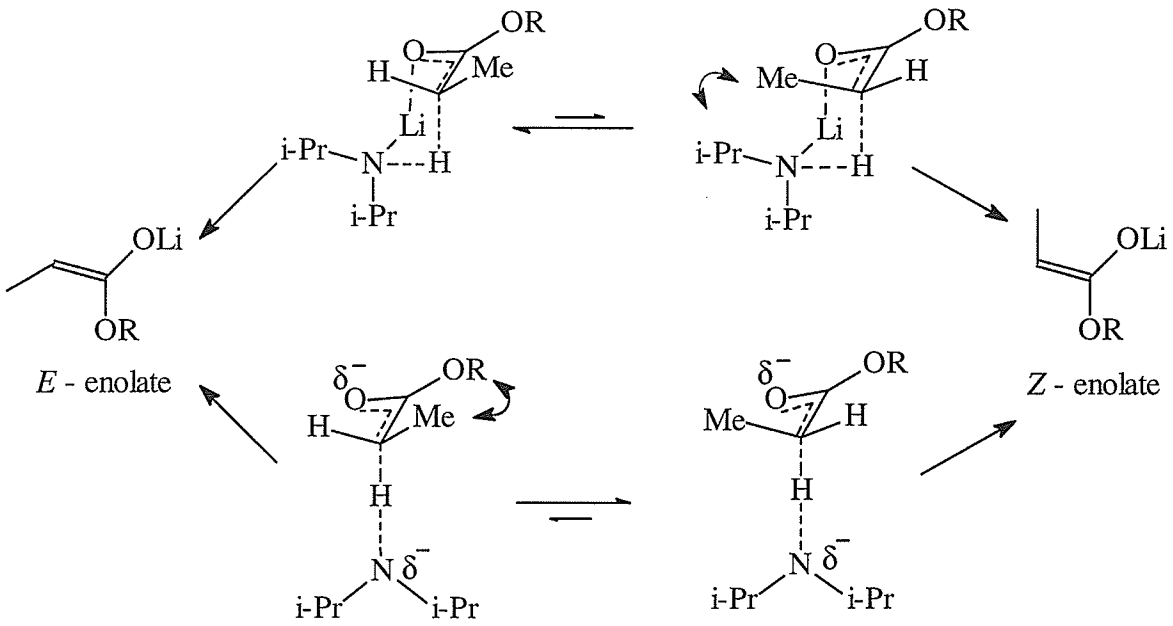

The stereochemical outcome of the aldol reaction using *Z* or *E* enolates has led to qualitative inferences about the transition state geometry that can be used to predict the likely products.[111,116] Simple diastereoselection may result in the preferential formation of either *syn* or *anti* products. The metal enolates are considered to react primarily through 6–membered pericyclic transition states that can adopt a chair (or boat) conformation, a proposal originally suggested by Zimmerman and Traxler (Scheme 1.43).[117-119] The metal enolate may in some cases be aggregated, but this does not seem

Scheme 1.43

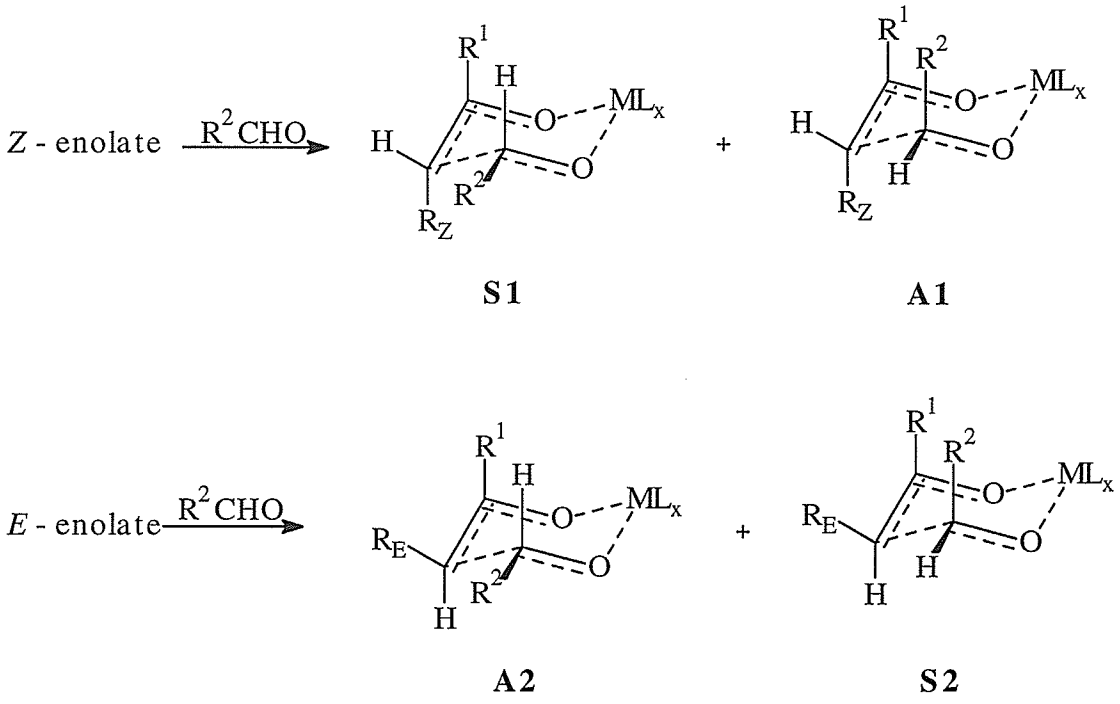

to effect the predicted outcome in most cases. The metal coordinates to the aldehyde and enforces a gauche relationship between the C=O of the aldehyde and the C=C of the enol. The preferred transition state will be the one which minimizes unfavorable steric interactions.

For either the *Z* or *E* enolate, with strongly coordinating metal ions (for example, Li, which has short M-O bonds) low stereoselectivity is observed when R^1 is small. This implies that the system shows no preference between **A** or **S** transition states. If R^1 is relatively large then high stereoselectivity will be observed for both enolates; *Z*-enolates will preferentially give *syn* transitions states **S1**, while *E*-enolates will give *anti* transition states **A2**.

The correlation between product stereochemistry and enolate geometry is often higher with *Z*-enolates. The rationale for this trend is not readily apparent using the

perfectly staggered chair models shown above. For the *Z*-enolate, the preferred transition state **S1** should have destabilizing interactions between R^2 and R_Z, which should reduce any preference between the two transition states. For the *E*-enolate, the R_E-R^2 interaction is gauche in both transition states so these effects could be expected to cancel and selectivity would be high.

Figure 1.21

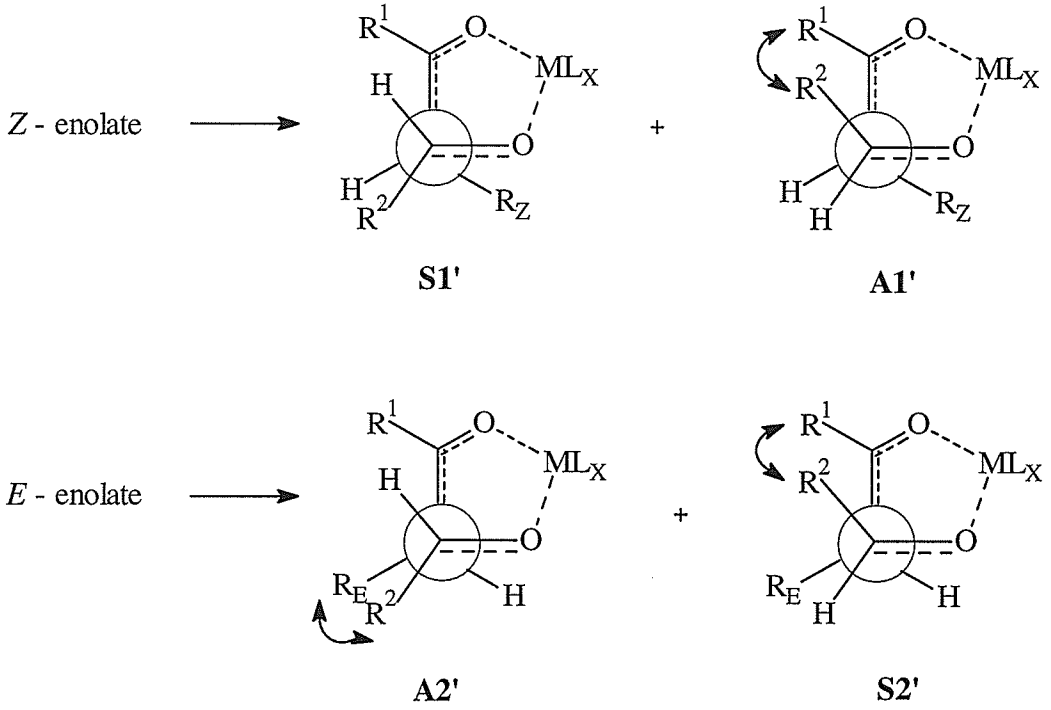

To account for the apparent discrepancy it has been proposed by such authors as Dubois and Heathcock[119-121] that the C=C to C=O torsion angle is closer to 90° (Figure 1.21). In this case, for the *Z*-enolate, R^2 remains far away from both alkyl substituents on the enolate in the preferred transition state **S1′** while the R^2–R^1 interaction remains significant in **A1′**. For the *E*-enolate, R^2 interactions remain significant in both transition states thus reducing the overall selectivity.

The choice of which pericyclic model is appropriate for a given reaction can be complicated, as some metal enolates (for example Sn, Ti, Zr) give the same *syn* products regardless of their stereochemistries. As an alternative to the above proposal of 90° torsion angles, Evans has suggested that boat transition states may become significant as R_Z or R_E become large and the O-M-O angle changes.[122] Nakamura and Kuwajima[123] have also proposed that a twist boat transition state for the *E*-titanium enolate is preferred, while for the *Z*-enolate, the chair transition state minimizes steric interactions.

An alternate approach to the classic aldol reaction is to pre-form the enolate and trap it as its silyl enol ether. The silyl enol ether can then be used in subsequent condensation reactions with an aldehyde in the presence of an activating agent. This method is referred to as a Mukaiyama reaction.[124] Contrary to the pericyclic arguments made above, the Mukaiyama reaction is considered to go through open transition states having either synclinal or antiperiplanar geometries, with no significant preference for either.[125] Unlike metal enolates where the pericyclic transition state imposes a *relative* stereochemical relationship on the developing chiral centers, the open transition states of the Mukaiyama reaction impose less stereochemical bias. Although there is no correlation of product stereochemistry to silyl enol ether geometry, there does persist in several instances a level of *syn* diastereoselectivity.[36]

The real power of carbonyl condensation reactions is displayed in stereoselective aldol additions. The use of chiral auxiliaries, chiral aldehydes and chiral ketones (or silyl enol ethers) has been extensively studied along with various metal enolates and Lewis acid activators.[41,56,59,118,119,126,127] Excellent enantio- and diastereoselectivities have been achieved in many of these situations by fine tuning of chiral substituents (R^1, R^2 and R_E

or R_Z in Scheme 1.43). For example Evans et al.[126] found that reaction of the boron enolate of compound **105** with isobutyraldehyde gave essentially one product (**106**) with 99.4% de (Scheme 1.44). Removal of the product from the chiral auxiliary resulted in a diastereoselective, and an overall enantioselective, synthesis.

Scheme 1.44

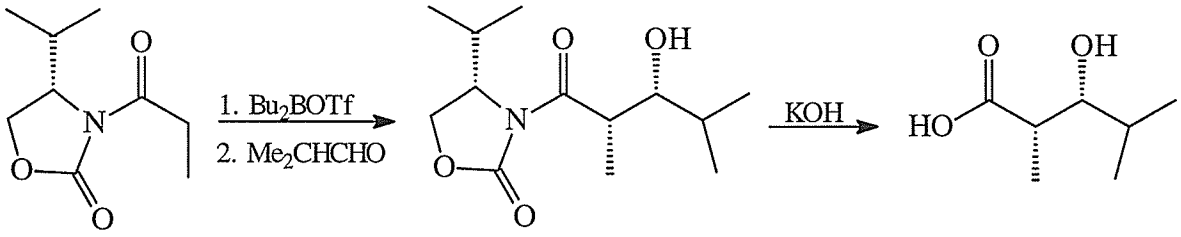

105 **106**

In the imine-aldol or Mannich like reactions, the substituent on the nitrogen imposes other steric constraints not found in the reaction of aldehydes by restricting the manner in which metals or Lewis acids can coordinate to the nitrogen. In the transition state, the imine prefers to lie with its substituents placed in axial positions allowing for formation of a pericyclic transition state, as in the aldol reaction. If the imine is considered to be in its more stable *E* geometry, reaction with a *Z* enolate through a chair transition state leads to the *anti* product (in contrast to *Z* enolates with aldehydes giving *syn* products). *Syn* products are formed through the boat transition states (Figure 1.22). With *E* enolates, it is the chair transition state that leads to *syn* products and the boat that gives the *anti* products. As with the classic aldol reaction, the chair transition states are again considered to be preferred.

Figure 1.22

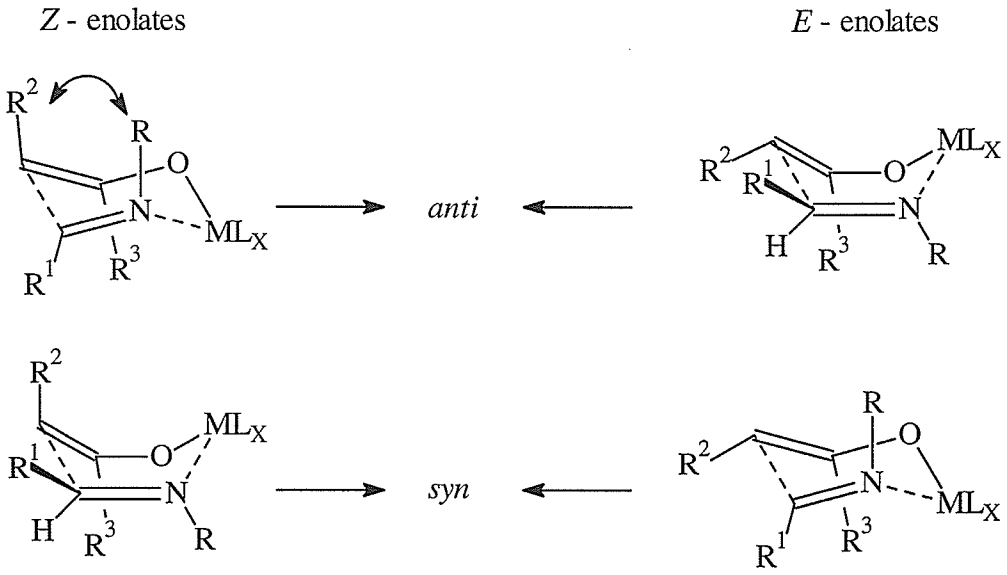

The simple stereoselection of lithium *ester* enolate-imine reactions has been extensively investigated, as this is a simple route for the synthesis of β-lactams, an important class of antibiotics.[128] In these instances, *E*-enolates give *cis* β-lactams with high diastereoselectivity but *Z*-enolates show little diastereoselectivity. These results are consistent with Evans' postulate of 6–membered cyclic transition states as shown above. The lack of selectivity with *Z*-enolates is attributed to the extra steric influence of the *N*-substituent. Unfortunately the diastereoselection of these reactions as a function of imine geometry has not been systematically studied. Fewer studies have also been done using ketone enolates. The possibility of *E* → *Z* isomerization of the imine has been postulated as a reason for changes in *syn/anti* diastereoselection, however this hypothesis has not been absolutely proven. The barrier to isomerization is considered by some to be too high.[129,130]

Several diastereoselective Mannich reactions have been reported over the years,[131-133] but until recently less work had been done on enantioselective reactions. In 1991 Corey et al.[129] reported the first example using a chiral boron ester enolate (Scheme 1.45a). In 1994 Yamamoto[134] reported an enantioselective reaction of a ketene silyl acetal using Lewis acid activation (1.45b). Both of these methods required stoichiometric amounts of a chiral component. In 1997, Kobayashi using a zirconium-BINAP catalyst[135] reported the first catalytic enantioselective Mannich reaction.

Scheme 1.45

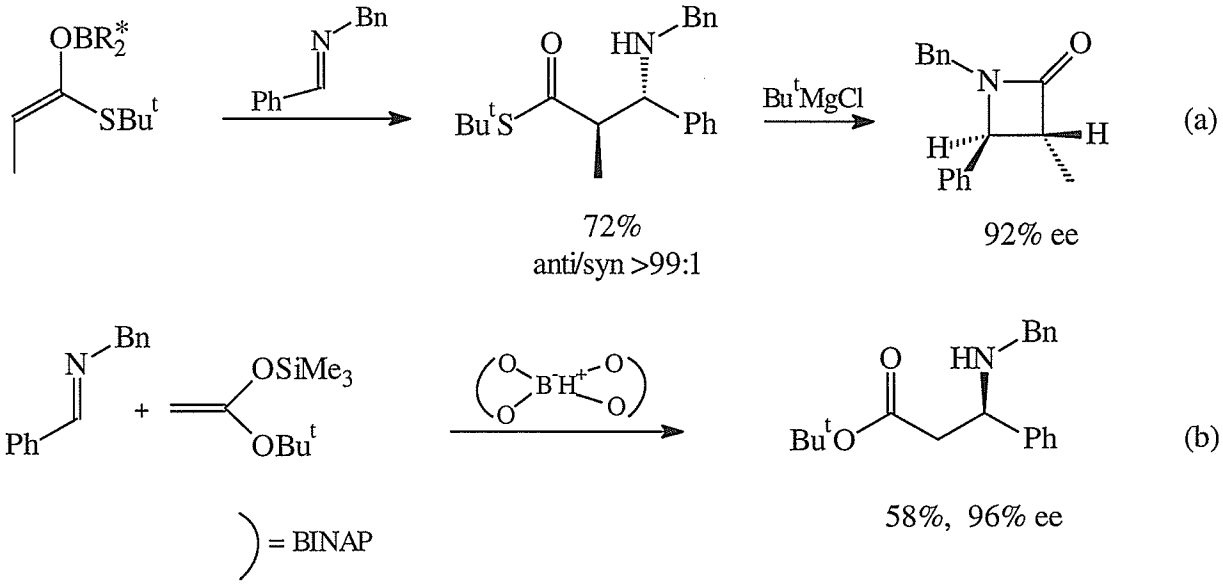

All of the diastereo- and enantioselective reactions mentioned above involved an ester-derived enolate. The imine-aldol reactions have been extensively studied with ester, amide or thioester partners. Reactions involving ketones, until recently, have been much less documented and they have still not been systematically studied.[106,128,136]

Thesis Objectives

1) To synthesize and study the reactions of a glucose based chiral glycine as a method of synthesizing amino acids.

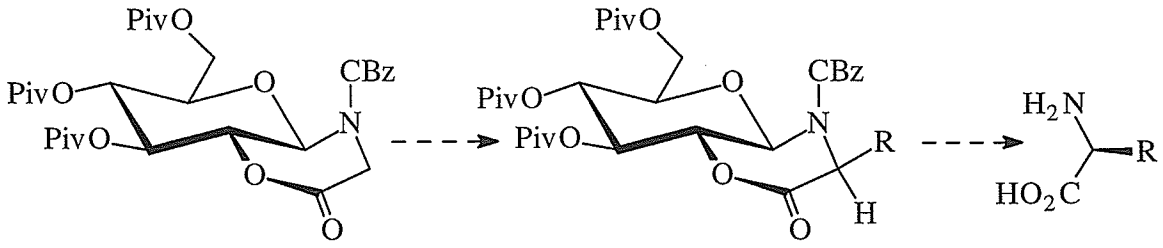

One of the classic approaches to the synthesis of novel amino acids is the 'chiral glycine' method. As mentioned earlier, cyclic chiral auxiliary based systems have typically given excellent diastereoselectivities. A rigid *bicyclic* system based on a glucose auxiliary would be expected to induce high diastereofacial bias in reactions of the enolate (or its equivalent) with electrophiles. Earlier research in our lab[137] established that a bicyclic oxazinone template could be prepared between glycine and glucose. These compounds showed excellent diastereoselectivities with good electrophiles, but the starting template degraded readily under the reaction conditions. Removal of the auxiliary from the amino acid product required harsh conditions.

In order to try and improve upon this earlier model, a new chiral template, employing different protecting groups on the sugar hydroxyls, is to be prepared and studied. Once this new chiral template is synthesized, its behavior towards various bases, electrophiles and cleavage conditions will be studied.

2) To develop a glucose based imine as a means of synthesizing γ-oxo-α-amino acids via a Mannich or aldol-like reaction.

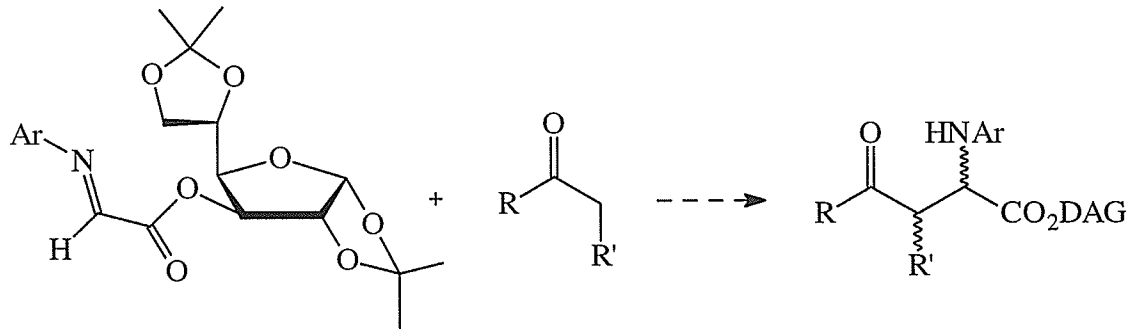

A second project using carbohydrate auxiliaries to synthesis α-amino acids focuses on the γ-oxo series of compounds. One of the most direct methods to synthesis γ-oxo-α-amino acids is by an aldol (or Mannich) like reaction between a glyoxylimine and a ketone. The approach to be undertaken, an asymmetric reaction of an imine with a ketone, is one method which is only now becoming more explored.

The first task will be to prepare a chiral glyoxylimine using diacetone D-glucose as the auxiliary. Once the chiral glyoxylimine is prepared, the reactivity and selectivity of the system will be explored using various reaction conditions and ketone partners. In order to test the simple diastereoselection of these reactions, as well as the viability of this experimental approach, an achiral model glyoxylimine will also be prepared. Conclusions drawn from the achiral experiments will be used as a starting point for the chiral auxiliary based reactions. Finally, removal of the amino acid products and their characterization will be undertaken.

Chapter 2

Results and Discussion

This chapter will be divided into two main sections. The first section discusses the synthesis and reactions of the glucose based bicyclic oxazinone, including cleavage of the amino acid from the auxiliary. The second and larger section will cover the development of a chiral glyoxylimine. This latter section is introduced with a discussion of a model study using an achiral glyoxylimine in the imine-aldol reaction. Finally, attempts to isolate the free γ-oxo-α-amino acids, and to characterize the compounds are addressed.

2.1 Oxazinone

One approach to the synthesis of α-amino acids is through the 'chiral glycine' method. Derivatization of glycine at the α position using nucleophilic or electrophilic glycine synthons leads to the synthesis of more complex α-amino acids. If the glycine residue is attached to a chiral auxiliary then the synthesis may be asymmetric. As discussed earlier (section 1.2), carbohydrates have been successfully used in the asymmetric synthesis of amino acids through such methods as the Ugi and Strecker syntheses.

In this study a bicyclic compound based on glucose and glycine was prepared. The formation of a fused ring system restricts the movement of the glycine fragment resulting in high diastereofacial discrimination.

2.1.1 Synthesis of the oxazinone

The synthesis of the glucose-derived oxazinone is shown in Scheme 2.1. Crystalline *N*-β-D-glucosylglycine ethyl ester **107** was prepared by a fellow student using a literature procedure.[138] Treatment with CBzCl and Hunigs' base in DMF gave the *N*-protected adduct **108** in 82% yield after column chromatography. The ester was cleaved using NaOH in EtOH and the product was isolated as its sodium salt, which was used without further purification. Suspension of the salt in pyridine followed by the addition of a catalytic amount of DMAP and an excess of pivaloyl chloride (PivCl) resulted in oxazinone formation and protection of the other hydroxyl groups in one step. Product **109** was isolated in 83% yield after chromatography. The product could be further purified by crystallization from MeOH (70%).

In the reaction with pivaloyl chloride it was found, by TLC monitoring, that the starting material was consumed rapidly and an intermediate compound formed. It appeared that cyclization had occurred rapidly followed by only di-pivaloylation of the remaining three hydroxyl groups. The third Piv group required prolonged reaction time (5 days) using ten equivalents of PivCl. Heating the mixture to 40 °C allowed completion of the reaction within 24 h. However even at the higher reaction temperature, reducing the amount of excess PivCl resulted in increased amounts of the di-pivaloyl products being isolated.

Scheme 2.1

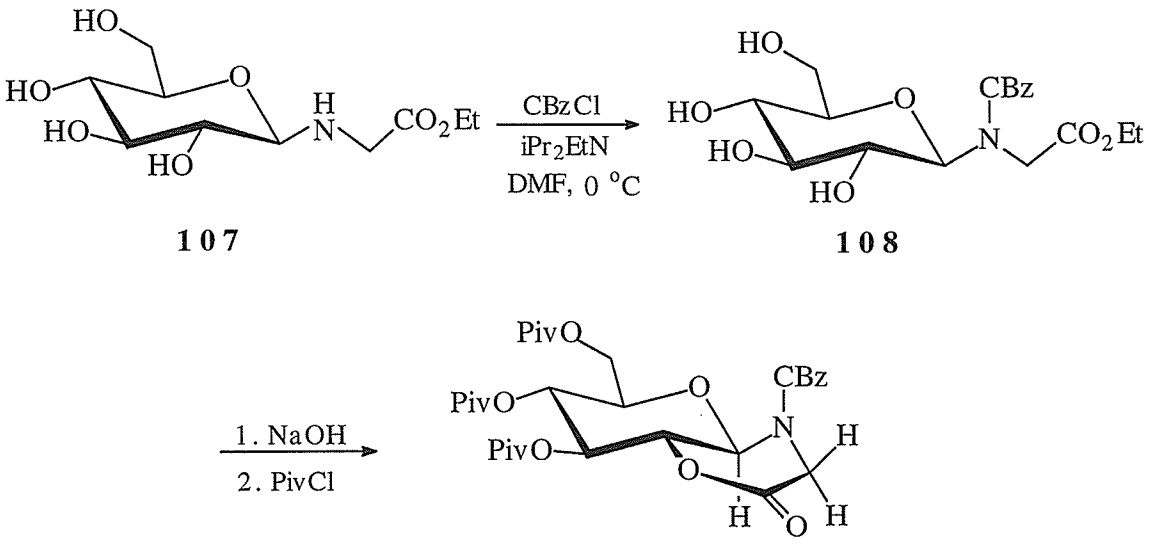

107 **108**

109

The conformation of the fused ring system was determined using nuclear Overhauser effect (nOe) analysis. Strong nOe was found between the anomeric proton and the 3 and 5 positions of the sugar ring (14% and 15% enhancements respectively) consistent with the expected chair conformation. Strong nOe between the pro-*S* hydrogen of the glycine moiety (top face of adduct as drawn) to the H-2 of the glucose ring (17%) was observed. No nOe was observed between the pro-*R* hydrogen and the anomeric proton. This indicated that the oxazinone ring was in a boat conformation, with the pro-*S* hydrogen of the glycine fragment lying in a flagpole position (Figure 2.1).

Figure 2.1

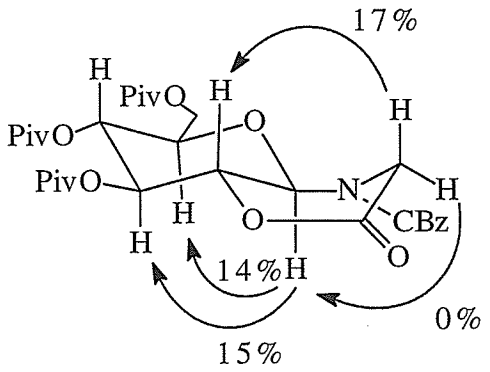

2.1.2 Reactions of the chiral oxazinone

Various alkylation reactions were performed using oxazinone **109**. Initial studies were carried out using methyl iodide (MeI) as the simplest alkylating agent. Earlier work, using a similar template, had led to the conclusion that a 10-fold excess of MeI gave the best results.[137] The results of the methylation reactions using template **109** are summarized in Table 2.1.

The reaction did not occur to any substantial degree unless the lithium salt of hexamethyldisilazide (HMDS) was used. In other instances such as with the less reactive NaHMDS, only starting material was recovered (91%). With the more reactive salt KHMDS, extensive degradation was observed along with the recovery of some starting material. In the absence of any additives such as HMPA little reaction was observed.

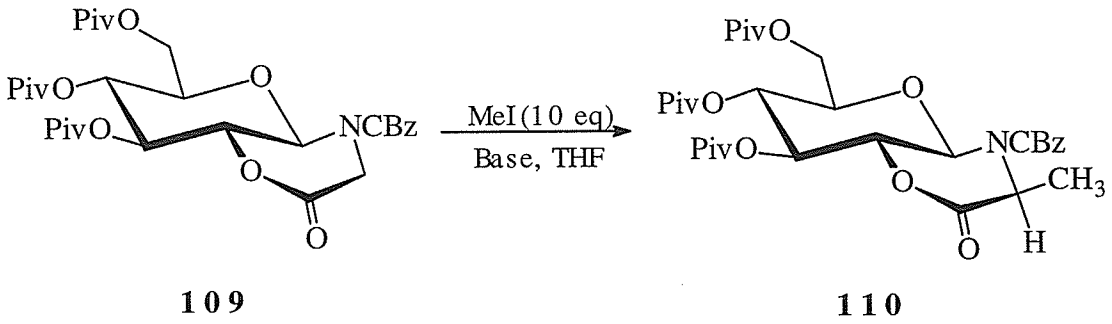

109 **110**

Table 2.1: Alkylation reactions of template **109** with MeI.

Base (eq)	**'Additives'**	**Time**	**Temp**	**Yield**[a]	**Recovered 109**
LiHMDS (1.1)	HMPA (10%)	2.5 h	– 100 °C	57%	7%
LiHMDS (1.2)	HMPA (10%)	20 min	– 100 °C	45%	trace
LiHMDS (1.1)	HMPA (20%)	30 min	– 78 °C	52%	10%
LiHMDS (1.2)	none	1 h	– 78 °C	trace	considerable
LiHMDS (1.2)	TMEDA (1.1)	1 h	– 78 °C	(60)[a]	(40)[b]
LiHMDS (1.2)	DME (solvent)	1 h	– 78 °C	25%	10%
NaHMDS (2)	HMPA (10%)	2.5 h	– 78 °C	trace	91%
KHMDS (1.2)	HMPA (10%)	1 h	– 78 °C	trace	considerable

[a]Yields reflect recovered **109**. [b]Estimated by ^{1}H NMR-the crude material was used to prepare the dimethyl compound **111**.

Additives such as HMPA have been used extensively when aggregation of the lithium enolates is suspected.[139,140] The best conditions were determined to be generation of the enolate at –100 °C using LiHMDS in THF containing 10% by volume of HMPA. The mono-methylated product was isolated in ~57% yield, based on recovered oxazinone.

The same reaction carried out at –78 °C gave a slightly lower yield. Use of TMEDA as an additive was also beneficial, while changing the solvent to DME gave lower yields.

No evidence of dimethylated compound (**111**) was seen in any of these reactions. This was confirmed by the preparation of compound **111**. This was achieved by re-subjecting the crude mixture of starting oxazinone **109** and mono-methyl product **110** to the same methylating reaction conditions. Comparison of the ^{1}H NMR spectra of the isolated products, and the reaction TLC, to those taken before the second methylation experiment clearly showed that dimethylated compound **111** had not been formed in the initial reaction.

Further alkylation reactions were then performed using allyl and ethyl bromide (Table 2.2). With allyl bromide, no reaction occurred when NaHMDS or KHMDS were used alone as the base. Using LiHMDS and HMPA at –78 °C, mono (**112**) and di-substituted (**113**) products (45%) were isolated, along with a small amount of recovered **109**. Only one mono-alkylated product was observed in the crude ^{1}H NMR spectra indicating that the diastereoselectivity exceeded the limits of NMR detection ($\geq$98% de).[141] No product was observed using LiHMDS/HMPA and the less reactive compound ethyl bromide at –78 °C, and decomposition of the enolate occurred if the reaction temperature was raised.

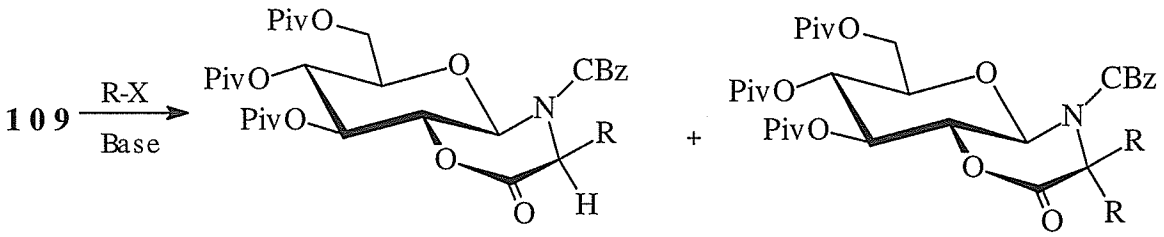

112, R = CH_2CHCH_2 **113,** R = CH_2CHCH_2

114, R = CH_3CH_2 **115,** R = CH_3CH_2

Table 2.2: Reactions of **109** using other electrophiles.

R – Br	Base	Additive (10%)	Combined Yield[a]	Products	Mono : Di ratio	Mono de[b]
allyl-	Na/KHMDS	HMPA	–	–	–	–
allyl-	LiHMDS (1.5)	HMPA	45%	**112 + 113**	1 : 1.1	>98%
allyl-	P4	none	70%	**112 + 113**	1 : 3.2	>98%
Et-	LiHMDS (1.2)	HMPA	–	–	–	–
Et-	P4	none	70%	**114 + 115**	2.2 : 1	>98%

[a]Yields reflect recovered **109**. [b]As determined by ^{1}H NMR

The phosphazene base 't-butyl P4' developed by Schwesinger,[142] was tried in both the allylation and ethylation reactions. The Pn base P4 is known to be of comparable basicity to KHMDS (p*K*a ~ 28 in THF) but it is less nucleophilic. The P4 base is a large molecule, which forms an extremely bulky cationic species after protonation (Figure 2.2). The $P4H^+$ system is able to delocalize the charge over each of the nitrogen and phosphorus atoms (17 resonance structures), giving a soft cation. The size and softness of the cation serves to keep it further away from the harder enolate partner, thus generating a 'naked enolate'.

Figure 2.2

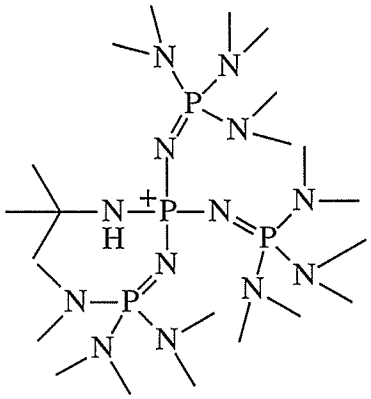

The P4 base cannot be used for methylations with MeI as the base itself is methylated with this reagent.[140] In reactions of **109** with allyl bromide using the P4 base, an improvement in the overall yield of the reaction was observed, increasing from 45% to 70%. Compound **113** accounted for most of the product isolated. With ethyl bromide the yield went from essentially zero at –78 °C to 70% at –100 °C. Compounds **114** and **115** along with recovered oxazinone **109** (8%) were isolated.

The observation that little alkylation occurred in the absence of additives such as HMPA and the positive effect of using the P4 base, which does not aggregate, suggested that the lithium enolates formed in these reactions were indeed aggregated. The presence of lithium aggregates in enolate solutions and the effects of additives on them have been studied primarily with the base LDA.[139,143,144] Seebach[145,146] has shown using X-ray structures and NMR analysis that the lithium is coordinated to the enolate oxygen and solvent molecules in a cube-like structure (Figure 2.3). This aggregate is assumed to remain in the solution state. Generally aggregation does not stop the reaction from taking place nor does it appear to alter the applicability of monomeric transition state models to describe the stereochemical outcome of such reactions. It may be postulated that it is the

presence of the sugar that lowers the reactivity of the aggregated enolate in this case. The other oxygens on the sugar moiety can participate in, and possibly stabilize this aggregate. It was observed that in the absence of HMPA, the aggregated enolate was stable towards degradation for prolonged periods (20 min). After addition of HMPA (or if HMPA was already present prior to enolate formation) degradation of the enolate became more evident. Addition of compounds such as HMPA opens up these tight aggregates by coordinating to the lithium and promoting the formation of open dimers, which are more accessible to an electrophile.

Figure 2.3

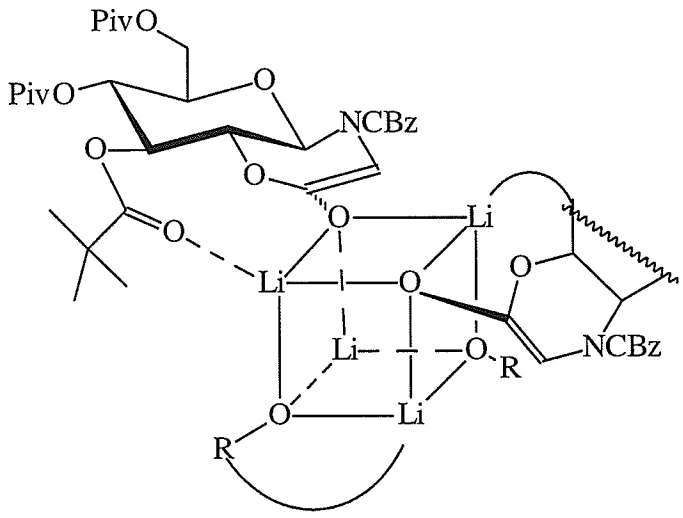

The enolate could be trapped as its silyl enol ether **116** using TBDMSCl (1.2 equiv) and LiHMDS at –78 °C (Scheme 2.2). In the absence of HMPA, no reaction was observed to occur. After addition of HMPA, **116** could be isolated in essentially quantitative yield. A ^{1}H NMR spectrum showed only a small amount of impurity due to the excess TBDMSCl added in the reaction. The compound **116** was used in subsequent

aldol reactions without further purification. These results suggested that the enolate could be generated quantitatively but the reactive center was inaccessible in the absence of co-solvents such as HMPA. This supported the hypothesis of an aggregated lithium enolate.

Scheme 2.2

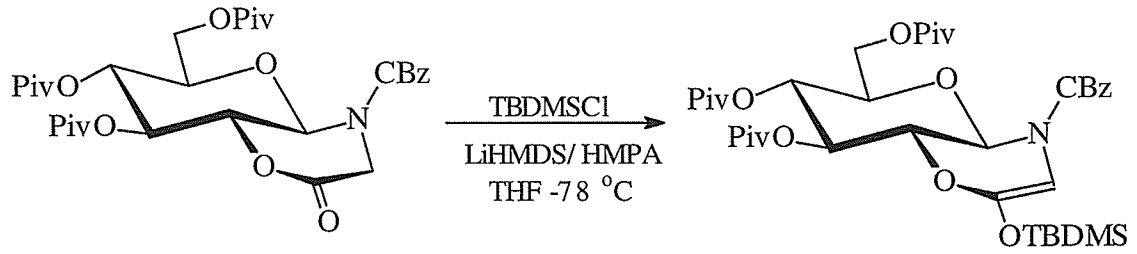

109 **116**

However even in the presence of HMPA, the yields were not as high as expected. The essentially quantitative recovery of the trapped silyl enolate under similar reaction conditions confirmed the enolate could be generated completely. The low alkylation yields may instead be a result of instability of the enolate in the sugar based oxazinone system. It is possible that a ketene elimination pathway could be occurring at a rate that can compete with allylation and which is faster then ethylation (Scheme 2.3). Kunz has shown that ketene eliminations can be facile with some sugar derived lithium ester enolates.[57] The presence of other oxygens on the sugar promotes strong intramolecular coordination of the lithium ion. The sugar then becomes a good leaving group, and degradation of the enolate can occur.

Scheme 2.3

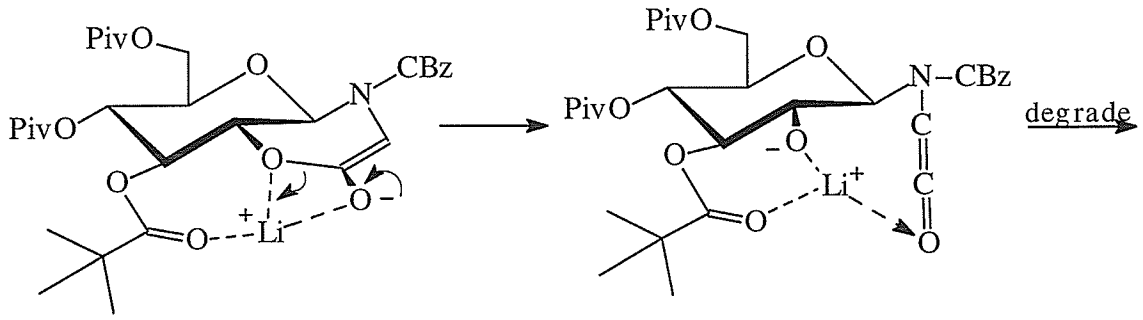

The improved yields using the non-aggregating P4 base also supports the theory of a tight lithium aggregate. With the P4 base, the so-called 'naked enolate' generated is more reactive and the reaction can be done at lower temperatures. With this base, at the lower temperature, the rates of both allylation and ethylation become more competitive with enolate degradation.

Dialkylation was also observed during the ethylation and allylation reactions. A possible explanation for this is the 'internal proton return' or 'conducted tour' phenomenon.[147,148] After enolate formation with a lithium amide base, the amine remains in close contact (coordination) with the lithium ion. The amine can shield the enolate from reaction or it can act as a proton donor. Within the close contact of a still somewhat aggregated or dimer type system, intra-aggregate proton transfer can occur (Figure 2.4). A neighboring enolate can remove the proton from a closely associated amine, which in turn can abstract a proton from a molecule that has already been alkylated. This internal transfer process can be much faster then alkylation. With less reactive electrophiles, this type of transfer is more apparent and dialkylation is observed to occur. It is possible that the individual molecules that undergo dialkylation are more accessible to the electrophile and lie at the outer edges of any aggregates. The diastereomeric monoalkylated isomers

of the products were never observed however. This suggests that the second alkylation occurs quickly. Seebach[148] has shown that when these enolate systems are quenched the proton delivered to the enolate is one associated on a nearby amine. Therefore the proton would be delivered to the same side from which it was removed so no stereochemical scrambling occurs.

Figure 2.4

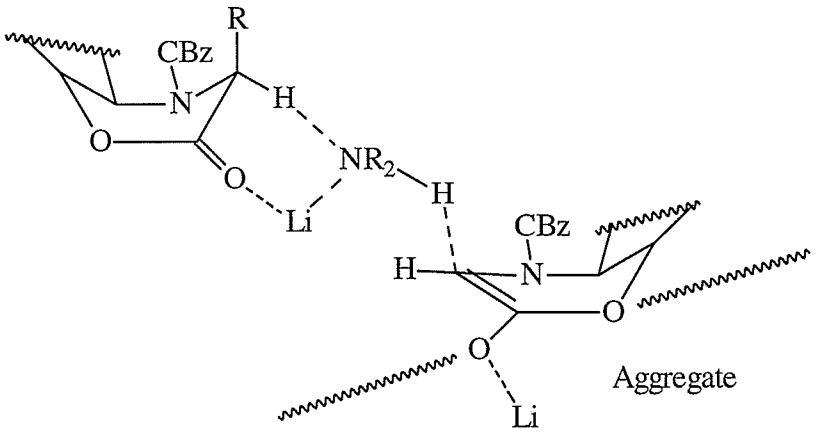

Aldol reactions of **109** with benzaldehyde were attempted under standard aldol reaction conditions by generation of the enolate *in situ* (Table 2.3, path a). Alternatively the trapped silyl enolate **116** was activated with a Lewis acid under Mukaiyama conditions (path b).

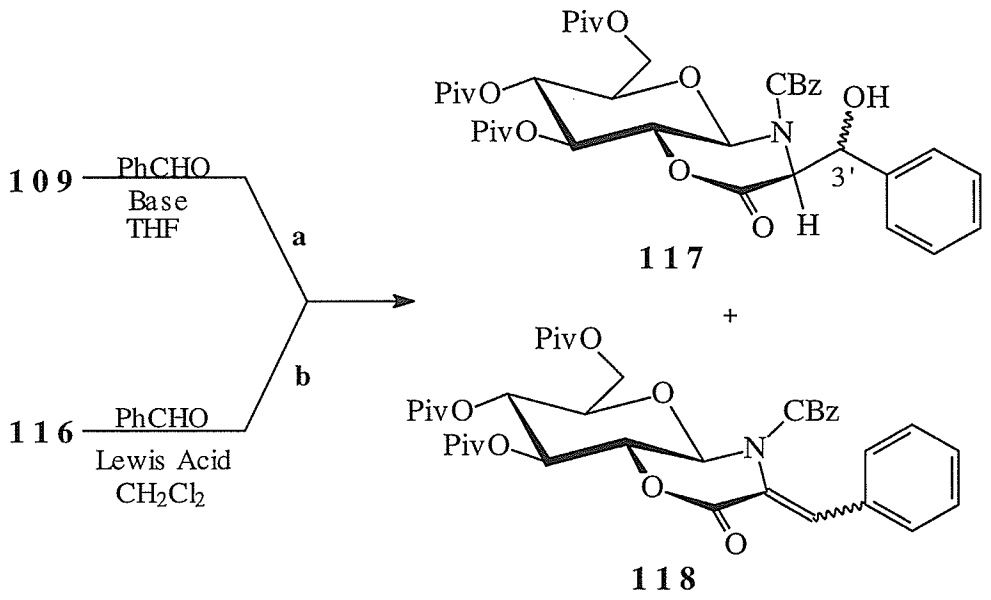

Table 2.3: Aldol reactions using template **109** or its trapped enolate **116**

Path	Base or Lewis Acid	Time	Temp (°C)	Recovered **109**	Yield **117**[a]	de of **117**
a	LiHMDS/HMPA	1 h	–78	18%	68%	34%
a	Et_3N/Bu_2BOTf	4 h	–78 → 0	considerable	–	–
b	TMSOTf	1 h	–78	43%	49%	75%
b	$Yb(OTf)_3$	30 min	25	13%	60%	N/D
b	$TiCl_4$	30 min	–78	–	trace	–

[a] Yield based on recovered oxazinone.

Generation of the enolate using LiHMDS and reaction with benzaldehyde (5 equivalents) gave **117** as a mixture of two diastereomers (de, 34%) at C-3′. Attempts to generate the dibutylboryl enolate using Et_3N/Bu_2BOTf failed, and only starting material and unidentified degradation products were observed. Using Mukaiyama conditions,

reaction of **116** with a catalytic amount of TMSOTf (10 mol%) gave a 49% yield of **117** having a 75% de. The major isomer was the same for both methods. Use of catalytic $Yb(OTf)_3$ (10 mol%) gave only 13% of **117** (undetermined de). A substantial amount of oxazinone **109** was recovered, accounting for most of the starting material (60%). When $TiCl_4$ was used to activate **116**, very little product was observed. A yellow precipitate developed on the addition of $TiCl_4$ to benzaldehyde, which did not disappear on addition of the silyl enol ether. We later learned that this insoluble $TiCl_4$-benzaldehyde complex can interfere in Mukaiyama aldol reactions, resulting in variable yields. In some cases this problem may be avoided by changing the order of reagent addition.[149]

The stereochemistry of the major monoalkylated products **110**, **112**, **114** and **117** was the same in each instance. Attack of the electrophile occurred to the pro-*S* face of the enolate. This may be understood by looking at the preferred conformation of the oxazinone ring. As stated earlier, the oxazinone ring exists in a boat conformation with the pro-*S* hydrogen lying in a flagpole position. After generation of the enolate, the electrophile may approach from either face as shown in Figure 2.5. The preferred direction of approach can be influenced by steric or stereoelectronic factors (or both). There appears to be little difference between the faces of the enolate from a steric point of view. Earlier work by another student (AM1 *semi empirical* or 6-31G* *ab initio* calculations) suggested that the *N*-CBz and the sugar substituents were not oriented in such a way as to offer much steric hindrance to either face.[137] Calculations carried out as a part of this thesis suggested that a stable *chair* conformer was not even a local minimum for these systems. The stereoselectivity observed in the present work may be explained by stereoelectronic arguments. The electrophile is expected to prefer an axial approach to

the 6-member cyclic enolate.[150] The electrophile then has two options. It can approach from the bottom face through a chair transition state or from the top face through a boat transition state (Figure 2.6). If the chair conformer is unstable as indicated in the earlier work, then it could also be expected that the chair transition state would also be destabilized relative to the boat transition state. Attack of the electrophile would then preferentially occur to the top or pro-*S* face of the molecule as observed.

Figure 2.5

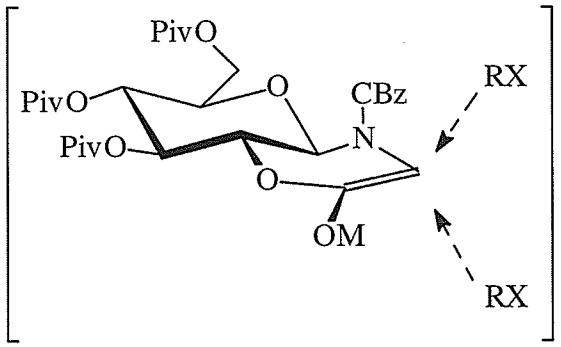

Figure 2.6

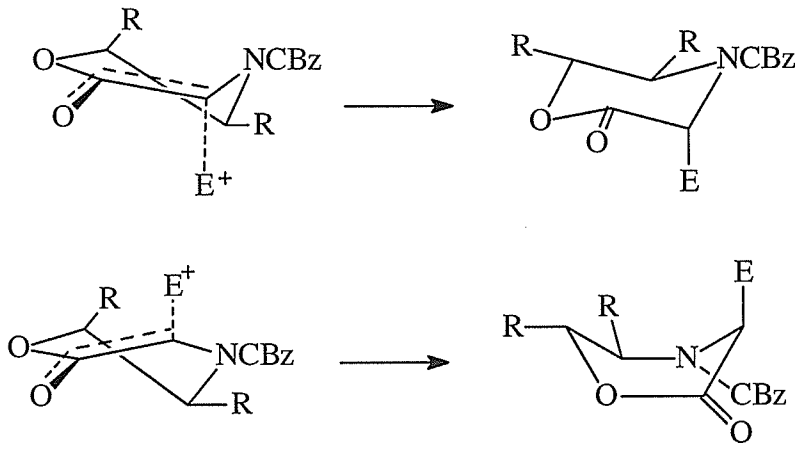

The nOe results for each of the mono-alkylated products confirmed that alkylation occurred to the top face in each instance (Figure 2.7). In each product, nOe between various protons on the sugar (C, D, E) showed that the chair conformation of the pyranose ring was retained. Little or no nOe (B) was observed between the anomeric proton and the pro-*R* hydrogen on the lower face of the molecule. Strong nOe (A) was always observed (17 – 20%) between the H-2 position of the glucose and the protons on the alkyl substituent.

Figure 2.7

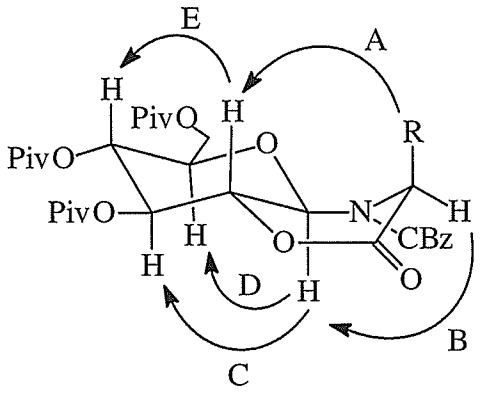

R	A	B	C	D	E
H	17%	0	14%	15%	–
Me	18%	0	17%	16%	11%
allyl	20%	–	–	–	13%
Et	19%	–	14%	15%	11%

The same preference held true for the aldol reaction with benzaldehyde. The facial selectivity with respect to the oxazinone moiety remained high (>98%), but there was less facial control with respect to the aldehyde partner. Under Mukaiyama reaction conditions, two aldol products (75% de) were isolated in ≤60% yield. Although the yield was slightly higher (68%) when the enolate was generated *in situ*, there was very little aldehyde diastereofacial selectivity in this case (34% de). In both cases the preference was for the same diastereomer, however the configuration at C-3′ carbinol carbon was not determined.

The results of methylation of the oxazinone **109** were then compared to an uncyclized analog of **109**, to explore the selectivity obtained using a more mobile system. The uncyclized analog **119** was prepared by treating ethyl ester compound **108** directly with PivCl (without prior ester cleavage) to give adduct **119** (Scheme 2.4). Compound **119** was then treated with 10 equivalents of MeI in the presence of LiHMDS and HMPA following a protocol similar to the oxazinone reactions. Unlike the oxazinone, the enolate obtained from **119** appeared to be less reactive at –78 °C. The reaction was allowed to warm slowly and the amount of HMPA and MeI was increased over a 2.5 h period. The reaction gave two products, **120**, and what appeared to be its diastereomer (35% de) by ^{1}H NMR spectra, in 62% yield after chromatography.

Scheme 2.4

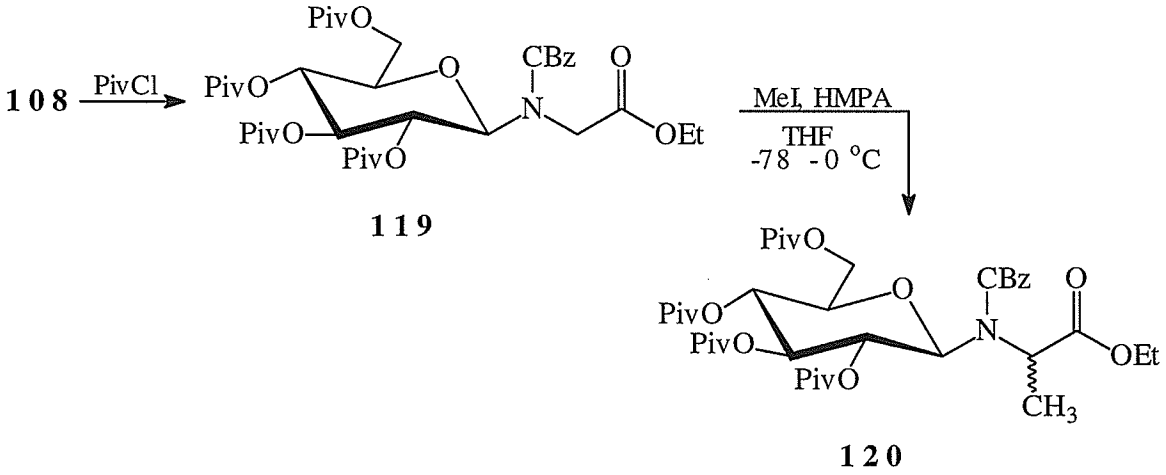

However only the major material **120** was isolated in sufficient quantity to obtain complete analytical data. The stereochemistry at the new center was not determined. The minor material, although it could not be completely separated from the major and starting

materials, had similar characteristic by ^{1}H NMR consistent with its being a diastereomer of **120**.

The selectivity obtained in alkylation reactions of the rigid oxazinone system **109** can be contrasted to that of similar reactions of the open analog **119** using MeI as the electrophile. Reaction of **119** gave only an apparent ~33% diastereoselectivity, indicating that for this model increasing the mobility of the glycine moiety reduces the overall facial discrimination. By cyclizing the glycine residue and making a rigid bicyclic system, the two faces become distinct and higher diastereofacial selectivity results. As shown, methylation of oxazinone **109** gave essentially one compound. These results confirm our hypothesis that a rigid bicyclic chiral glycine would afford superior selectivity to a flexible acyclic chiral glycine.

The final step in the preparation of the free amino acid involved deprotection and cleavage from the auxiliary. It was found that removal of the amino acid was best achieved by first cleaving the *N*-CBz protection group, as the unprotected glycosylamines are labile under mildly acidic conditions.[151] The *N*-CBz group was first removed using H_2 in the presence of a catalytic amount of Pd/C (10 mol%) in MeOH. The reaction was completed in 5 – 10 min at room temperature. Filtration of the solution through Celite followed by dilution with an equal volume of 1 M HCl/MeOH readily cleaved the lactone and glycosidic linkages (Scheme 2.5). The sugar was isolated in essentially quantitative yields as a mixture of anomers. *L*-Alanine was isolated in 95% yield as a mixture of the carboxylic acid and methyl ester (2:1). Left for a prolonged period in the presence of aqueous HCl, the ester was gradually cleaved to give *L*-alanine $[\alpha]_D = +9.3$ (*c* 0.30 6 N HCl) (literature $[\alpha]_D = +13.7$ (*c* 2, 6 N HCl)).[152]

Scheme 2.5

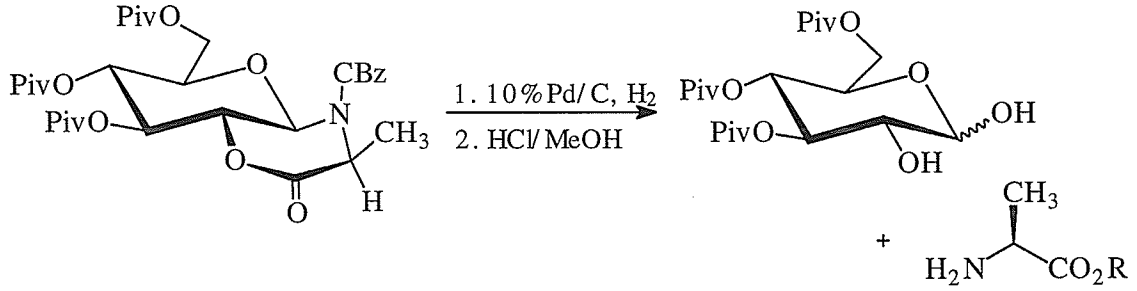

2.2 Glyoxylimines in the synthesis of γ-oxo-α-amino acids.

The γ-oxo and related γ-hydroxy amino acids are an interesting class of naturally occurring compounds that has drawn increased attention in recent years. However, the presence of the oxo substituent also makes them a synthetic challenge. There are, as discussed earlier, various approaches to the synthesis of these compounds, either as racemic mixtures[93,95] or as pure enantiomers.[6,8] A closer look at the functional pattern of these compounds shows a similarity with that of the products derived from the aldol reaction (Figure 2.8).

Figure 2.8

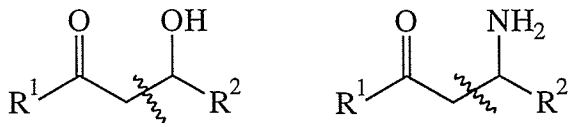

In the classic aldol reaction, the carbonyl-containing fragment comes from a ketone while the alcohol fragment comes from an aldehyde. If an imine (aldimine) is used instead of the aldehyde, the expected product is an amine. An aldol-like reaction

using a glyoxylimine (i.e. $R^2 = CO_2R'$) and a ketone would therefore give the desired γ-oxo-α-amino acids in one step. The extra steric influence of substituents on the imine nitrogen, which is not present with aldehydes, might also be expected to play a role in diastereoselection, as it restricts the manner in which a Lewis acid or a metal can coordinate. The stereoelectronic nature of the *N*-substituent also has an effect on the reaction. *N*-oxidation, *N*-acylation, and *N*-sulfonation all increase the electrophilicity of the α-carbon.[106] However, the ease of removal of these substituents after the reaction, must also be taken into consideration, and this is not always easy. For example the removal of the *N*-*p*-toluenesulfonyl group typically requires strongly acidic conditions such as 30% HBr/acetic acid[85] which could harm other acid sensitive groups in the molecule. A common *N*-substituent used in the synthesis of β-lactams is the *p*-methoxyphenyl group that can be removed using a metal oxidant. These conditions are relatively mild and suitable for our purposes. For this study, three glyoxylimines were prepared and their reactions studied. These imines were used in both Mukaiyama aldol reactions (Section 2.2.2) and enolate based reactions (Section 2.2.3). Various attempts were made to cleave the protecting and auxiliary groups from the resulting products in order to release the free amino acids. Several approaches were also undertaken to determine the absolute configurations of the products. These are discussed in Section 2.2.4.

2.2.1 Synthesis of the glyoxylimines and silyl enols.

Three glyoxylimines were prepared for study in the aldol reactions. The first glyoxylimine was the achiral methyl glyoxylimine **121** used to explore simple *syn/anti* diastereoselection (Scheme 2.6).

Scheme 2.6

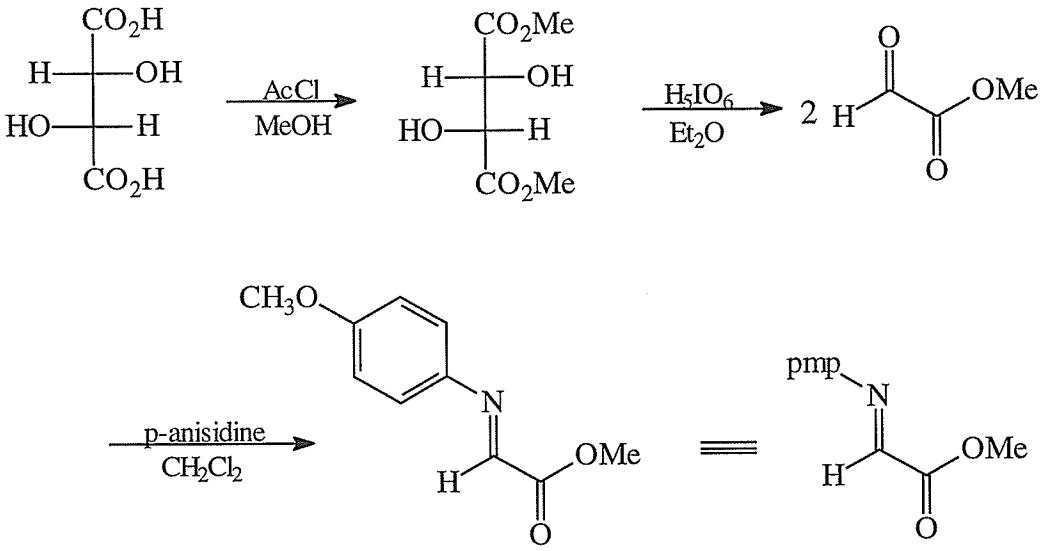

121

Dimethyl *d*-tartrate was synthesized in 95% yield by esterification of *d*-tartaric acid with acidic methanol. Oxidative cleavage using periodic acid, following the procedure of Horne et al.[153] gave the crude glyoxal intermediate. Subsequent condensation with *p*-anisidine gave the desired methyl glyoxylimine **121** as a brown oil, in 92% yield. The product could be purified using bulb-to-bulb vacuum distillation, but it was generally pure enough, as judged by ^{1}H NMR analysis, to use crude.[154] The imine was found to be unstable over long storage times and was used within a few weeks of synthesis.

The diacetone D-glucosylimine **123** was prepared starting from diacetone D-glucose (DAG-OH). The basic strategy was to introduce the glyoxyl group through oxidative cleavage of an alkene attached to the DAG auxiliary. The first approach was based on the symmetrical fumarate system, which on oxidative cleavage would give two molecules of the desired intermediate. The initial step involved acylation of the 3-position hydroxyl group. Fumaric acid and fumaryl chloride were tested in an attempt to synthesize the symmetrical diester. Oxidative cleavage of the double bond would then give the desired glyoxyl ester (Scheme 2.7). Unfortunately the use of fumaryl chloride with either DMAP or sodium carbonate

Scheme 2.7

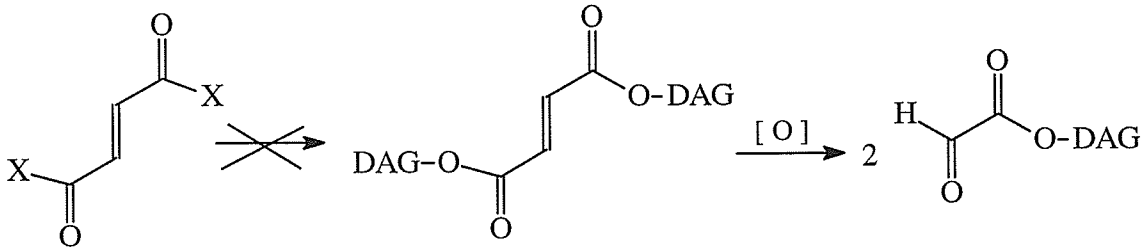

X = OH, Cl

led only to apparent polymerization of the acyl chloride. Attempts to use fumaric acid with a DCC/DMAP coupling technique also failed.

On the other hand, the *crotonate* ester **122** could be successfully prepared. Various approaches were tested to determine the optimum conditions for this reaction. The reaction of crotonyl chloride with diacetone D-glucose employing NaH as the base gave acceptable yields (50 – 70%). The use of butyl lithium gave a 66% yield plus a

byproduct that appeared to have arisen from the loss of the 5,6-isopropylidene group, followed by triacylation. Under optimized conditions, ester **122** was prepared using a DCC/DMAP coupling of crotonic acid and diacetone D-glucose (Scheme 2.8). One equivalent each of DCC and crotonic acid were initially added to a solution of DAG-OH in CH_2Cl_2. Once the reaction appeared to halt (as judged by TLC), a further 0.5 equivalents of each was added. After diluting the reaction with ether, cooling, filtering and repeating several times to remove the dicyclohexylurea byproducts, ester **122** was isolated in excellent yield (93%). Addition of the excess reagents in the initial step gave lower yields as these reagents underwent side reactions that halted the desired process

Scheme 2.8

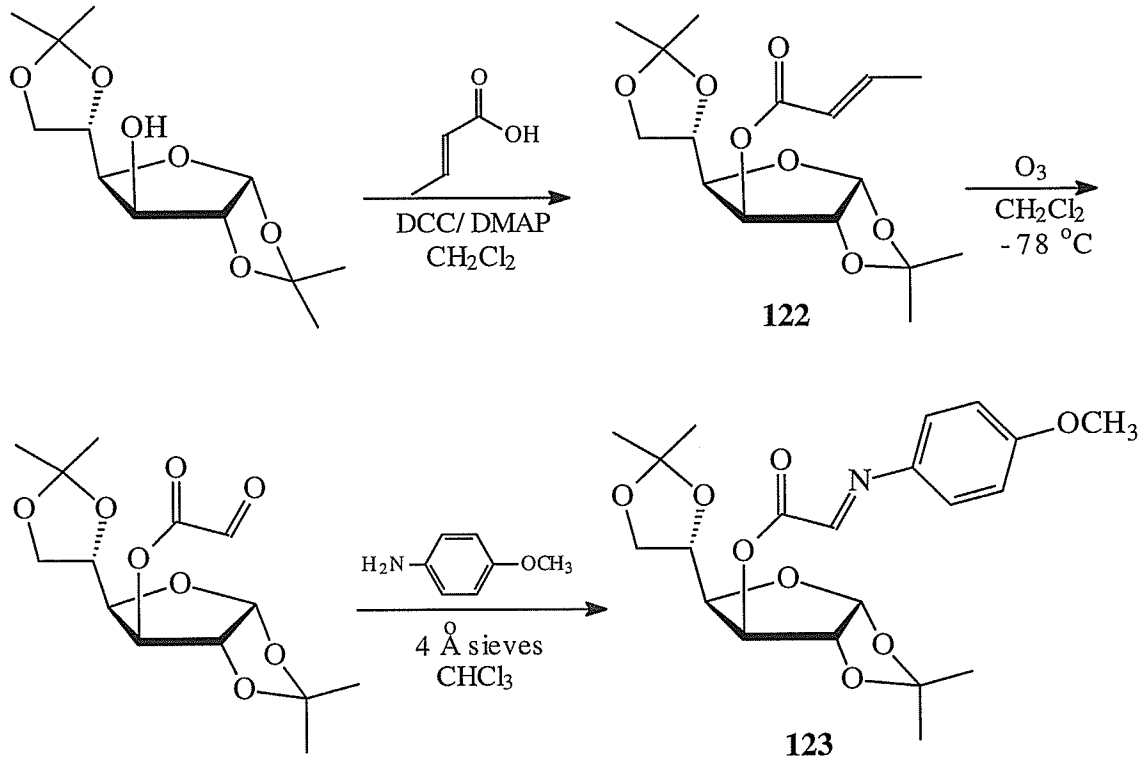

before complete consumption of the starting material. The alkene group in **122** was cleaved using ozone at –78 °C and the reaction was quenched with a large excess of Me_2S. Slow warming was required to ensure complete cleavage of the ozonide to give an 84% yield of the desired intermediate as colorless foam that could be used without further purification. With rapid warming, a product that appeared to be the ozonide was obtained in solution. This decomposed when the solution was concentrated, giving diacetone D-glucose. Chromatographic purification of the mixture was then necessary, reducing the yield (~30%) of the desired product significantly.

The ozonolysis of vinylic esters gives an intermediate ozonide that has been shown in some instances to undergo acyl migration.[155] Subsequent fragmentation then releases the alcohol portion of the ester (Scheme 2.9). The apparent persistence of our glucose-based ozonide on fast workup, and subsequent warming and concentration, could promote such a migration process. The other products, being volatile, could not be isolated by the procedure employed.

Scheme 2.9

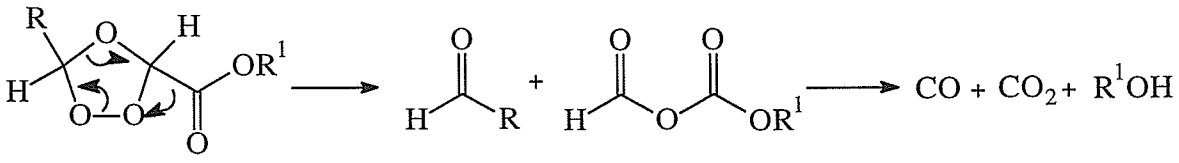

The glyoxylimine **123** was obtained as a stable yellow foam (87%) by condensation of the crude glyoxyl ester with *p*-anisidine in freshly distilled $CHCl_3$ over activated 4 Å molecular sieves. It was determined that the imine was in the expected *E*

geometry by a nuclear Overhauser effect (nOe) experiment. Strong nOe (14.1%) was observed between the α-H and the aromatic ortho hydrogens (Figure 2.9).

Figure 2.9

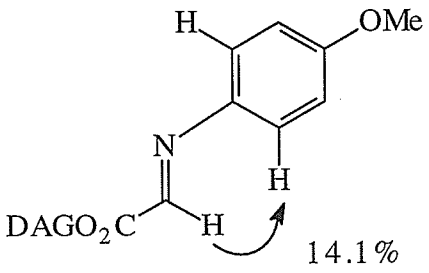

The third glyoxylimine was derived from diacetone D-allose (**124**) which itself was prepared by oxidation/reduction of diacetone D-glucose. Diacetone D-glucose was oxidized in 93% yield using PDC and acetic anhydride over crushed 3 Å molecular sieves (Scheme 2.10). [156,157] Subsequent reduction of the resulting ketone using $NaBH_4$ gave the epimeric sugar **124** in good yield (82%). Only a small amount of diacetone D-glucose

Scheme 2.10

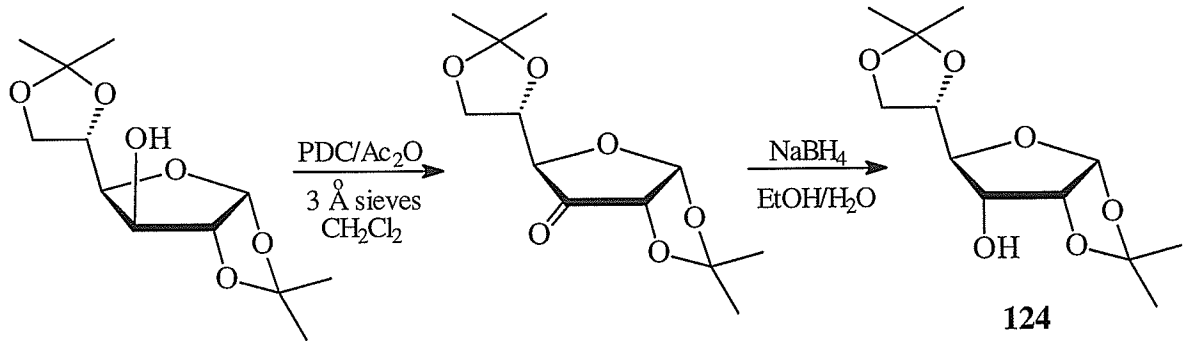

124

was seen in the ^1H NMR spectra of **124**. The product was used without further purification. Following a protocol similar to that shown in Scheme 2.8 the allose

crotonate **125** was prepared in 81% yield after recrystallization from hexanes. The ozonolysis of **125** was not optimized in this case and chromatographic purification was required, resulting in only a 33% yield for this step. The imine **126** was subsequently prepared in 71% yield. The three glyoxylimines used in this study are shown in Figure 2.10.

Figure 2.10

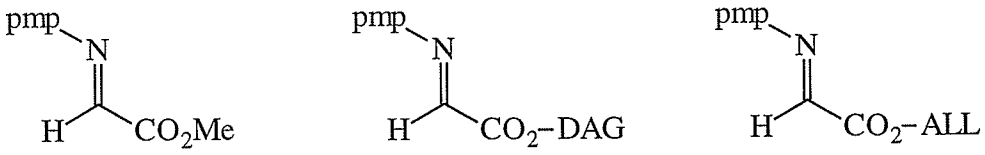

121 **123** **126**

pmp = $CH_3OC_6H_4$, DAG = diacetone D-glucose, ALL = diacetone D-allose

The silyl enol ethers of the various ketones were also required for the Mukaiyama aldol reactions. The trimethylsilyl (TMS) enols of acetophenone (**127a**), propiophenone (**127b**), deoxybenzoin (**127c**), diphenyl acetone (**127d**), and cyclohexanone (**127e**) were prepared using the procedure of Cazeau[158] (Scheme 2.11). Cyclohexanone gave modest yields (53%) while the other silyl enol ethers were obtained in ca. 80% yields. It was determined that the *Z*-silyl enol ether was formed in each case (except for cyclohexanone, which necessarily forms the *E* silyl enol ether).[159-161]

Scheme 2.11

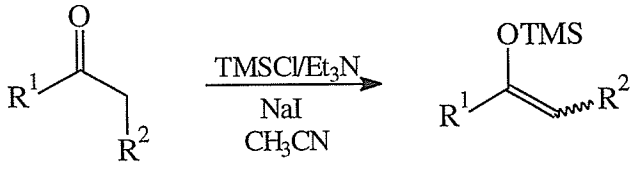

127a R^1 = Ph, R^2 = H
127b R^1 = Ph, R^2 = Me
127c R^1 = Ph, R^2 = Ph
127d R^1 = CH_2Ph, R^2 = Ph
127e $R^1 + R^2 = (CH_2)_4$

2.2.2 Mukaiyama aldol reactions.

The first reactions studied were the Mukaiyama aldol-like reactions of glyoxylimines **121** and **123** with the silyl enol ethers. In an attempt to establish the degree of simple *syn/anti* diastereoselectivity, enols **127a-e** were first condensed with methyl glyoxylimine **121**. These results are summarized in Table 2.4. Two general methods were used for these reactions. Method **A** involved addition of a stoichiometric amount of promoter, usually $BF_3{\cdot}OEt_2$, to a cooled solution of **121** and the silyl enol ether. Other promoters that were used on a catalytic scale are noted in Table 2.4. Method **B** (entries 1-4) involved generation of the imine **121** in the presence of 5 mol% $Yb(OTf)_3$ and subsequent reaction with the silyl enol ether in a one-pot procedure.[162] After work up, the pure amino ketones were obtained by chromatography and their structures determined by ^{1}H NMR spectroscopy and X-ray analysis. The selectivities for these reactions were determined by ^{1}H NMR spectroscopy or by HPLC analysis of the crude product mixtures.

Addition reactions using Method **B** afforded moderately good yields but only low *syn/anti* diastereoselectivity with a slight preference for the *syn* diastereomer. Using

more catalyst (10%, entry 2) had no effect on the diastereoselectivity, while changing the solvent to acetonitrile (entry 4) gave only a small increase in favor of the *syn* compound.

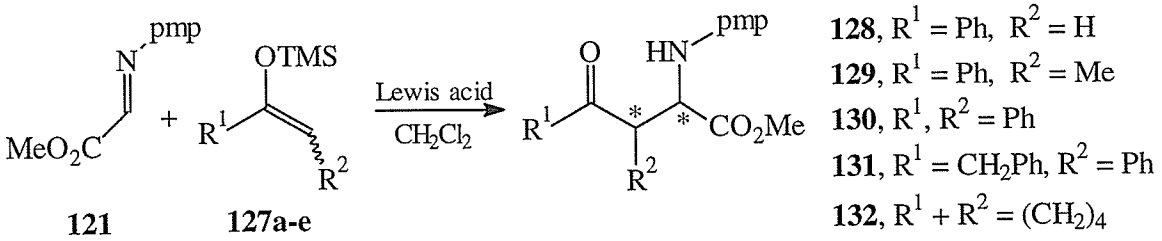

121 **127a-e**

Table 2.4: Mukaiyama aldol reactions of glyoxylimine **121** with various silyl enol ethers.

	Silyl Enol Ether (eq)	Method (cat eq.)	Reaction Time	Product(s)	Yield (%)	Selectivity *Syn* : *Anti*
1	**127a** (2.0)	**B** (5%)	1 h	**128**	50	N/A
2	**127b** (1.2)	**B** (10%)	1 h	**129a + 129b**	45	1.2:1
3	**127b** (2.0)	**B** (5%)	30 min	**129a + 129b**	61	1.2:1
4	**127b** (1.2)	**B** (5%)	1.5 h	**129a + 129b**	40	2:1
5	**127b** (1.1)	**A** (1.0)	2 h	**129a + 129b**	60	3:2
6	**127c** (1.1)	**A** (1.0)	30 min	**130a + 130b**	37	2:1
7	**127d** (1.1)	**A** (1.0)	30 min	**131**	40	0:100
8	**127e** (1.1)	**A** (1.0)	30 min	**132a + 132b**	44	1.2:1
9	**127b** (1.5)	**A**(TMSOTf-10%)[a]	3.5 h	**129a + 129b**	trace	4:3
10	**127b** (1.1)	**A**($TiCl_4$-10%)[b]	3 h	**129a + 129b**	trace	3:1
11	**127b** (1.1)	**A**($SnCl_4$-10%)[b]	3 h	**129a + 129b**	trace	2:1

[a] Reaction allowed to warm to room temp.

[b] Lewis acid is added to the imine @ –78°C, followed by the silyl enol ether.

Method **A** gave marginally better results than did method **B**. In most cases the reactions afforded low to moderate yields and low diastereoselectivities for the *syn* products. For the reaction of enol ether **127b** with **121** using method **A**, only $BF_3{\cdot}OEt_2$ was found to be an effective Lewis acid promoter (compare entry 5 with 9 – 11). The low yields obtained using catalytic TMSOTf, $TiCl_4$ and $SnCl_4$ could be a result of 'catalyst trapping'. Kobayashi et al.[136] have studied reactions of imines in the presence of Lewis acid catalysts. Kobayashi found that some Lewis acids seemed to be trapped by the basic nitrogen of the reactant or the product. This removes the catalyst from the catalytic cycle and halts the reaction. Therefore the Lewis acid catalyzed addition of nucleophiles to electrophilic imines can be difficult. The use of lanthanide derived Lewis acids has met with better success. Annunziata et al.[163] have observed (by ^1H NMR spectral shifts) that, in the presence of an imine and an aldehyde, $Yb(OTf)_3$ preferentially coordinates to the imine nitrogen. Imines are therefore readily activated with this reagent. The large size and soft nature of the Lanthanide metal ion means that after the reaction, the Yb^{3+} will not remain tightly associated to the harder N^- center and the catalytic cycle may continue. Stoichiometric amounts of other Lewis acids often have worked better but both $TiCl_4$ and $SnCl_4$ give variable results in the literature.[95,162] In the presence of $BF_3{\cdot}OEt_2$, enols **127c** and **127e** displayed similar behavior to **127b** in the reaction with **121**, giving low selectivities and moderate yields.

Surprisingly a change in selectivity was observed in the reaction of the diphenylacetone-derived enol **127d** with imine **121**. In this instance, only the *anti* product **131** was obtained. This result may be rationalized by looking at the possible transition states for this reaction. Most experimental evidence suggests that Mukaiyama

reactions proceed through open transition states of either synclinal or antiperiplanar geometry.[125] There is no intrinsic preference for either of these geometries. Six possible transition states can be proposed based on (a) the preference of the imine for the *E* geometry and (b) the coordination of the Lewis acid *syn* to the ester substituent (Figure 2.11). Destabilizing steric interactions between the Lewis acid and the R group, and between the OTMS and ester groups are expected for (**A**) and (**F**). Electrostatic destabilization due the dipole alignment of the OTMS and imine double bond, as well as steric hindrance with the OTMS group are expected in transition states (**B**) and (**D**).[125] This suggests that the antiperiplanar transition state (**C**) leading to the *syn* products and synclinal transition state (**E**) leading to the *anti* products are expected to have the least unfavorable steric or electrostatic interactions.

Figure 2.11

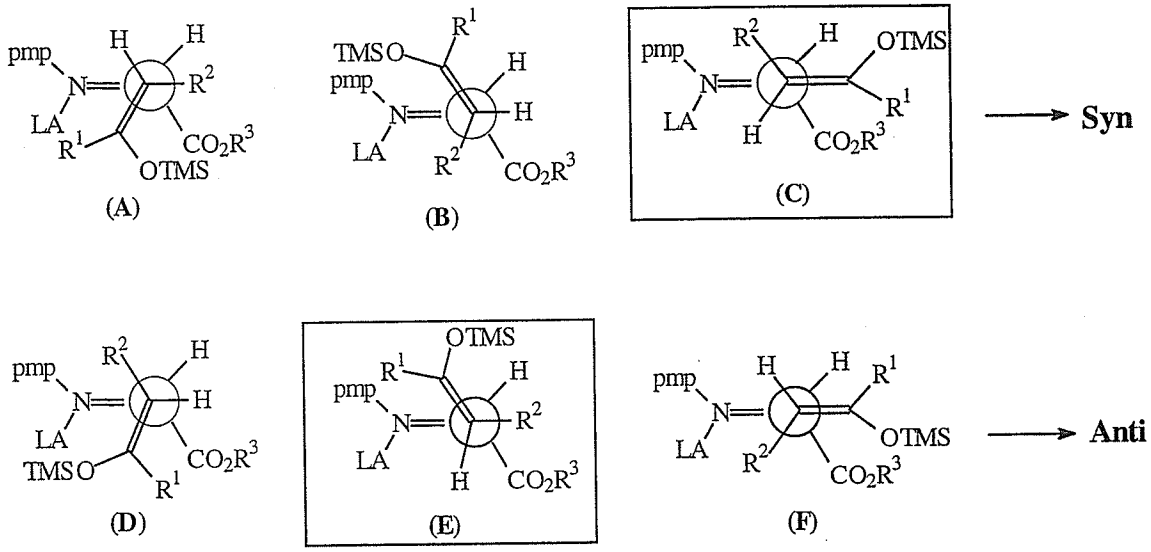

A lowest energy conformer search (Merck/X force field, Spartan SGI version 5.0) suggested that for **127d** R^1 (CH_2Ph) prefers an orientation in which the phenyl moiety is on the same side of the alkene plane as the OTMS substituent (Figure 2.12). The imine will approach the silyl enol ether from the opposite face, and will encounter little steric conflict between R^1 and the pmp group in transition state (**E**), while the R^2-pmp interaction in (**C**) remains significant. In contrast, with silyl enol ether **127b** (R^1 = Ph, R^2 = Me), transition state (**C**) is apparently slightly preferred.

Figure 2.12

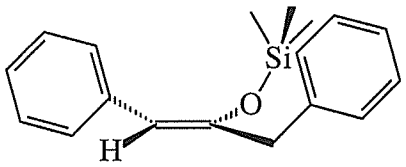

Similar reactions were tried with chiral glyoxylimine **123** (Table 2.5). Enol ether **127b** reacted with **123** in the presence of $Sc(OTf)_3$ or $Yb(OTf)_3$ to afford compounds **133** in good yield (60 – 80%) but apparently low diastereoselectivity (*syn*:*anti*, 1:1). There was also a small diastereofacial (*anti*$_1$:*anti*$_2$, <4:1) selectivity in favor of *anti* product **133d**. The assignment of the various reaction products as diastereomers, in this and the other cases, was determined by separation of the products as much as possible by column chromatography and preparative HPLC. The ^1H and ^{13}C NMR spectra for the pure compounds were consistent with the assigned structures. Comparison of the ^1H and ^{13}C NMR spectral characteristics for compounds that could not be separated with those of the pure materials from each reaction suggested that these materials were also diastereomers.

The assignment of the relative stereochemistry for these compounds is discussed in the next section (section 2.2.4).

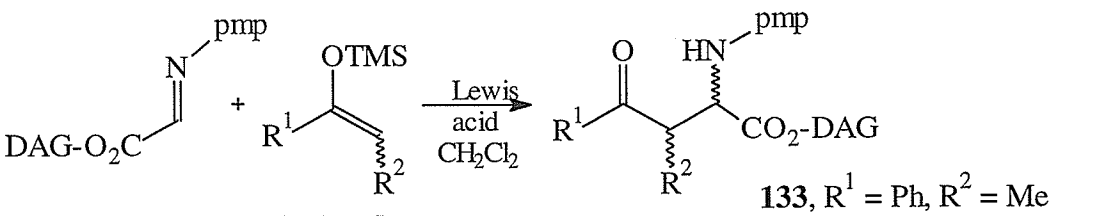

123 **127b,c,d**

133, R^1 = Ph, R^2 = Me
134, R^1, R^2 = Ph
135, R^1 = CH_2Ph, R^2 = Ph

Table 2.5: Mukaiyama reactions of chiral glyoxylimine **123** with various silyl enol ethers.

	Lewis Acid		**Final**		**Yield**	**Selectivity**	
Enol (eq)	**(eq)**	**Time**	**T (°C)**	**Products**	**(%)**	***Syn*:*Anti***	***Anti*$_1$:*Anti*$_2$**
127b (1.2)	$Yb(OTf)_3$ (0.2)	30 min	25	**133a-d**	>60	1:1.4	1:1.1
127b (1.5)	$Sc(OTf)_3$ (0.1)	20 min	25	**133a-d**	80	1:1	1:4
127c (1.1)	$BF_3{\cdot}OEt_2$ (3)	2 h	–78	—	0	—	—
	+$Yb(OTf)_3$ (0.1)	30 min	–20	**134a-c**	42	7:1	*a*
127d (1.1)	$BF_3{\cdot}OEt_2$ (3)	2 h	–78	—	0	—	—
	+$Yb(OTf)_3$ (0.1)	30 min	–20	**135a-d**	60	1:3	1:3

[a] Compound Syn_2 major.

For enols **127c** and **127d** the reactions were attempted in THF and contrary to earlier results, no reaction took place even in the presence of a large excess of $BF_3{\cdot}OEt_2$. This is presumably due to coordination of the Lewis acid with the oxygens on the sugar

moiety. Subsequent addition of $Yb(OTf)_3$ (10 mol%) to the solutions already containing $BF_3{\cdot}OEt_2$ gave the respective products **134** and **135** with low diastereoselectivity and modest yields. With silyl enol ether **127c**, *syn* product **134c** was slightly preferred, while for silyl enol ether **127d**, *anti* product **135c** was the major isomer.

This slight change in diastereomer preference suggests the glucose unit is exerting only a modest steric influence in the transition state. The modest facial selectivity is likely due to the mobility of the side chain. A conformational analysis of the glucose moiety of this imine was undertaken. The starting structure was initially based on X-ray structural coordinates of a similar 3-*O* ester compound.[164] A low energy conformer search and geometry optimization (SYBYL force field) was then done on the imine side

Figure 2.13

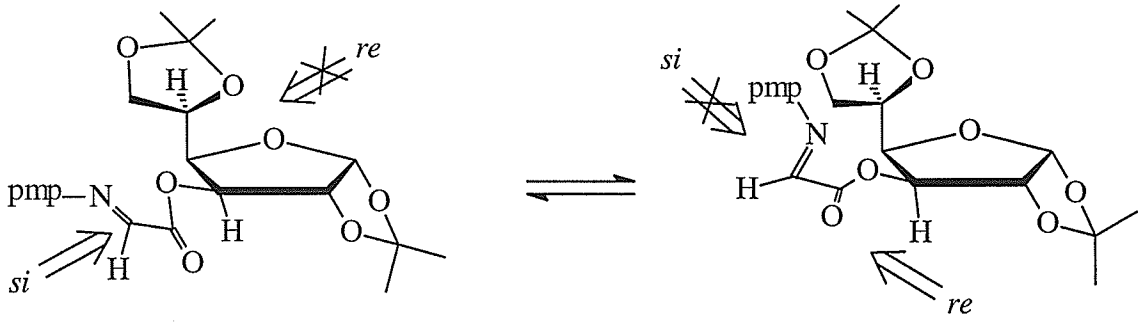

(G) **(H)**

E = 33.2 kcal/mol E = 34.7 kcal/mol

chain. The results (Figure 2.13) (Spartan SGI version 5.0) suggest that, for a given low energy conformation of the 5,6-isopropylidene group, a small rotation in the HC–O–(C=O) dihedral can expose either the *si* or *re* face to attack. In conformer (**G**), the imine side chain is facing outwards, away from the glucose moiety, leaving the *si* face

open and the *re* face only partially blocked to nucleophilic attack. In conformer (**H**), the imine has rotated such that the *si* face is now almost completely blocked and the *re* face exposed. The difference in the strain energies between these conformers was calculated to be ~0.7 kcal/mol, therefore both are likely to be populated under the reaction conditions used.

The planar nature of the α-ester function seems to have been a drawback to these reactions. The bulky substituent is placed too far away from the reactive center to consider applying Felkin-Ahn (or Cram) models for selectivity.[38] These models have predictive value for the preferred direction of nucleophilic attack only when chiral centers are in the α or β positions.[125] Any facial bias must be based only on hindered approach of the electrophile past the glucose moiety. Due to the modest results in these reactions, it was postulated that an enolate approach would be more suitable. As stated, the Mukaiyama reactions go through open antiperiplanar or synperiplanar transition states with little preference for either. In contrast, metal-based enolate reactions are known to react through cyclic transition states. The existence of pericyclic chair or boat transition states in these reactions can often exert more stereocontrol.

2.2.3A Enolate reactions

Reactions of glyoxylimine **121** with titanium (IV) enolates of acetophenone and propiophenone afforded adducts in ca. 40% yields. In the case of the propiophenone derived compound, *anti* product **129b** was favored. This suggested that a change in the

transition states from the open type predicted for the Mukaiyama reactions had indeed occurred. Representative results are shown in Table 2.6.

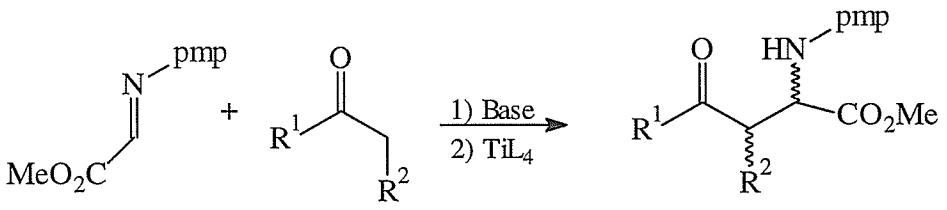

128, R^1 = Ph, R^2 = H
129, R^1 = Ph, R^2 = CH_3

Table 2.6: Aldol reactions of **121** with various titanium enolates.

Base	TiL_4	Ketone	Product(s)	Reaction Time	Selectivity *Syn* : *Anti*
LDA	Ti(*i*OPr)$_4$	acetophenone	**128**	1 h	N/A
LiHMDS	Ti(*i*OPr)$_4$	propiophenone	**129a + 129b**	1 h	1:20
Et_3N[a]	$TiCl_4$	propiophenone	**129a + 129b**	30 min	2:3

[a] Ti enolate formed directly using Method D.

It is notable that with increased bulk of the metal ligands, there is an increase in simple diastereoselection for reactions with propiophenone. Generation of the sterically demanding 'ate' complex [ROTi(*i*OPr)$_4^-$ Li^+][165] from Ti(*i*OPr)$_4$ gave very good results (**129a:129b**, 1:20). With Ti(*i*OPr)$_4$, the *i*OPr ligands are poorer leaving groups and remain associated to the titanium center. This provides more steric bulk around the enolate giving good diastereoselectivity for the reaction. With $TiCl_4$ only modest

selectivity (**129a:129b**, 2:3) was observed. Because the Cl^- ligands are smaller it means that steric hindrance around the enolate is lower, and lower selectivity was observed.

Considering the possible pericyclic transition states as postulated by Evans,[118] two models can be proposed based on an *E* imine and either a chair (**I**) or a boat (**J**) transition state (Figure 2.14). In **I**, potential 1,3-diaxial strain exists among the ester, the R^1 group and the metal ligands. The presence of the nitrogen substituent also adds a pmp-to-R^2 interaction.

Figure 2.14

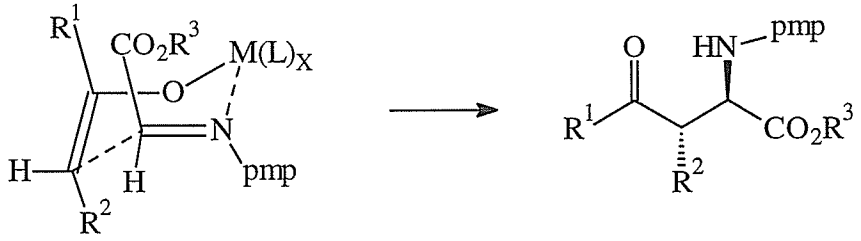

(I)

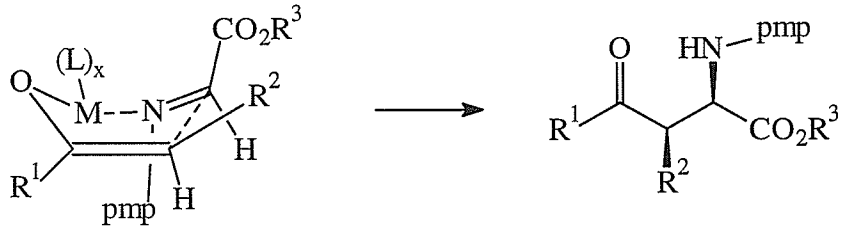

(J)

The boat transition state **J** contains gauche strain between the metal ligand and the pmp group and between the ester and R^2 groups. For the reactions mentioned in Table 2.6, it is conceivable that with small metal ligands such as Cl, the 1,3-diaxial strain in **I** makes the two transition states closer in energy. As a result little diastereoselectivity

would be expected. In the reaction of the 'ate' complexes formed from Ti(*i*OPr)$_4$, the number of ligands associated to the metal is higher and the ligands themselves are larger. In this situation, the gauche interactions in transition state **J** become more destabilizing and the chair form becomes increasingly preferred.

The reactions of the auxiliary based imine **123** were next tried with acetophenone and propiophenone (Tables 2.7 and 2.8). Due to the increased size of the ester substituent, the effective size of the metal enolate was expected to be more important in these reactions. These effects were determined by successive changes to the metal ligands, as the Ti (IV) reagent was varied from $TiCl_4$ to Ti(*i*OPr)$_4$.[166] The transmetallated enolates were generated using two methods. When Ti(IV) bearing two or more chloride ligands was used, the titanium enolate was generated directly from the ketone using Et_3N (method D). The bulkier enolates in which the metal ion carried one or no Cl ligands, were made by generation of the lithium enolate using 1.1 – 1.2 equivalents of LDA and then subsequent addition of two equivalents (with respect to lithium) of the titanium species (method C). Preliminary work established that, unlike reactions involving the methyl glyoxylimine **121**, no aldol product was observed when only one equivalent of the enolate was used. Acceptable results were obtained using six equivalents of enolate.[167] In reactions of the sterically less demanding Ti(IV) enolate of acetophenone (Table 2.7), product was obtained at both –78 °C and –40 °C, but the reactions displayed no diastereofacial selectivity. A modest preference for the *R* (**136a**) isomer was obtained from reactions employing the lithium enolate. The absolute configurations of the products were determined by transesterification of **136b** to the isopropyl ester (see section

2.2.4 and experimental) and comparison of the products' optical rotation with the literature values.[96]

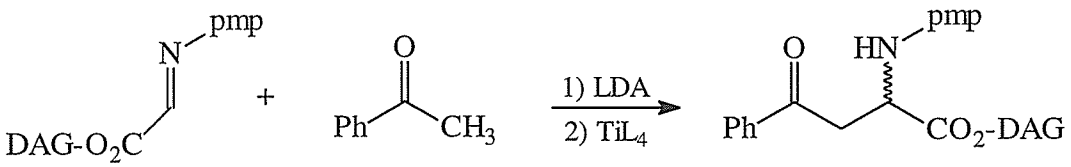

123 **136a,b**

Table 2.7: Reactions of glyoxylimine **123** with various metal enolates of acetophenone.

Added TiL_4	Equiv Ketone	Reaction Time	Yield (%)	Final Temp (°C)	Selectivity 136a:136b
Ti(*i*OPr)$_4$	1.1	3.5 h	0	RT	—
Ti(*i*OPr)$_4$	6	2 h	46	–40	1:1
Ti(*i*OPr)$_4$	6	2 h	59	–78	1:1
LDA only	6	1 h	48	–78	2.8:1

In contrast, the reactions of **123** with the enolate of propiophenone (Table 2.8) produced no products at –78 °C with the bulkier enolates. Enolates generated from Ti(IV) species having two or more isopropoxide ligands required a higher temperature (–40 °C) during the aldol reaction. Also noticeable was the consistently low *syn*:*anti* selectivity (<1:3.5).

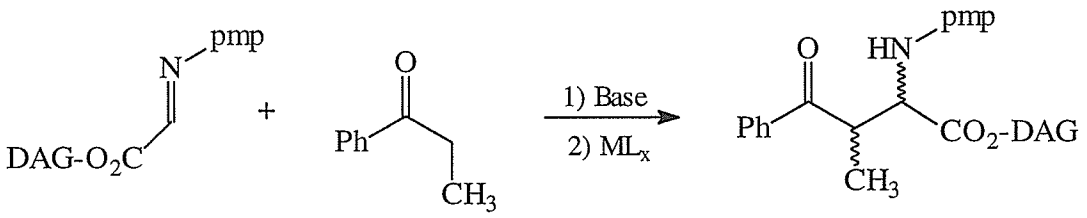

123 **133a-d**

Table 2.8: Reactions of **123** with various metal enolates of propiophenone.

		Reaction	Yield	Final Rxn	Selectivity	
	ML_x	Time	(%)	Temp (°C)	*Syn* : *Anti*[a]	$Anti_1$: $Anti_2$
1	$Ti(iOPr)_4$	4 h	0	–78		
2	$Ti(iOPr)_4$	3 h	48	–40	1:3	5.3:1
3	$ClTi(iOPr)_3$	2.5 h	50	–40	1:1	2:1
4	$Cl_2Ti(iOPr)_2$	4 h	81	–40	1:1.8	3.4:1
5	$Cl_2Ti(iOPr)_2$	5.5 h	79	–40	1:2.5	2.5:1
6	$Cl_3Ti(iOPr)$	1 h	46	–78	1:3.5	1:1
7	none added	2 h	36	–78	1:3	6.8:1
8	$MgBr_2$	1 h	46	–78	1:3.5	14:1

[a] Diastereomer ratio is that of major two products only.

The apparent diasterofacial preference also appeared to be reversed from that of the Mukaiyama reactions, *anti* compound **133a** being the preferred product based on analysis of the ^{1}H NMR spectra. The small difference between entries 2 and 3 suggested that the generation of an 'ate' complex as opposed to a simple enolate had only a modest effect. The yields fluctuated with the metal enolate used, the highest occurring with

$Cl_2Ti(iOPr)_2$. Good facial discrimination was achieved with the magnesium enolate (14:1). The lack of any general trend in these reactions suggested that the carbohydrate auxiliary played only a relatively weak role. The diastereoselectivity, facial selectivity and yield seemed to vary independently of each other.

The low diastereoselectivities observed could be a result of isomerization taking place under the conditions of the reaction. It was observed in each of these reactions that the low yields of addition products were accompanied by the formation of a significant amount of the free diacetone D-glucose ($\leq$50%). This suggested that degradation of the product was taking place during the reaction by one of two possible pathways (**P1** Scheme 2.12 or **P2** Scheme 2.13). Due to the unreactive nature of the imine, as stated earlier, a large excess (6 equiv.) of enolate was required. The products of these reactions contain a β-H adjacent to a ketone. This hydrogen would be expected to have a similar pKa to that of the corresponding hydrogen in the starting ketones. Removal of this hydrogen (Pathway **P1**) by either the excess enolate or by proton transfer to the now more basic *N*-metalloamine would result in stereochemical scrambling at the β position upon quenching, thus lowering the *syn/anti* selectivity (Scheme 2.12). Once this new enolate is formed it can undergo cyclization to the lactone with concurrent loss of the sugar moiety. This byproduct could then tautomerize to give a conjugated furan byproduct (**137**).

Scheme 2.12

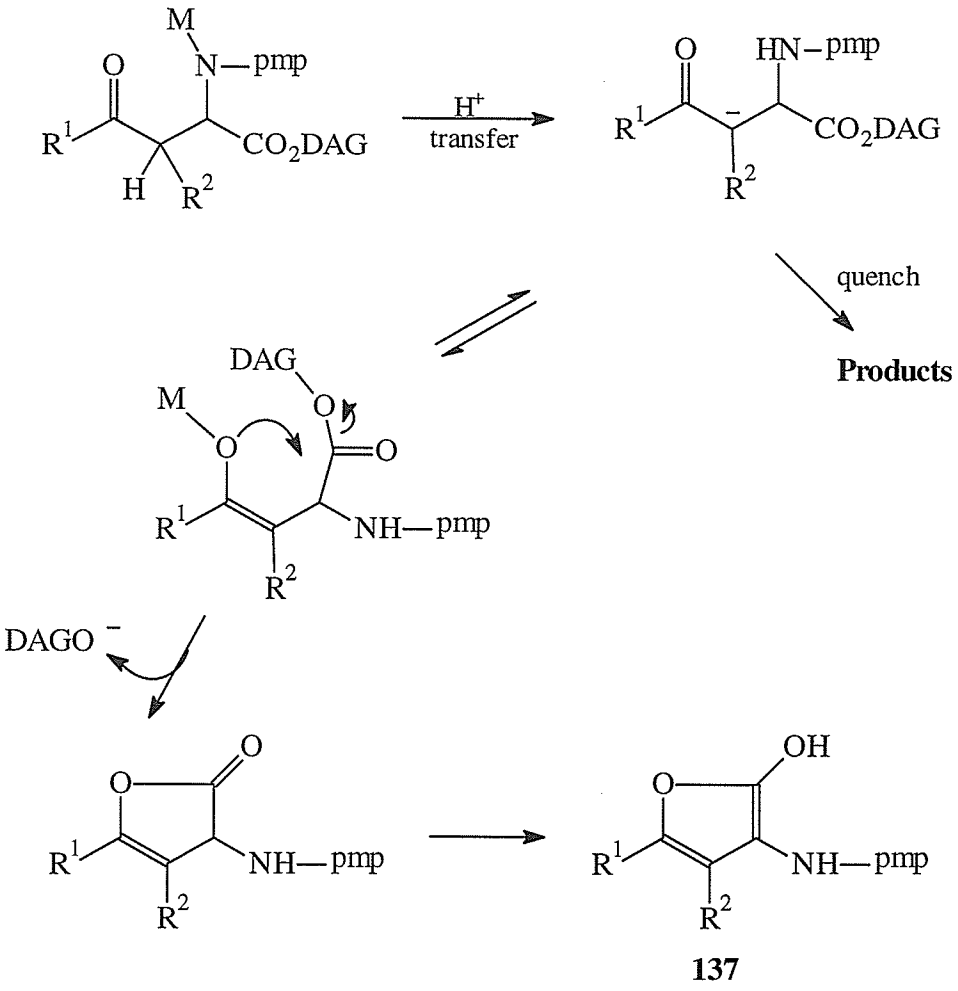

137

An alternate degradation pathway **P2** was also proposed to account for the loss of the sugar moiety. If instead the α-H were removed, the sugar could be lost through a ketene elimination pathway (Scheme 2.13), similar to one suggested by Kunz (section 1.2).[46,57] Kunz noted that enolates generated from an acylated glucofuranose auxiliary provided a favorable geometry for a polydentate lithium chelate. This resulted in the carbohydrate becoming a suitable leaving group due to the neutralization of the developing charge, and hence increased the tendency towards ketene elimination,

analogous to the path shown. By changing to the C-3 epimeric sugar Kunz found that the lithium chelate did not form and the elimination no longer occurred.

Scheme 2.13

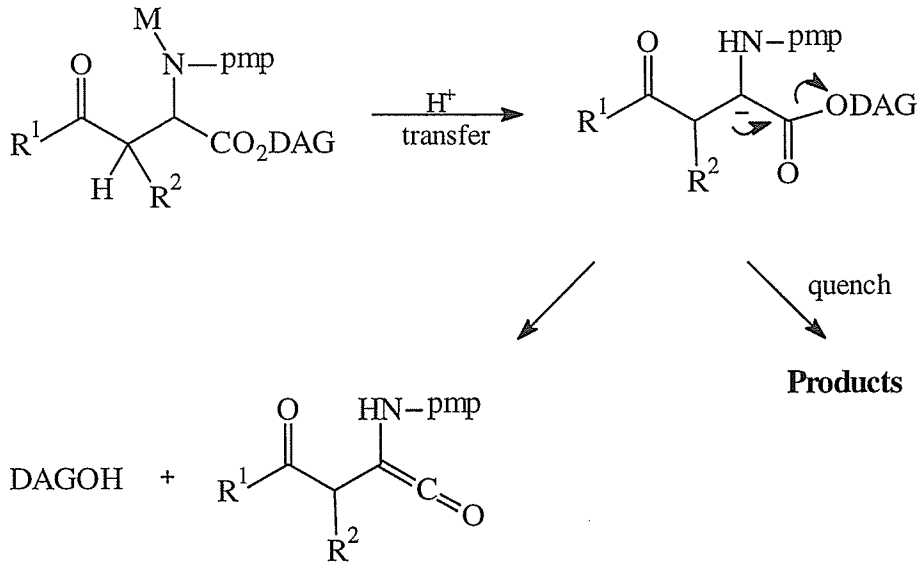

Unfortunately, in our reactions the possible byproducts that may have conclusively determined whether one or both paths were being followed could not be isolated. We did see evidence that path **P1** was possible in attempts to deprotect compound **131** using LiOH/THF. Under these basic reaction conditions, a product was isolated whose ^{1}H NMR spectrum (see insert pg 114) was consistent with a furan species such as **137**. The sensitivity of the products of our reactions towards basic cleavage conditions has led to problems in the determination of their absolute stereochemistry, which will be discussed later (section 2.2.4)

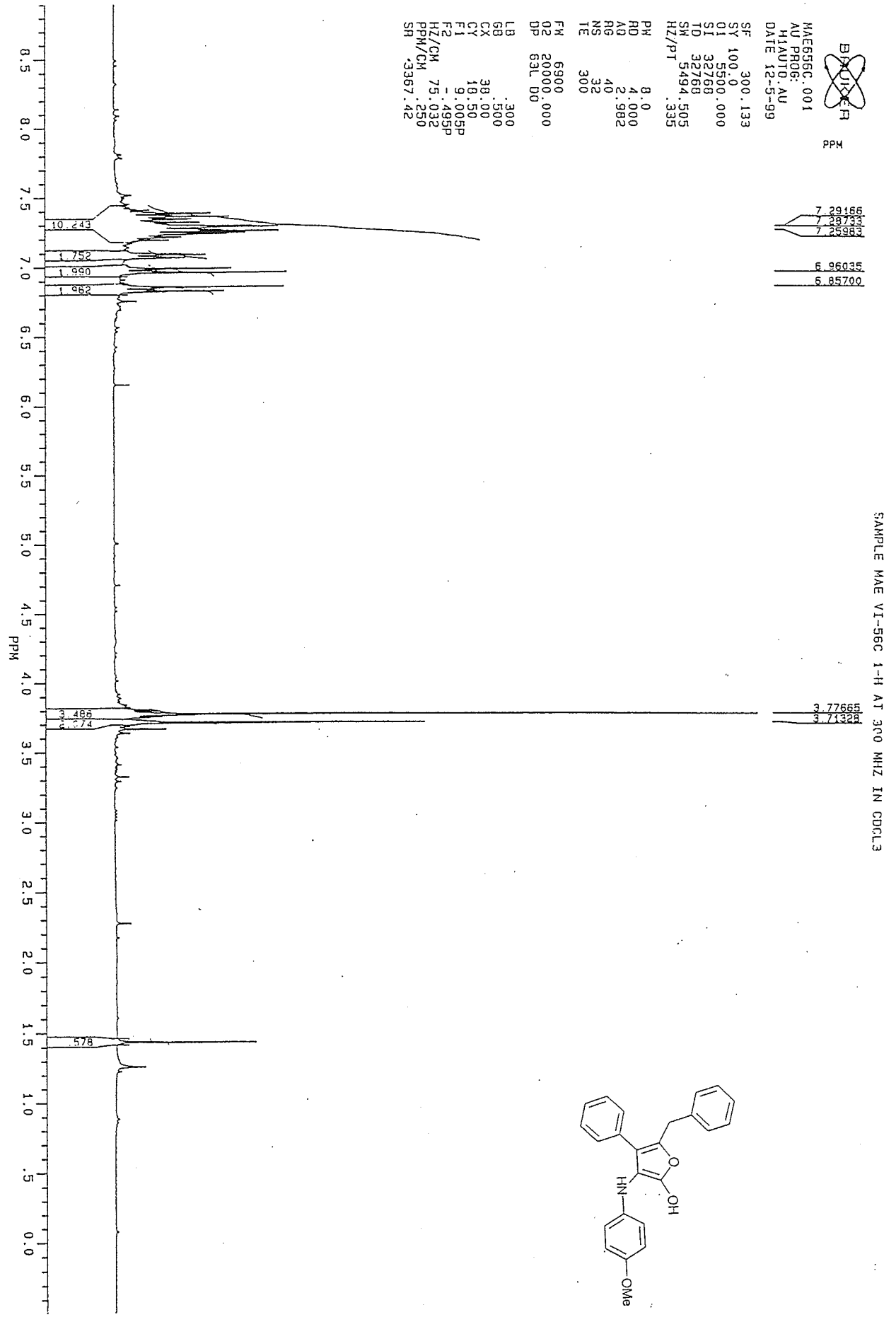
MAE656C.001
AU PROG:
H1AUTO.AU
DATE 12-5-99
SF 300.133
SY 100.0
O1 5500.000
SI 32768
TD 32768
SW 5494.505
HZ/PT .335
PW 8.0
RD 4.000
AQ 2.982
RG 40
NS 32
TE 300
FW 6900
O2 20000.000
DP 63L D0
LB .300
GB .500
CX 38.00
CY 18.50
F1 9.005P
F2 -.495P
HZ/CM 75.032
PPM/CM .250
SR -3367.42
PPM
7.29166
7.28733
7.25983
6.96035
6.85700
3.77665
3.71328
10.243
1.752
1.990
1.962
3.486
3.474
.578
SAMPLE MAE VI-56C 1-H AT 300 MHZ IN CDCL3
HN
OH
OMe

Scheme 2.14

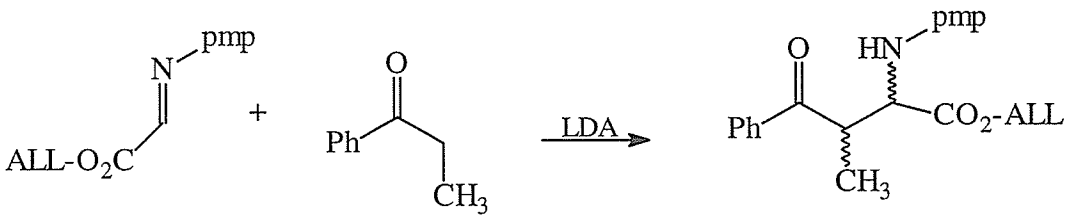

126 **138a-d**

Following the approach taken by Kunz, the C-3 epimeric allose glyoxylimine **126** was prepared as described in Section 2.1. Imine **126** was then reacted with propiophenone enolates (Scheme 2.14). The diastereoselectivities of these reactions were lower (*syn*:*anti* 7:2, $anti_1$:$anti_2$ 1:1) than was observed in the reactions of the glucose analog, which was not unexpected given the remoteness of sugar protecting groups to the reactive center. The yield however was not increased (54%). This suggested that a ketene elimination path such as **P2** was a less probable process for the DAG imine **123** than the alternate path **P1**.

2.2.3B Enolate reactions using inverse addition

With the likely interference of a competing degradation pathway, a milder method was sought to improve the *syn/anti* selectivity. Use of a cerium enolate was chosen based on literature references.[168,169] These reported that cerium enolates often gave better yields then the lithium enolates in situations where side reactions such as enolization of the products could occur.

It was also considered that chelating agents that would take advantage of the other oxygens of the glucose unit and restrict the mobility of the imine might also improve the

syn/anti diastereoselectivity. To this end a change in the order of reagent addition was necessary. This required that the imine is cooled to the reaction temperature and the cold enolate added by *cannula*. It was found that even in the absence of any transmetallating agents or additives to imine **123**, a substantial increase in selectivity was obtained (Table 2.9).

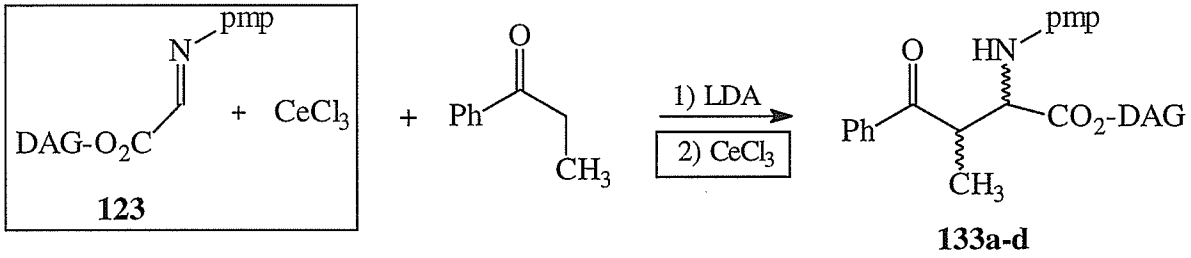

Table 2.9: Modes of $CeCl_3$ addition to reactions of **123** and acetophenone.

$CeCl_3$ added to (eq)	**Time**	**Yield (%)**	**Selectivity** *Syn* : *Anti*	**Selectivity** $Anti_1$: $Anti_2$
none added	20 min	54	1:3.4	24:1
enolate (1)	30 min	54	1:2.3	6.5:1
enolate (2)	5 min	62	1:2	8.6:1
enolate (2), imine (1)	5 min	71	2:5	15:1
imine (1)	10 min	68	1:2.7	12.4:1

Variations on this process were studied. The cerium salt was added in three different manners (method E). The enolates were generated using 1.1 – 1.2 equivalents of LDA. The lithium enolate could then be transmetallated with $CeCl_3$. Alternately, $CeCl_3$

was added to the imine **123** in an attempt to restrict the mobility of the side chain. Finally a combination of these two methods was used and $CeCl_3$ was added to both reaction partners. In each case the enolate was then cannulated into the cooled solution of the imine. Although no improvement in the overall *syn/anti* selectivity was achieved over our established procedures, there was in each case a significant increase in the facial diastereoselectivity as a result of this inverse reaction procedure. Compound **133a** became significantly more preferred.

The use of LDA alone gave the largest facial preference in the addition reactions ($anti_1$:$anti_2$ 24:1). Addition of one equivalent of $CeCl_3$ to the enolate prior to adding it to **123** showed no benefit. However adding two equivalents of $CeCl_3$ resulted in an increased yield. The use of the cerium enolate did have a positive effect on yield, as did addition of $CeCl_3$ to the imine **123**. Prior association of $CeCl_3$ with an imine species has also been observed by others to improve yields.[169]

Addition of the reagent to both partners showed no clear benefit. The fact that the *syn/anti* diastereoselectivity was not significantly affected as the yield improved suggested that these phenomena were not related. Once deprotonation of the product has occurred (Scheme 2.12) loss of the sugar moiety is likely faster than reprotonation causing the loss in yield only. The low *syn/anti* diastereoselectivity is probably a result of poor discrimination between competitive pericyclic transition states (Figure 2.14).

The requirement for two equivalents of $CeCl_3$ may be understood from arguments used with the generation of titanium enolates by transmetallation (Section 2.2.3A). Thornton et al.[165] observed that transmetallations of the lithium enolates with one equivalent of $Ti(iOPr)_4$ or $ClTi(iOPr)_3$ resulted in little change in selectivity in the aldol

reactions with respect to the lithium enolate. They explained this in terms of the close association of a lithium titanium-'ate' complex (Scheme 2.15).

Scheme 2.15

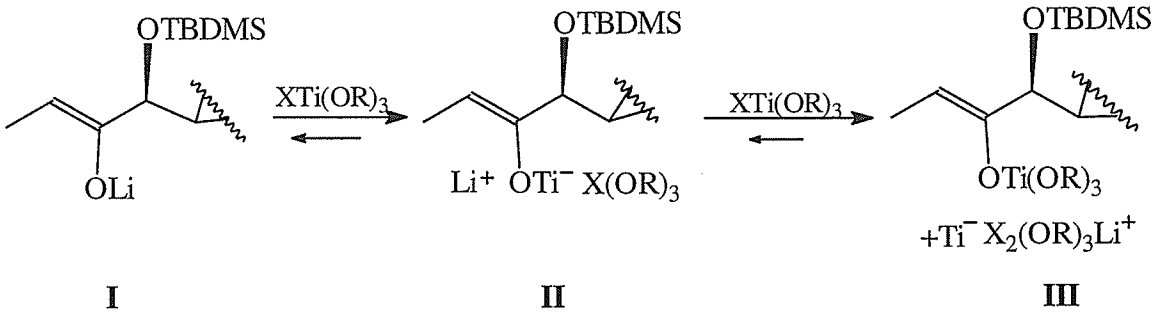

I **II** **III**

The fraction of aldol products formed from each of the complexes **I** – **III** is determined by the relative stability of the transition structure for that route. The amount of lithium enolate **I** present at equilibrium is expected to be small. But this species is more reactive, so it may significantly contribute to product formation when only one equivalent of $XTi(OR)_3$ is added. When two or more equivalents of titanium reagents are added it appears that the lithium is more effectively removed from the coordination sphere (**III**) of the enolate and the outcome of the reaction now relies on the properties of the new metal. It can be postulated that a similar effect may be occurring in our case with $CeCl_3$.

Concurrently with this work we studied a select few other ketones (Table 2.10). The last four entries show the effect of changing the enolate geometry. For diphenylacetone, the *E* and *Z* enolates were formed in approximately equal amounts (determined by trapping studies), which resulted in little selectivity, as expected. The

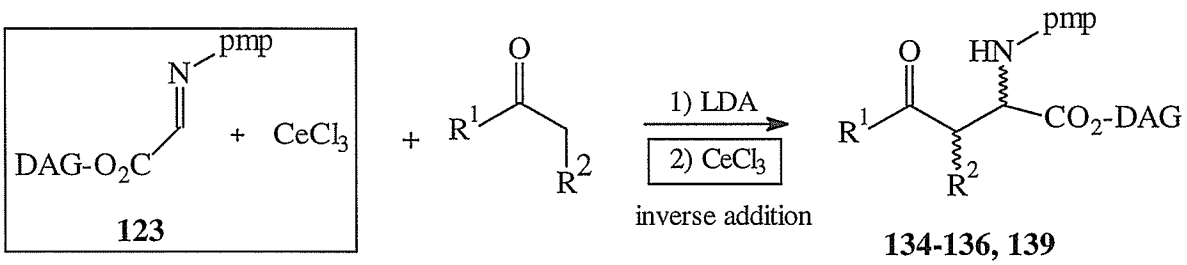

Table 2.10: Aldol reactions of **123** with various ketones.

	$CeCl_3$ added to			Yield	Selectivity	
R^1, R^2	(eq)	Time	Products	(%)	*Syn*:*Anti*	$Anti_1$:$Anti_2$
Ph, H	imine (1)	5 min	**136a+136b**	61	3.4:1[a]	
Ph, H	ketone (1)	10 min	**136a+136b**	44	2.3:1[a]	
Ph, Ph	none added	5 min	**134a**	22	0:100	100:0
Ph, Ph	imine(1), ketone (2)	40 min	**134a**	32	0:100	100:0
CH_2Ph, Ph	none added	1 h	**135a-d**	55	1:2.4	5:1
CH_2Ph, Ph	imine (1)	5 min	**135a-d**	57	1:1.7	2:3
$(CH_2)_4$	none added	30 min	**139a-d**	51	1:1.8	1:2
$(CH_2)_4$	imine (1)	10 min	**139a-d**	44	1:1.8	1:3

[a] Selectivity is for *R*:*S*.

cyclohexanone enolate is of course *E* and again little selectivity was observed. It has been shown in reactions with aldehydes that the correlation of enolate geometry with aldol configurations is stronger for *Z* enolates than for *E* enolates (Section 1.4).[111] Acetophenone gave only modest selectivity in favor of the *R* diastereomer. Low selectivity in the aldol reactions of unsubstituted methyl ketones has been reported in the

literature[126] and was not unexpected. For imine **123**, an impressive level of selectivity was obtained in the reaction of deoxybenzoin, where only the one *anti* product **134a** was observed by ^{1}H NMR or HPLC. In this case, an optimum balance of steric interactions in the transition state must have been achieved. The low yield may be attributed to increased acidity of the β-H of this product, which suggests the degradation path **P1** (Scheme 2.12) is quite favorable in this case. In these instances a large amount of the free diacetone glucose (~ 50%) accounted for the bulk of the consumed reactant.

2.2.4 Deprotection and characterization attempts

The synthesized γ-oxo-α-amino acids next required characterization. In order to achieve this, it was necessary to remove the ester substituent and the *N*-protecting group. Several approaches were investigated. First the determination of the relative stereochemistries of the chiral centers in each compound was necessary. This was attempted using two methods, ^{1}H NMR analysis and X-ray crystallography. Secondly, if possible, the absolute configuration of each compound was determined. Several methods were investigated. We attempted to obtain good quality crystals of the DAG and camphorsulfonate derivatives of the γ-oxo-α-amino acids, suitable for X-ray crystallographic analysis. ^{1}H NMR techniques using MPA and MTPA amides were also investigated. Palladium complexes were also synthesized for CD spectral analysis. Only three related compounds could be found in searches of the literature (see Figure 2.16).[96,98] In order to relate the configurations of the compounds prepared in this research to those literature analogs, it was necessary to change the protecting groups in our compounds.

The various methods tested to remove/replace the protecting groups of the prepared compounds will also be discussed.

Simple diastereoselectivity

Analysis of the ^{1}H NMR spectra was considered as the easiest method to determine simple diastereoselection. As mentioned earlier, the functional pattern of these compounds is quite similar to that of the β-hydroxy ketones. It is well known that these compounds often hydrogen bond internally giving distinct differences for $J_{\alpha\beta}$. The vicinal coupling constant for the *syn* isomer (2 – 6 Hz) is less than that of the *anti* isomers (7 – 10 Hz).[119]

The various rotamers for β-hydroxy ketones are shown in Figure 2.15. It can be seen that for the *syn* compounds rotamers **K** and **L** are capable of internal H-bonding. Both of these rotamers experience gauche interactions between H_α and H_β. According to the Karplus relationship[170,171] their coupling constants are expected to be small ($J_g = 4 – 5$ Hz for 60° angle). The anti compounds also have two H-bonded rotamers, **K′** and **L′**. However in **K′**, H_α and H_β have a gauche relationship and in **L′** they have a trans relationship. The $J_{\alpha\beta}$ value will be a weighted population average of the J values for each of these two rotamers, and therefore larger than would be expected for the corresponding syn diastereomers. The actual values, however, will depend on the substituents R, R^1 and R^2, which affect the population of each of the rotamers.

Figure 2.15

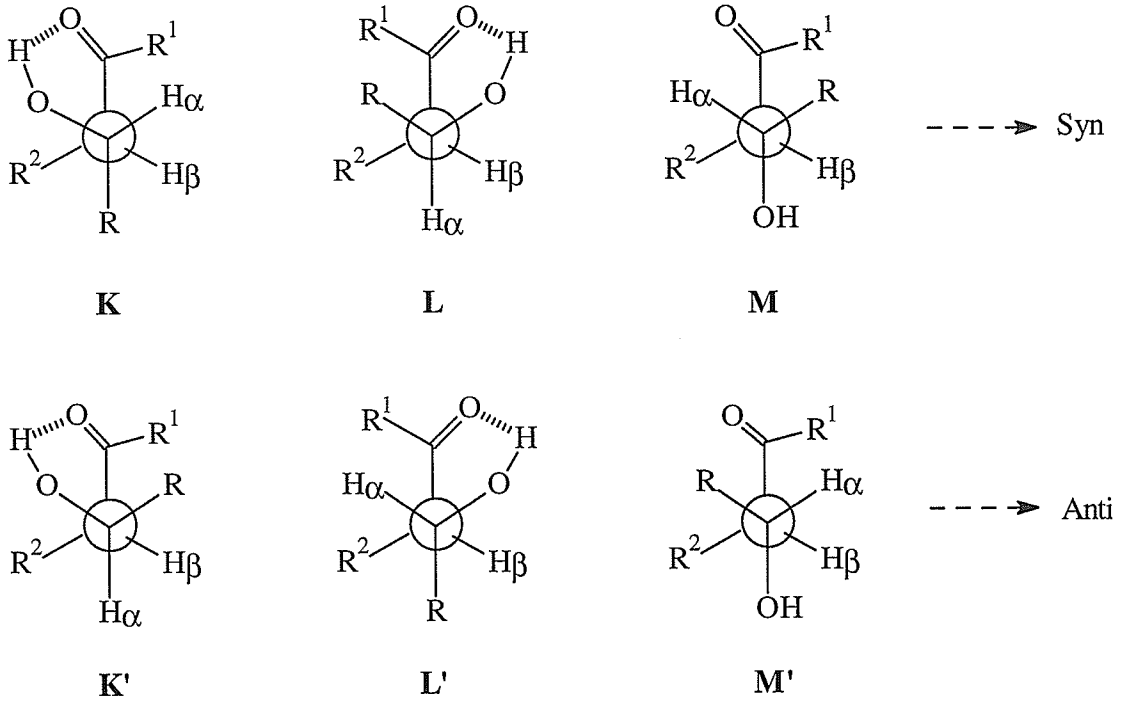

The coupling constants for H_α and H_β were determined for each of the methyl ester products obtained in this thesis (Table 2.11). As can be seen there is little difference between the $J_{\alpha\beta}$ values for the *syn* and the *anti* compounds. Compounds **129a** and **129b** appear at first glance to have almost identical coupling constants and chemical shifts for H_α and H_β. The $J_{\alpha\beta}$ values are borderline between the two idealized ranges described above. For both **130a** and **130b**, $J_{\alpha\beta}$ lies in the expected range (7 – 10 Hz) for *anti* compounds, while for **132a** and **132ab**, $J_{\alpha\beta}$ lies in the expected region (2 – 5 Hz) for *syn* compounds. It is therefore impossible to determine *syn/anti* configurations using this method. It is expected that the rotamers **M** and **M′** are significantly populated for these compounds.

Suitable crystals for X-ray crystallographic analysis were obtained for at least one compound of each of the diastereomeric pairs; **129b**, **131**, **130a** and **132b**. ORTEP plots of the crystal structures are shown on the following pages (For data tables see Appendix 1). The relative configurations of these compounds were thus assigned using X-ray crystallography.

Table 2.11: ^{1}H NMR data of adducts.

Compound	$J_{\alpha\beta}$ (Hz)	H_α and H_β δ (ppm)	
129a	6.6	4.39	4.00
129b	7.0	4.37	4.01
130a	8.8	4.78	5.11
130b	8.6	4.77	5.00
131	8.5	4.55	4.22
132a	5.2	4.25	2.81
132b	4.0	4.00	3.13

The *relative* stereochemistries of the DAG products were determined by transesterification to their methyl esters using NaOH/MeOH. Their HPLC retention times were compared to authentic samples of known relative configuration. Although isomerization does occur to some extent in the transesterification process, the relative stereochemistries of the major isomers could be determined by this method.

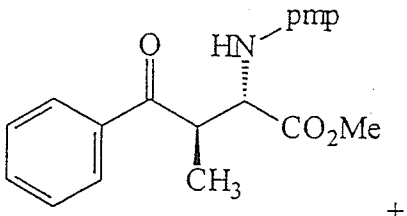
pmp
HN
O
CO2Me
CH3

+ enantiomer

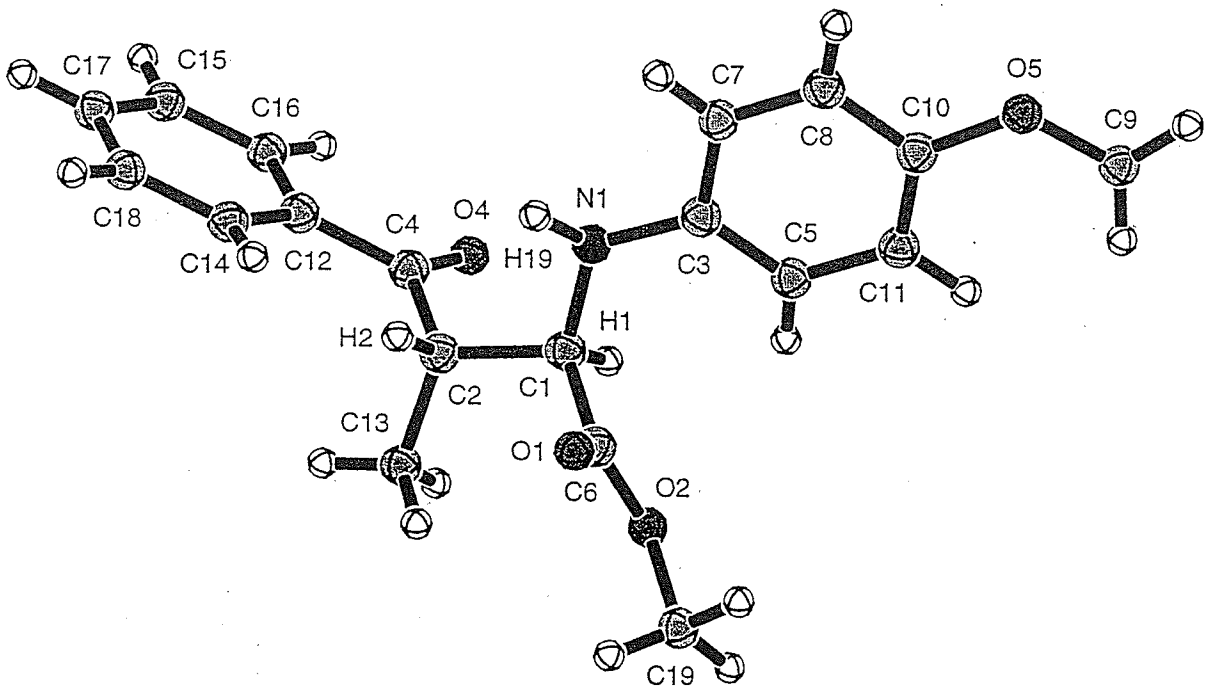
C17
C15
C16
C18
C14
C12
C4
O4
H19
N1
C7
C8
C10
O5
C9
C3
C5
C11
H2
H1
C2
C1
C13
O1
C6
O2
C19

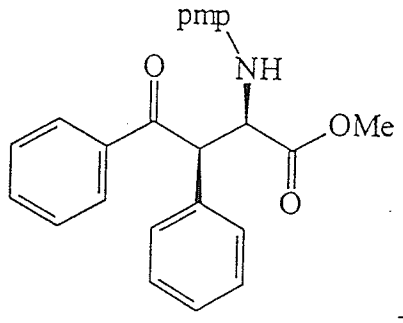
pmp
NH
O
OMe
O

+ enantiomer

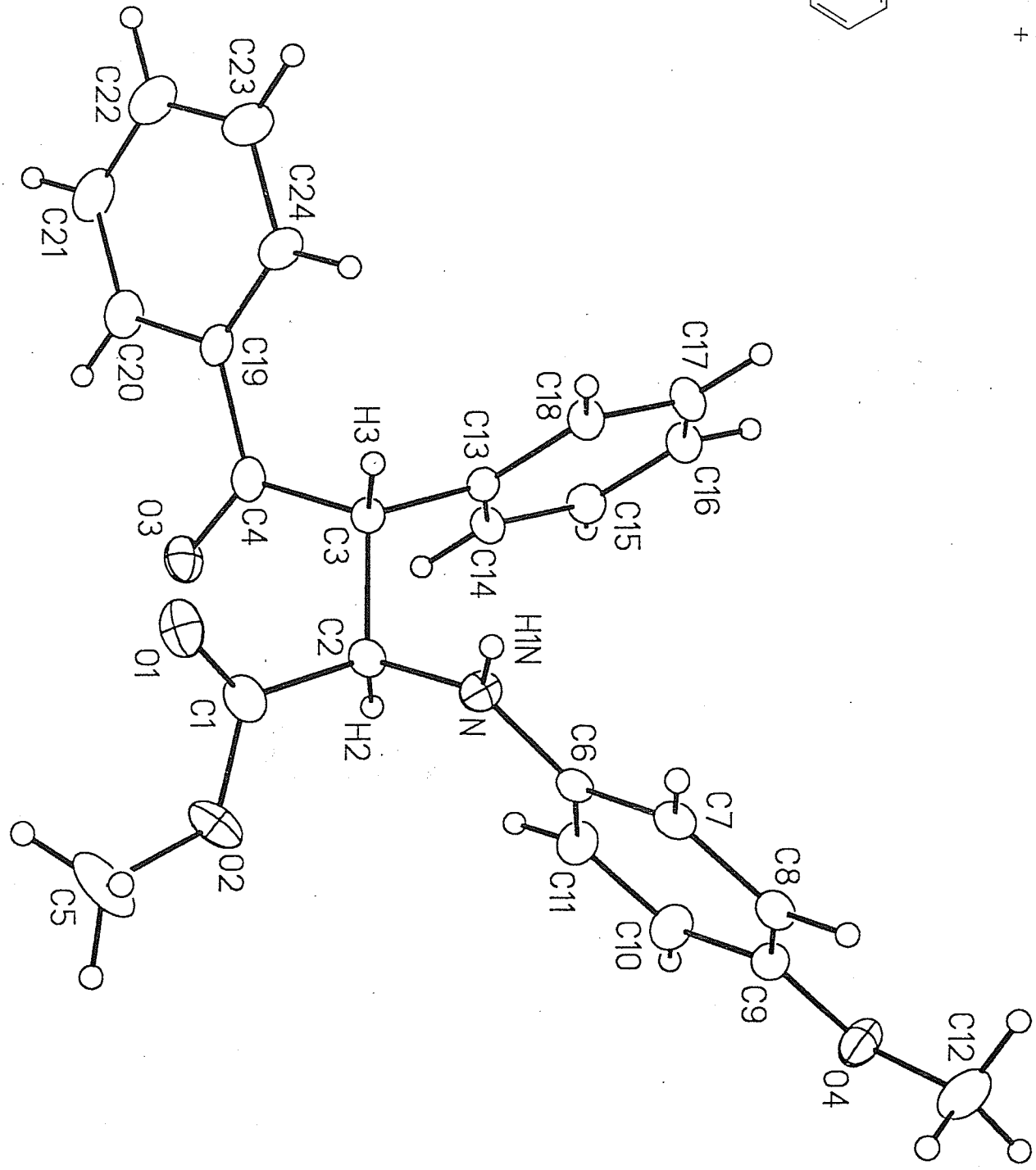
C22
C23
C24
C21
C20
C19
C17
C18
H3
C13
C16
C15
O3
C4
C3
C14
H1N
O1
C2
C1
H2
N
C6
C7
C8
C11
C10
C9
O2
C5
O4
C12

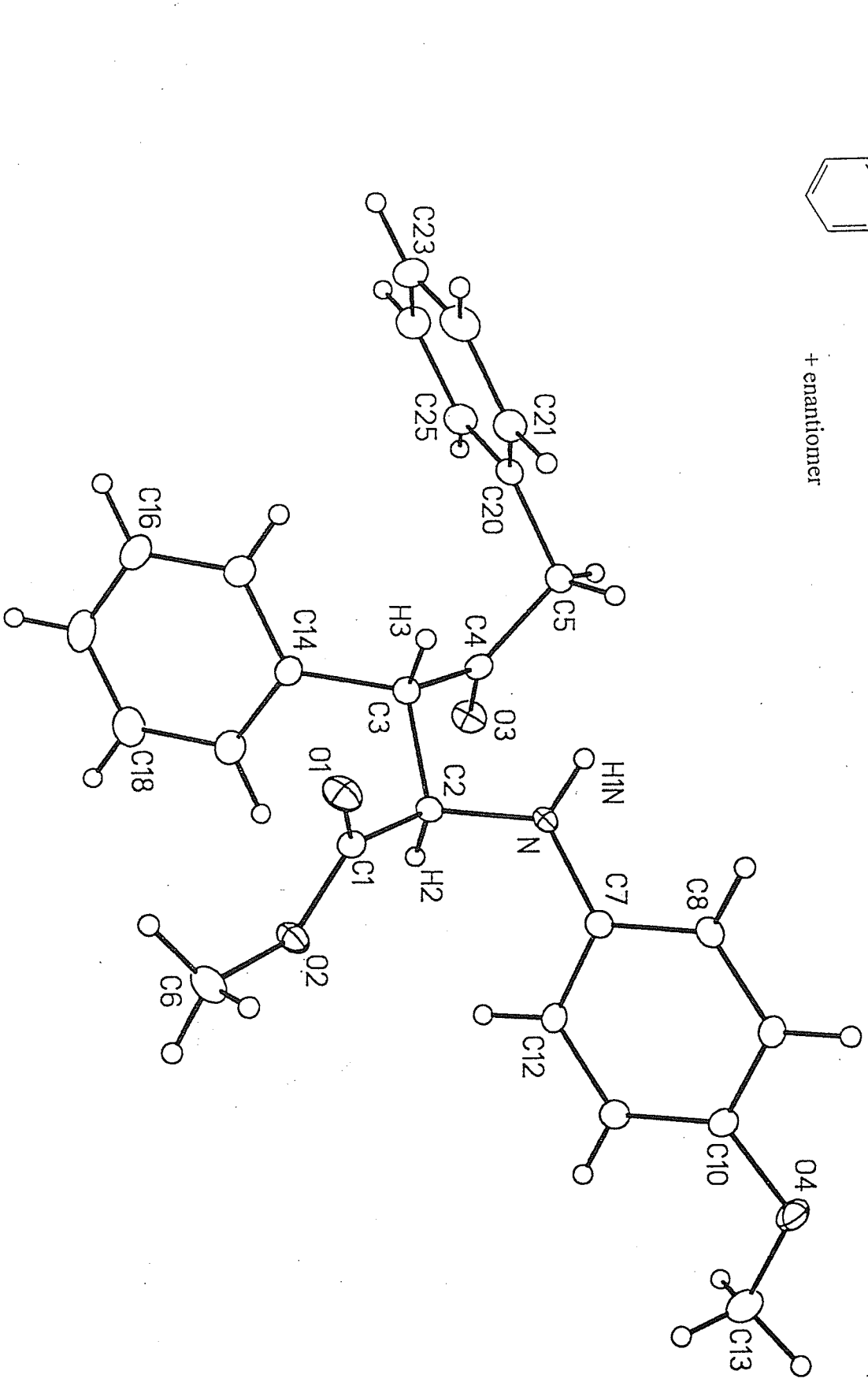
pmp
NH
O
OMe
+ enantiomer
C23
C25
C21
C20
C5
C16
C14
H3
C4
C3
O3
C18
O1
C2
H1N
N
C1
H2
C7
C8
O2
C6
C12
C10
O4
C13

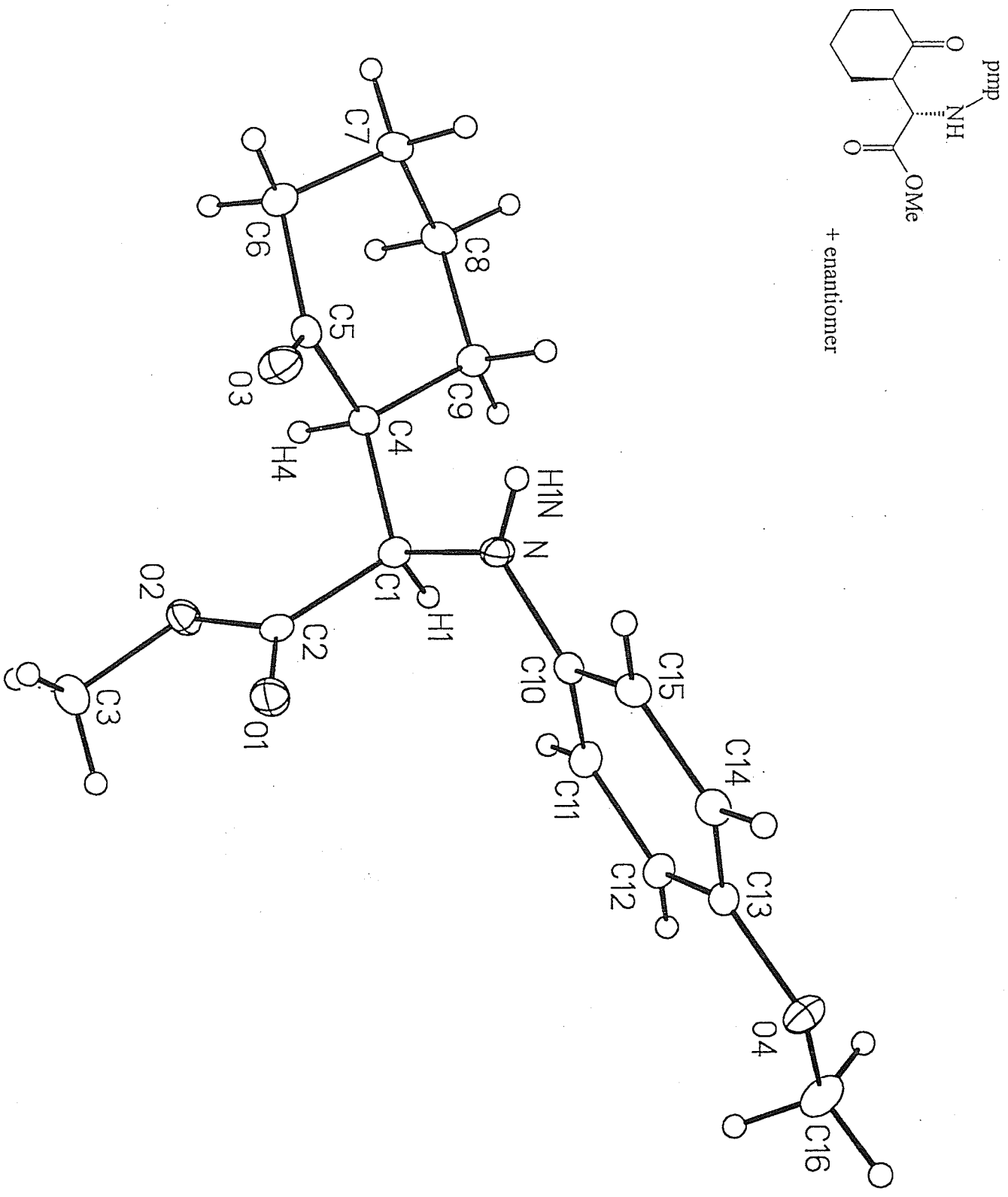
pmp
NH
O
OMe
+ enantiomer
C7
C6
C8
C5
O3
C9
C4
H4
H1N
N
C1
H1
O2
C2
O1
C3
C10
C15
C11
C14
C12
C13
O4
C16

Absolute Diastereoselectivity

Various approaches were tried to determine the *absolute* stereochemistry of these compounds. These included synthesis of camphorsulfonamide derivatives, Mosher's (MTPA) and MPA amides, transformation to literature compounds **140 – 142** (Figure 2.16) and synthesis of a palladium complex to analyze using circular dichroism (CD) spectra.

We hoped that crystal structures of the DAG esters would permit us to deduce the configurations of each of the compounds prepared. However, unlike the methyl ester derivatives, the DAG-esters did not produce suitable crystals for X-ray analysis. Derivatization with another crystalline chiral compound was therefore attempted. The *N*-pmp protecting group was removed from a mixture of **129a** and **129b** (~3:2) using ceric ammonium nitrate (CAN).[172] The free amine was then treated with (1*S*)-(+)-camphorsulfonyl chloride (Scheme 2.16) and Hunig's base to give a mixture of four compounds, in 75% yield, whose ^{1}H NMR spectra were consistent with compounds **143a-d**.

Scheme 2.16

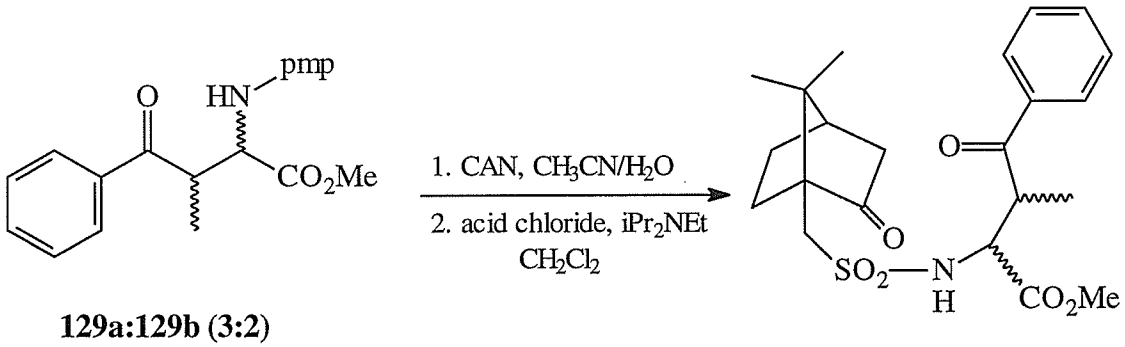

129a:129b (3:2)

143a-d

These compounds were separated by preparative HPLC. Unfortunately suitable crystals for X-ray analysis were not obtained; therefore the materials were not characterized further. Alternate ways to determine the absolute configurations of our products were sought.

Literature analogs of some of the compounds prepared are shown in Figure 2.16.[96,98] Compound **136b** was converted to **140** by solvolysis in Na*i*OPr/*i*PrOH. Comparison of the optical rotation of **140** prepared in this way with data from the literature permitted us to assign the configuration of the α center of our compound as *S* (Literature $[\alpha]_D$ = +30.4 (*c* 0.54 $CHCl_3$),[96] found +26.7 (*c* 0.06 $CHCl_3$)). Attempts to prepare **141** and **142** or their enantiomers from **133** and **139** respectively were unsuccessful.

Figure 2.16

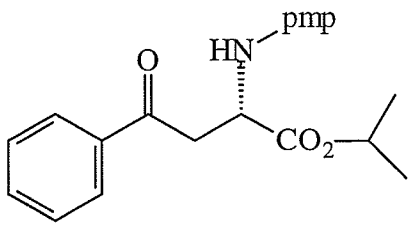

140

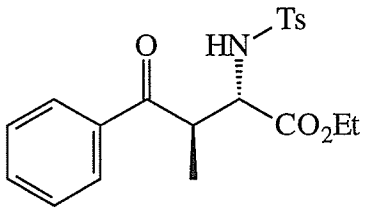

141

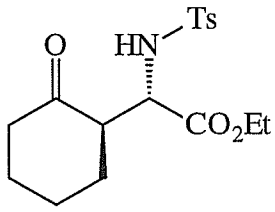

142

Tosylation of compounds' **133a-d** directly using $TsCl/Et_3N$ or TsCl/NaH were unsuccessful. Removal of the *N*-pmp substituent using ceric ammonium nitrate (CAN) followed by tosylation of the free amine was also unsuccessful.

Attempts to effect cleavage of either the DAG or methyl esters, or approaches to transesterify to active esters, were also problematic. Three typical approaches were tried:

acid catalysts, base catalysts and nucleophilic cleavage. These attempts are summarized in Table 2.12 for the methyl ester compound **131** and Table 2.13 for various DAG-esters.

Table 2.12. Cleavage attempts for methyl ester **131**.

Reagent, Conditions	Solvent	Time	Result (TLC)
0.1 N KOH (2 equiv)	EtOH/THF	3 d	several byproducts
LiOH (2 equiv)	THF	2.5 h	furan **137** (57%)
2 N HCl		1 h	p-anisidine recovered
Dowex 50 (H^+), Δ	H_2O/THF	16 h	s/m + byproducts
30% HBr/AcOH		2 d	s/m + diastereomer (10%)
1% w/v H_2SO_4 or AcOH	wet Et_2O	12 d	s/m
1 % w/v HCl or AcCl	wet Et_2O	12 d	several byproducts
1 % w/v pTsA	wet Et_2O	12 d	s/m + byproducts
1 % w/v TFA	wet Et_2O	12 d	s/m + byproducts
Subtilisin, 0.1 M buffer	DMF	6 d	s/m
Chymotrypsin, 0.1 M buffer	DMF	6 d	s/m

In summary, basic conditions[95,173] led to isomerization (presumably at the β-center, adjacent to the carbonyl) or to incomplete cleavage accompanied by production of several byproducts. For compound **131** attempts to cleave the methyl ester with LiOH/MeOH yielded a furan product **137** ($R^1 = CH_2Ph$, $R^2 = Ph$). As previously mentioned (Section 2.2.3), this result suggested that degradation of the DAG products was possible under the basic conditions of the reaction. Acidic reagents[83,85,95] either did

nothing, or promoted degradation of the starting material, giving several byproducts. Even for the DAG esters (Table 2.13), attempted transesterification using reagents such as NaSBu,[174] $Me_2AlStBu$,[175,176] or reagents such as LiOTMS[177] and KOTMS[178] (which are considered to react under relatively mild, neutral conditions) caused isomerization along with ester cleavage. Suitable conditions for enzymatic cleavage of the methyl ester with Subtilisin or Chymotrypsin[179,180] were not found.

Table 2.13. Methods tested to cleave **133** or **134** DAG esters.

Compounds	Reagents/Conditions	Solvent	Time	Results
133a-d	AcCl	MeOH	16 h	s/m
133a-d	TFA:$CHCl_3$ (1:1), Δ		30 min	byproducts, possibly acid
133a-d	pTsA RT→ Δ	MeOH	4 d	byproducts, possibly acid
133a-d	Dowex 50 (H^+), Δ	THF/H_2O	48 h	possible acid, could not purify
133a-d	$Me_2AlStBu$ (2 eq), 0 °C	CH_2Cl_2	2 d	s/m + 8% DAGOH
133a-d	KOTMS (1.1 eq)	THF	16 h	RCO_2K (80%) + DAGOH (100%)
133c	NaOMe (0.03 M)	MeOH	30 min	methyl ester-S:A 1:1
133c	NaOMe (0.03 M)	MeOH	5 min	methyl ester-S:A 2:1
133c	KCN (0.02 M)	MeOH	20 min	methyl ester-S:A 1.2:1
134a-c	NaSBu (1.5 eq)	THF	15 min	DAGOH + possible product
134a-c	LiOTMS (1.1 eq)	THF	2 d	s/m

Using X-ray analysis and transesterification techniques as mentioned earlier, the *relative* stereochemistry of the products had already been determined. It is therefore only necessary to determine the absolute stereochemistry at one center in the molecule. The other center will then be known by inference. The most straightforward method left was to determine the stereochemistry of the α center. Three methods were tried: synthesis of a palladium complex for CD study and derivatization of the amine to form the Mosher's[181] and MPA amides[182,183] for ^{1}H NMR study.

A survey of the literature uncovered a technique for determining the configuration of the α-center of an amino acid based on circular dichroism (CD).[184] Although CD techniques have been used for many years to find absolute configurations, interpreting the shape of the spectral curve for this purpose typically relies on knowing the conformation of the molecule in solution.[185] This new technique involved a palladium complex to which the amino acid binds in a predictable manner. The complex acts to lock the molecule into a rigid conformation about the α center. The sign of the Cotton Effect (CE) for a given wavelength can then be correlated to the configuration of the α center. Urriolabeitia and Diaz-de-Villegas[184,186,187] determined that *L*-amino acids give a negative CE band at 265 – 280 nm and a weaker positive CE band at 305 – 320 nm. *D*-amino acids give bands of opposite signs in these same regions. The palladium precursor **144** was synthesized using literature procedures (Scheme 2.17).[188]

Scheme 2.17

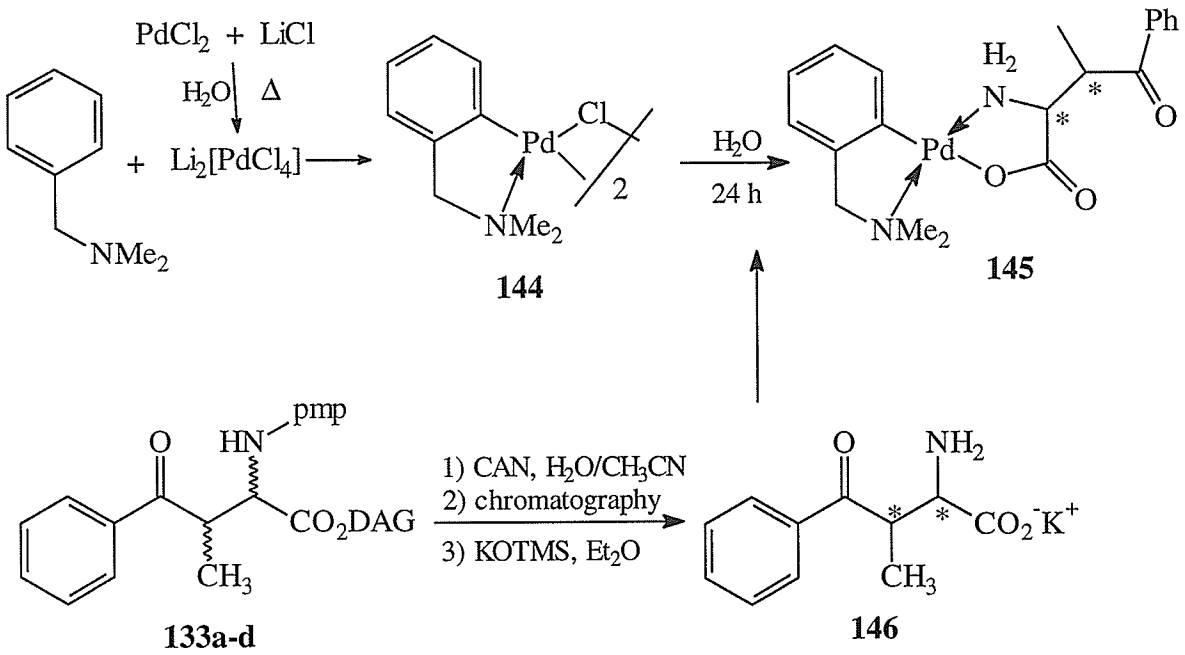

The *N*-pmp group was cleaved from a diastereomeric mixture of **133a-d**, and one diastereomer was found to separate from the other three by column chromatography. The glucose moiety of this diastereomer was then cleaved using KOTMS, and the resulting potassium salt **146** was condensed with the dimeric palladium complex to give **145**. ^{1}H NMR of **145** or **146** showed that isomerization had occurred during the cleavage of the glucose unit. Chromatographic, or crystallization methods to purify either of these compounds was not found.

The absolute configurations of amino acids may also be determined from the ^{1}H NMR spectra of amide derivatives formed from chiral reagents such as α-methoxyphenylacetic acid (MPA) and α-methoxytrifluoromethylphenylacetic acid (MTPA). These methods generally require that two conditions be met: (a) derivatives of a pure stereoisomer of an amino acid must be prepared using *both* enantiomers of MPA

or MTPA so that their ^{1}H NMR spectra can be compared, and (b) the derivatives must have one predominant conformer resulting in different shielding environments for the two α substituents. Analysis of the differences in various proton chemical shifts between the diastereomeric derivatives (i.e. $\Delta\delta^{SR}$ = δ (*S*-MTPA compound) – δ (*R*-MTPA compound)) then allows the configuration of the chiral center to be determined.

The Mosher's amides of **129a** and **129b** were studied (Scheme 2.18). A mixture of **129a** and **129b** (1.2:1) were *N*-deprotected using ceric ammonium nitrate, and condensed with the acid chloride prepared from (*R*)-MTPA.[189,190] The four amides **147a-d** were separated by HPLC and their ^{1}H NMR spectra were recorded.

Scheme 2.18

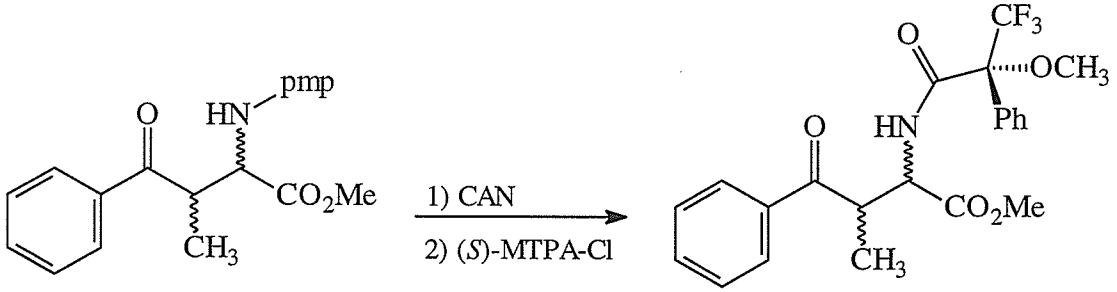

129a:129b, (1.2:1) **147a-d**

Typically the *R* and *S*-MTPA amides of the same diastereomer are prepared, however preparation of the *R*-MTPA amides from both members of an enantiomeric pair can be considered equivalent by ^{1}H NMR. For example, if enantiomeric compounds *RR* and *SS* are derivatized with (*R*)-MTPA the resulting compounds are *RR-R* and *SS-R*. However, *SS-R* is the enantiomer of *RR-S* and will therefore be indistinguishable by ^{1}H NMR. Mosher's model for such compounds predicts trends in $\Delta\delta^{SR}$ assuming that the

amide has only three conformers, defined by the CF_3–C–C=O dihedral. Two of the conformers are antiperiplanar (ap_1 and ap_2), differing only in the rotation of the phenyl ring plane (Figure 2.17). The third conformer is synperiplanar (sp), which is assumed to be the lowest in energy. The ^1H NMR spectrum is interpreted in terms of the shielding effects expected from the sp conformer.[181]

Figure 2.17

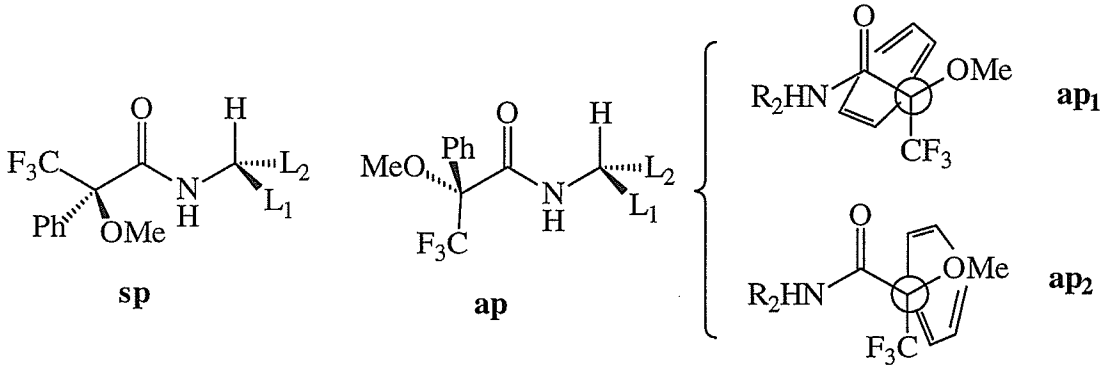

For an *L*-amino acid ester, $\Delta\delta^{S-R}$ of the ester substituent will be a positive value due to decreased shielding effects ($\Delta\delta^{S-R} > 0$). The configuration of the *L*-amino acids from each of the *syn* **147a,b** and *anti* **147c,d** pairs were assigned based on this premise. A comparison of the other $\Delta\delta^{S-R}$ values was then made (Table 2.14). As shown in the table, the *anti* pair of compounds gave consistent results with this hypothesis. The other hydrogens in the molecule all show increased shielding effects ($\Delta\delta^{S-R} < 0$). However for the *syn* pair the β-H and the methyl ester both exhibited decreased shielding effects ($\Delta\delta^{S-R} > 0$), which called into question the reliability of this method.

Table 2.14: ^{1}H NMR data for MTPA amides.

	$\Delta\delta^{S-R}$ in ppm	
Substituent	***Syn* 147(a-b)**	***Anti* 147(c-d)**
CO_2Me	+ 0.018	+ 0.027
β-H	+ 0.030	- 0.061
γ-Me	- 0.031	- 0.224
o-Ph	- 0.055	- 0.066
m-Ph		- 0.030
p-Ph	- 0.012	

The final approach involved a promising new technique based on MPA amides recently reported by Riguera et al.[183] The MPA amides have only two important conformers, the ap and the sp,[†] with the former being more stable (Figure 2.18).[191] Riguera's method employed Ba^{2+} complexation to stabilize the sp conformer preferentially. Riguera et al. reported that the shielding effects of the MPA phenyl group on protons in L_1 and L_2 changed in a predictable manner on complexation, and they gave an empirical rule for assigning the configuration of the α center based on the differences between the chemical shifts ($\Delta\delta^{Ba}$) observed in the absence and presence of Ba^{2+}.

[†]Conformer sp in the MTPA analog corresponds to conformer ap for MPA. For MTPA, CF_3 and C=O are used to define the ap/sp relationship, while OMe and C=O are used for MPA.

Figure 2.18

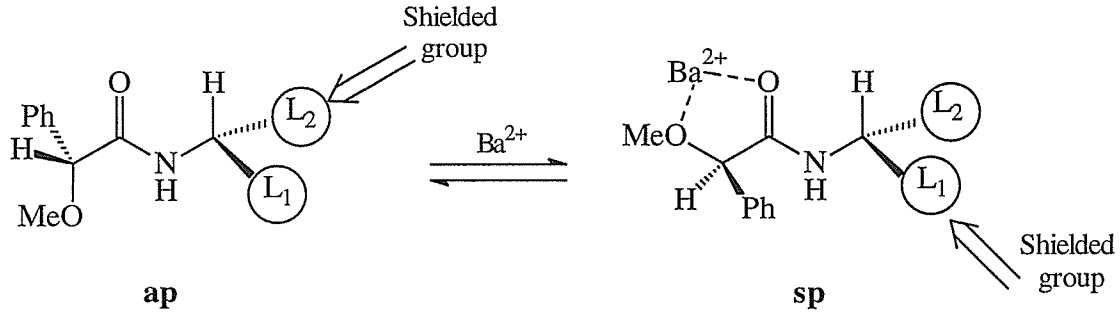

They demonstrated the successful application of this method to a variety of amines and amino acids. A further advantage was that both enantiomers of MPA were not needed, thus simplifying the process. We tested this technique on several of the prepared γ-oxo-α-amino acids.

In order to test the effects of Ba^{2+} complexation, (*R*)-MPA derivatives were prepared from the racemic γ-oxo-α-amino acid, methyl esters **128**, **130** and **131**. The resulting pairs of diastereomeric amides **148 – 150**, were separated whenever possible (Figure 2.19). In order to test whether isomerization was occurring in the synthesis of the amides, compound **148a** was also prepared from the enantiomerically and diastereomerically pure *S* amino acid **136b** obtained using our chiral auxiliary. No loss of stereochemical integrity was observed. Based on Riguera's observations, each member of a given pair prepared from the racemate was expected to display complementary behavior (i.e. the signs of $\Delta\delta^{Ba}$ observed for L_1 and L_2 should be opposite for each), consistent with presence of both an α-*R* and an α-*S* amide.

Figure 2.19

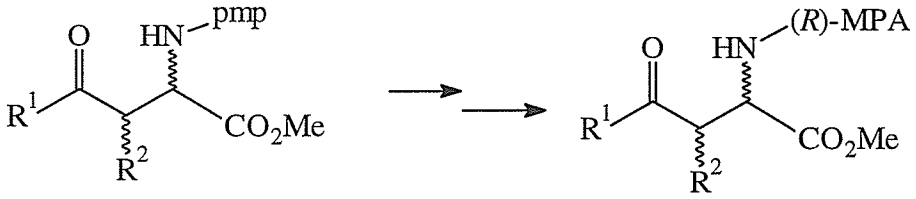

128	R^1 = Ph, R^2 = H	**148a** (2*S*) **148b** (2*R*)
130a	*syn* R^1 = Ph, R^2 = Ph	**149 a/b**
130b	*anti*	**149 c/d**
131	*anti* R^1 = CH_2Ph, R^2 = Ph	**150 a/b**

Table 2.15: ^{1}H NMR data for MPA adducts.

Compound	CO_2Me	β-H	γ-R_1 [b]
148a	- .001	+ .027 (+ .018)	+ .007 (+ .010)
148b	+ .027	+ .067 (+ .053)	+ .029
149a[a]	+ .013	–	–
149b[a]	+ .011	–	–
149c	- .025	- .035	+ .010 (+ .007)
149d	- .017	- .014	+ .003 (+ .003)
150a	- .006	- .022	- .012 (- .008)
150b	- .007	- .006	+ .002 (+ .003)

[a] Compounds were not separable. NMR data was obtained from the mixture of diastereomers.

[b] Data are for phenyl-ortho (meta), or for **150a/b**-CH_2.

The ^{1}H NMR spectra of the MPA amides were then obtained in CD_3CN before and after the addition of two equivalents of barium perchlorate (see examples in Appendix 2). The $\Delta\delta^{Ba}$ ((δ in presence of Ba) – (δ in absence of Ba)) values for signals expected to be diagnostic are displayed in Table 2.15.

For compound **148a**, there was a small increase in shielding on the ester group (L_1 in Figure 2.8, $\Delta\delta^{Ba}$ <0) and decreased shielding on the other substituents ($\Delta\delta^{Ba}$ >0) on addition of Ba^{2+}, consistent with Riguera et al.'s observations for the *S* configuration. However, for compound **148b** the method failed. The methyl ester group, as expected, showed decreased shielding ($\Delta\delta^{Ba}$ >0), but so did the two β hydrogens and the phenyl hydrogens. The other amides showed similar inconsistencies. The *anti* pair of amides **149c/d** both exhibited increased shielding of their ester groups and their β hydrogens ($\Delta\delta^{Ba}$ <0). The γ-phenyl hydrogens were deshielded in the cases where their shifts could be determined ($\Delta\delta^{Ba}$ >0). *Anti* compounds **150a/b** behaved similarly with both the ester and β hydrogens showing increased shielding ($\Delta\delta^{Ba}$ <0). The γ-CH_2's behaved differently, with **150a** displaying an increase and **150b** a decrease in shielding. For *syn* compounds **149c/d** both methyl esters were deshielded ($\Delta\delta^{Ba}$ >0). The β-H's in this pair overlapped with the α-H's and could not be distinguished. Because of these ambiguities, the MPA/Ba^{2+} method could not be used to determine the absolute configurations of our γ-oxo-α-amino acids.

Two distinct inconsistencies were observed in our experiments with these amides. First, with the exception of **148a/b**, in each pair of diastereomeric amides the resonances of the ester groups shifted in the same direction on addition of Ba^{2+}. Second, for a given

compound the signs of the $\Delta\delta^{Ba}$s observed for L_1 and L_2 were often the same. Several arguments can be proposed to explain these inconsistencies. The proximity of L_1 or L_2 to the MPA or MTPA phenyl ring and the ring plane orientation is considered to cause the shielding/deshielding influences in each rotamer. A conformationally mobile side chain containing another aromatic ring could interfere by creating other shielding influences that were unaccounted for in the model used. Also the MPA and the MTPA methods require that one conformer dominate at equilibrium. The presence of two or more conformers of similar energy could cause opposing shielding/deshielding influences that would result in smaller values for $\Delta\delta$ and reduce the reliability of the configurational assignment. This has been observed to occur for MTPA esters.[192] Alternatively, the γ-oxo functionality in MPA amides may provide competing modes of barium complexation. This could influence the conformation of the L_1/L_2 side chain instead of the ap/sp population as desired. Since the MPA/Ba^{2+} method is based on rationalizing the $\Delta\delta^{Ba}$ s resulting from the ap/sp conformational shift, it might not give consistent results in such cases.

Conclusions

Two research projects presented at the beginning of this thesis were successfully undertaken. Both approaches were based on the synthesis and use of carbohydrate auxiliary systems.

First, a rigid bicyclic carbohydrate template **109** was prepared. Alkylation reactions with methyl iodide, allyl bromide and ethyl bromide were then carried out using this template. Compound **109** showed excellent diastereofacial control (>98%) for the monoalkylated product in each of these reactions. With the less reactive nucleophiles, dialkylation was significant. This dialkylation is postulated to be a result of an 'internal proton return' mechanism. Aggregation of the lithium enolates was also implicated in the low yields obtained as trapping studies with TBDMSCl, indicated that the enolate was being formed quantitatively. Use of the P4 base was required for less reactive electrophiles. The template **109** was also tested in aldol reactions with benzaldehyde. Standard aldol and Mukaiyama methods were attempted. Again the template showed excellent diastereofacial control (>98%) to the oxazinone ring. Facial control of the aldehyde was lower in these reactions.

A mild method was found to remove the new amino acid from the auxiliary. Removal of the *N*-CBz group using H_2 and Pd/C occurred rapidly. Minimal workup to remove the catalyst and diluting the mixture with acidic methanol resulted in the cleavage of the ester and anomeric linkages in one step. The sugar and free amino acid could both be recovered in excellent yield.

Two limitations of the system were the modest yields and the occurrence of dialkylation, which could not be completely overcome. The glucose-based oxazinone did have many characteristics of a good auxiliary based system. The starting materials were inexpensive. The starting template was easily prepared from common reagents in good overall yield. The reactions themselves showed high diastereocontrol. After the reactions, the auxiliary could be removed and isolated quantitatively under mild conditions.

The second approach involved the synthesis of chiral diacetone D-glucose glyoxylimine **123**. An achiral methyl glyoxylimine (**121**) was used in model studies. These imines were readily prepared and isolated in good yields. Mannich or aldol-like reactions were then carried out with these reagents. The model achiral imine (**121**) showed slight *syn* selectivity ($\leq$2:1) in Mukaiyama reactions with the silyl enol ethers of various ketones. An exception to this was the reaction with the silyl enol ether of diphenylacetone, which gave only one product, *anti* isomer **131**. A change to titanium enolate reactions showed a change in selectivity in favor of the *anti* products with propiophenone. The bulk of the titanium enolate was shown to have a significant effect on the overall diastereoselectivity. The smaller enolate prepared with $TiCl_4$ showed low selectivity (de, 20%), while Ti(*i*OPr)$_4$ gave much better results (de, 90%). These observations gave a starting point for the chiral auxiliary based system.

With chiral imine **123**, reactions of the titanium enolate with propiophenone gave consistently low *syn*:*anti* selectivity ($\leq$3.5:1) for products **133**. The amount of isomer **133a** obtained, varied with the metal used in the enolate. A significant improvement in the *anti* diastereoselectivity was obtained by inverting the order of reagent addition and

having both partners cooled to the reaction temperature. With the lithium enolate, **133a** was prepared with 92% de. The *syn*:*anti* selectivity could not be improved. Yields for these reactions were modest at best. A change to the cerium enolate improved the yield (71%) at some sacrifice to selectivity (de, ≤88%). Other ketones tested generally did not fair as well. The most ideal system was obtained using deoxybenzoin with **123**. Only one isomer, *anti* **134a**, was observed indicating an ideal match had been found. However the yields for this system were lower then usual (32%).

Two limiting conditions of this system were identified. The metal used in the enolate had significant effect on the reaction, and directly affected the yield obtained. The loss of yield is attributed to decomposition of the enolate with concurrent loss of the sugar. This decomposition was promoted by the acidic nature of the hydrogen α to the carbonyl and the excess base used in the reaction.

Removal of the *N*-protecting group and the ester groups and assignment of the absolute stereochemistries of each product turned out to be problematic. Removal of the *N*-pmp group could be carried out with relative ease. Attempts to characterize the products through derivatization with MPA, MTPA or camporsulfonamide groups by ^{1}H NMR or X-ray techniques were not successful. Various attempts to remove the sugar met with limited success.

In this project, the carbohydrate provided less stereocontrol than did the previous oxazinone based system. The flexibility of this auxiliary system and the remoteness of the reactive center to the auxiliary appeared to reduce the systems effectiveness. The sensitivity of the γ-oxo-α-amino acid adducts to various cleavage conditions had the most significant effect making the removal of the sugar auxiliary difficult to achieve.

Experimental

General.

Solvents and reagents were dried and/or purified using standard procedures.[193] Diacetone D-glucose was recrystallized from ether. *p*-Anisidine was sublimed at 40 °C under vacuum. $CeCl_3$ was dried in a drying pistol with slow heating to 140 °C. Removal of urea impurities from DCC was accomplished by dissolving DCC in CH_2Cl_2, filtering and then evaporating the solvent. Reactions requiring an inert atmosphere were conducted under a positive pressure of argon or nitrogen in glassware oven dried overnight at 120 – 140 °C. Reaction temperatures recorded are bath temperatures. 'Drying' of organic extracts refers to the use of anhydrous $MgSO_4$.

Nuclear magnetic resonance spectra were acquired on Bruker AM 300 or AMX 500 instruments in $CDCl_3$ at 300 K unless otherwise noted. Compounds were visualized on analytical thin layer chromatograms (TLC) by UV light or by 5% H_2SO_4 in ethanol. Flash chromatography was performed on silica gel 60, eluting with the solvent mixtures indicated. Melting points were determined in open capillaries and are uncorrected. Optical rotations were recorded at room temperature in a microcell, 1 dm path length. Diastereomers were separated by HPLC using Porasil® μ–1 analytical and μ–5 preparative columns eluting with ≤1% *i*PrOH/hexanes. High-resolution mass spectra (HRMS) were acquired on a VG7070E-HF mass spectrometer using EI and FAB ionization. Microanalyses were obtained on pure compounds or diastereomeric mixtures by Guelph Laboratories, Guelph, ON. Where applicable, analyses are reported for the

major diastereomer only. X-ray crystal structures were acquired at the University of Alberta (Dr. Robert McDonald) or the University of Manitoba (Ms. Angela Toms).

The various $XTi(OR)_n$ species were synthesized according to the procedure of Denmark.[166]

N-(β-D-Glucopyranosyl)-*N*-(benzyloxycarbonyl)glycine ethyl ester (108).

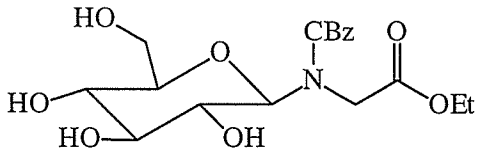

N-(β-D-Glucopyranosyl)glycine ethyl ester[137,138] (**107**) (5.00 g, 18.9 mmol) was added to dry DMF (25 mL) and flame dried 4Å molecular sieves (1 g). The solution was cooled to 0 °C. Di(isopropyl)ethylamine (3.60 mL, 20.7 mmol) was added, followed by dropwise addition of benzyl chloroformate (4.0 mL, 28.0 mmol). After 2.5 h, the solution was filtered through Celite and concentrated under vacuum. The residue was evaporated twice with small portions of toluene, and dried under high vacuum. Column chromatography (1 : 1 → 1 : 2, hexanes : EtOAc) gave **108** (6.17 g, 82%).

^{1}H NMR (DMSO-d_6, 383 K): δ 1.18 (t, 3H, J = 7.1 Hz, CH_3), 3.14-3.36 (m, 4H, H-2, H-3, H-4, H-5), 3.50 (ddd, 1H, J = 11.6, 4.8 and 5.6 Hz, H-6), 3.69 (ddd, 1H, J = 11.6, 2.6 and 5.1 Hz, H-6′), 3.82 (dd, 1H, J = 5.1 and 5.6 Hz, O*H*), 3.94 (d, 1H, J = 17.5 Hz, C*H*CO), 4.07 (d, 1H, J = 17.5 Hz, C*H*CO), 4.12 (q, 2H, J=7.1 Hz, CH_2CH$_3$), 4.29 (d, 1H,

J = 4.1 Hz, O*H*), 4.45 (d, 1H, *J* = 4.8 Hz, O*H*), 4.49 (d, 1H, *J* = 3.4 Hz, O*H*), 5.07 (d, 1H, *J* = 8.9 Hz, H-1), 5.14 (s, 2H, CH_{2CBz}), 7.35 (m, 5H, H_{Ar}).

(4a*R*,6*R*,7*R*,8*S*,8a*R*)-4-(Benzyloxycarbonyl)-6-(pivaloyloxy)methyl-7,8-bis(pivaloyloxy)-6H-pyrano[3,2-b]-1,4-oxazin-2-one (109).

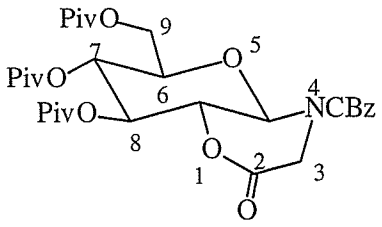

Ester **108** (2.0 g, 5.0 mmol) was dissolved in EtOH (10 mL) and aqueous NaOH (0.3 M, 20 mL, 6 mmol) was added. After 1.5 h the solution was adjusted to pH 8.5 – 9.0 with Amberlite IR-120 (H^+) resin. The solution was filtered and concentrated. The residue was re-evaporated from toluene to give the crude sodium salt.

The salt was suspended in dry pyridine (15 mL) containing a catalytic amount of DMAP (0.03 g, 0.25 mmol). Pivaloyl chloride (6.2 mL, 50 mmol) was added dropwise *via* syringe. After 1 h, the mixture was heated to 40 °C for 16 h. The solution was concentrated, and the residue was re-evaporated from toluene. The crude material was adsorbed onto silica gel (10 mL) and applied to dry silica (4 cm × 5.5 cm) in a fritted funnel. Portion wise elution (6 : 1, hexanes : EtOAc) gave 2.52 g (83%) of white powder, which was crystallized from methanol, yielding 2.12 g (70%) of **109**.

Fine needle-like crystals. Mp 210–211 °C.

^{1}H NMR ($CDCl_3$): δ 1.16, 1.18, 1.21 (3 × s, 27H, C(CH_3)$_3$), 3.90 (br m, 1H, H-6), 4.05 (d, 1H, J = 17.0 Hz, H-3), 4.10-4.20 (m, 2H, H-9, H-9′), 4.27 (dd, 1H, J = 9.5 and 10.1 Hz, H-8a), 4.85 (br d, 1H, J = 17.0 Hz, H-3′), 5.00 (d, 1H, J = 9.5 Hz, H-4a), 5.15-5.26 (m, 3H, CH_{2CBz}, H-7), 5.52 (dd, 1H, J = 10.1 and 8.9 Hz, H-8), 7.30-7.40 (m, 5H, H_{Ar}).

^{13}C NMR ($CDCl_3$): δ 26.5, 27.0, 27.1 (C(CH_3)$_3$), 38.8, 38.9 (C(CH$_3$)$_3$), 44.4 (C-3), 61.4 (C-9), 67.7 (C-7), 68.7 (CH_{2CBz}), 71.0 (C-8), 74.6 (C-8a), 74.9 (C-6), 81.3 (C-4a), 128.1, 128.6, 128.7 (C_{Ar}), 135.2, (4° C_{Ar}), 154.4 (C=O$_{CBz}$), 166.3 (C=O$_{oxazinone}$), 176.4, 176.9, 177.9 (C=O$_{piv}$).

Anal. Calcd. for $C_{31}H_{43}NO_{11}$: C, 61.47; H, 7.16; N, 2.31. Found: C, 61.38; H, 7.24; N, 2.23.

$[\alpha]_D$ = +47.2 (*c* 0.50, $CHCl_3$).

(3*S*,4a*R*,6*R*,7*R*,8*S*,8a*R*)-3-Methyl-4-(benzyloxycarbonyl)-6-(pivaloyloxy)methyl-7,8-bis(pivaloyloxy)-6H-pyrano[3,2-b]-1,4-oxazin-2-one (110).

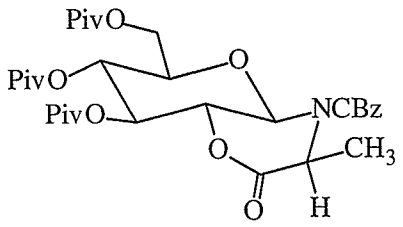

A solution of oxazinone **109** (242.3 mg, 0.4 mmol) in THF (4.5 mL) and HMPA (0.5 mL) was cooled to –95 °C. A solution of freshly prepared LiHMDS* in THF (1 M,

440 μL, 0.440 mmol) was added. The mixture was stirred at –95°C for 1 h, then methyl iodide (250 μL, 4.02 mmol) was added. After 1.5 h, the reaction was quenched by pouring into water (15 mL). The aqueous layer was extracted with Et_2O (2 × 15 mL). The organic layers were combined, washed with water (2 × 10 mL), dried, and evaporated to provide an oil. Chromatography (4 : 1, hexanes : EtOAc) afforded **110** (131.5 mg, 57%) as a glassy solid, as well as unreacted **109** (18.5 mg).

*__Note__: Other bases or solvents used as described in Table 2.1.

Glass-like solid. Mp 152–153 °C.

^{1}H NMR ($CDCl_3$): δ 1.16, 1.20, 1.22 (3 × s, 27H, C(CH_3)$_3$), 1.64 (d, 3H, J = 7.6 Hz, CH_3), 3.86 (ddd, 1H, J = 10.1, 4.5 and 1.7 Hz, H-6), 4.10 (dd, 1H, J = 4.5 and 12.6 Hz, H-9), 4.19 (dd, 1H, J = 1.7 and 12.6 Hz, H-9′), 4.31 (dd, 1H, J = 9.6 and 10.0 Hz, H-8a), 4.95 (d, 1H, J = 9.6 Hz, H-4a), 4.97 (q, 1H, J = 7.6 Hz, H-3′), 5.18 (dd, 1H, J = 8.9 and 10.1 Hz, H-7), 5.20 (m, 2H, CH_{2Cbz}), 5.45 (dd, 1H, J = 10.0 and 8.9 Hz, H-8), 7.35-7.45 (m, 5H, H_{Ar}).

^{13}C NMR ($CDCl_3$): δ 19.8 (CH_3), 27.0, 27.1 (C(CH_3)$_3$), 38.8, 38.9 (C(CH_3)$_3$), 52.5 (C-3), 61.4 (C-9), 67.9 (C-7), 68.5 (CH_{2Cbz}), 71.3 (C-8), 73.3 (C-8a), 74.9 (C-6), 80.7 (C-4a), 128.0, 128.6, 128.7 (C_{Ar}), 135.3, (4° C_{Ar}), 154.5 (C=O_{CBz}), 168.4 (C=$O_{oxazinone}$), 176.5, 176.9, 177.8 (C=O_{piv}).

Anal. Calcd. for $C_{32}H_{45}NO_{11}$: C, 62.02; H, 7.32; N, 2.26. Found: C, 62.07; H, 7.43; N, 2.23.

$[\alpha]_D$ = +53.4 (*c* 0.50, $CHCl_3$).

(4a*R*,6*R*,7*R*,8*S*,8a*R*)-3,3-Dimethyl-4-(benzyloxycarbonyl)-6-(pivaloyloxy)methyl-7,8-bis(pivaloyloxy)-6H-pyrano[3,2-b]-1,4-oxazin-2-one (111).

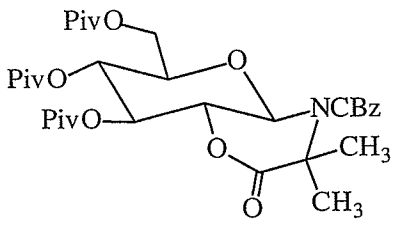

A crude mixture of **109** and **110** (~0.3 mmol) in THF (1 mL) and HMPA (0.2 mL) was cooled to –78 °C. LiHMDS in THF was added (1.1 M, 0.45 mL) followed by MeI (186 μL, 30 mmol). The reaction was allowed to warm slowly over 2 h to 0 °C. The mixture was then worked up as for **110**. Chromatography (6 : 1, hexanes : EtOAc) gave products **111** (30 mg) and **110** (16.4 mg).

Glass-like solid. Mp 59–61 °C.

^{1}H NMR ($CDCl_3$): δ 1.14, 1.19, 1.21 (3 × s, 27H, C(CH_3)$_3$), 1.75, 1.88 (2 × s, 6H, CH_3), 3.71 (ddd, 1H, J = 10.1, 3.5, and 2.2 Hz, H-6), 3.9-4.0 (m, 2H, H-9, H-9′), 4.28 (dd, 1H, J = 9.4 and 9.9 Hz, H-8a), 4.97 (d, 1H, J = 9.4 Hz, H-4a), 5.14 (d, 1H, J = 12.2 Hz, CH_{CBz}), 5.17 (dd, 1H, J = 8.9 and 10.1 Hz, H-7), 5.19 (d, 1H, J = 12.2 Hz, CH_{CBz}), 5.40 (dd, 1H, J = 9.9 and 8.9 Hz, H-8), 7.3-7.4 (m, 5H, H_{Ar}).

^{13}C NMR ($CDCl_3$): δ 26.6 (CH_3), 27.0, 27.05, 27.1 (C(CH_3)$_3$), 27.3 (CH_3) 38.8, 38.9 (C(CH_3)$_3$), 61.0, 61.1 (C-3, C-9), 67.7 (C-7), 68.8 (CH_{2Cbz}), 71.5 (C-8), 72.6 (C-8a), 74.5 (C-6), 81.2 (C-4a), 128.1, 128.5, 128.6 (C_{Ar}), 135.6, (4° C_{Ar}), 153.8 (C=O_{CBz}), 170.6 (C=$O_{oxazinone}$), 176.3, 177.0, 177.8 (C=O_{piv}).

Anal. calcd. for $C_{33}H_{47}NO_{11}$: C, 62.54; H, 7.47; N, 2.21. Found: C, 62.47; H, 7.68; N, 2.17.

$[\alpha]_D$ = +46.4 (*c* 0.50, $CHCl_3$).

(3*S*,4a*R*,6*R*,7*R*,8*S*,8a*R*)-3-Allyl-4-(benzyloxycarbonyl)-6-(pivaloyloxy)methyl-7,8-bis(pivaloyloxy)-6H-pyrano[3,2-b]-1,4-oxazin-2-one (112) and (4a*R*,6*R*,7*R*,8*S*,8a*R*)-3,3-diallyl-4-(benzyloxycarbonyl)-6-(pivaloyloxy)methyl-7,8-bis(pivaloyloxy)-6H-pyrano[3,2-b]-1,4-oxazin-2-one (113).

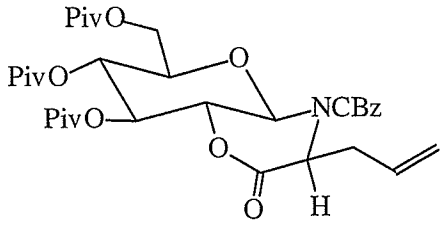

112

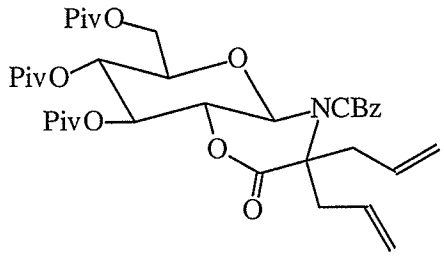

113

Oxazinone **109** (91 mg, 0.15 mmol) was dissolved in THF (1 mL). Allyl bromide (130 μL, 1.5 mmol) was added and the solution was cooled to –78 °C. A solution of LiHMDS* in hexanes (1 M, 225 μL, 0.225 mmol) was then added. The mixture was stirred for 1 h, but no reaction was observed. HMPA (150 μL) was added to the vigorously stirred solution and the reaction was allowed to proceed for 20 min. The flask was removed from the cooling bath, and phosphate buffer (2 mL, 1M, pH 7) was added, followed by Et_2O (5 mL). The solution was poured into Et_2O (15 mL) and the phases

were separated. The organic layer was washed with water (3 × 2 mL), dried and evaporated. Column chromatography (9 : 1, hexanes : EtOAc) yielded **113** (25.1 mg, 25%), **112** (22 mg, 23.2%) and unreacted **109** (2.2 mg).

*__Note__: Other HMDS salts used as described in Table 2.2. Same procedure used in attempted ethylation of **109**.

112: Mp 137.5–138.5 °C.

^{1}H NMR ($CDCl_3$): δ 1.16, 1.19, 1.22 (3 × s, 27H, C(CH_3)$_3$), 2.70 (m, 2H, CH_{2allyl}) 3.86 (m, 1H, H-6), 4.08 (dd, 1H, J = 4.2 and 12.5 Hz, H-9), 4.19 (dd, 1H, J = 1.9 and 12.5 Hz, H-9′), 4.37 (dd, 1H, J = 9.6 and 10.0 Hz, H-8a), 4.90 (br m, 1H, H-3′), 4.95 (d, 1H, J = 9.6 Hz, H-4a), 5.1-5.3 (m, 5H, H-7, CH_{2Cbz}, CH_{2vinyl}), 5.44 (dd, 1H, J = 10.0 and 8.9 Hz, H-8), 5.82 (dddd, 1H, J = 7.3, 7.3, 10.1 and 16.8 Hz, CH_{vinyl}), 7.35-7.45 (m, 5H, H_{Ar}).

^{13}C NMR ($CDCl_3$): δ 27.0, 27.1 (C(CH_3)$_3$), 38.3 (CH_{2allyl}), 38.8, 38.9 (C(CH_3)$_3$), 56.7 (C-3), 61.2 (C-9), 67.8 (C-7), 68.5 (CH_{2Cbz}), 71.3 (C-8), 73.1 (C-8a), 74.8 (C-6), 80.7 (C-4a), 119.8 (CH_{2vinyl}), 127.9, 128.5, 128.6 (C_{Ar}), 131.5 (CH_{vinyl}), 135.3 (4° C_{Ar}), 154.8 (C=O_{Cbz}), 167.3 (C=$O_{oxazinone}$), 176.4, 176.9, 177.8 (C=O_{piv}).

Anal. Calcd. for $C_{34}H_{47}NO_{11}$: C, 63.24; H, 7.34; N, 2.17. Found: C, 63.12; H, 7.46; N, 2.08.

$[\alpha]_D$ = +54.4 (*c* 0.32, $CHCl_3$).

113: Mp 131–133 °C.

^{1}H NMR ($CDCl_3$): δ 1.13, 1.18, 1.22 (3 × s, 27H, C(CH_3)$_3$), 2.67 (dd, 1H, J = 13.6 and 8.6 Hz, $CH_{\beta allyl}$), 2.84 (ddd, 1H, J = 14.3, 5.6 and 1.5 Hz, $CH_{\alpha allyl}$), 3.15 (ddd, 1H, J =

13.6, 6.4 and 1.0 Hz, C$H_{\beta allyl}$), 3.35 (dd, 1H, J = 14.3 and 8.9 Hz, C$H_{\alpha allyl}$), 3.70 (ddd, 1H, J = 10.0, 3.0 and 2.5 Hz, H-6), 3.95 (m, 2H, H-9, H-9′), 4.23 (dd, 1H, J = 9.3 and 10.0 Hz, H-8a), 4.80 (d, 1H, J = 9.3 Hz, H-4a), 4.9-5.1 (m, 2H, C$H_{2\alpha vinyl}$), 5.14 (dd, 1H, J = 8.9 and 10.0 Hz, H-7), 5.12 (d, 1H, J = 12.1 Hz, CH_{CBz}), 5.22 (d, 1H, J = 12.1 Hz, CH_{CBz}), 5.18-5.26 (m, 2H, C$H_{2\beta vinyl}$), 5.37 (dd, 1H, J = 10.0 and 8.9 Hz, H-8), 5.45 (dddd, 1H, J = 5.6, 8.9, 10.4 and 16.7 Hz, C$H_{\alpha vinyl}$), 5.89 (dddd, 1H, J = 6.4, 8.6, 10.5, and 17.0 Hz, C$H_{\beta vinyl}$), 7.35-7.45 (m, 5H, H_{Ar}).

^{13}C NMR ($CDCl_3$): δ 27.0, 27.1 (C(CH_3)$_3$), 38.7, 38.9 (C(CH_3)$_3$), 42.1, 43.5 (CH_{2allyl}), 60.9 (C-9), 67.6 (C-7), 67.9 (CH_{2Cbz}), 69.8 (C-3), 71.2 (C-8), 72.4 (C-8a), 74.2 (C-6), 80.4 (C-4a), 120.5, 120.7 (CH_{2vinyl}), 128.2, 128.5, 128.6 (C_{Ar}), 131.3, 132.5, (CH_{vinyl}), 135.5 (4° C_{Ar}), 154.1 (C=O_{CBz}), 169.6 (C=$O_{oxazinone}$), 176.3, 177.0, 177.7 (C=O_{piv}).

Anal. Calcd. for $C_{37}H_{51}NO_{11}$: C, 64.80; H, 7.50; N, 2.04. Found: C, 64.75; H, 7.65; N, 2.00

$[\alpha]_D$ = +78.0 (*c* 0.50, $CHCl_3$).

Allylation of 109 using P4 Base.

Following the procedure of Pietzonka and Seebach,[194] oxazinone **109** (30 mg, 0.05 mmol) in THF (0.5 mL) at –95 °C was treated with allyl bromide (13 μL, 0.15 mmol) and a solution of P4 base in hexanes (1M, 0.055 mmol, 55 μL). After 40 min the solution was warmed and the solvent evaporated. The residue was re-dissolved in Et_2O and

filtered. Chromatography (6 : 1, hexanes : EtOAc) of the crude product gave **113** (16.4 mg, 52.7%), **112** (5.8 mg, 16.7%) and recovered **109** (2.5 mg).

(3*S*,4a*R*,6*R*,7*R*,8*S*,8a*R*)-3-Ethyl-4-(benzyloxycarbonyl)-6-(pivaloyloxy)-methyl-7,8-bis(pivaloyloxy)-6H-pyrano[3,2,b]-1,4-oxazin-2-one (114) and (4a*R*,6*R*,7*R*,8*S*,8a*R*)-3,3-diethyl-4-(benzyloxycarbonyl)-6-(pivaloyloxy)methyl-7,8-bis(pivaloyloxy)-6H-pyrano[3,2,b]-1,4-oxazin-2-one (115).

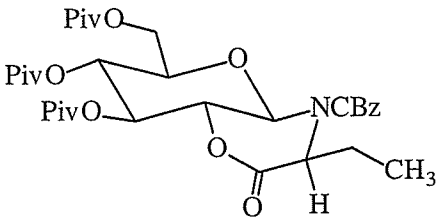

114

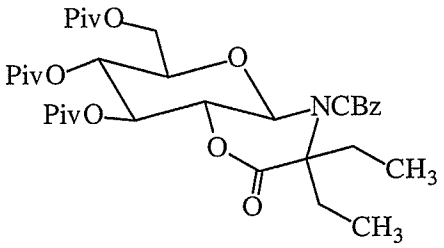

115

Following the procedure of Pietzonka and Seebach,[194] oxazinone **109** (60 mg, 0.1 mmol) and ethyl bromide (37 μL, 0.5 mmol) were dissolved in THF (1.0 mL) and the solution cooled to –95 °C. P4 base (1M, 0.1 mmol, 0.1 mL) was added. After 20 min the solution was worked up as above for the allylation. Chromatography (6 : 1, hexanes : EtOAc) yielded **114** (27.5 mg, 48%), **115** (13.4 mg, 22%) and unreacted **109** (5 mg).

114: Glass-like solid. Mp 137–139 °C.

^{1}H NMR ($CDCl_3$): δ 1.10 (t, 3H, J = 7.4 Hz, CH_2CH_3), 1.16, 1.19, 1.21 (3 × s, 27H, $C(CH_3)_3$), 1.96 (m 2H, CH_2CH_3), 3.86 (br m, 1H, H-6), 4.06 (dd, 1H, J = 4.4 and 12.5

Hz, H-9), 4.21 (dd, 1H, J = 1.8 and 12.5 Hz, H-9′), 4.31 (dd, 1H, J = 9.6 and 10.0 Hz, H-8a), 4.79 (br m, 1H, H-3′), 4.96 (d, 1H, J = 9.6 Hz, H-4a), 5.1-5.2 (m, 3H, H-7, CH_{2Cbz}), 5.45 (dd, 1H, J = 10.0 and 8.9 Hz, H-8), 7.30-7.45 (m, 5H, H_{Ar}).

^{13}C NMR ($CDCl_3$): δ 10.6 (CH_2CH_3), 27.0, 27.1 ($C(CH_3)_3$), 27.4 (CH_2CH_3), 38.8, 38.9 ($C(CH_3)_3$), 58.2 (C-3), 61.3 (C-9), 67.9 (C-7), 68.5 (CH_{2Cbz}), 71.4 (C-8), 73.1 (C-8a), 74.8 (C-6), 80.9 (C-4a), 127.9, 128.5, 128.7 (CH_{Ar}), 135.3 (4° C_{Ar}), 155.0 ($C{=}O_{Cbz}$), 167.7 ($C{=}O_{oxazinone}$), 176.4, 176.9, 177.8 ($C{=}O_{piv}$).

Anal. Calcd. for $C_{33}H_{47}NO_{11}$: C, 62.54; H, 7.48; N, 2.21. Found: C, 62.03; H, 7.68; N, 2.11.

$[\alpha]_D$ = +44.4 (*c* 0.64,$CHCl_3$).

115: Glass-like solid. Mp 93–95 °C.

^{1}H NMR ($CDCl_3$): δ 0.66 (t, 3H, J = 7.5 Hz, CH_2CH_3), 1.04 (t, 3H, J = 7.5 Hz, CH_2CH_3), 1.14, 1.20, 1.22 (3 × s, 27H, $C(CH_3)_3$), 2.0-2.2 (m 2H, CH_2CH_3), 2.27 (m 1H, CH_2CH_3), 2.55 (m 1H, CH_2CH_3), 3.75 (ddd, 1H, J = 10.0, 3.2 and 5.7 Hz, H-6), 3.9-4.0 (m, 2H, H-9, H-9′), 4.14 (dd, 1H, J = 9.3 and 9.9 Hz, H-8a), 4.91 (d, 1H, J = 9.3 Hz, H-4a), 5.1-5.25 (m, 3H, H-7, CH_{2Cbz}), 5.41 (dd, 1H, J = 9.9 and 9.0 Hz, H-8), 7.3-7.4 (m, 5H, H_{Ar}).

^{13}C NMR ($CDCl_3$): δ 8.9, 9.9 (CH_2CH_3), 27.0, 27.1 ($C(CH_3)_3$), 30.7, 32.9 (CH_2CH_3), 38.8, 38.9 ($C(CH_3)_3$), 61.1 (C-9), 67.7 (C-7), 67.9 (CH_{2Cbz}), 71.3, 71.4 (C-8, C-3), 72.7 (C-8a), 74.4 (C-6), 81.0 (C-4a), 128.3, 128.5, 128.6 (CH_{Ar}), 135.6 (4° C_{Ar}), 154.2 ($C{=}O_{Cbz}$), 170.0 ($C{=}O_{oxazinone}$), 176.4, 177.1, 177.8 ($C{=}O_{piv}$).

Anal. Calcd. for $C_{35}H_{51}NO_{11}$: C, 63.52; H, 7.77; N, 2.12. Found: C, 63.78; H, 8.00; N, 2.04.

$[\alpha]_D = +36.8$ (*c* 0.34, $CHCl_3$).

(4a*R*,6*R*,7*R*,8*S*,8a*R*)-2-*t*-Butyldimethylsilyloxy-4-(benzyloxycarbonyl)-6-(pivaloyloxy)methyl-7,8-bis(pivaloyloxy)-4*H*,6*H*-(4a,7,8,8a)-tetrahydro)pyrano[3,2-b]-1,4-oxazine (116).

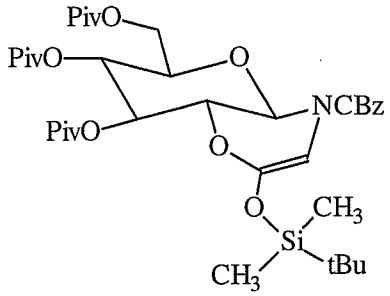

Oxazinone **109** (100 mg, 0.17 mmol) was dissolved in THF (1 mL), and TBDMSCl (29.8 mg, 0.198 mmol) in THF (0.2 mL) was added. The solution was cooled to –78 °C and LiHMDS (1 M, 198 μL, 0.198 mmol) was added. After 20 min, only starting material was evident by TLC, and HMPA (0.1 mL) was added. After 5 min, the solution was quenched with phosphate buffer (2 mL, 1M, pH 7) and diluted with Et_2O (5 mL). The mixture was poured into Et_2O (15 mL) and the phases separated. The organic layer was washed with water (2 × 2 mL) and brine (2 mL), dried and evaporated to afford **116**. ^{1}H NMR of the crude product showed signals consistent with **116** as well as HMPA and excess silyl materials. Chromatography (7 : 1, hexanes : EtOAc) yielded **116** (63%). Mp 122–123 °C.

^{1}H NMR ($CDCl_3$): δ 0.13, 0.14 (2 × s, 6H, SiCH_3), 0.89 (s, 9H, SiC(CH_3)$_3$), 1.16, 1.18, 1.22 (3 × s, 27H, C(CH_3)$_3$), 3.85 (dd, 1H, J = 8.5 and 10.1 Hz, H-8a), 3.85 (m, 1H, H-6), 4.1-4.2 (m, 2H, H-9, H-9′), 4.72 (d, 1H, J = 8.5 Hz, H-4a), 5.17 (dd, 1H, J = 9.0 and 10.1 Hz, H-7), 5.11 (d, 1H, J = 12.4 Hz, CH_{CBz}), 5.27 (d, 1H, J = 12.4 Hz, CH_{CBz}), 5.42 (dd, 1H J = 10.1 and 9.0 Hz, H-8), 5.81 (s, 1H, H-3), 7.30-7.40 (m, 5H, H_{Ar}).

^{13}C NMR ($CDCl_3$): δ –5.0, –4.6 (SiCH$_3$), 17.9 (SiC(CH$_3$)$_3$), 25.3 (SiC(CH$_3$)$_3$), 27.0, 27.1, 27.2 (C(CH$_3$)$_3$), 38.8, 38.9 (C(CH$_3$)$_3$), 61.6 (C-9), 67.8 (C-7), 68.0 (CH$_{2Cbz}$), 71.8 (C-8), 74.8 (C-6), 76.7 (C-8a), 81.2 (C-4a), 89.3 (C-3), 127.8, 128.2, 128.5 (C_{Ar}), 135.9 (4° C_{Ar}), 153.3 (C=O$_{Cbz}$), 147.4 (C=O$_{oxazinone}$), 176.5, 177.1, 178.0 (C=O$_{piv}$).

Anal. Calcd. for $C_{37}H_{57}NO_{11}Si$: C, 61.73; H, 7.98; N, 1.95. Found: C, 61.48; H, 8.12; N, 1.91.

$[\alpha]_D$ = –30.8 (*c* 0.50, $CHCl_3$).

(3*S*,4a*R*,6*R*,7*R*,8*S*,8a*R*)-3-(Hydroxybenzyl)-4-(benzyloxycarbonyl)-6-(pivaloyloxy)methyl-7,8-bis(pivaloyloxy)-6H-pyrano[3,2-b]-1,4-oxazin-2-one (117a) and its epimeric compound (117b) and (4a*R*,6*R*,7*R*,8*S*,8a*R*)-3-(phenylmethylene)-4-(benzyloxycarbonyl)-6-(pivaloyloxy)methyl-7,8-bis(pivaloyloxy)-6H-pyrano[3,2-b]-1,4-oxazin-2-one (118).

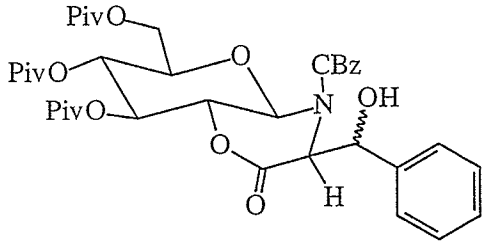

117a and **117b**

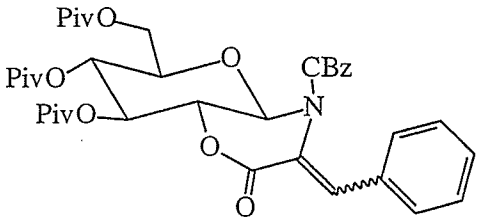

118

To oxazinone **109** (60 mg, 0.1 mmol) in THF at –78 °C was added LiHMDS in THF (1 M, 0.12 mL, 0.12 mmol) then benzaldehyde (50 μL, 0.5 mmol). After 30 min, only starting material was evident by TLC, and HMPA (0.1 mL) was added. The solution was quenched after a further 30 min with phosphate buffer (2 mL, 1 M, pH 7) and diluted with Et_2O (15 mL). The layers were separated and the water layer extracted with Et_2O (5 mL). The combined organic layers were washed with water (2 × 3 mL), dried and evaporated. Chromatography (5 : 1 → 4 : 1, hexanes : EtOAc) gave **118** (3.2 mg, 5.6%) and a mixture of **117a**:**117b** (39.6 mg, 68.2%) as well as recovered **109** (10.6 mg). A quantity of **117a** and **117 b** were separated by further column chromatography. The stereochemistry of these compounds was not assigned.

117a: White powder. Mp 95–97 °C.

^{1}H NMR ($CDCl_3$): δ 1.16, 1.20, 1.25 (3 × s, 27H, C(CH_3)$_3$), 2.62 (br, 1H, O*H*), 3.87 (br m, 1H, H-6), 4.12 (dd, 1H, *J* = 3.9 and 12.4 Hz, H-9), 4.24 (dd, 1H, *J* = 2.0 and 12.4 Hz, H-9′), 4.74 (br, 1H , H-4a), 4.8-5.0 (m, 3H, H-8a, CH_{2CBz}), 5.06 (d, 1H, *J* = 2.5 Hz, H-3), 5.19 (dd, 1H, *J* = 9.8 and 9.1 Hz, H-7), 5.29 (br m, 1H, H-10), 5.43 (dd, 1H, *J* = 8.8 and 9.8 Hz, H-8), 7.0-7.5 (m, 10H, H_{Ar}).

^{13}C NMR ($CDCl_3$): δ 27.0, 27.1 (C(CH_3)$_3$), 38.8, 38.86, 38.9 ($C(CH_3)_3$), 61.2 (C-9), 62.7 (C-3), 68.0 (C-7), 68.4 (CH_{2Cbz}), 71.2 (C-8), 72.8 (C-8a), 74.6 (C-6), 75.2 (C-10), 80.5 (C-4a), 126.9, 127.9, 128.3, 128.4, 128.5, 128.7 (C_{Ar}), 135.0, 138.8 (4° C_{Ar}), 154.9 (C=O_{CBz}), 167.5 (C=$O_{oxazinone}$), 176.4, 177.1, 177.8 (C=O_{piv}).

Anal. Calcd. for $C_{38}H_{49}NO_{12}$: C, 64.12; H, 6.94; N, 1.97. Found: C, 64.05; H, 7.22; N, 1.97.

$[\alpha]_D$ = –6.2 (*c* 0.50, $CHCl_3$).

117b: Mp 98–100 °C.

^{1}H NMR (500 MHz, $CDCl_3$, 310 K): δ 1.15, 1.18, 1.25 (3 × s, 27H, C(CH_3)$_3$), 2.95 (br, 1H, O*H*), 3.81 (br m, 1H, H-6), 4.10-4.13 (m, 3H, H-9, H-9′, H-8a), 4.86 (d, 1H, *J* = 9.5 Hz, H-4a), 5.02 (dd, 1H, *J* = 9.5 and 9.3 Hz, H-7), 5.14 (br, 1H, H-3), 5.17 (br, 2H, CH_{2CBz}), 5.24 (br, 1H, H-10), 5.34 (dd, 1H, *J* = 9.4 and 9.5 Hz, H-8), 7.3-7.5 (m, 10H, H_{Ar}).

^{13}C NMR (125.8 MHz, $CDCl_3$, 310 K): δ 27.0, 27.2 (C(CH_3)$_3$), 38.8, 38.86, 38.9 ($C(CH_3)_3$), 61.5 (C-9), 64.1 (C-3), 67.9 (C-7), 69.0 (CH_{2Cbz}), 71.1 (C-8), 72.8 (C-8a),

74.8 (C-6), 76.0 (C-10), 80.4 (C-4a), 126.3, 128.1, 128.7, 128.8 (C_{Ar}), 135.0, 139.1 (4° C_{Ar}), 165.0 (C=$O_{oxazinone}$), 176.4, 176.9, 177.9 (C=O_{piv}).

Anal. Calcd. for $C_{38}H_{49}NO_{12}$: C, 64.12; H, 6.94; N, 1.97. Found: C, 64.18; H, 6.77; N, 2.47.

$[\alpha]_D$ = +63.6 (*c* 0.14, $CHCl_3$).

118: Possible mixture of E/Z isomers.

^{1}H NMR ($CDCl_3$): δ 1.16, 1.18, 1.23 (3 × s, 27H, C(CH_3)$_3$), 3.9-4.0 (m, 1H, H-6), 4.1-4.2 (m, 3H,H-9, H-9′, H-8a), 5.11 (d, 1H , J = 9.5 Hz, H-4a), 5.16 (d, 1H, J = 10.0 Hz, H-7), 5.18 (d, 1H, J = 12.3 Hz, CH_{CBz}), 5.30 (d, 1H, J = 12.3 Hz, CH_{CBz}), 5.53 (dd, 1H, J = 9.1 and 10.0 Hz, H-8), 7.22 (s, 1H, H-10), 7.3-7.7 (m, 10H, H_{Ar}).

Alternate synthesis of 117a, 117b and 118.

To the TBDMS trapped oxazinone **116** (0.1 mmol) in CH_2Cl_2 (1 mL) was added benzaldehyde (10 μL, 0.1 mmol) and the solution was cooled to –78 °C. A catalytic amount of TMSOTf* (10mol%, 2 μL, 0.01 mmol) was added. After 1 h the solution was quenched with water and extracted with CH_2Cl_2 (2 × 10 mL). The combined organic layers were dried and the solvent evaporated. Chromatography then gave **118** (3.6 mg, 5.2%), a mixture of **117a**:**117b** (19.4 mg, 48.6%) and recovered oxazinone **109** (26 mg).

***Note**: Other catalysts used as described in Table 2.3

N-(2,3,4,6-Tetra-*O*-pivaloyl-β-D-glucopyranosyl)-*N*-(benzyloxycarbonyl)glycine, ethyl ester (119).

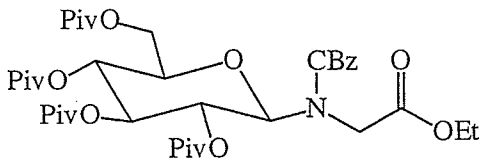

Ester **108** (5.0 g, 18.9 mmol) was suspended in dry pyridine (25 mL) containing a catalytic amount of DMAP (0.03 g, 0.25 mmol). Pivaloyl chloride (12.4 mL, 100 mmol) was added dropwise *via* syringe. After 1 h, the mixture was heated to 40 °C for 24 h. The solution was concentrated, and the residue was re-evaporated from toluene. Purification by column chromatography (7 : 1, hexanes : EtOAc) gave **119** (10.3 g, 76%) as an oil which crystallized on standing.

White powder. Mp 111–113 °C.

^{1}H NMR (DMSO-d_6, 500 MHz, 373 K): δ 1.03, 1.07, 1.11, 1.15 (4 × s, 36H, C(CH_3)$_3$), 1.0-1.2 (m, 3H, CH_2CH_3), 3.86 (d, 1H, J = 17.7 Hz, Hα), 3.96 (d, 1H, J = 17.7 Hz, Hα′), 3.97 (dd, 1H, J = 4.4 and 12.4 Hz, H-6), 4.0-4.1 (m, 2H, CH_2CH_3), 4.08 (dd, 1H, J = 2.0 and 12.4 Hz, H-6′), 4.14 (ddd, 1H, J = 2.0, 4.4, and 10.0 Hz, H-5), 5.0-5.1 (m, 4H, H-2, H-4, CH_{2CBz}), 5.44 (dd, 1H J = 9.4 and 9.4 Hz, H-3), 5.67 (d, 1H, J = 9.3 Hz, H-1), 7.3-7.4 (m, 5H, H_{Ar}).

^{13}C NMR (DMSO-d_6, 125.76 MHz, 373 K): δ 13.3 (CH_2CH_3), 26.0, 26.1, 26.2, 26.3 (C(CH_3)$_3$), 37.6, 37.7 (C(CH$_3$)$_3$), 43.3 (Cα), 59.7 (CH_2CH_3), 61.0 (C-6), 66.7 (CH_{2CBz}),

67.1 (C-4), 68.2 (C-2), 72.2 (C-3), 72.6 (C-5), 82.0 (C-1), 126.8, 127.0, 127.4, 127.7 (C_{Ar}), 135.5 (4° C_{Ar}), 154.2 (C=O_{Cbz}), 167.6 (C=$O_{oxazinone}$), 175.2, 175.4, 175.6 (C=O_{piv}). Anal. Calcd. for $C_{38}H_{57}NO_{13}$: C, 62.02; H, 7.81; N, 1.90. Found: C, 61.95; H, 8.14; N, 1.95.

$[\alpha]_D$ = +22.2 (*c* 0.50, $CHCl_3$).

N-(2,3,4,6-Tetra-*O*-pivaloyl-β-D-glucopyranosyl)-*N*-(benzyloxycarbonyl)-α-methyl-glycine, ethyl ester (120).

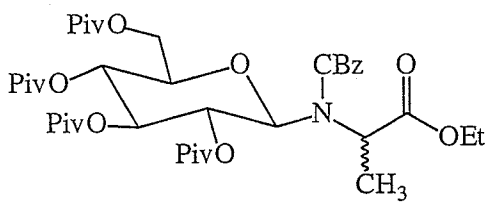

To LiHMDS (0.16 mL, 1.0 M, 1.7 mmol) in THF (1 mL) was added compound **119** (0.1 g, 0.14 mmol) followed by MeI (85 μL, 1.4 mmol) and then HMPA (0.1 mL). After 1 h little reaction was observed and further LiHMDS (0.16 mL), HMPA (0.1 mL) and MeI (0.1 mL) were added and the solution allowed to warm slowly to 0 °C over 2.5 h. The reaction was worked up as for the methylation of **109**. Column chromatography (7 : 1, hexanes : EtOAc) gave **120** in 42% yield plus a minor product (~20%).

Mp 61–63 °C.

^{1}H NMR (DMSO-d_6, 500 MHz, 373 K): δ 1.06, 1.07, 1.12, 1.15 (4 × s, 36H, C(CH_3)$_3$), 1.0-1.2 (m, 3H, CH_2CH_3), 1.41 (d, 3H, J = 6.8 Hz, $CH_3\alpha$), 3.8-4.0 (m, 3H, H-6, CH_2CH_3), 4.1-4.2 (m, 2H, H-6′, H-5), 4.28 (q, 1H, J = 6.8 Hz, Hα), 5.0-5.1 (m, 3H, H-4,

CH_{2CBz}), 5.20 (dd, 1H J = 9.2 and 8.9 Hz, H-2), 5.39 (dd, 1H, J = 8.9 and 9.6 Hz, H-3), 5.73 (d, 1H, J = 9.2 Hz, H-1), 7.3-7.4 (m, 5H, H_{Ar}).

^{13}C NMR (DMSO-d_6, 125.76 MHz, 373 K): δ 13.1 (CH_2CH_3), 16.1 ($CH_3\alpha$), 25.9, 26.0, 26.1, 26.2 ($C(CH_3)_3$), 37.5, 37.6, 37.7 ($C(CH_3)_3$), 51.0 (Cα), 59.7 (CH_2CH_3), 61.0 (C-6), 66.5 (CH_{2CBz}), 67.2 (C-4), 68.3 (C-2), 72.6 (C-3), 73.1 (C-5), 83.1 (C-1), 127.0, 127.2, 127.5 (C_{Ar}), 135.3 (4° C_{Ar}), 153.6 (C=O_{Cbz}), 169.3 (C=$O_{oxazinone}$), 174.5, 175.1, 175.6, 176.2 (C=O_{piv}).

Anal. Calcd. for $C_{39}H_{59}NO_{13}$: C, 62.47; H, 7.93; N, 1.87. Found: C, 62.45; H, 8.19; N, 1.98.

$[\alpha]_D$ = +32.9 (*c* 0.42, $CHCl_3$).

Cleavage of the amino acid from the auxiliary.

Compound **110** (56 mg, 0.09 mmol) was dissolved in MeOH (1 mL) and cooled to 0 °C. 10 % Pd/C (9 mg, 10 mol%) was added and the solution vigorously stirred under an atmosphere of H_2. After 15 min the solution was filtered through Celite and diluted to 2 mL. HCl in MeOH (1 M, 0.2 mmol, 0.2 mL) was added and the solution stirred overnight. The excess solvent was evaporated and the products were separated on Amberlite IR (H^+) 120 resin (7 : 1, MeOH : H_2O) to give the sugar (38.5 mg, 100%) and the amino acid as a 1:2 mixture of the acid and methyl ester (11.6 mg, 95%). Left for a prolonged period (~7 days) in the presence of aqueous HCl, the ester was gradually cleaved to give *L*-alanine $[\alpha]_D$ = + 9.3 (*c* 0.30 6 N HCl) (literature $[\alpha]_D$ = + 13.7 (*c* 2, 6 N HCl)).[152]

Dimethyl *d*-tartrate.

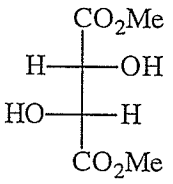

Acetyl chloride (10 mol%, 1.5 mL, 20 mmol) was added to MeOH (450 mL). d-Tartaric acid (30 g, 0.2 mol) was added and the solution refluxed under a soxhlet (containing 4Å sieves) for 16 h. The bulk of the MeOH was evaporated and the remaining solution diluted with Et_2O (200 mL). The solution was neutralized by the addition of solid $KHCO_3$ (5 g) and a small amount of water, dried with $CaSO_4$, then filtered and evaporated giving 34 g (95%) of dimethyl d-tartrate as a thick oil. A ^1H NMR of the product was consistent with the literature.[195]

Methyl glyoxylate hemiacetal.

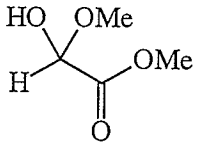

Following the procedure of Horne,[153] to a rapidly stirred solution of dimethyl d-tartrate (1.6 g, 9 mmol) in 35% THF/ether (20 mL) at 0 °C was added portion wise finely pulverized H_5IO_6 (2.1 g, 9 mmol). The solution was allowed to warm to room temperature over 1 h and left for a further 30 min. The solution was diluted with Et_2O (30 mL), filtered, dried with $MgSO_4$ and K_2CO_3 and the solvent evaporated. The residue

was re-dissolved in a small amount of MeOH and evaporated to give a clear oil of the methyl glyoxyl as a mixture of hemiacetals 1.33 g (83%). The reaction was monitored by watching for the disappearance of the starting material by TLC (5% MeOH/ether chromic acid spray).

Methyl glyoxylimine (121).

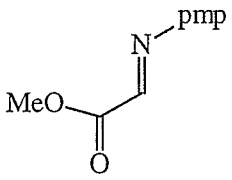

p-Anisidine (0.62 g, 5.0 mmol) and $MgSO_4$ (1.0 g) were added to CH_2Cl_2 (10 mL) and the solution cooled to 0 °C. Crude methyl glyoxyl hemiacetal (0.66 g, 5.5 mmol) was added. The solution was stirred for 1 h, filtered and evaporated to give **121** as a brown oil 0.88 g (92%) which was essentially one material by ^1H NMR.[196] The crude product was used within several days.

3-*O*-Crotonyl-1,2:5,6-di-*O*-isopropylidene-D-glucofuranose (122).

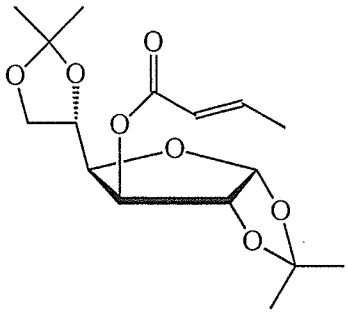

Crotonic acid (1.49 g, 17 mmol) and DMAP (0.21g, 1.7 mmol) were dissolved in CH_2Cl_2 (30 mL). Diacetone D-glucose (4.51 g, 17 mmol) was added and the solution cooled to 0 °C. DCC (3.57 g, 17 mmol) was then added and the reaction warmed to room temperature. After ~5 min a fine precipitate formed. After 2.5-3 h, additional portions of crotonic acid (0.75 g, 8.7 mmol) and DCC (1.79 g, 8.7 mmol) were added and the reaction was stirred overnight. After cooling to 0 °C the solution was filtered through Celite and the solvent evaporated. The residue was re-dissolved in a small amount of Et_2O, cooled, filtered and concentrated. This process was repeated until no further precipitate was detected. The product crystallized on standing to yield 5.30 g (93%) of **122** as white needles.

Mp 64–66 °C. Lit. mp 65.5–67 °C[197]

^{1}H NMR ($CDCl_3$): δ 1.30, 1.31, 1.41, 1.52 (4 × s, 12H, CH_3), 1.90 (dd, 3H, J = 1.6 and 6.9 Hz, H-4′), 4.0-4.1 (m, 2H, H-6a, H-6b), 4.2-4.3 (m, 2H, H-4, H-5), 4.51 (d, 1H, J = 3.7 Hz, H-2), 5.30 (d, 1H, J = 2.4 Hz, H-3), 5.8-5.9 (m, 1H, H-2′), 5.87 (d, 1H, J = 3.7 Hz, H-1), 7.02 (dq, 1H, J = 6.9 and 15.5 Hz, H-3′).

^{13}C NMR ($CDCl_3$): δ 18.1 (C-4′), 25.3, 26.3, 26.8, 26.9 (4 × CH_3), 67.1 (C-6), 72.6 (C-5), 75.9 (C-3), 79.8 (C-4), 83.4 (C-2), 105.1 (C-1), 109.3, 112.3 (4° $C_{acetonide}$), 122.0 (C-2′), 146.2 (C-3′), 164.9 (C-1′).

$[\alpha]_D$ = –43.2 (*c* 0.5 $CHCl_3$). Lit: $[\alpha]_D^{25}$ = –48.4 (*c* 4.7 $CHCl_3$).[197]

3-*O*-[(*N*-*p*-Anisyl)-imino acetate]-1,2:5,6-di-*O*-isopropylidene-D-glucofuranose (123).

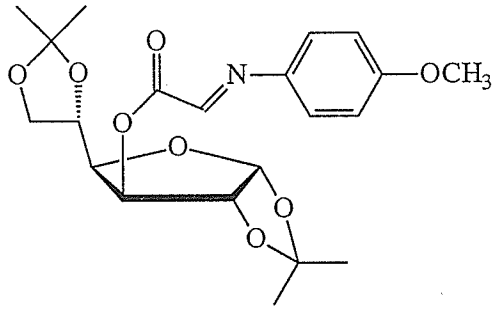

A solution of **122** (2.5 g, 7.6 mmol) in CH_2Cl_2 (100 mL) at –78 °C was treated with a stream of O_3 until a faint blue color persisted (~ 2 h). The solution was purged with O_2, quenched with an excess of Me_2S (10 mL), and allowed to warm slowly overnight to room temperature. The solution was poured into water (20 mL) and washed through an extraction cascade of H_2O, saturated $NaHCO_3$ and brine (20 mL each). The aqueous layers were extracted with CH_2Cl_2 (2 × 15 mL). The combined organic extracts were dried and evaporated to yield a colorless foam 2.03 g (84%). The crude product was re-dissolved in freshly distilled $CHCl_3$ over activated 4Å sieves (2 g) and the mixture cooled to 0 °C. *p*-Anisidine (0.79 g, 6.4 mmol) was added. After 16 h, the solution was filtered through Celite and the solvent evaporated to afford **123** (2.36 g, 87%) as a pale yellow foam.

Mp 50–52 °C.

^{1}H NMR ($CDCl_3$): δ 1.31, 1.33, 1.43, 1.55 (4 × s, 12H, CH_3), 3.85 (s, 3H, OCH_3), 4.0-4.2 (m, 2H, H-6a, H-6b), 4.3-4.4 (m, 2H, H-4, H-5), 4.63 (d, 1H, J = 3.7 Hz, H-2), 5.48 (d,

1H, J = 2.1 Hz, H-3), 5.96 (d, 1H, J = 3.7 Hz, H-1), 6.9-7.4 (m, 4H, H_{pmp}), 7.95 (s, 1H, H-2′).

^{13}C NMR ($CDCl_3$): δ 25.3, 26.3, 26.8, 26.9 (4 × CH_3), 55.6 (OCH_3), 67.2 (C-6), 72.6 (C-5), 77.3 (C-3), 79.8 (C-4), 83.3 (C-2), 105.2 (C-1), 109.4, 112.4 (2 × 4° $C_{acetonide}$), 114.6 , 123.9 (C_{pmp}), 141.1 (4° C_{pmp}), 146.2 (C-2′), 160.9, 162.2 (C-1′, 4° C_{pmp}).

Anal. Calcd for $C_{21}H_{27}NO_8$: C, 59.85; H, 6.46; N, 3.32. Found: C, 60.19; H, 6.70; N, 3.49.

$[\alpha]_D$ = –41.6 (*c* 0.5 $CHCl_3$).

Oxidation of 1,2:5,6-di-*O*-isopropylidene-D-glucofuranose.

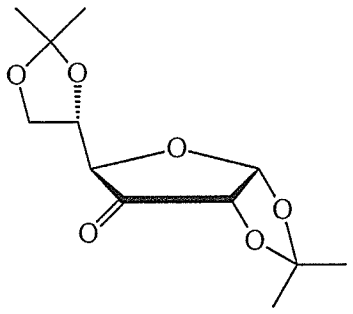

Following a modification of literature procedures[156,157] diacetone D-glucose (2.72 g, 10.4 mmol) was dissolved in a minimum amount of CH_2Cl_2 and stirred over activated crushed 3 Å molecular sieves. To this were added PDC (2.36 g, 6.3 mmol) and a solution of acetic anhydride (2.95 mL, 31 mmol) in CH_2Cl_2 (30 mL). After 2.5 h, TLC (2 : 1, hexanes : EtOAc) showed a low running streaky spot. The mixture was slowly poured onto a short Celite-topped column of silica, which was covered by a layer of EtOAc. The heavily colored chromium salts precipitated out and the column was topped up

periodically with EtOAc as the reaction mixture was added. The solution was concentrated and the filtration step repeated as long as the solution still retained colour. Re-evaporation from toluene yielded 2.51 g (93%) of crude product, which was used without further purification.

1,2:5,6-Di-*O*-isopropylidene-D-allofuranose (124).

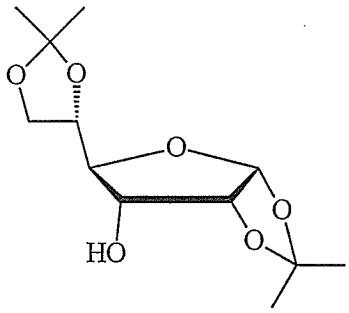

The crude oxidation product above (2.51 g, 9.7 mmol) was dissolved in 3 : 7, EtOH/H_2O (20 mL).[198] Excess EtOH was added as necessary to get complete dissolution. $NaBH_4$ (0.446 g, 11.8 mmol) was then added portion wise with stirring and slight cooling. After 30 min most of the solvent was evaporated, with water (10 mL) added twice with evaporation after each addition to ensure removal of the EtOH. The product was extracted from the remaining aqueous layer with CH_2Cl_2 (4 × 20 mL). The organic layer was dried and evaporated to give white crystals 2.08 g (82%). A ^1H NMR spectrum showed only a trace amount of the epimeric glucose sugar.

3-*O*-Crotonyl-1,2:5,6-di-*O*-isopropylidene-D-allofuranose (125).

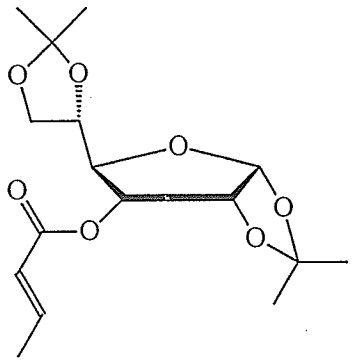

Synthesized as for the glucose ester **122**. Crotonic acid (0.84 g, 9.7 mmol), DMAP (95 mg, 0.78 mmol) and **124** (2.02 g, 7.8 mmol) were dissolved in CH_2Cl_2 (50 mL). After several hours, more crotonic acid (0.33 g, 3.8 mmol) and DCC (0.80 g, 3.8 mmol) were added. The product was worked up as for **122**. Crystallization from hexanes in two batches yielded **125** as colorless needles (2.07 g, 81%).

Mp 84–85 °C.

^{1}H NMR ($CDCl_3$): δ 1.32, 1.34, 1.40, 1.54 (4 × s, 12H, CH_3), 1.93 (dd, 3H, J = 1.7 and 6.7 Hz, H-4′), 3.90 (dd, 1H, J = 8.5 and 5.9 Hz, H-6a), 4.06 (dd, 1H, J = 8.5 and 6.8 Hz, H-6b), 4.20 (dd, 1H, J = 4.1 and 8.6 Hz, H-4), 4.30 (m, 1H, H-5), 4.84 (dd, 1H, J = 3.8 and 5.0 Hz, H-2), 4.92 (dd, 1H, J = 5.0 and 8.6 Hz, H-3), 5.82 (d, 1H, J = 3.7 Hz, H-1), 5.92 (dq, 1H, J = 1.7 and 15.5 Hz, H-2′), 7.04 (dq, 1H, J = 7.0 and 15.5 Hz, H-3′).

^{13}C NMR ($CDCl_3$): δ 18.2 (C-4′), 25.1, 26.3, 26.7 (4 × CH_3), 65.6 (C-6), 72.3 (C-3), 75.1 (C-5), 77.6 (C-4), 77.9 (C-2), 104.1 (C-1), 110.0, 113.1 (4° $C_{acetonide}$), 121.8 (C-2′), 146.2 (C-3′), 165.4 (C-1′).

Anal. Calcd for $C_{16}H_{24}O_7$: C, 58.53; H, 7.37. Found: C, 58.86; H, 7.57.

$[\alpha]_D$ = +117.6 (*c* 0.50 $CHCl_3$).

3-*O*-[(*N*-*p*-Anisyl)imino acetate]-1,2:5,6-di-*O*-isopropylidene-D-allofuranose (126).

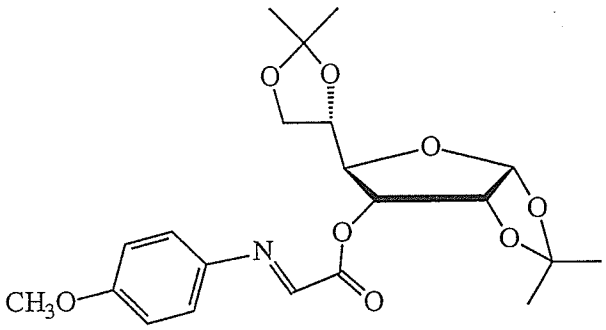

Synthesized as for imine **123**. Compound **125** (0.6 g, 1.83 mmol) was dissolved in CH_2Cl_2 (30 mL), cooled to –78 °C and a stream of O_3 passed through. After a faint blue color persisted (~ 2 h), the solution was purged with N_2 and quenched with an excess of Me_2S (10 mL). Incomplete quench of the ozonide necessitated chromatography through a silica plug (4 : 1→ 1 : 1, hexanes : EtOAc) giving a clear oil (0.15 g, 33%). The crude material was re-dissolved in freshly distilled $CHCl_3$ (15 mL) over activated 4Å sieves. *p*-Anisidine (0.59 g, 0.48 mmol) was added. After 16 h the solution was filtered through Celite and the solvent evaporated yielding 0.144 g (71%) of **126** as an oil. Product crystallized on standing.

Mp 79–81 °C.

^{1}H NMR ($CDCl_3$): δ 1.34, 1.43, 1.57 (3 × s, 12H, CH_3), 3.84 (s, 3H, OCH_3), 3.99 (dd, 1H, *J* = 8.6 and 5.5 Hz, H-6a), 4.10 (dd, 1H, *J* = 8.6 and 6.5 Hz, H-6b), 4.3-4.4 (m, 2H,

H-4, H-5), 4.94 (dd, 1H, J = 3.8 and 5.0 Hz, H-2), 5.10 (dd, 1H, J = 8.0 and 5.0 Hz, H-3), 5.87 (d, 1H, J = 3.7 Hz, H-1), 6.9-7.4 (m, 4H, H_{pmp}), 7.98 (s, 1H, H-2′).

^{13}C NMR ($CDCl_3$): δ 25.0, 26.4, 26.7 (4 × CH_3), 55.6 (OCH_3), 65.7 (C-6), 73.6 (C-3), 75.1 (C-5), 77.6, 77.8 (C-2, C-4), 104.2 (C-1), 110.1, 113.4 (4° $C_{acetonide}$), 114.6, 123.9 (C_{pmp}), 141.2 (4° C_{pmp}), 146.3 (C-2′), 160.8, 162.3 (C-1′, 4° C_{pmp}).

Anal. Calcd for $C_{21}H_{27}NO_8$: C, 59.85; H, 6.46; N, 3.32. Found: C, 59.58; H, 6.82; N, 3.25.

$[\alpha]_D$ = +136.3 (*c* 0.58 $CHCl_3$).

Synthesis of silyl enols 127a-e.

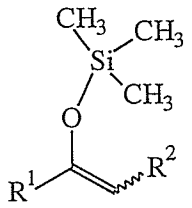

127a, R^1 = Ph, R^2 = H
127b, R^1 = Ph, R^2 = Me
127c, R^1 = Ph, R^2 = Ph
127d, R^1 =CH_2Ph, R^2 = Ph
127e, $R^1 + R^2 = (CH_2)_4$

Following the procedure of Cazeau,[158] sodium iodide (94 mg, 6.25 mmol) was dissolved in acetonitrile (6 mL) at room temperature under N_2. The ketone (5 mmol) was added followed by a prepared solution of 1:1, Et_3N: TMSCl (1.66 mL, 6.25 mmol) and the reaction stirred for 30 min. The reaction mixture was diluted with cold pentane (10 mL) and washed with water (2 mL). The organic layer was dried and the solvent evaporated. The products were left under high vacuum, for a few minutes only, to remove residual solvent. Products were used without further purification. Typical yields 78 – 89%. Products were determined to be predominately the Z-isomers (>98%)

(exception **127e** derived from cyclohexanone) by comparison of their ^{1}H NMR spectra with the literature.[159-161]

Example methods for Mukaiyama reactions

Method A. To a solution of **121** (150 mg, 0.78 mmol) in CH_2Cl_2 (5 mL) was added the TMS enolate of deoxybenzoin **127c** (23 mg, 0.85 mmol). The solution was cooled to –78 °C and $BF_3{\cdot}OEt_2$ (95 μL, 0.78 mmol) was added. After 30 min, the reddish reaction mixture was poured into saturated aqueous $NaHCO_3$ (10 mL). The phases were separated and the water layer was washed with Et_2O (2 × 10 mL). The combined organic layers were washed with brine, dried and the solvent evaporated. The crude product was purified by column chromatography (4 : 1, hexanes : EtOAc) to yield 113 mg (38%) of **130** as a mixture of isomers. The diastereomers were separated by preparative HPLC (~1% *i*PrOH/hexanes, Porasil® column).

Note 1. When catalytic (10 mol%) $TiCl_4$, $SnCl_4$ or TMSOTf were used, the Lewis acid was added to the imine first at –78 °C and then the silyl enol ether was added.

Note 2. Reactions using $Yb(OTf)_3$ or $Sc(OTf)_3$ were done at room temperature.

Method B. A solution of *p*-anisidine (123 mg, 1.0 mmol) in CH_2Cl_2 (2 mL) was treated with $Yb(OTf)_3$ (31 mg, 0.05 mmol) and anhydrous $MgSO_4$ (300 mg). Methyl glyoxyl hemiacetal (120 mg, 1.0 mmol) in CH_2Cl_2 (1 mL) was added and the solution turned a brownish color. After 30 min, silyl enol ether **127b** (413 mg, 2 mmol) in CH_2Cl_2 (1 mL) was added. After 1.5 h, H_2O (3 mL) was added and the product was extracted with CH_2Cl_2 (2 × 10 mL). The combined organic layers were dried and the solvent

evaporated. Column chromatography (4 : 1, hexanes : EtOAc) yielded 201 mg (61%) of **129** as a mixture of isomers. The diastereomers were separated by preparative HPLC (~1% *i*PrOH/hexanes, Porasil® column).

Example methods for enolate reactions.

Method C: Transmetallating conditions. Propiophenone (37 μL, 0.28 mmol) in THF (0.3 mL) was added to a solution of freshly prepared base (LDA or LiHMDS) (0.03 mmol) in THF (2 mL) at –78 °C. After 20 min, $Ti(iOPr)_4$ (0.18 mL, 0.61 mmol) was added. The solution was allowed to warm to ~ –40 °C over 1 h, held at that temperature for 30 min, then cooled to –78 °C. Imine **121** (48 mg, 0.25 mmol) in THF (0.5 mL) was then added, and the reaction allowed to warm slowly to ~ –30 °C over 1 h. The reaction was quenched with saturated NH_4Cl (2 mL) and the product extracted with Et_2O (3 × 15 mL). The combined organic layers were dried and the solvent evaporated. Column chromatography (3 : 1, hexanes : EtOAc) yielded 8 mg (10%) of **129** as a mixture of isomers.

Method D: Direct titanium enolate formation. $TiCl_4$ (1 M, 0.55 mL, 0.55 mmol) was added drop wise to a solution of propiophenone (66 μL, 0.55 mmol) in CH_2Cl_2 (2 mL) at –78 °C, giving a yellow slurry. After 2 min, Et_3N (84 μL, 0.60 mmol) was added and the reddish solution was stirred for 1 h. Imine **121** (92.3 mg, 0.5 mmol) in CH_2Cl_2 (0.5 mL) was then added. The reaction was quenched after 30 min with aqueous NH_4Cl (1 mL) and worked up as in method C to give 0.106 mg (65%) of **129** as a mixture of isomers.

Method C and D variant: Alternate quench for DAG products. The reactions were quenched with glacial acetic acid (~1 mL) followed by phosphate buffer (~2 mL, 1.0 M, pH 7) and the solution faded to a pale yellow. The products were extracted with Et_2O (2 × 10 mL). The combined extracts were washed with H_2O and $NaHCO_3$ (2 mL each), dried and evaporated. Products purified as usual.

Method E: Inverse addition. $CeCl_3$ (295 mg, 1.2 mmol) was placed in a side arm to one reaction flask. The flask and side arm were gently flame dried under vacuum and purged with argon. LDA (0.72 mmol) in THF (3.8 mL) was prepared in this flask and cooled to –78 °C. Propiophenone (80 μL, 0.6 mmol) in THF (0.2 mL) was added, with rinsing. After ~20 min the $CeCl_3$ from the side arm was added and the solution stirred for a further 1.5 h. In a separate flask, imine **123** (42 mg, 0.1 mmol) and $CeCl_3$ (25 mg, 0.1 mmol) were completely dissolved in THF (1 mL) (~1 h to dissolve) to give a brownish solution, which was then cooled to –78 °C. The enolate solution was then cannulated into the imine solution. After 5 min the reaction was quenched with glacial acetic acid (0.5 mL) then poured into Et_2O (10 mL). The organic layer was washed with H_2O, 2 × $NaHCO_3$ and brine (5 mL each). The organic layer was then dried and the solvent evaporated. Column chromatography (4 : 1, hexanes : EtOAc) yielded 34.4 mg (62%) of **133a-d**. Isomer ratios as given in text.

Variation: Either of the $CeCl_3$ addition steps may be left out as indicated in text. Without the $CeCl_3$, the imine solution may be cooled immediately.

2-(*N*-*p*-Anisyl)amino-4-oxo-phenylbutanoic acid, methyl ester (128).

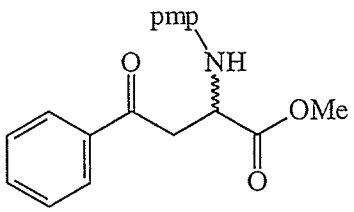

Fine white needles. Mp 85–87 °C.

^{1}H NMR ($CDCl_3$): δ 3.54 (d, 1H, J = 5.4 Hz, H-3), 3.72, 3.73 (2 × s, 6H, CO_2CH_3, OCH_3), 4.23 (br s, 1H, N*H*), 4.56 (t, 1H, J = 5.4 Hz, H-2), 6.6-6.8 (m, 4H, H_{pmp}), 7.4-8.0 (m, 5H, H_{Ph}).

^{13}C NMR ($CDCl_3$): δ 41.2 (C-3), 52.5 (CO_2CH_3), 54.4 (C-2), 55.8 (OCH_3), 114.9, 115.7, 128.2, 128.7, 133.6 (C_{Ar}), 136.5, 140.5, 153.1 (4° C_{Ar}), 173.7 (C-1), 197.3 (C-4).

Anal. Calcd for $C_{18}H_{19}NO_4$: C, 69.00; H, 6.10; N, 4.47. Found: C, 68.78; H, 6.15; N, 4.46.

(2*S*,3*S*) and (2*R*,3*R*)-2-(*N*-*p*-Anisyl)amino-3-methyl-4-oxo-phenylbutanoic acid, methyl ester (129a).

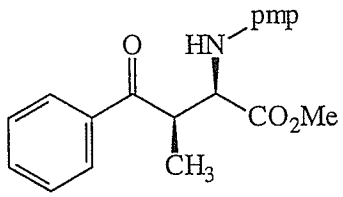

+ enantiomer

White powder. Mp 77–79 °C.

^{1}H NMR ($CDCl_3$): δ 1.35 (d, 3H, J = 7.1 Hz, CH_3), 3.66 (s, 3H, CO_2CH_3), 3.73 (s, 3H, OCH_3), 4.00 (dt, 1H, J = 7.1 and 6.6 Hz, H-3), 4.39 (d, 1H, J = 6.6 Hz, H-2), 6.5-6.8 (m, 4H, H_{pmp}), 7.4-8.0 (m, 5H, H_{Ph}).

^{13}C NMR ($CDCl_3$): δ 13.7 (CH_3), 44.0 (C-9), 52.3 (CO_2CH_3), 55.7 (OCH_3), 60.4 (C-2), 114.8, 115.7, 128.4, 128.8, 133.3 (C_{Ar}), 136.0, 140.7, 153.1 (4° C_{Ar}), 173.4 (C-1), 201.4 (C-4).

HRMS for $C_{19}H_{21}NO_4$: 327.1470. Found: 327.1468.

(2*S*,3*R*) and (2*R*,3*S*)-2-(*N*-*p*-Anisyl)amino-3-methyl-4-oxo-phenylbutanoic acid, methyl ester (129b).

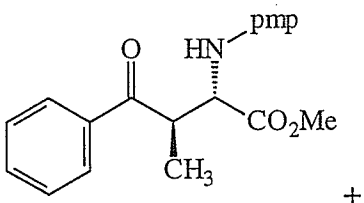

+ enantiomer

White powder. Mp 112–114 °C.

^{1}H NMR ($CDCl_3$): δ 1.30 (d, 3H, J = 7.1 Hz, CH_3), 3.63 (s, 3H, CO_2CH_3), 3.73 (s, 3H, OCH_3), 4.01 (dt, 1H, J = 7.0 and 7.1 Hz, H-3), 4.37 (d, 1H, J = 7.0 Hz, H-2), 6.6-6.8 (m, 4H, H_{pmp}), 7.4-8.0 (m, 5H, H_{Ph}).

^{13}C NMR ($CDCl_3$): δ 14.9 (CH_3), 43.4 (C-3), 52.0 (CO_2CH_3), 55.7 (OCH_3), 61.2 (C-2), 114.8, 115.9, 128.3, 128.7, 133.3 (C_{Ar}), 136.5, 141.0, 153.1 (4° C_{Ar}), 173.7 (C-1), 201.8 (C-4).

HRMS for $C_{19}H_{21}NO_4$: 327.1470. Found: 327.1470.

X-ray suitable crystals were obtained by slow recrystallization from hexanes/EtOAc.

For X-ray crystal structural data see appendix.

(2*R*,3*R*) and (2*S*,3*S*)-2-(*N*-*p*-Anisyl)amino-4-oxo-3-phenyl-phenylbutanoic acid, methyl ester (130a).

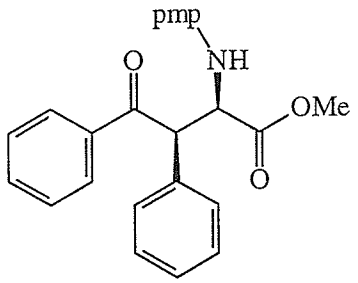

+ enantiomer

White powder. Mp 151–153 °C.

^{1}H NMR ($CDCl_3$): δ 3.68 (s, 3H, CO_2CH_3), 3.72 (s, 3H, OCH_3), 4.78 (d, 1H, J = 8.8 Hz, H-2), 5.11 (d, 1H, J = 8.8 Hz, H-3), 6.5-6.7 (m, 4H, H_{pmp}), 7.1-8.0 (m, 10H, H_{Ph}).

^{13}C NMR ($CDCl_3$): δ 52.4 (CO_2CH_3), 55.7 (OCH_3), 56.3 (C-3), 61.0 (C-2), 114.7, 115.9 (C_{pmp}), 127.9, 128.6, 128.9, 129.1, 129.2, 133.2 (C_{Ar}), 135.0, 136.1 (4° C_{Ar}), 140.6, 153.0 (4° C_{pmp}), 173.8 (C-1), 197.9 (C-4).

Anal. Calcd for $C_{24}H_{23}NO_4$: C, 74.02; H, 5.95; N, 3.60. Found: C, 74.03; H, 6.05; N, 3.58.

X-ray sutiable crystals were obtained by slow recrystallization from hexanes/EtOAc.

For X-ray crystal structural data see appendix.

(2*S*,3*R*) and (2*R*,3*S*)-2-(*N*-*p*-Anisyl)amino-4-oxo-3-phenyl-phenylbutanoic acid, methyl ester (130b).

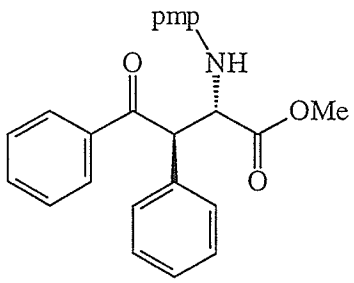

+ enantiomer

White powder. Mp 108–111 °C.

^{1}H NMR ($CDCl_3$): δ 3.37 (s, 3H, CO_2CH_3), 3.72 (s, 3H, OCH_3), 4.77 (d, 1H, J = 8.6 Hz, H-2), 5.00 (d, 1H, J = 8.0 Hz, H-3), 6.6-6.8 (m, 4H, H_{pmp}), 7.1-8.0 (m, 10H, H_{Ph}).

^{13}C NMR ($CDCl_3$): δ 51.9 (CO_2CH_3), 55.7 (OCH_3), 57.0 (C-3), 62.7 (C-2), 114.7, 116.6 (C_{pmp}), 128.0, 128.6, 128.9, 129.0, 129.1, 133.2 (C_{Ar}), 134.8, 136.6 (4° C_{Ar}), 141.0, 153.4 (4° C_{pmp}), 173.8 (C-1), 197.1 (C-4).

(2*R*,3*S*) and (2*S*,3*R*)-2-(*N*-*p*-Anisyl)amino-4-oxo-3-phenyl-phenylpentanoic acid, methyl ester (131).

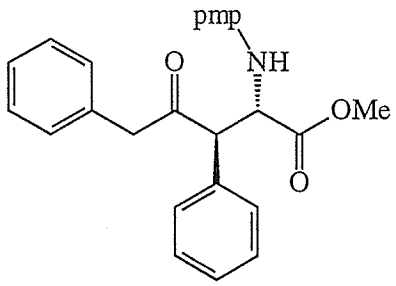

+ enantiomer

White powder. Mp 116–117 °C.

^{1}H NMR ($CDCl_3$): δ 3.33 (s, 3H, CO_2CH_3), 3.70 (s, 2H, H-5), 3.72 (s, 3H, OCH_3), 4.22 (d, 1H, J = 8.5 Hz, H-3), 4.55 (d, 1H, J = 8.5 Hz, H-2), 6.5-6.8 (m, 4H, H_{pmp}), 7.0-7.4 (m, 10H, H_{Ph}).

^{13}C NMR ($CDCl_3$): δ 49.7 (C-5), 51.9 (CO_2CH_3), 55.7 (OCH_3), 60.3 (C-3), 61.6 (C-2), 114.7, 116.4 (C_{pmp}), 127.2, 128.2, 128.7, 128.9, 129.4, 129.8 (C_{Ar}), 133.43, 133.9 (4° C_{Ar}), 140.9, 153.3 (4° C_{pmp}), 173.4 (C-1), 205.1 (C-4).

Anal. Calcd for $C_{25}H_{25}NO_4$: C, 74.42; H, 6.25; N, 3.47. Found: C, 73.25; H, 6.13; N, 3.38.

X-ray sutiable crystals were obtained by slow recrystallization from hexanes/EtOAc.

For X-ray crystal structural data see appendix.

(1′*R*,2*R*) and (1′*S*,2*S*)-Methyl-2-(*N*-*p*-anisyl)amino-2-(2′-oxocyclohexyl) acetate (132a).

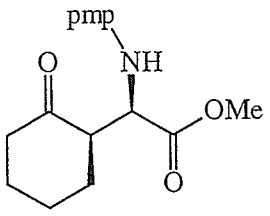

+ enantiomer

Diastereomers **132a** and **132b** were separated by column chromatography (3 : 1, hexanes : EtOAc).

Yellow oil.

^{1}H NMR ($CDCl_3$): δ 1.5-2.5 (m, 8H, H-3′, H-4′, H-5′, H-6′), 2.81 (m, 1H, H-1′), 3.69 (s, 3H, CO_2CH_3), 3.74 (s, 3H, OCH_3), 4.25 (d, 1H, J = 5.2 Hz, H-2), 6.7-6.8 (m, 4H, H_{pmp}). ^{13}C NMR ($CDCl_3$): δ 24.8, 26.9, 29.7 (C-4′, C-5′, C-6′), 41.9 (C-3′, 52.2 (CO_2CH_3), 53.6 (C-1′), 55.8 (OCH_3), 58.1 (C-2), 114.8, 116.0 (C_{pmp}), 141.0, 153.1 (4° C_{pmp}), 174.0 (C-1), 210.0 (C-2′).

Anal. Calcd for $C_{16}H_{21}NO_4$: C, 65.96; H, 7.26; N, 4.81. Found: C, 66.14; H, 7.54; N, 4.83.

(1′*S*,2*R*) and (1′*R*,2*S*)-Methyl-2-(*N*-*p*-anisyl)amino-2-(2′-oxocyclohexyl) acetate (132b).

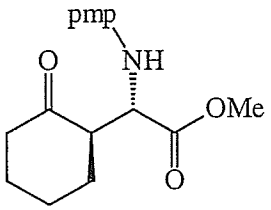

+ enantiomer

White powder. Mp 102–104 °C.

^{1}H NMR ($CDCl_3$): δ 1.5-2.5 (m, 8H, H-3′, H-4′, H-5′, H-6′), 3.13 (m, 1H, H-1′), 3.68 (s, 3H, CO_2CH_3), 3.73 (s, 3H, OCH_3), 4.00 (d, 1H, J = 4.0 Hz, H-2), 6.5-6.8 (m, 4H, H_{pmp}). ^{13}C NMR ($CDCl_3$): δ 24.7, 26.9, 30.7 (C-4′, C-5′, C-6′), 41.9 (C-3′), 52.3 (CO_2CH_3), 53.7 (C-1′), 55.8 (OCH_3), 59.0 (C-2), 114.9, 115.5 (C_{pmp}), 142.1, 152.8 (4° C_{pmp}), 173.7 (C-1), 211.0 (C-2′).

X-ray sutiable crystals were obtained by slow recrystallization from hexanes/EtOAc.

For X-ray crystal structural data see appendix.

1′,2′:5′,6′-Di-*O*-isopropylidene-D-glucofuranos-3′-yl 2-(*N*-*p*-anisyl)amino-3-methyl-4-oxo-phenylbutanoate (133).

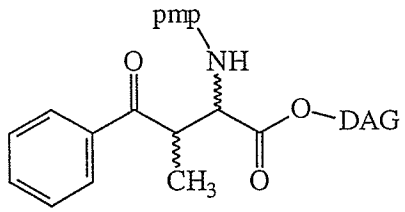

Compounds **133a** (*anti*$_1$) and **133b** (*syn*$_1$) could not be separated by preparative HPLC. The relative stereochemistries were assigned by taking a mixture enriched with **133a** and cleaving it to the methyl ester as stated in the text. Comparison of HPLC retention times were then made with samples of the methyl esters prepared using the achiral imine **121**.

133c: **(2,3 *syn*$_2$).** White solid. Mp 149–151 °C.

^{1}H NMR ($CDCl_3$): δ 1.21, 1.24, 1.35, 1.47 (4 × s, 12H, C*H*$_3$), 1.40 (d, 3H, *J* = 7.2 Hz, CHC*H*$_3$), 3.73 (s, 3H, OC*H*$_3$), 3.8-4.2 (m, 6H, N*H*, H-3, 2H-6′, H-4′, H-5′), 4.30 (d, 1H, *J* = 3.6 Hz, H-2′), 4.40 (br, 1H, H-2), 5.22 (d, 1H, *J* = 2.9 Hz, H-3′), 5.63 (d, 1H, *J* = 3.6 Hz, H-1′), 6.5-6.8 (m, 4H, H$_{pmp}$), 7.4-8.0 (m, 5H, H$_{Ph}$).

^{13}C NMR ($CDCl_3$): δ 14.7 (CH*C*H$_3$), 25.2, 26.2, 26.8, 26.9 (4 × *C*H$_3$), 44.1 (C-3), 55.8 (O*C*H$_3$), 60.3, (C-2), 67.4 (C-6′), 72.3 (C-5′), 76.9 (C-3′), 79.7 (C-4′), 82.8 (C-2′), 105.1

(C-1′), 109.4, 112.3 (4° $C_{acetonide}$), 114.9, 115.4, 128.5, 128.9, 133.5 (C_{Ar}), 135.8, 140.5, 153.1 (4° C_{Ar}), 172.1 (C-1), 201.6 (C-4).

Anal. Calcd for $C_{30}H_{37}NO_9$: C, 64.85; H, 6.71; N, 2.52. Found: C, 65.07; H, 7.03; N, 2.53.

$[\alpha]_D = -61.0$ (*c* 0.20 $CHCl_3$).

133d: **(2,3 *anti*$_2$).** White solid. Mp 130–132 °C.

^{1}H NMR ($CDCl_3$): δ 1.23, 1.26, 1.37, 1.47 (4 × s, 12H, C*H*$_3$), 1.3-1.4 (m, 3H, CHC*H*$_3$), 3.72 (s, 3H, OC*H*$_3$), 3.79 (br s, 1H, N*H*) 3.9-4.2 (m, 5H, H-3, 2H-6′, H-4′, H-5′), 4.15 (d, 1H, *J* = 3.6 Hz, H-2′), 4.41 (br, 1H, H-2), 5.21 (d, 1H, *J* = 2.7 Hz, H-3′), 5.59 (d, 1H, *J* = 3.6 Hz, H-1′′), 6.5-6.8 (m, 4H, H_{pmp}), 7.4-8.0 (m, 5H, H_{Ph}).

^{13}C NMR ($CDCl_3$): δ 14.0 (CH*C*H$_3$), 25.2, 26.1, 26.7, 26.9 (4 × *C*H$_3$), 44.1 (C-3), 55.7 (O*C*H$_3$), 60.7, (C-2), 67.3 (C-6′), 72.5 (C-5′), 76.8 (C-3′), 79.9 (C-4′), 82.0 (C-2′), 105.1 (C-1′), 109.4, 112.3 (4° $C_{acetonide}$), 114.8, 116.3, 128.3, 128.9, 133.4 (C_{Ar}), 135.8, 140.5, 153.5 (4° C_{Ar}), 171.5 (C-1), 201.1 (C-4).

$[\alpha]_D = +36.0$ (*c* 0.30 $CHCl_3$).

1′:2′:5′,6′-Di-*O*-isopropylidene-D-glucofuranos-3′-yl 2-(*N*-*p*-anisyl)amino-4-oxo-3-phenyl-phenylbutanoate (134).

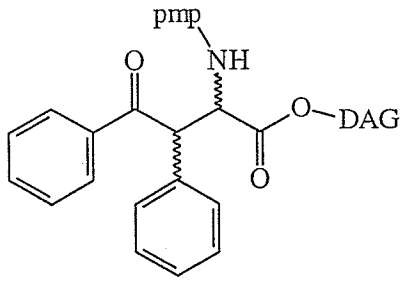

134a: **(2,3 *anti*$_1$).** White powder. Mp 155–157 °C.

^{1}H NMR ($CDCl_3$): δ 1.15, 1.21, 1.32, 1.45 (4 × s, 12H, C*H*$_3$), 3.6-3.7 (m, 1H, H-5'), 3.70 (s, 3H, OC*H*$_3$), 3.83 (dd, 1H, *J* = 8.6 and 6.2 Hz, H-6′a), 3.93 (dd, 1H, *J* = 8.6 and 4.2 Hz, H-6′b), 3.97 (d, 1H, *J* = 3.7, H-2′), 4.06 (dd, 1H, *J* = 7.7 and 2.9 Hz, H-4′), 4.69 (d, 1H, *J* = 7.5 Hz, H-2), 4.98 (d, 1H, *J* = 3.0 Hz, H-3′), 5.17 (d, 1H, *J* = 7.5 Hz, H-3), 5.72 (d, 1H, *J* = 3.7 Hz, H-1′), 6.6-6.8 (m, 4H, H$_{pmp}$), 7.2-8.0 (m, 10H, H$_{Ph}$).

^{13}C NMR ($CDCl_3$): δ 25.1, 26.1, 26.7, 26.8 (4 × *C*H$_3$), 55.7 (O*C*H$_3$), 56.2 (C-3), 63.3 (C-2), 66.9 (C-6′), 72.1 (C-5′), 76.6 (C-3′), 79.5 (C-4′), 82.9 (C-2′), 105.0 (C-1′), 109.2, 112.2 (4° C$_{acetonide}$), 114.6, 116.9, 128.0, 128.6, 128.9, 129.0, 129.3, 133.3 (C$_{Ar}$), 135.0, 136.3, 140.9, 153.6 (4° C$_{Ar}$), 171.9 (C-1), 197.8 (C-4).

Anal. Calcd for $C_{35}H_{39}NO_9$: C, 68.05; H, 6.36; N, 2.27. Found: C, 68.10; H, 6.66; N, 2.39.

$[\alpha]_D = -67.4$ (*c* 0.50 $CHCl_3$).

134b: **(2,3 *syn*$_1$).** White powder. Mp 173–175 °C.

^{1}H NMR ($CDCl_3$): δ 1.15, 1.28, 1.33, 1.48 (4 × s, 12H, CH_3), 3.78 (s, 3H, OCH_3), 3.7-3.8 (m, 1H, H-5′), 3.81 (dd, 1H, J = 8.6 and 6.1 Hz, H-6′a), 3.89 (dd, 1H, J = 8.6 and 4.6 Hz, H-6′b), 4.09 (dd, 1H, J = 8.2 and 2.9 Hz, H-4′), 4.43 (d, 1H, J = 3.7, H-2′), 4.72 (d, 1H, J = 8.6 Hz, H-2), 5.13 (d, 1H, J = 8.6 Hz, H-3), 5.22 (d, 1H, J = 2.9 Hz, H-3′), 5.80 (d, 1H, J = 3.7 Hz, H-1′), 6.5-6.7 (m, 4H, H$_{pmp}$), 7.1-8.0 (m, 10H, H$_{Ph}$).

^{13}C NMR ($CDCl_3$): δ 25.1, 26.2, 26.8, 26.9 (4 × CH_3), 55.7 (OCH_3), 56.6 (C-3), 61.4 (C-2), 67.1 (C-6′), 72.0 (C-5′), 76.9 (C-3′), 79.7 (C-4′), 82.9 (C-2′), 105.1 (C-1′), 109.2, 112.3 (4° C$_{acetonide}$), 114.7, 115.8, 127.9, 128.6, 128.9, 129.0, 129.1, 133.4 (C$_{Ar}$), 135.2, 135.9, 140.4 (4° C$_{Ar}$), 172.3 (C-1), 198.2 (C-4).

$[\alpha]_D$ = –146.2 (*c* 0.26 $CHCl_3$).

134c: **(2,3 *syn*$_2$).** White powder. Mp 120–122 °C.

^{1}H NMR ($CDCl_3$): δ 1.20, 1.33, 1.42, 1.46 (4 × s, 12H, CH_3), 3.71 (s, 3H, OCH_3), 4.0-4.1 (m, 2H, H-2′, H-6′a), 4.1-4.3 (m, 3H, H-4′, H-5′, H-6′b), 4.81 (d, 1H, J = 8.3 Hz, H-2), 5.08 (d, 1H, J = 8.3 Hz, H-3), 5.22 (d, 1H, J = 2.7 Hz, H-3′), 5.48 (d, 1H, J = 3.6 Hz, H-1′), 6.6-6.8 (m, 4H, H$_{pmp}$), 7.2-8.0 (m, 10H, H$_{Ph}$).

^{13}C NMR ($CDCl_3$): δ 25.3, 26.1, 26.7, 26.9 (4 × CH_3), 55.7 (OCH_3), 56.3 (C-3), 61.4 (C-2), 67.2 (C-6′), 72.5 (C-5′), 76.6 (C-3′), 79.8 (C-4′), 83.0 (C-2′), 105.1 (C-1′), 109.4, 112.2 (4° C$_{acetonide}$), 114.6, 116.8, 128.0, 128.6, 128.9, 129.1, 129.2, 133.3 (C$_{Ar}$), 134.8, 135.9, 140.4, 153.6 (4° C$_{Ar}$), 171.8 (C-1), 197.3 (C-4).

$[\alpha]_D$ = +87.0 (*c* 0.29 $CHCl_3$).

1′,2′:5′,6′-Di-*O*-isopropylidene-D-glucofuranos-3′-yl 2-(*N*-*p*-anisyl)amino-4-oxo-3-phenyl-phenylpentanoate (135).

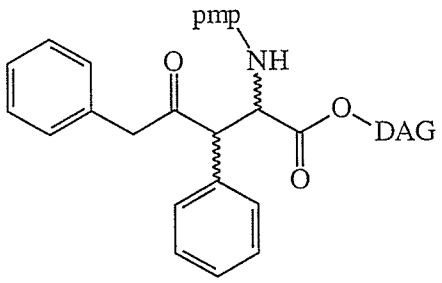

135a: **(2,3 *anti*$_1$).** Mp 133–135 °C.

^{1}H NMR ($CDCl_3$): δ 1.18, 1.20, 1.32, 1.44 (4 × s, 12H, CH_3), 3.6-3.7 (m, 1H, H-5′), 3.70 (s, 3H, OCH_3), 3.71 (s, 2H, 2H-5), 3.8-4.0 (m, 3H, H-2′, H-6′a, H-6′b), 4.02 (dd, 1H, J = 3.0 and 8.0 Hz, H-4′), 4.39 (d, 1H, J = 7.6 Hz, H-3), 4.52 (d, 1H, J = 7.6 Hz, H-2), 4.94 (d, 1H, J = 3.0 Hz, H-3′), 5.66 (d, 1H, J = 3.7 Hz, H-1′), 6.5-6.7 (m, 4H, H_{pmp}), 7.0-7.4 (m, 10H, H_{Ph}).

^{13}C NMR ($CDCl_3$): δ 25.2, 26.1, 26.6, 26.8 (4 × CH_3), 49.2 (C-5), 55.7 (OCH_3), 59.8 (C-3), 62.1 (C-2), 67.0 (C-6′), 72.0 (C-5′), 77.0 (C-3′), 79.5 (C-4′), 82.8 (C-2′), 105.0 (C-1′), 109.2, 112.2 (4° $C_{acetonide}$), 114.7, 116.8, 127.2, 128.3, 128.7, 129.1, 129.5, 129.7 (C_{Ar}), 133.3, 134.2, 140.7, 153.6 (4° C_{Ar}), 171.4 (C-1), 205.9 (C-4).

Anal. Calcd for $C_{36}H_{41}NO_9$: C, 68.45; H, 6.54; N, 2.22. Found: C, 68.76; H, 6.47; N, 2.43.

$[\alpha]_D$ = –93.2 (*c* 0.46 $CHCl_3$).

135b: **(2,3 *syn*$_1$).** Mp 143–145 °C.

^{1}H NMR ($CDCl_3$): δ 1.12, 1.17, 1.30, 1.39 (4 × s, 12H, CH_3), 2.94 (d, 1H, J = 3.7 Hz, H-2′), 3.70 (br s, 5H, 2H-5, OCH_3), 3.9-4.0 (m, 4H, H-4′, H-5′, H-6′a, H-6′b), 4.12 (d, 1H, J = 10.0 Hz, H-3), 4.64 (d, 1H, J = 10.0 Hz, H-2), 4.92 (d, 1H, J = 1.5 Hz, H-3′), 5.13 (d, 1H, J = 3.7 Hz, H-1′), 6.6-6.8 (m, 4H, H $_{pmp}$), 7.0-7.4 (m, 10H, H $_{Ph}$).

^{13}C NMR ($CDCl_3$): δ 25.1, 26.0, 26.5, 26.8 (4 × CH_3), 50.1 (C-5), 55.6 (OCH_3), 60.1 (C-2), 61.3 (C-3), 67.1 (C-6′), 72.1 (C-5′), 76.2 (C-3′), 79.5 (C-4′), 82.4 (C-2′), 105.0 (C-1′), 109.3, 111.9 (4° C $_{acetonide}$), 114.7, 116.8, 127.4, 128.4, 128.8, 129.0, 129.7, 129.8 (C $_{Ar}$), 133.1, 133.6, 140.3, 153.7 (4° C $_{Ar}$), 172.2 (C-1), 204.0 (C-4).

$[\alpha]_D$ = +86.7 (c 0.21 $CHCl_3$).

135c: **(2,3 *anti*$_2$).** Mp 123–125 °C.

^{1}H NMR ($CDCl_3$): δ 1.20, 1.30, 1.43, 1.47 (4 × s, 12H, CH_3), 3.35 (br d, 1H, N*H*), 3.66 (s, 2H, 2H-5), 3.70 (s, 3H, OCH_3), 3.93 (d, 1H, J = 3.6 Hz, H-2′), 4.0 (dd, 1H, J = 3.7 and 7.8 Hz, H-6′a), 4.1-4.2 (m, 3H, H-4′, H-5′, H-6′b), 4.28 (d, 1H, J = 8.2 Hz, H-3), 4.66 (br d, 1H, J = 8.2 Hz, H-2), 5.18 (d, 1H, J = 1.7 Hz, H-3′), 5.52 (d, 1H, J = 3.6 Hz, H-1′), 6.5-6.7 (m, 4H, H $_{pmp}$), 7.0-7.4 (m, 10H, H $_{Ph}$).

^{13}C NMR ($CDCl_3$): δ 25.2, 26.1, 26.7, 26.9 (4 × CH_3), 48.3 (C-5), 55.7 (OCH_3), 59.9, 60.2, (C-2, C-3), 67.2 (C-6′), 72.3 (C-5′), 76.7 (C-3′), 79.8 (C-4′), 83.0 (C-2′), 105.1 (C-1′), 109.4, 112.2 (4° C $_{acetonide}$), 114.5, 116.9, 127.1, 128.3, 128.6, 129.1, 129.5, 129.6 (C $_{Ar}$), 133.6, 133.9, 140.3, 153.6 (4° C $_{Ar}$), 172.0 (C-1), 205.2 (C-4).

$[\alpha]_D$ = +191.8 (c 0.17 $CHCl_3$).

135d: **(2,3 *syn*$_2$).** Mp 180–182 °C.

^{1}H NMR ($CDCl_3$): δ 1.13, 1.29, 1.34, 1.50 (4 × s, 12H, CH_3), 3.50 (br s, 1H, N*H*), 3.68 (s, 3H, OCH_3), 3.72 (s, 2H, 2H-5), 3.7-3.9 (m, 2H, H-5′, H-6′a), 3.90 (dd, 1H, J = 4.4 and 8.4 Hz, H-6′b), 4.09 (dd, 1H, J = 2.9 and 8.1 Hz, H-4′), 4.33 (d, 1H, J = 9.1 Hz, H-3), 4.39 (d, 1H, J = 3.6 Hz, H-2′), 4.56 (br d, 1H, J = 9.1 Hz, H-2), 5.21 (d, 1H, J = 2.9 Hz, H-3′), 5.80 (d, 1H, J = 3.6 Hz, H-1′), 6.4-6.7 (m, 4H, H$_{pmp}$), 6.9-7.4 (m, 10H, H$_{Ph}$). $[\alpha]_D$ = –86.0 (*c* 0.10 $CHCl_3$).

1′,2′;5′,6′-Di-*O*-isopropylidene-D-glucofuranos-3′-yl 2-(*N*-*p*-anisyl)amino-4-oxophenylbutanoate (136).

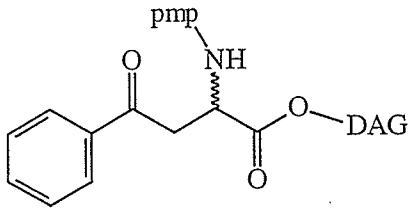

To freshly prepared LDA (0.96 mmol) in THF (5 mL) at –78 °C was added a solution of acetophenone (93 μL, 0.80 mmol) in THF (0.5 mL). After 20 min, a solution of the imine **123** (56 mg, 0.13 mmol) in THF (0.5 mL) was added, with rinsing (0.2 mL). The solution turned a darker yellow. The reaction was quenched after 1 h with saturated aqueous NH_4Cl, diluted with Et_2O (10 mL) and the layers separated. The water layer was extracted with Et_2O (2 × 15 mL), and the combined organic layers washed with H_2O (5 mL), dried and evaporated. Column chromatography (3 : 1, hexanes : EtOAc) yielded

34.1 mg (48%) of isomers **136**. The diastereomers were separated by preparative HPLC (~1% *i*PrOH/hexanes, Porasil® column).

136a: (*R*) isomer. White powder. Mp 122–123 °C.

^{1}H NMR ($CDCl_3$): δ 1.26, 1.27, 1.38, 1.49 (4 × s, 12H, CH_3), 3.53 (dd, 1H, *J* = 17.3 and 4.9 Hz, H-3a), 3.60 (dd, 1H, *J* = 17.3 and 5.8 Hz, H-3b), 3.74 (s, 3H, OCH_3), 3.9-4.2 (m, 4H, H-4′, H-5′, H-6′, H-6″), 4.42 (d, 1H, *J* = 3.6 Hz, H-2′), 4.53 (dd, 1H, *J* = 5.8 and 4.9 Hz, H-2), 5.27 (d, 1H, *J* = 2.7 Hz, H-3′), 5.58 (d, 1H, *J* = 3.6 Hz, H-1′), 6.6-6.8 (m, 4H, H_{pmp}), 7.4-8.0 (m, 5H, H_{Ph}).

^{13}C NMR ($CDCl_3$): δ 25.3, 26.2, 26.8, 26.9 (4 × CH_3), 41.1 (C-3), 54.4 (C-2), 55.8 (OCH_3), 67.3 (C-6′), 72.4 (C-5′), 77.0 (C-3′), 79.7 (C-4′), 82.8 (C-2′), 105.1 (C-1′), 109.4, 112.3 (4° $C_{acetonide}$), 115.0, 115.6, 128.1, 128.8, 133.8 (C_{Ar}), 136.2, 140.4, 153.2 (4° C_{Ar}), 171.9 (C-1), 197.3 (C-4).

Anal. Calcd for $C_{29}H_{35}NO_9$: C, 64.31; H, 6.51; N, 2.95. Found: C, 64.23; H, 6.62; N, 2.63;

$[\alpha]_D$ = –23.6 (*c* 0.2 $CHCl_3$).

136b: (*S*) isomer. Clear oil.

^{1}H NMR ($CDCl_3$): δ 1.11, 1.28, 1.34, 1.49 (4 × s, 12H, CH_3), 3.58 (dd, 1H, *J* = 17.8 and 5.2 Hz, H-3a), 3.67 (dd, 1H, *J* = 17.8 and 5.0 Hz, H-3b), 3.73 (s, 3H, OCH_3), 3.8-4.0 (m, 3H, H-5′, H-6′, H-6″), 4.12 (dd, 1H, *J* = 3.0 and 8.2 Hz, H-4′), 4.20 (d, 1H, *J* = 10.4 Hz, N*H*), 4.39 (d, 1H, *J* = 3.7 Hz, H-2′), 4.58 (dd, 1H, *J* = 5.2 and 5.0 Hz, H-2), 5.23 (d, 1H,

J = 3.0 Hz, H-3′), 5.83 (d, 1H, J = 3.7 Hz, H-1′), 6.6-6.8 (m, 4H, H_{pmp}), 7.4-8.0 (m, 5H, H_{Ph}).

^{13}C NMR ($CDCl_3$): δ 25.0, 26.2, 26.8, 26.9 (4 × CH_3), 41.7 (C-3), 54.4 (C-2), 55.7 (OCH_3), 67.3 (C-6'), 72.1 (C-5′), 77.0 (C-3′), 79.9 (C-4''), 83.0 (C-2′), 105.2 (C-1′), 109.3, 112.3 (4° $C_{acetonide}$), 114.9, 116.0, 128.1, 128.8, 133.7 (C_{Ar}), 136.2, 140.6, 153.5 (4° C_{Ar}), 172.6 (C-1), 197.2 (C-4).

$[\alpha]_D = -17.3$ (c 0.15 $CHCl_3$).

The configuration was assigned by conversion to the isopropyl ester. A small amount of **136b** (3 mg, 0.006 mmol) was dissolved in NaO*i*Pr/*i*PrOH (~0.04 M) at 0 °C and the reaction was monitored by TLC (2 : 1, hexanes : EtOAc). The reaction was quenched with H_2O and the product extracted with Et_2O (2 × 3 mL). The solution was dried and the solvent evaporated. Column chromatography (4 : 1, hexanes : EtOAc) yielded 1 mg of the isopropyl ester identified by comparison of its ^1H NMR spectra and optical rotation with the literature. $[\alpha]_D = +26.7$ (c 0.06 $CHCl_3$). Lit: $[\alpha]_D^{25} = +30.4$ (c 0.54 $CHCl_3$).[96]

2-(*S*)-(*N*-*p*-anisyl)amino-4-oxo-phenylbutanoic acid, methyl ester (128a).

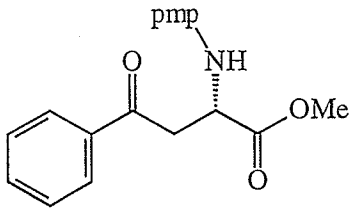

Compound **136b** (9.5 mg, 0.018 mmol) was dissolved in a NaOMe/MeOH (~0.05 M, 0.5 mL) solution. After 10 min the mixture was diluted with H_2O (2 mL) and extracted with Et_2O (2 × 5 mL). The combined organic layers were washed with a phosphate buffer solution (1 mL × 0.1 M, pH 7), dried and evaporated. Column chromatography (4 : 1, hexanes : EtOAc) yielded **128a** (3.3 mg, 60%).

1′,2′:5′,6′-Di-*O*-isopropylidene-D-allofuranos-3′-yl 2-(*N*-*p*-anisyl)amino-3-methyl-4-oxo-phenylbutanoate (138).

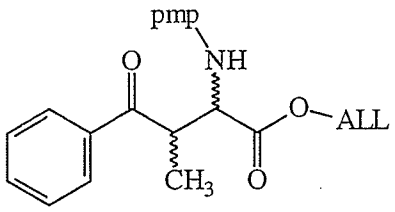

Compounds **138c** (*anti*$_1$) and **138d** (*anti*$_2$) could not be separated by preparative HPLC. Relative stereochemistries were assigned by cleavage to the methyl ester. Comparisons of HPLC retention times were then made with those of samples of the methyl esters prepared using the achiral imine **121**.

138a: **(2,3 *syn*$_1$).** White solid. Mp 95–97 °C.

^{1}H NMR ($CDCl_3$): δ 1.20, 1.33, 1.38, (3 × s, 12H, C*H*$_3$), 1.39 (m, 3H, CHC*H*$_3$), 3.72 (s, 3H, OC*H*$_3$), 3.79 (dd, 1H, *J* = 8.5 and 6.3 Hz, H-6′a), 3.9-4.2 (m, 3H, H-3, H-6′b, H-4′), 4.23 (ddd, 1H, *J* = 4.2, 6.3 and 6.5 Hz, H-5′), 4.3-4.4 (br d, 2H, H-2, N*H*), 4.7-4.8 (m,

2H, H-3′, H-2′), 5.77 (d, 1H, J = 3.6 Hz, H-1′), 6.6-6.8 (m, 4H, H_{pmp}), 7.4-8.0 (m, 5H, H_{Ph}).

^{13}C NMR ($CDCl_3$): δ 15.4 ($CHCH_3$), 25.2, 26.2, 26.5, 26.6 (4 × CH_3), 43.3 (C-3), 55.8 (OCH_3), 61.2, (C-2), 65.6 (C-6′), 73.4 (C-3′), 75.0 (C-5′), 77.2, 77.4 (C-2′, C-4′), 104.1 (C-1′), 110.0, 113.0 (4° $C_{acetonide}$), 114.8, 116.2, 128.5, 128.7, 133.3 (C_{Ar}), 136.4, 141.0, 153.2 (4° C_{Ar}), 172.5 (C-1), 201.8 (C-4).

Anal. Calcd for $C_{30}H_{37}NO_9$: C, 64.85; H, 6.71; N, 2.52. Found: C, 65.01; H, 7.06; N, 2.76.

$[\alpha]_D$ = +75.3 (*c* 0.30 $CHCl_3$).

138b: **(2,3 *syn*$_2$).** White solid. Mp 118–120 °C.

^1H NMR ($CDCl_3$): δ 1.24, 1.29, 1.33, 1.45 (4 × s, 12H, CH_3), 1.36 (d, 3H, J = 7.1 Hz, $CHCH_3$), 3.65 (m, 1H, H-6′a), 3.72 (s, 3H, OCH_3), 3.9-4.2 (m, 4H, H-3, H-6′b, H-4′, H-5′), 4.40 (d, 1H, J = 7.5 Hz, H-2), 4.7-4.8 (m, 2H, H-2′, H-3′), 5.78 (d, 1H, J = 3.8 Hz, H-1′), 6.6-6.8 (m, 4H, H_{pmp}), 7.4-8.0 (m, 5H, H_{Ph}).

^{13}C NMR ($CDCl_3$): δ 15.4 ($CHCH_3$), 25.1, 26.2, 26.6, 26.8 (4 × CH_3), 43.2 (C-3), 55.7 (OCH_3), 61.6, (C-2), 65.5 (C-6′), 73.6 (C-3′), 75.1 (C-5′), 77.5, 77.8 (C-4′, C-2′), 104.2 (C-1′), 109.9, 113.0 (4° $C_{acetonide}$), 114.7, 116.3, 128.4, 128.8, 133.4 (C_{Ar}), 136.5, 141.0, 153.3 (4° C_{Ar}), 172.5 (C-1), 201.6 (C-4).

$[\alpha]_D$ = +51.8 (*c* 0.43 $CHCl_3$).

1″,2″:5″,6″-Di-*O*-isopropylidene-D-glucofuranos-3″-yl 2-(*N*-*p*-anisyl)amino-2-(2′-oxocyclohexyl) acetate (139).

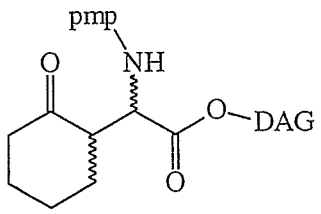

139a: **(1′,2 *anti*$_1$).** Yellow oil.

^{1}H NMR ($CDCl_3$): δ 1.13, 1.29, 1.32, 1.49 (4 × s, 12H, CH_3), 1.5-2.5 (m, 8H, H-3′, H-4′, H-5′, H-6′), 3.25 (m, 1H, H-1′), 3.51 (m, 1H, H-5″), 3.72 (s, 3H, OCH_3), 3.81 (dd, 1H, *J* = 8.7 and 6.1 Hz, H-6″a), 3.87 (dd, 1H, *J* = 8.7 and 4.5 Hz, H-6″b), 3.97 (d, 1H, *J* = 3.1, H-2), 4.03 (dd, 1H, *J* = 8.9 and 2.9 Hz, H-4″), 4.14 (br, 1H, N*H*), 4.48 (d, 1H, *J* = 3.6 Hz, H-2″), 5.15 (d, 1H, *J* = 2.9 Hz, H-3″), 5.92 (d, 1H, *J* = 3.6 Hz, H-1″), 6.5-6.8 (m, 4H, H$_{pmp}$).

^{13}C NMR ($CDCl_3$): δ 24.7, 25.0, 26.3, 26.8, 26.9, 27.0, 30.6 (4 × CH_3, 4 × CH_2), 42.0 (C-3′), 54.0 (C-1′), 55.7 (OCH_3), 59.0 (C-2), 67.3 (C-6″), 71.7 (C-5″), 76.9 (C-3″), 79.8 (C-4″), 82.8 (C-2″), 105.2 (C-1″), 109.2, 112.3 (4° C$_{acetonide}$), 114.8, 115.5 (C$_{Ar}$), 142.1, 152.9 (4° C$_{Ar}$), 172.7 (C-1), 211.6 (C-2′).

Anal. Calcd for $C_{27}H_{37}NO_9$: C, 62.41; H, 7.17; N, 2.70. Found: C, 62.53; H, 7.58; N, 2.75.

$[\alpha]_D$ = –143.6 (*c* 0.14 $CHCl_3$).

139b: **(1′,2 *syn*$_1$).** Yellow oil.

^{1}H NMR ($CDCl_3$): δ 1.25, 1.31, 1.39, 1.48 (4 × s, 12H, C*H*$_3$), 1.5-2.5 (m, 8H, H-3′, H-4′, H-5′, H-6′), 3.05 (m, 1H, H-1′), 3.73 (s, 3H, OC*H*$_3$), 3.9-4.3 (m, 6H, H-2, H-4″, H-5″, H-6″, N*H*), 4.22 (d, 1H, J = 3.6 Hz, H-2″), 5.20 (d, 1H, J = 2.6 Hz, H-3″), 5.52 (d, 1H, J = 3.6 Hz, H-1″), 6.6-6.8 (m, 4H, H$_{pmp}$).

^{13}C NMR ($CDCl_3$): δ 24.6, 25.3, 26.2, 26.8, 26.9, 27.0, 30.7 (4 × *C*H$_3$, 4 × *C*H$_2$), 41.8 (C-3′), 53.5 (C-1′), 55.8 (O*C*H$_3$), 59.3 (C-2), 67.3 (C-6″), 72.4 (C-5″), 76.7 (C-3″), 79.8 (C-4″), 82.7 (C-2″), 105.0 (C-1″), 109.4, 112.4 (4° C$_{acetonide}$), 114.8, 115.7 (C$_{Ar}$), 142.0, 153.1 (4° C$_{Ar}$), 171.8 (C-1), 210.9 (C-2′).

$[\alpha]_D$ = –12.8 (*c* 0.50 $CHCl_3$).

139c: **(1′,2 *syn*$_2$).** White fluffy crystals. Mp 164–166 °C.

^{1}H NMR ($CDCl_3$): δ 1.20, 1.29, 1.35, 1.49 (4 × s, 12H, C*H*$_3$), 1.6-2.5 (m, 8H, H-3′, H-4′, H-5′, H-6′), 2.87 (m, 1H, H-1′), 3.73 (s, 3H, OC*H*$_3$), 3.85 (br, 1H, N*H*), 3.9-4.2 (m, 5H, H-2, H-4″, H-5″, H-6″), 4.47 (d, 1H, J = 3.6 Hz, H-2″), 5.23 (d, 1H, J = 2.8 Hz, H-3″), 5.77 (d, 1H, J = 3.6 Hz, H-1″), 6.6-6.8 (m, 4H, H$_{pmp}$).

^{13}C NMR ($CDCl_3$): δ 24.9, 25.2, 26.3, 26.8, 26.9, 27.4, 30.6 (4 × *C*H$_3$, 4 × *C*H$_2$), 42.0 (C-3′), 53.8 (C-1′), 55.7 (O*C*H$_3$), 58.3 (C-2), 67.3 (C-6″), 72.3 (C-5″), 76.7 (C-3″), 79.7 (C-4″), 82.7 (C-2″), 105.2 (C-1″), 109.3, 112.3 (4° C$_{acetonide}$), 114.9, 115.7 (C$_{Ar}$), 140.6, 153.2 (4° C$_{Ar}$), 172.3 (C-1), 210.6 (C-2′).

$[\alpha]_D$ = –93.9 (*c* 0.23 $CHCl_3$).

139d: **(1′,2 *anti*$_2$).** Yellow oil.

^{1}H NMR ($CDCl_3$): δ 1.24, 1.29, 1.39, 1.48 (4 × s, 12H, C*H*$_3$), 1.5-2.5 (m, 8H, H-3′, H-4′, H-5′, H-6′), 2.84 (ddd, 1H, *J* = 11.4, 5.3 and 6.6 Hz, H-1′), 3.73 (s, 3H, OC*H*$_3$), 3.80 (br, 1H, N*H*), 3.9-4.2 (m, 4H, H-4″, H-5″, H-6″), 4.19 (d, 1H, *J* = 3.6 Hz, H-2″), 4.24 (d, 1H, *J* = 5.3 Hz, H-2), 5.20 (d, 1H, *J* = 2.9 Hz, H-3″), 5.71 (d, 1H, *J* = 3.6 Hz, H-1″), 6.7-6.8 (m, 4H, H$_{pmp}$).

^{13}C NMR ($CDCl_3$): δ 24.9, 25.3, 26.2, 26.7, 26.8, 26.9, 29.8 (4 × *C*H$_3$, 4 × *C*H$_2$), 41.9 (C-3′), 53.9 (C-1′), 55.7 (O*C*H$_3$), 58.6 (C-2), 67.2 (C-6″), 72.4 (C-5″), 76.6 (C-3″), 79.8 (C-4″), 83.0 (C-2″), 105.2 (C-1″), 109.3, 112.2 (4° C$_{acetonide}$), 114.8, 116.7 (C$_{Ar}$), 140.9, 153.5 (4° C$_{Ar}$), 172.4 (C-1), 210.1 (C-2′).

$[\alpha]_D$ = +10.5 (*c* 0.76 $CHCl_3$).

Example of *N*-oxidative deprotection.

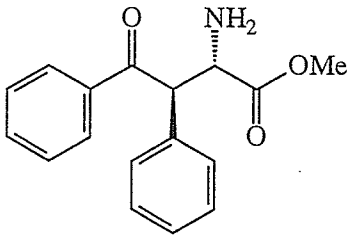

To **130b** (5 mg, 0.013 mmol) in acetonitrile (0.5 mL) was added a solution of ceric ammonium nitrate (CAN) (21 mg, 0.039 mmol) in water (0.2 mL).[172] The solution immediately turned a dark reddish color that gradually faded to a pale orange. After 10 min Et_2O and H_2O (1 mL each) were added. The layers were separated and the H_2O layer

washed with Et_2O (1 mL). The combined organic layers were washed with a solution of 1:2, $NaHCO_3$: 10% $Na_2S_2O_3$ (0.5 mL), then 10% $Na_2S_2O_3$ (2 × 0.2 mL), dried and evaporated. Yield 3.2 mg (89%). The products were generally used without further purification.

Synthesis of Pd complex (145).

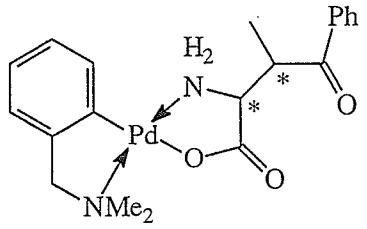

The *N*-pmp protecting group was removed from a mixture of **133a-d** using ceric ammonium nitrate (CAN) as described above. One diastereomeric product was found to separate from the others using column chromatography (EtOAc). A sample of this material (4.3 mg, 0.009 mmol) was dissolved in Et_2O (0.5 mL) and KOTMS (1.5 mg, 0.011 mmol) was added. After 30 min the mixture was diluted with H_2O and the products extracted with Et_2O until no further DAGOH was removed. The aqueous layer was evaporated to dryness to give crude **146**. This material was dissolved in fresh H_2O and the Pd-dimer **144** (2.5 mg) was added with vigorous stirring. After 16 h the product was extracted with CH_2Cl_2 (3 × 2 mL). The organic layers were dried and the solvent evaporated to give 3.8 mg (88%) of product. A ^1H NMR spectrum of compound **145** or **146** showed two products (2 : 3).

Synthesis of MTPA amides 147a-d

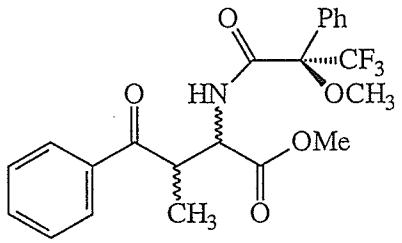

The free amino compounds were prepared from a mixture of **129a** and **129b** using the CAN method described earlier. To a solution of these free amines (56 mg, 0.25 mmol) and iPr_2NEt (66 μL, 0.38 mmol) in CH_2Cl_2 (2 mL) was added (*S*)-MTPACl (57 μL, 0.3 mmol)[190] and the solution was stirred for 48 h. The reaction was quenched with water (2 mL). The phases were separated and the water layer washed with Et_2O (15 mL). The combined organic extracts were washed with aqueous 10% HCl, Na_2CO_3, H_2O (1 mL each), dried and evaporated. Column chromatography (4 : 1, hexanes : EtOAc) gave the products **147a-d** (66 mg, 60%). The four diastereomers were separated by HPLC (0.5% *i*OPrOH/hexanes) and their ^1H NMR spectra recorded.

147a: ***syn.*** ^1H NMR ($CDCl_3$): δ 1.28 (d, 3H, J = 7.1 Hz, CH_3), 3.42 (s, 3H, OCH_3), 3.76 (s, 3H, CO_2CH_3), 4.20 (m, 1H, H-3), 4.88 (m, 1H, H-2), 7.1-8.0 (m, 11H, H_{Ph}, N*H*).

147b: ***syn.*** ^1H NMR ($CDCl_3$): δ 1.30(d, 3H, J = 7.0 Hz, CH_3), 3.36 (s, 3H, OCH_3), 3.74 (s, 3H, CO_2CH_3), 4.17 (m, 1H, H-3), 4.90 (m, 1H, H-2), 7.3-8.0 (m, 11H, H_{Ph}, N*H*).

147c: ***anti.*** ^1H NMR ($CDCl_3$): δ 1.09 (d, 3H, J = 7.1 Hz, CH_3), 3.67 (s, 6H, OCH_3, CO_2CH_3), 4.29 (m, 1H, H-3), 5.02 (dd, 1H, J = 6.6 Hz, H-2), 7.3-8.0 (m, 11H, H_{Ph}, N*H*).

147d: ***anti.*** ^1H NMR ($CDCl_3$): δ 1.31 (d, 3H, J = 7.2 Hz, CH_3), 3.47 (s, 3H, OCH_3), 3.64 (s, 3H, CO_2CH_3), 4.34 (m, 1H, H-3), 5.05 (dd, 1H, J = 6.6 Hz, H-2), 7.3-8.0 (m, 11H,

H_{Ph}), 8.33 (br d, 1H, N*H*).

Example synthesis of MPA amides (149c/d).

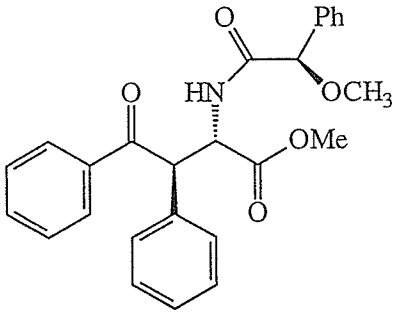

+ other anti diastereomer

To the free amine prepared from **130b** (3.2 mg, 0.011 mmol) in CH_2Cl_2 (0.5 mL) was added (*R*)-α-methoxyphenylacetic acid (MPA) (2.2 mg, 0.013 mmol) followed by DCC (2.9 mg, 0.014 mmol). After a few minutes a fine white precipitate was observed. After 15 min the solution was filtered and evaporated. The residue was re-dissolved in cold Et_2O, filtered through Celite and evaporated. This was repeated until no further precipitate was observed. The diastereomers **149c/d** were separated by column chromatography (2 : 1, hexanes: EtOAc). ^1H NMR spectra were run in CD_3CN. $Ba(ClO_4)_2$ (2eq) was then added and a second spectra was run. $\Delta\delta^{Ba}$s were then calculated for relevant protons ($\Delta\delta^{Ba}$ = (δ in the presence of Ba^{2+}) – (δ original spectra)). Alternatively, if racemization became a problem due to long reaction times, the amides were prepared by *in situ* generation of the MPA chloride.[182]

Examples of these spectral comparisons are shown in Appendix 2.

List of References

(1) Parlington, J. R. *A History of Chemistry*; MacMillan & Co. Ltd.: Toronto, **1964**; Vol. 4.

(2) March, J. *Advanced Organic Chemistry*; 4th ed.; Wiley-Interscience: New York, **1992**, p. 107.

(3) McMurry, J. *Organic Chemistry*, 1st ed.; Brooks/Cole: California, **1984**, p. 40.

(4) Palomo, C.; Oiarbide, M.; Azipurua, J. M.; González, A.; García, J. M.; Landa, C.; Odriozola, I.; Linden, A. *J. Org. Chem.* **1999**, *64*, 8193-8200.

(5) Reetz, M. T. *Chem. Rev.* **1999**, *99*, 1121-1162.

(6) Jackson, R. F. W.; Wishart, N.; Wood, A.; James, K.; Wythes, M. J. *J. Org. Chem.* **1992**, *57*, 3397-3404.

(7) Swindell, C. S.; Tao, M. *J. Org. Chem.* **1993**, *58*, 5889-5891.

(8) Kober, R.; Papadopoulos, K.; Miltz, W.; Enders, D.; Steglich, W. *Tetrahedron* **1985**, *41*, 1693-1701.

(9) Hattori, K.; Miyata, M.; Yamamoto, H. *J. Am. Chem. Soc.* **1993**, *115*, 1151-1152.

(10) Pons, D.; Savignac, M.; Genet, J.-P. *Tetrahedron Lett.* **1990**, *31*, 5023-5026.

(11) Barluenga, J.; Fernández-Marí, F.; Viado, A. L.; Aguilar, E.; Olano, B. *J. Org. Chem.* **1996**, *61*, 5659-5662.

(12) Food & Drug Administration, policy statements, 1992.

(13) Stinson, S. C. *Chem. Eng. News* **1999**; Vol. 77, p 101-120.

(14) Ledbetter, E. *Modern Drug Discovery* **2000**; Vol. 3, p 25-28.

(15) Brennan, M. B. *Drug Discovery Today* **1999**; Vol. 77, p 91-99.

(16) Procter, G. *Asymmetric Synthesis*; Oxford University Press: New York, **1996**.

(17) Ikan, R. *Natural Products*; 2nd ed.; Academic Press, Inc.: New York, **1991**.

(18) Coppola, G. M.; Schuster, H. F. *Asymmetric Synthesis*; Wiley-Interscience: New York, **1987**.

(19) Crosby, J. *Tetrahedron* **1991**, *47*, 4789-4846.

(20) Reider, P. J.; Davis, P.; Hughes, D. L.; Grabowski, E. J. J. *J. Org. Chem.* **1987**, *52*, 955-957.

(21) Buisson, D.; Azerad, R. *Tetrahedron Lett.* **1986**, *27*, 2631-2634.

(22) Blaser, H.-U. *Chem. Rev.* **1992**, *92*, 935-952.

(23) Chida, N.; Yamada, K.; Ogawa, S. *Chem. Lett.* **1992**, 687-690.

(24) Bols, M. *Carbohydrate Building Blocks*; Wiley-Interscience: Toronto, **1996**.

(25) Boons, G.-J.; Hale, K. J. *Organic Synthesis with Carbohydrates*; Blackwell Science, Inc: Malden, **2000**.

(26) Shinozaki, K.; Mizuno, K.; Oda, H.; Masaki, Y. *Chem. Lett.* **1992**, 2265-2268.

(27) Wasserman, H. H.; Gambale, R. J. *J. Am. Chem. Soc.* **1985**, *107*, 1423-1424.

(28) Nógrádi, M. *Stereoselective Synthesis*; 2nd ed.; VCH: New York, **1995**.

(29) Pfenninger, A. *Synthesis* **1986**, 89-116.

(30) Jones, J. B. In *Asymmetric Synthesis*; Morrison, J. D., Ed.; Academic Press, Inc.: New York, **1985**; Vol. 5, p 309-345.

(31) Duthaler, R. O.; Hafner, A.; Riediker, M. *Org. Synth. Organomet., Proc. Symp.* **1991**, *3*, 285-309.

(32) Whitcombe, M. J.; Alexander, C.; Vulfson, E. N. *Synlett* **2000**, 911-923.

(33) Gamez, P.; Dunjic, B.; Pinel, C.; Lemaire, M. *Tetrahedron Lett.* **1995**, *36*, 8779-8782.

(34) Jalander, L.; Strandberg, R. *Acta. Chem. Scand. B* **1983**, *37*, 15-19.

(35) Davis, F. A.; Reddy, R. E.; Szewczyk, J. M. *J. Org. Chem.* **1995**, *60*, 7037-7039.

(36) Evans, D. A.; Yang, M. G.; Dart, M. J.; Duffy, J. L.; Kim, A. S. *J. Am. Chem. Soc.* **1995**, *117*, 9598-9599.

(37) Masamune, S.; Choy, W.; Petersen, J. S.; Sita, L. R. *Angew. Chem. Int. Ed. Engl.* **1985**, *24*, 1-76.

(38) Mengel, A.; Reiser, O. *Chem. Rev.* **1999**, *99*, 1191-1223.

(39) Roush, W. R.; Adam, M. A.; Walts, A. E.; Harris, D. J. *J. Am. Chem. Soc.* **1986**, *108*, 3422-3434.

(40) Roush, W. R.; Hoong, L. K.; Palmer, M. A. J.; Park, J. C. *J. Org. Chem.* **1990**, *55*, 4109-4117.

(41) Ahn, K. H.; Lee, S.; Lim, A. *J. Org. Chem.* **1992**, *57*, 5065-5066.

(42) Ojima, I.; Habus, I. *Tetrahedron Lett.* **1990**, *31*, 4289-4292.

(43) Seyden-Penne, J. *Chiral Auxiliaries and Ligands in Asymmetric Synthesis*; Wiley-Interscience: New York, **1995**.

(44) Hultin, P. G.; Earle, M. A.; Sudharshan, M. *Tetrahedron* **1997**, *53*, 14823-14870.

(45) Kunz, H. *Pure & Appl. Chem.* **1995**, *67*, 1627-1635.

(46) Kunz, H.; Ruck, K. *Angew. Chem. Int. Ed. Engl.* **1993**, *32*, 336-358.

(47) Kunz, H.; Pfrengle, W. *Tetrahedron* **1988**, *44*, 5487-5494.

(48) Kunz, H.; Pfrengle, W. *J. Am. Chem. Soc.* **1988**, *110*, 651-652.

(49) Kunz, H.; Sager, W. *Angew. Chem. Int. Ed. Engl.* **1987**, *26*, 557-559.

(50) Kunz, H.; Sager, W.; Schanzenbach, D.; Decker, M. *Ann,* **1991**, 649-654.

(51) Kunz, H.; Sager, W.; Pfrengle, W.; Schanzenbach, D. *Tetrahedron Lett.* **1988**, *29*, 4397-4400.

(52) Kunz, H.; Pfrengle, W.; Rück, K.; Sager, W. *Synthesis* **1991**, 1039-1042.

(53) Lowe, R. F.; Stoodley, R. J. *Tetrahedron Lett.* **1994**, *35*, 6351-6354.

(54) Cousins, R. P. C.; Curtis, A. D. M.; Ding, W. C.; Stoodley, R. J. *Tetrahedron Lett.* **1995**, *36*, 8689-8692.

(55) Solladie, G.; Clair, J.-F. S.; Philippe, M.; Semeria, D.; Maignan, J. *Tetrahedron Asymmetry* **1996**, *7*, 2359-2364.

(56) Heathcock, C. H.; White, C. T.; Morrison, J. J.; VanDerveer, D. *J. Org. Chem.* **1981**, *46*, 1296-1309.

(57) Kunz, H.; Mohr, J. *J. Chem. Soc., Chem. Commun.* **1988**, 1315-1317.

(58) Mulzer, J.; Hiersemann, M.; Buschmann, J.; Luger, P. *Ann.* **1996**, 649-654.

(59) Evans, D. A.; Takacs, J. M.; McGee, L. R.; Ennis, M. D.; Mathre, D. J.; Bartoli, J. *Pure Appl. Chem.* **1981**, *53*, 1109-1127.

(60) Köll, P.; Lutzen, A. *Tetrahedron Asymmetry* **1996**, *7*, 637-640.

(61) Banks, M. R.; Cadogan, J. I. G.; Gosney, I.; Hodgson, P. K. G.; Thorburn, P. *Chiral'95* Europe, **1995**.

(62) Banks, M. R.; Cadogan, J. I. G.; Gosney, I.; Gaur, S.; Hodgson, P. K. G. *Tetrahedron Asymmetry* **1994**, *5*, 2447-2458.

(63) Banks, M. R.; Blake, A. J.; Cadogan, J. I. G.; Dawson, I. M.; Gosney, I.; Grant, K. J.; Gaur, S.; Hodgson, P. K. G.; Knight, K. S.; Smith, G. W.; Stevenson, D. E. *Tetrahedron* **1992**, *48*, 7979-8006.

(64) Izumi, Y.; Chibata, I.; Itoh, T. *Angew. Chem. Int. Ed. Engl.* **1978**, *17*, 176-183.

(65) Evans, D. A.; Britton, T. C.; Ellman, J. A.; Dorow, R. L. *J. Am. Chem. Soc.* **1990**, *112*, 4011-4030.

(66) Duthaler, R. O. *Tetrahedron* **1994**, *50*, 1539-1650.

(67) Greenstein, J. P.; Winitz, M., Eds; *Chemistry of the Amino Acids*; Kreiger Publishing Co.: Florida, **1961**; Vol. 1.

(68) Barrett, G. C. *Chemistry and Biochemistry of the Amino Acids*; Chapman and Hall: New York, **1985**.

(69) O'Donnell, M. J.; Chen, N.; Zhou, C.; Murray, A.; Kubiak, C. P.; Yang, F.; Stanley, G. G. *J. Org. Chem.* **1997**, *62*, 3962-3975.

(70) Oppolzer, W. *J. Pure Appl. Chem.* **1990**, *62*, 1241-1250.

(71) Williams, R. M. *Synthesis of Optically Active α-Amino Acids*; Pergamon Press: New York, **1989**.

(72) Schöllkopf, U. In *Topics in Current Chemistry*; Boschke, D. F. L., Ed.; Springer-Verlag: New York, **1983**; Vol. 109, p 65-84.

(73) Seebach, D.; Juaristi, E.; Miller, D. D.; Schickli, C.; Weber, T. *Helv. Chim. Acta* **1987**, *70*, 237-261.

(74) Williams, R. M. *Aldrichimica Acta* **1992**, *25*, 11-25.

(75) Sinclair, P. J.; Zhai, D.; Reibenspies, J.; Williams, R. M. *J. Am. Chem. Soc.* **1986**, *108*, 1103-1104.

(76) Williams, R. M.; Im, M.-N. *J. Am. Chem. Soc.* **1991**, *113*, 9276-9286.

(77) Williams, R. M.; Sinclair, P. J.; Zhai, D.; Chen, D. *J. Am. Chem. Soc.* **1988**, *110*, 1547-1557.

(78) Williams, R. M.; Fegley, G. J. *Tetrahedron Lett.* **1992**, *33*, 6755-6758.

(79) Bender, D. M.; Williams, R. M. *J. Org. Chem.* **1997**, *62*, 6690-6691.

(80) Williams, R. M.; Fegley, G. J. *J. Am. Chem. Soc.* **1991**, *113*, 8796-8806.

(81) Decker, H.; Zahner, H.; Heitsch, H.; Konig, W. A.; Fiedler, H.-P. *J. Gen. Microbiology* **1991**, *137*, 1805-1813.

(82) Jackson, R. F. W.; Rettie, A. B.; Wood, A.; Wythes, M. J. *J. Chem. Soc. Perkin 1* **1994**, 1719.

(83) Jackson, R. F. W.; Turner, D.; Block, M. H. *J. Chem. Soc. Chem. Commun.* **1995**, 2207-2208.

(84) Gair, S.; Jackson, R. F. W.; Brown, P. A. *Tetrahedron Lett.* **1997**, *38*, 3059-3062.

(85) Salituro, F. G.; McDonald, I. M. *J. Org. Chem.* **1988**, *53*, 6138-6139.

(86) König, W. A.; Hass, W. *Ann.* **1980**, 622-628.

(87) Barrett, A. G. M.; Dhanak, D.; Lebold, S. A.; Russell, M. A. *J. Org. Chem.* **1991**, *56*, 1894-1901.

(88) Saksena, A. K.; Lovey, R. G.; Girjavallabhan, V. M.; Guzik, H.; Ganguly, A. K. *Tetrahedron Lett.* **1993**, *34*, 3267-3270.

(89) Barrett, A. G. M.; Lebold, S. A. *J. Org. Chem.* **1991**, *56*, 4875-4884.

(90) Berrée, F.; Chang, K.; Cobas, A.; Rapoport, H. *J. Org. Chem.* **1996**, *61*, 715-721.

(91) Mooiweer, H. H.; Ettema, K. W. A.; Hiemstra, H.; Speckamp, W. N. *Tetrahedron* **1990**, *46*, 2991-2998.

(92) Roos, E. C.; Lopez, M. C.; Brook, M. A.; Hiemstra, H.; Speckamp, W. N.; Kaptein, B.; Kamphius, J.; Shoemaker, H. E. *J. Org. Chem.* **1993**, *53*, 3259-3268.

(93) Merla, B.; Grumbach, H.-J.; Risch, N. *Synthesis* **1998**, 1609-1614.

(94) Loh, T.-P.; Wei, L.-L. *Tetrahedron Lett.* **1998**, *39*, 323-326.

(95) Bretschneider, T.; Miltz, W.; Munster, P.; Steglich, W. *Tetrahedron* **1988**, *44*, 5403-5414.

(96) Hagiwara, E.; Fujii, A.; Sodeoka, M. *J. Am. Chem. Soc.* **1998**, *120*, 2474-2475.

(97) Fujii, A.; Hagiwara, E.; Sodeoka, M. *J. Am. Chem. Soc.* **1999**, *121*, 5450-5458.

(98) Ferraris, D.; Young, B.; Cox, C.; III, W. J. D.; Dudding, T.; Lectka, T. *J. Org. Chem.* **1998**, *63*, 6090-6091.

(99) Ferraris, D.; Young, B.; Dudding, T.; Lectka, T. *J. Am. Chem. Soc.* **1998**, *120*, 4548-4549.

(100) Krüger, J.; Carreira, E. M. *J. Am. Chem. Soc.* **1998**, *120*, 837-838.

(101) Barluenga, J.; Viado, A. L.; Aguilar, E.; Olano, S. F. B. *J. Org. Chem.* **1993**, *58*, 5972-5975.

(102) Danishefsky, S. J.; Pearson, W. H.; Segmuller, B. E. *J. Am. Chem. Soc.* **1985**, *107*, 1280-1285.

(103) Crossley, M. J.; Fung, Y. M.; Kyriakopoulos, E.; Potter, J. J. *J. Chem. Soc. Perkin Trans. 1* **1998**, 1123-1130.

(104) Panek, J. A.; Yang, M.; Mular, I. *J. Org. Chem.* **1992**, *57*, 4063-4064.

(105) Arend, M.; Westermann, B.; Risch, N. *Angew. Chem. Int. Ed. Engl.* **1998**, *37*, 1044-1070.

(106) Heathcock, C. H. *The Bimolecular Aliphatic Mannich and Related Reactions*; Pergamon Press: New York, **1991**; Vol. 2, Chapter 4.1.

(107) Tramontini, M.; Angiolini, L. *Tetrahedron* **1990**, *46*, 1791-1837.

(108) Mannich, C.; Krösche, W. *Arch. Chem.* **1913**, *250*, 647-667.

(109) Scheibler, H.; Voß, J. *Chem. Ber.* **1920**, *53*, 388-410.

(110) Levine, R. *Chem. Rev.* **1954**, *54*, 467-573.

(111) Heathcock, C. H. *Modern Synthetic Methods*; Scheffield, R., Ed.; Weinheim/UCH: 1**992**, p 1-102.

(112) Dubois, J.-E.; Dubois, M. *Tetrahedron Lett.* **1967**, *43*, 4215-4219.

(113) Ireland, R. E.; Willard, A. K. *Tetrahedron Lett.* **1975**, *46*, 3975-3978.

(114) Ireland, R. E.; Mueller, R. H.; Willard, A. K. *J. Am. Chem. Soc.* **1976**, *98*, 2868-2877.

(115) Xie, L.; Isenberger, K. M.; Held, G.; Dahl, L. M. *J. Org. Chem.* **1997**, *62*, 7516-7519.

(116) Li, Y.; Padden-Row, M. N.; Houk, K. N. *J. Org. Chem.* **1990**, *55*, 481-493.

(117) Zimmerman, H. E.; Traxler, M. D. *J. Am. Chem. Soc.* **1957**, *79*, 1920-1923.

(118) Evans, D. A.; Nelson, J. V.; Taber, T. R. In *Topics in Stereochemistry*; Allinger, N. L., Eliel, E. L., Wilen, S. H., Eds.; Wiley: Toronto, **1982**; Vol. 13, p 1-115.

(119) Heathcock, C. H. In *Asymmetric Synthesis*; Morrison, J. D., Ed.; Academic Press: New York, **1984**; Vol. 3, p 111-212.

(120) Dubois, J.-E.; Fellmann, P. *Tetrahedron Lett.* **1975**, *14*, 1225-1228.

(121) Fellmann, P.; Dubois, J.-E. *Tetrahedron* **1978**, *34*, 1349-1357.

(122) Evans, D. A.; McGee, L. R. *Tetrahedron Lett.* **1980**, *21*, 3975-3978.

(123) Nakamura, E.; Kuwajima, I. *Tetrahedron Lett.* **1983**, *24*, 3343-3346.

(124) Mukaiyama, T.; Banno, K.; Narasaka, K. *J. Am. Chem. Soc.* **1974**, *96*, 7503-7509.

(125) Evans, D. A.; Dart, M. J.; Duffy, J. L.; Yang, M. G. *J. Am. Chem. Soc.* **1996**, *118*, 4322-4343 and references therein.

(126) Evans, D. A.; Bartroli, J.; Shih, T. L. *J. Am. Chem. Soc.* **1981**, *103*, 2127-2129.

(127) Loh, T.-P.; Chua, G.-L.; Vittal, J. J.; Wong, M.-W. *J. Chem. Soc. Chem. Commun.* **1998**, 861-862.

(128) Hart, D. J.; Ha, D.-C. *Chem. Rev.* **1989**, *89*, 1447-1465.

(129) Corey, E. J.; Decicco, C. P.; Newbold, R. C. *Tetrahedron Lett.* **1991**, *32*, 5287-5290.

(130) Bernardi, A.; Gennari, C.; Raimondi, L.; Villa, M. B. *Tetrahedron Lett.* **1997**, *53*, 7705-7714.

(131) Fujisawa, T.; Kooriyama, Y.; Shimizu, M. *Tetrahedron Lett.* **1996**, *37*, 3881-3884.

(132) Matsumura, Y.; Tomita, T. *Tetrahedron Lett.* **1994**, *35*, 3737-3740.

(133) Seebach, D.; Betschart, C.; Schiess, M. *Helv. Chi. Acta* **1984**, *67*, 1593-1597.

(134) Ishihara, K.; Miyata, M.; Hattori, K.; Tada, T.; Yamamoto, H. *J. Am. Chem. Soc.* **1994**, *116*, 10520-10524.

(135) Ishitani, H.; Ueno, M.; Kobayashi, S. *J. Am. Chem. Soc.* **1997**, *119*, 7153-7154.

(136) Kobayashi, S.; Ishitani, H. *Chem. Rev.* **1999**, *99*, 1069-1094.

(137) Keynes, M. N. M.Sc., University of Manitoba, **1996**.

(138) Wolfrom, M. L.; Schuetz, R. D.; Cavalieri, L. F. *J. Am. Chem. Soc.* **1949**, *71*, 3518-3523.

(139) Rück, K. *Angew. Chem. Int. Eng.* **1995**, *34*, 433435.

(140) Solladie-Cavallo, A.; Csaky, A. G.; Gantz, I.; Suffert, J. *J. Org. Chem.* **1994**, *59*, 5343-5346.

(141) Akitt, J. W. *NMR and Chemistry* Chapman & Hall: New York, 1992.

(142) Schwesinger, R.; Schlemper, H. *Angew. Chem. Int. Eng.* **1987**, *26*, 1167-1169.

(143) Bernstein, M. P.; Romesberg, F. E.; Fuller, D. J.; Harrison, A. T.; Collum, D. B.; Liu, Q.-Y.; Williard, P. G. *J. Am. Chem. Soc.* **1992**, *114*, 5100-5110.

(144) Henderson, K. W.; Dorigo, A. E.; Liu, Q.-Y.; Williard, P. G.; Schleyer, P. v. R.; Bernstein, P. R. *J. Am. Chem. Soc.* **1996**, *118*, 1339-1347.

(145) Amstutz, R.; Schweizer, W. B.; Seebach, D.; Dunitz, J. D. *Helv. Chim. Acta* **1981**, *64*, 2617-2621.

(146) Seebach, D.; Amstutz, R.; Dunitz, J. D. *Helv. Chim. Acta* **1981**, *64*, 2622-2626.

(147) Polt, R.; Seebach, D. *J. Am. Chem. Soc.* **1989**, *111*, 2622-2632.

(148) Laube, T.; Dunitz, J. D.; Seebach, D. *Helv. Chim. Acta* **1985**, *68*, 1373-.

(149) Heathcock, C. H.; Davidson, S. K.; Hug, K. T.; Flippin, L. A. *J. Org. Chem.* **1986**, *51*, 3027-3037.

(150) Eliel, E. L.; Wilen, S. H.; Mander, L. N. In *Stereochemistry of Organic Compounds*; Wiley: New York, **1994**, p 734.

(151) Spevak, W.; Dasgupta, F.; Hobbs, C. J.; Nagy, J. O. *J. Org. Chem.* **1996**, *61*, 3417-3422.

(152) *Merck Index*; Budavari, S., Ed.; Merck & Co. Inc.: Whitehouse, NJ, **1996**; Vol. 12.

(153) Horne, D.; Gaudino, J.; Thompson, W. J. *Tetrahedron Lett.* **1984**, *25*, 3529-3532.

(154) Aizpurua, J. M., personal communication, **1996**.

(155) *Ozonation in Organic Chemistry*; Bailey, P. S.; Trahanovsky, W., Eds.; Academic Press: New York, **1978**; Vol. 39-I.

(156) Czernecki, S.; Georgoulis, C.; Stevens, C. L.; Vijayakumaran, K. *Tetrahedron Lett.* **1985**, *26*, 1699-1702.

(157) Andersson, F.; Samuelsson, B. *Carb. Res.* **1984**, *129*, C1-C3.

(158) Cazeau, P.; Moulines, F.; Laporte, O.; Duboudin, F. *J. Organometal. Chem.* **1980**, *201*, C9-C13.

(159) Middleton, W. J.; Bingham, E. M. *J. Am. Chem. Soc.* **1980**, *102*, 4845-4846.

(160) House, H. O.; Czuba, L. J.; Gall, M.; Olmstead, H. D. *J. Org. Chem.* **1969**, *34*, 2324-2336.

(161) Ishihara, K.; Hanaki, N.; Funahashi, M.; Miyata, M.; Yamamoto, H. *Bull. Chem. Soc. Jpn.* **1995**, *68*, 1721-1730.

(162) Kobayashi, S.; Araki, M.; Yasuda, M. *Tetrahedron Lett.* **1995**, *36*, 5773-5776.

(163) Annunziata, R.; Maura; Cinquini; Cozzi, F.; Molteni, V.; Schupp, O. *J. Org. Chem.* **1996**, *61*, 8293-8296.

(164) Ojala, W. H.; Gleason, W. B.; Connelly, M. P. E.; Wallis, R. R.; Kremer, J. J. *Acta Cryst.* **1996**, *C52*, 155-158.

(165) Siegel, C.; Thornton, E. R. *J. Am. Chem. Soc.* **1989**, *111*, 5722-5728.

(166) Denmark, S. E.; Moon, Y.-C.; Senanayake, C. B. W. *J. Am. Chem. Soc.* **1990**, *112*, 311-315.

(167) Fujisawa, T.; Ukaji, Y.; Noro, T.; Date, K.; Shimizu, M. *Tetrahedron Lett.* **1991**, *32*, 7563-7566.

(168) Bloch, R. *Chem. Rev.* **1998**, *98*, 1407-1438.

(169) Imamoto, T. *Comprehensive Organic Synthesis*; **1980**, Vol. 1, p 231-250 and reference 30 therein.

(170) Haasnoot, C. A. G.; Leeuw, F. A. A. M. d.; Altona, C. *Tetrahedron* **1980**, *36*, 2783-2792.

(171) Karplus, M. *J. Am. Chem. Soc.* **1963**, *85*, 2870.

(172) Georg, G. I.; Kant, J.; Gill, H. S. *J. Am. Chem. Soc.* **1987**, *109*, 1129-1135.

(173) Mori, K.; Tominaga, M.; Takigawa, T.; Matsui, M. *Synthesis* **1973**, 790-791.

(174) McMurry, J. *Organic Reactions*; Dauben, W. G., Ed.; Wiley: New York, **1976**; Vol. 24, p 187-224.

(175) Hatch, R. P.; Weinreb, S. M. *J. Org. Chem.* **1977**, *42*, 3960-3961.

(176) Cohen, T.; Gapinski, R. E. *Tetrahedron Lett.* **1978**, *45*, 4319-4322.

(177) Seyferth, D.; Alleston, D. L. *Inorg. Chem.* **1963**, *2*, 418-420.

(178) Laganis, E. D.; Chenard, B. L. *Tetrahedron Lett.* **1984**, *25*, 5831-5834.

(179) Wu, S.-H.; Lo, L.-C.; Chen, S.-T.; Wang, K.-T. *J. Org. Chem.* **1989**, *54*, 4220-4222.

(180) Tong, J. H.; Petitclerc, C.; D'Iorio, A.; Benoiton, N. L. *Can. J. Biochem.* **1971**, *49*, 877-881.

(181) Kusumi, T.; Fukushima, T.; Ohtani, I.; Kakisawa, H. *Tetrahedron Lett* **1991**, *32*, 2939-2942.

(182) Trost, B. M.; Bunt, R. C.; Pulley, S. R. *J. Org. Chem.* **1994**, *59*, 4202-4205.

(183) López, B.; Quiñoá, E.; Riguera, R. *J. Am. Chem. Soc.* **1999**, *121*, 9724-9725.

(184) Diaz-de-Villegas, M. D.; Urriolabeitia, E. P. *J. Chem. Ed.* **1999**, *76*, 77-78.

(185) Lightner, D. A.; Gurst, J. E. *Organic Conformational Analysis and Stereochemistry form Circular Dichroism Spectroscopy*; Wiley-VCH: New York, **2000**.

(186) Cantin, O.; Cativiela, C.; Diaz-de-Villegas, M. D.; Navarro, R.; Urriolabeitia, E. P. *Tetrahedron Asymmetry* **1996**, *7*, 2695-2702.

(187) Navarro, R.; Garcia, J.; Urriolabeitia, E. P.; Cativiela, C.; Diaz-de-Villegas, M. D. *J. Organomet. Chem.* **1995**, *490*, 35-43.

(188) Cope, A. C.; Friedrich, E. C. *J. Am. Chem. Soc.* **1968**, *90*, 909-913.

(189) Dale, J. A.; Dull, D. L.; Mosher, H. S. *J. Org. Chem.* **1969**, *34*, 2543-2549.

(190) Hoye, T. R.; Renner, M. K. *J. Org. Chem.* **1996**, *61*, 2056-2064.

(191) Seco, J. M.; Latypov, S. K.; Quiñoá, E.; Riguera, R. *J. Org. Chem.* **1997**, *62*, 7569-7574.

(192) Latypov, S. K.; Seco, J. M.; Quiñoá, E.; Riguera, R. *J. Org. Chem.* **1996**, *61*, 8569-8577.

(193) Perrin, D. D.; Armarego, W. L. F. *Purification of Laboratory Chemicals*; 3 ed.; Pergamon Press: New York, **1988**.

(194) Pietzonka, T.; Seebach, D. *Chem Ber.* **1991**, *124*, 1837-1843.

(195) Nakajima, M.; Komioka, K.; Iitaka, Y.; Koga, K. *Tetrahedron* **1993**, *49*, 10793-10806.

(196) Kronenthal, D. R.; Han, C. Y.; Taylor, M. K. *J. Org. Chem.* **1982**, *47*, 2765-2768.

(197) Corbett, W. M.; McKay, J. E. *J. Chem. Soc.* **1961**, 2930-2935.

(198) Baker, D. C.; Horton, D.; Charles G. Tindall, J. *Carb. Res.* **1972**, *24*, 192-197.

APPENDIX 1

University of Manitoba Department of Chemistry

STRUCTURE REPORT

Date: 21 March 2000

Compound: 2-(*p*-anisyl)amino-3-methyl-4-oxo-phenylbutanoic acid, methyl ester

Formula: $C_{19}H_{21}NO_4$

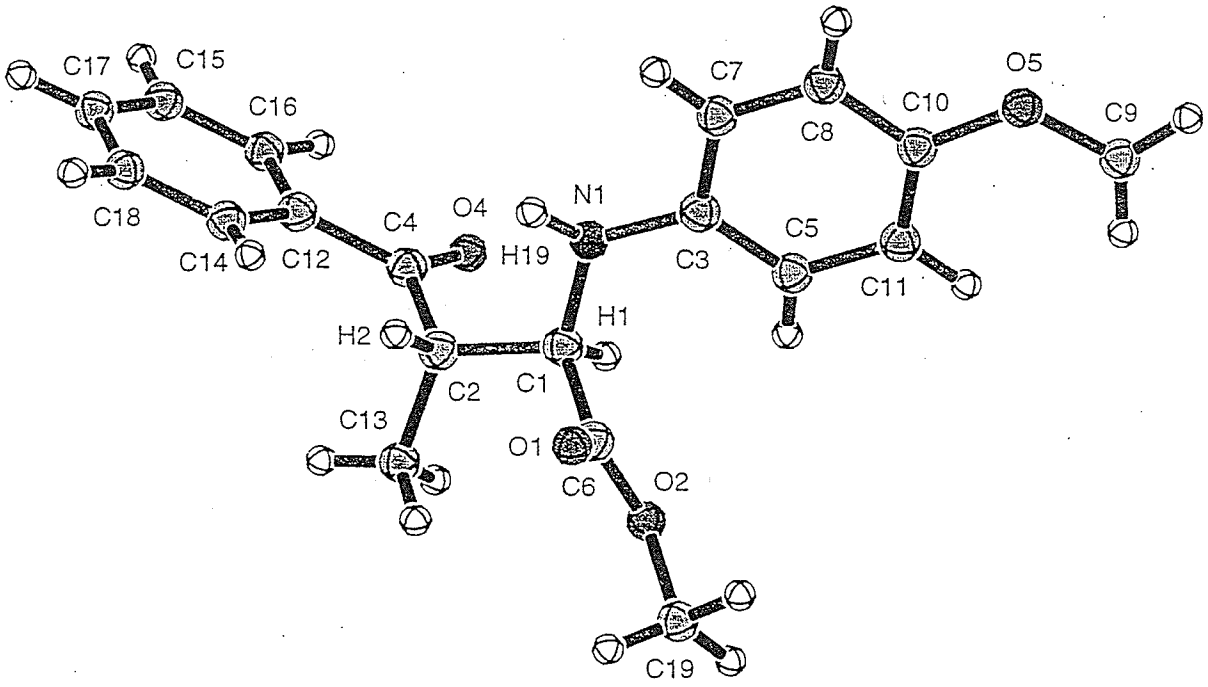

Experimental

Data Collection

A colourlessneedle needle crystal of $O_4NC_{19}H_{21}$ having approximate dimensions of 0.35 x 0.18 x 0.05 mm was mounted on a glass fiber. Al l measurements were made on a Rigaku AFC6S diffractometer with graphite monochromated Cu-Kα radiation.

Cell constants and an orientation matrix for data collection, obtained from a least-squares refinement using the setting angles of 25 carefully centered reflections in the range $45.00 < 2\theta < 65.00°$ corresponded to a primitive monoclinic cell with dimensions:

a = 8.317(2) Å
b = 23.833(3) Å β = 110.46(2)°
c = 9.560(2) Å
V = 1775.5(6) Å^3

For Z = 4 and F.W. = 327.38, the calculated density is 1.22 g/cm^3. The systematic absence of:

h0l : h ≠ 2n
0k0: k ≠ 2n

uniquely determine the space group to be:

$P2_1/a$ (#14)

The data were collected at a temperature of 23 ± 1 °C using the ω-2θ scan technique to a maximum 2θ value of 110.1°. Omega scans of several intense reflections, made prior to data collection, had an average width at half-height of 0.00° with a take-off angle of 6.0°. Scans of $(1.20 + 0.30 \tan\theta)°$ were made at a speed of 8.0° /min (in omega). The weak reflections ($I < 6.0\sigma(I)$) were rescanned (maximum of 10 scans) and the counts were accumulated to ensure good counting statistics. Stationary background counts were recorded on each side of the reflection. The ratio of peak counting time to background counting time was 2:1. The diameter of the incident beam collimator was 1.0 mm, the crystal to detector distance was 285 mm, and the detector aperture was 6.0 x 6.0 mm (horizontal x vertical).

Data Reduction

Of the 2695 reflections which were collected, 2313 were unique (R_{int} = 0.040). The intensities of three representative reflections were measured after every 200 reflections. No decay correction was applied.

The linear absorption coefficient, μ, for Cu-Kα radiation is 7.0 cm^{-1}. An empirical absorption correction based on azimuthal scans of several reflections was applied which resulted in transmission factors ranging from 0.96 to 1.00. The data were corrected for Lorentz and polarization effects.

Structure Solution and Refinement

The structure was solved by direct methods[1] and expanded using Fourier techniques.[2] The non-hydrogen atoms were refined anisotropically. Hydrogen atoms were refined isotropically. The final cycle of full-matrix least-squares refinement[3] was based on 1317 observed reflections ($I > 3.00\sigma(I)$) and 301 variable parameters and converged (largest parameter shift was 1.77 times its esd) with unweighted and weighted agreement factors of:

$$R = \Sigma \big| \, |Fo| - |Fc| \, \big| / \Sigma |Fo| = 0.040$$
$$R = \sqrt{(\Sigma w(|Fo| - |Fc|)^2 / \Sigma w Fo^2)} = 0.036$$

The standard deviation of an observation of unit weight[4] was 1.54. The weighting scheme was based on counting statistics and included a factor ($p = 0.025$) to down weight the intense reflections. Plots of $(\Sigma w(|Fo| - |Fc|)^2$ versus $|Fo|$, reflection order in data collection, sin θ/λ and various classes indices showed no unusual trends. The maximum and minimum peaks on the final difference Fourier map corresponded to 0.14 and –0.13 $e^-/Å^3$, respectively.

Neutral atom scattering factors were taken from Cromer and Waber.[5] Anomalous dispersion effects were included in Fcalc;[6] the values for $\Delta f'$ and $\Delta f''$ were those of Creagh and McAuley.[7] The values for the mass attenuation coefficients are those of Creagh and Hubbel.[8] All calculations were performed using the teXsan[9] crystallographic software package of Molecular Structure Corporation.

References

(1) MITHRIL84: Gilmore,C.J.; MITHRIL- an integrated direct methods computer program. J. Appl. Cryst. 17, 42-46, Univ. of Glasgow, Scotland, (1984).

(2) DIRDIF94: Beurskens, P.T., Admiraal, G., Beurskens, G., Bosman, W.P., de Gelder, R., Israel, R. and Smits, J.M.M. (1994). The DIRDIF-94 program system, Technical Report of the Crystallography Laboratory, University of Nijmegen, The Netherlands.

(3) Least-Squares:

Function minimized: $\Sigma w(|Fo| - |Fc|)^2$
Where $w = 1/\sigma^2(Fo) = [\sigma^2_C(Fo) + (p^2/4)Fo]^{-1}$

$\sigma_c(Fo)$ = e.s.d. based on counting statistics
p = p-factor

(4) Standard deviation of an observation of unit weight:

$$\sqrt{(\Sigma w(|Fo| - |Fc|)^2/No - Nv)}$$

Where: No = number of observations
Nv = number of variables

(5) Cromer, D. T. & Waber, J. T.; "International Tables for X-ray Crystallography", Vol. IV, The Kynoch Press, Birmingham, England, Table 2.2A (1974).

(6) Ibers, J. A. &Hamilton, W. C.; Acta Crystallogr., 17, 781 (1964).

(7) Creagh, D. C. & McAuley, W.J.; "International Tables for Crystallography", Vol. C, (A.J.C. Wilson, ed.), Kluwer Academic Publishers, Boston, Table 4.2.6.8, pages 219-222 (1992).

(8) Creagh, D. C. &Hubbel l, J.H.; "International Tables for Crystallography", Vol. C, (A.J.C. Wilson, ed.), Kluwer Academic Publishers, Boston, Table 4.2.4.3, pages 200-206 (1992).

(9) teXsan : Crystal Structure Analysis Package, Molecular Structure Corporation (1985&1992).

EXPERIMENTAL DETAILS

A. Crystal Data

Empirical Formula	$O_4NC_{19}H_{21}$
Formula Weight	327.38
Crystal Color, Habit	colourlessneedle, needle
Crystal Dimensions	0.35 x 0.18 x 0.05 mm
Crystal System	monoclinic
Lattice Type	Primitive
No. of Reflections Used for Unit	
Cell Determination (2θ range)	25 (45.0 - 65.0°)
Omega Scan Peak Width	
at Half-height	0.00°
Lattice Parameters	a = 8.317(2)Å
	b = 23.833(3)Å
	c = 9.560(2)Å
	β =110.46(2)°
	V = 1775.5(6)Å^3
Space Group	$P2_1/a$ (#14)
Z value	4
D_{calc}	1.225 g/cm^3
F_{000}	696.00
μ(CuKα)	7.02 cm

B. Intensity Measurements

Diffractometer	Rigaku AFC6S
Radiation	CuKα (λ = 1.54178 Å)
	graphite monochromated

Take-off Angle	6.0°
Detector Aperture	6.0 mm horizontal
	6.0 mm vertical
Crystal to Detector Distance	285 mm
Voltage, Current	0kV, 0mA
Temperature	23.0 °C
Scan Type	ω-2θ
Scan Rate	8.0°/min (in ω) (up to 10 scans)
Scan Width	$(1.20 + 0.30 \tan\theta)°$
$2\theta_{max}$	110.1
No. of Reflections Measured	Total: 2695
	Unique: 2313 (R_{int} = 0.040)
Corrections	Lorentz-polarization
	Absorption
	(trans. factors: 0.9589 - 1.0000)

C. Structure Solution and Refinement

Structure Solution	Direct Methods (MITHRIL84)
Refinement	Full-matrix least-squares
Function Minimized	$\Sigma w(\|Fo\| - \|Fc\|)^2$
Least Squares Weighted	$w = 1/\sigma^2(Fo) = [\sigma^2_C(Fo) + (p^2/4)Fo]^{-1}$
p-factor	0.0250
Anomalous Dispersion	All non-hydrogen atoms
No. Observations (I > 3.00σ(I))	1317
No. Variables	301
Reflection/Parameter Ratio	4.38
Residuals: R; Rw	0.040; 0.036
Goodness of Fit Indicator	1.54
Max Shift/Error in Final Cycle	1.77

Maximum Peak in Final Diff. Map	0.14 e^- / Å^3
Minimum Peak in Final Diff. Map	0.13 e^- / Å^3

Table 1. Atomic coordinates and B_{iso}/B_{eq}

atom	x	y	z	B_{eq}
O(1)	-1.2161(4)	-0.4915(1)	-0.9230(3)	6.73(9)
O(2)	-1.2083(4)	-0.5044(1)	-0.6879(3)	6.71(9)
O(4)	-0.6703(5)	-0.5890(1)	-0.5782(4)	9.8(1)
O(5)	-0.8002(5)	-0.2517(1)	-0.6887(4)	8.8(1)
N(1)	-0.8462(4)	-0.4821(1)	-0.7849(4)	5.5(1)
C(1)	-0.9506(6)	-0.5193(2)	-0.7322(5)	5.0(1)
C(2)	-0.9312(6)	-0.5784(2)	-0.7843(5)	5.1(1)
C(3)	-0.8396(5)	-0.4244(2)	-0.7553(4)	4.7(1)
C(4)	-0.7480(6)	-0.5995(2)	-0.7088(5)	6.2(1)
C(5)	-0.9037(6)	-0.3999(2)	-0.6555(5)	5.5(1)
C(6)	-1.1393(6)	-0.5031(2)	-0.7949(5)	5.4(1)
C(7)	-0.7628(5)	-0.3897(2)	-0.8299(5)	5.3(1)
C(8)	-0.7523(6)	-0.3331(2)	-0.8054(5)	6.5(1)
C(9)	-0.8452(9)	-0.2247(2)	-0.5801(7)	7.8(2)
C(10)	-0.8175(6)	-0.3092(2)	-0.7046(5)	5.7(1)
C(11)	-0.8931(6)	-0.3425(2)	-0.6300(5)	5.5(1)
C(12)	-0.6713(6)	-0.6371(2)	-0.7931(5)	5.4(1)
C(13)	-1.0505(9)	-0.6204(2)	-0.7497(7)	7.6(2)
C(14)	-0.7494(7)	-0.6482(2)	-0.9421(5)	6.5(1)
C(15)	-0.4437(8)	-0.6991(3)	-0.7913(9)	8.7(2)
C(16)	-0.5162(7)	-0.6630(2)	-0.7170(6)	7.1(2)
C(17)	-0.5246(9)	-0.7093(2)	-0.9406(8)	8.1(2)
C(18)	-0.6757(8)	-0.6840(2)	-1.0144(7)	7.9(2)
C(19)	-1.3903(9)	-0.4918(4)	-0.7335(8)	9.8(2)

(continued)

atom	x	y	z	Beq
H(1)	-0.912(4)	-0.518(1)	-0.619(4)	4.3(7)
H(2)	-0.961(4)	-0.578(1)	-0.897(4)	4.0(7)
H(3)	-0.952(4)	-0.420(1)	-0.599(4)	4.4(8)
H(4)	-0.718(4)	-0.405(1)	-0.899(4)	4.4(8)
H(5)	-0.705(5)	-0.310(2)	-0.858(4)	7(1)
H(8)	-0.933(4)	-0.326(1)	-0.549(4)	5.1(8)
H(9)	-1.016(6)	-0.627(2)	-0.628(5)	10(1)
H(10)	-1.031(5)	-0.658(2)	-0.780(5)	8(1)
H(11)	-1.174(6)	-0.609(2)	-0.802(5)	10(1)
H(12)	-0.850(5)	-0.627(2)	-1.001(4)	7(1)
H(13)	-0.333(7)	-0.717(2)	-0.740(6)	12(1)
H(14)	-0.473(6)	-0.736(2)	-0.993(5)	9(1)
H(15)	-0.725(6)	-0.692(2)	-1.119(5)	9(1)
H(18)	-0.462(5)	-0.652(2)	-0.610(5)	8(1)
H(19)	-0.847(6)	-0.491(2)	-0.886(5)	10(1)
H(20)	-1.445(6)	-0.519(2)	-0.811(5)	9(1)
H(21)	-1.406(7)	-0.487(3)	-0.629(6)	15(1)
H(22)	-1.399(9)	-0.450(3)	-0.763(8)	16(2)
H(23)	-0.819(5)	-0.184(2)	-0.578(5)	9(1)
H(24)	-0.767(9)	-0.242(3)	-0.468(8)	17(1)
H(25)	-0.932(8)	-0.237(3)	-0.554(7)	14(1)

$B_{eq} = 8/3\pi^2(U_{11}(aa^*)^2 + U_{22}(bb^*)^2 + U_{33}(cc^*)^2 + 2U_{12}aa^*bb^*\cos\gamma + 2U_{13}aa^*cc^*\cos\beta + 2U_{23}bb^*cc^*\cos\alpha)$

Table 2. Anisotropic Displacement Parameters

atom	U11	U22	U33	U12	U13	U23
O(1)	0.092(2)	0.104(2)	0.062(2)	0.014(2)	0.029(2)	0.000(2)
O(2)	0.088(2)	0.110(2)	0.072(2)	-0.005(2)	0.047(2)	-0.011(2)
O(4)	0.156(3)	0.125(3)	0.061(2)	0.043(2)	-0.001(2)	-0.016(2)
O(5)	0.176(4)	0.062(2)	0.128(3)	-0.009(2)	0.092(3)	-0.003(2)
N(1)	0.088(3)	0.064(2)	0.070(2)	-0.009(2)	0.043(2)	-0.007(2)
C(1)	0.079(3)	0.062(3)	0.055(3)	-0.003(2)	0.031(2)	-0.002(2)
C(2)	0.084(3)	0.056(3)	0.059(3)	0.001(2)	0.030(3)	-0.001(2)
C(3)	0.067(3)	0.060(3)	0.053(2)	-0.002(2)	0.023(2)	0.002(2)
C(4)	0.106(4)	0.063(3)	0.061(3)	0.006(3)	0.022(3)	0.005(2)
C(5)	0.100(4)	0.065(3)	0.060(3)	-0.010(2)	0.046(3)	0.000(2)
C(6)	0.092(4)	0.059(3)	0.062(3)	-0.006(2)	0.037(3)	-0.008(2)
C(7)	0.080(3)	0.067(3)	0.067(3)	-0.003(2)	0.040(3)	-0.002(2)
C(8)	0.111(4)	0.066(3)	0.088(3)	-0.012(3)	0.056(3)	0.004(3)
C(9)	0.144(6)	0.063(4)	0.101(4)	0.000(4)	0.058(4)	-0.011(3)
C(10)	0.094(4)	0.054(3)	0.071(3)	-0.002(2)	0.032(3)	0.000(2)
C(11)	0.095(4)	0.062(3)	0.063(3)	-0.005(2)	0.040(3)	-0.002(2)
C(12)	0.077(3)	0.054(2)	0.074(3)	0.000(2)	0.026(3)	0.005(2)
C(13)	0.129(5)	0.066(3)	0.111(5)	-0.017(4)	0.066(4)	-0.009(3)
C(14)	0.089(4)	0.082(3)	0.074(4)	0.020(3)	0.024(3)	-0.008(3)
C(15)	0.089(5)	0.107(5)	0.142(6)	0.029(4)	0.052(5)	0.029(4)
C(16)	0.084(4)	0.087(4)	0.088(4)	0.006(3)	0.014(3)	0.016(3)
C(17)	0.110(5)	0.092(4)	0.126(5)	0.018(4)	0.066(5)	0.006(4)
C(18)	0.104(5)	0.101(4)	0.096(4)	0.026(3)	0.038(4)	-0.013(3)
C(19)	0.084(5)	0.181(7)	0.117(5)	-0.001(5)	0.046(4)	-0.044(5)

The general temperature factor expression:

$\exp(-2\pi^2(a^{*2}U_{11}h^2 + b^{*2}U_{22}k^2 + c^{*2}U_{33}l^2 + 2a^*b^*U_{12}hk + 2a^*c^*U_{13}hl + 2b^*c^*U_{23}kl))$

University of Alberta Department of Chemistry
Structure Determination Laboratory

STRUCTURE REPORT

SDL Code: MAN9904
Date: 22 April 1999

Compound: 2-(*p*-Anisyl)amino-4-oxo-3-phenyl phenylbutanoic acid, methyl ester
Formula: $C_{24}H_{23}NO_4$

Supervisor: Philip Hultin, Department of Chemistry, University of Manitoba

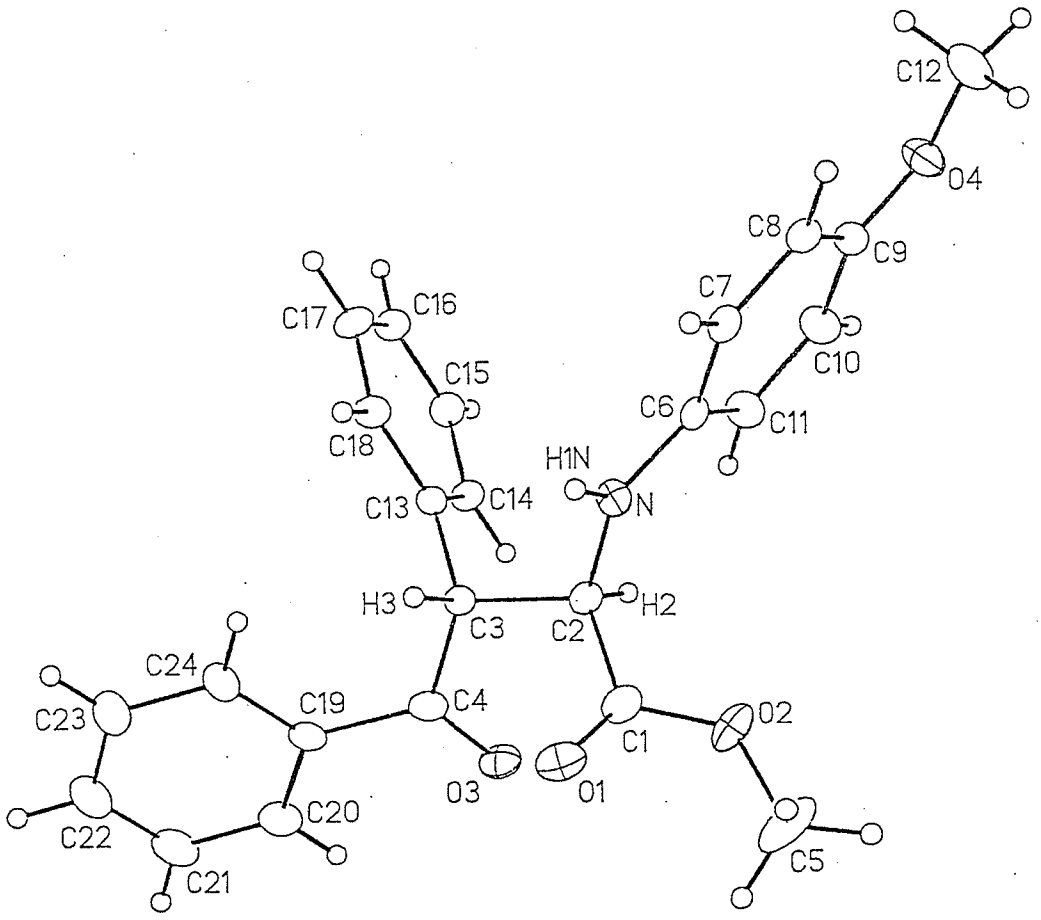

Table 1. Crystallographic Experimental Details

A. Crystal Data	
formula	$C_{24}H_{23}NO_4$
formula weight	389.43
crystal dimensions (mm)	$0.38 \times 0.12 \times 0.06$
crystal system	orthorhombic
space group	*Pbca* (No. 61)
unit cell parameters[a]	
a (Å)	9.8190 (9)
b (Å)	18.0568 (17)
c (Å)	23.008 (2)
V (Å^3)	4079.3 (7)
Z	8
ρcalcd (g cm^{-3})	1.268
μ (mm^{-1})	0.086
B. Data Collection and Refinement Conditions	
diffractometer	Bruker P4/RA/SMART 1000 CCD[b]
radiation (λ [Å])	graphite-monochromated Mo Kα (0.71073)
temperature (°C)	–80
scan type	ϕ rotations (0.3°) / ω scans (0.3°) (20 s exposures)
data collection 2θ limit (deg)	51.40
total data collected	20773 ($-11 \le h \le 11$, $-21 \le k \le 22$, $-27 \le l \le 28$)
independent reflections	3866
number of observations (*NO*)	1658 [$F_o^2 \ge 2\sigma(F_o^2)$]
structure solution method	direct methods (*SHELXS–86*[c])
refinement method	full-matrix least-squares on F^2 (*SHELXL–93*[d])
absorption correction method	*SADABS*
range of transmission factors	0.9674–0.5551
data/restraints/parameters	3866 [$F_o^2 \ge -3\sigma(F_o^2)$] / 0 / 262
goodness-of-fit (S)[e]	0.801 [$F_o^2 \ge -3\sigma(F_o^2)$]
final R indices[f]	
$R1$ [$F_o^2 \ge 2\sigma(F_o^2)$]	0.0464
$wR2$ [$F_o^2 \ge -3\sigma(F_o^2)$]	0.1034
largest difference peak and hole	0.191 and –0.231 e Å^{-3}

[a]Obtained from least-squares refinement of 3768 centered reflections.

[b]Programs for diffractometer operation, data collection, data reduction and absorption

correction were those supplied by Bruker.

[c]Sheldrick, G. M. *Acta Crystallogr.* **1990**, *A46*, 467–473.

Table 1. Crystallographic Experimental Details (continued)

[d]Sheldrick, G. M. *SHELXL-93*. Program for crystal structure determination. University of Göttingen, Germany, 1993. Refinement on F_o^2 for all reflections (all of these having $F_o^2 \geq -3\sigma(F_o^2)$). Weighted R-factors wR_2 and all goodnesses of fit S are based on F_o^2; conventional R-factors R_1 are based on F_o, with F_o set to zero for negative F_o^2. The observed criterion of $F_o^2 > 2\sigma(F_o^2)$ is used only for calculating R_1, and is not relevant to the choice of reflections for refinement. R-factors based on F_o^2 are statistically about twice as large as those based on F_o, and R-factors based on ALL data will be even larger.

[e]$S = [\Sigma w(F_o^2 - F_c^2)^2/(n-p)]^{1/2}$ (n = number of data; p = number of parameters varied; $w = [\sigma^2(F_o^2) + (0.0378P)^2]^{-1}$ where $P = [\mathrm{Max}(F_o^2, 0) + 2F_c^2]/3$).

[f]$R_1 = \Sigma||F_o| - |F_c||/\Sigma|F_o|$; $wR_2 = [\Sigma w(F_o^2 - F_c^2)^2/\Sigma w(F_o^4)]^{1/2}$.

Table 2. Atomic Coordinates and Equivalent Isotropic Displacement Parameters

Atom	*x*	*y*	*z*	U_{eq}, Å^2
O1	-0.12816(19)	-0.07251(10)	-0.03118(8)	0.0549(6)*
O2	-0.30427(18)	-0.06292(11)	-0.09314(8)	0.0598(6)*
O3	-0.37224(17)	-0.03239(10)	0.05448(8)	0.0499(5)*
O4	-0.38662(18)	0.27962(11)	-0.24433(8)	0.0601(6)*
N	-0.17681(19)	0.08777(11)	-0.07707(9)	0.0386(6)*
C1	-0.2215(3)	-0.03750(16)	-0.05136(12)	0.0425(7)*
C2	-0.2533(2)	0.04191(14)	-0.03662(10)	0.0335(6)*
C3	-0.2128(2)	0.06059(13)	0.02606(10)	0.0306(6)*
C4	-0.2760(2)	0.00641(14)	0.06920(12)	0.0377(7)*
C5	-0.2714(3)	-0.13562(18)	-0.11631(15)	0.0852(12)*
C6	-0.2300(2)	0.13339(14)	-0.12016(11)	0.0320(6)*
C7	-0.1433(2)	0.16720(14)	-0.15975(11)	0.0368(7)*
C8	-0.1906(3)	0.21533(15)	-0.20198(11)	0.0401(7)*
C9	-0.3278(3)	0.23090(15)	-0.20542(11)	0.0422(7)*
C10	-0.4158(3)	0.19732(16)	-0.16698(12)	0.0500(8)*
C11	-0.3686(3)	0.14891(15)	-0.12484(11)	0.0456(8)*
C12	-0.3024(3)	0.31033(19)	-0.28805(12)	0.0754(10)*
C13	-0.2523(2)	0.13971(13)	0.04088(10)	0.0317(6)*
C14	-0.3885(2)	0.15894(14)	0.04857(10)	0.0368(7)*
C15	-0.4249(3)	0.23194(15)	0.05908(11)	0.0437(7)*
C16	-0.3264(3)	0.28620(15)	0.06181(11)	0.0457(7)*
C17	-0.1918(3)	0.26803(15)	0.05437(11)	0.0465(7)*
C18	-0.1551(2)	0.19492(15)	0.04425(10)	0.0394(7)*
C19	-0.2194(3)	0.00278(14)	0.12930(12)	0.0369(7)*
C20	-0.2867(3)	-0.03840(16)	0.17105(14)	0.0578(8)*
C21	-0.2377(4)	-0.04277(18)	0.22727(15)	0.0706(10)*
C22	-0.1209(4)	-0.00654(18)	0.24254(14)	0.0679(10)*
C23	-0.0515(3)	0.03442(17)	0.20148(13)	0.0622(9)*
C24	-0.1006(3)	0.03920(16)	0.14523(12)	0.0488(8)*

Anisotropically-refined atoms are marked with an asterisk (*). The form of the anisotropic displacement parameter is: $\exp[-2\pi^2(h^2a^{*2}U_{11} + k^2b^{*2}U_{22} + l^2c^{*2}U_{33} + 2klb^*c^*U_{23} + 2hla^*c^*U_{13} + 2hka^*b^*U_{12})]$.

Table 3. Selected Interatomic Distances (Å)

Atom1	Atom2	Distance	Atom1	Atom	Distance
O1	C1	1.207(3)	C8	C9	1.379(3)
O2	C1	1.340(3)	C9	C10	1.377(3)
O2	C5	1.453(3)	C10	C11	1.385(3)
O3	C4	1.224(3)	C13	C14	1.393(3)
O4	C9	1.381(3)	C13	C18	1.383(3)
O4	C12	1.415(3)	C14	C15	1.387(3)
N	C2	1.454(3)	C15	C16	1.378(3)
N	C6	1.391(3)	C16	C17	1.373(3)
C1	C2	1.506(3)	C17	C18	1.388(3)
C2	C3	1.534(3)	C19	C20	1.383(3)
C3	C4	1.526(3)	C19	C24	1.388(3)
C3	C13	1.519(3)	C20	C21	1.382(4)
C4	C19	1.492(3)	C21	C22	1.367(4)
C6	C7	1.388(3)	C22	C23	1.380(4)
C6	C11	1.394(3)	C23	C24	1.384(3)
C7	C8	1.384(3)			

Table 4. Selected Interatomic Angles (deg)

Atom1	Atom2	Atom3	Angle	Atom1	Atom2	Atom3	Angle
C1	O2	C5	116.0(2)	O4	C9	C10	115.7(3)
C9	O4	C12	117.8(2)	C8	C9	C10	119.1(3)
C2	N	C6	126.8(2)	C9	C10	C11	121.1(3)
O1	C1	O2	123.9(3)	C6	C11	C10	120.5(2)
O1	C1	C2	124.7(3)	C3	C13	C14	120.6(2)
O2	C1	C2	111.2(2)	C3	C13	C18	120.9(2)
N	C2	C1	106.92(19)	C14	C13	C18	118.4(2)
N	C2	C3	110.05(19)	C13	C14	C15	120.4(2)
C1	C2	C3	111.6(2)	C14	C15	C16	120.2(2)
C2	C3	C4	111.4(2)	C15	C16	C17	120.0(3)
C2	C3	C13	110.58(19)	C16	C17	C18	119.9(2)
C4	C3	C13	110.67(19)	C13	C18	C17	121.1(2)
O3	C4	C3	120.1(2)	C4	C19	C20	119.3(3)
O3	C4	C19	121.3(2)	C4	C19	C24	122.5(2)
C3	C4	C19	118.7(2)	C20	C19	C24	118.2(3)
N	C6	C7	119.9(2)	C19	C20	C21	121.0(3)
N	C6	C11	122.7(2)	C20	C21	C22	120.3(3)
C7	C6	C11	117.4(3)	C21	C22	C23	119.7(3)
C6	C7	C8	122.1(2)	C22	C23	C24	120.1(3)
C7	C8	C9	119.8(2)	C19	C24	C23	120.7(3)
O4	C9	C8	125.1(2)				

Table 5. Torsional Angles (deg)

Atom1	Atom2	Atom3	Atom4	Angle	Atom1	Atom2	Atom3	Atom4	Angle
C5	O2	C1	O1	-3.3(4)	C3	C4	C19	C24	-8.8(4)
C5	O2	C1	C2	172.1(2)	N	C6	C7	C8	-177.4(2)
C12	O4	C9	C8	6.9(4)	C11	C6	C7	C8	0.9(4)
C12	O4	C9	C10	-174.4(2)	N	C6	C11	C10	177.1(2)
C6	N	C2	C1	113.6(3)	C7	C6	C11	C10	-1.1(4)
C6	N	C2	C3	-125.1(2)	C6	C7	C8	C9	0.1(4)
C2	N	C6	C7	-172.6(2)	C7	C8	C9	O4	177.9(2)
C2	N	C6	C11	9.2(4)	C7	C8	C9	C10	-0.8(4)
O1	C1	C2	N	89.0(3)	O4	C9	C10	C11	-178.2(2)
O1	C1	C2	C3	-31.3(3)	C8	C9	C10	C11	0.6(4)
O2	C1	C2	N	-86.4(2)	C9	C10	C11	C6	0.4(4)
O2	C1	C2	C3	153.3(2)	C3	C13	C14	C15	-176.6(2)
N	C2	C3	C4	-172.09(19)	C18	C13	C14	C15	0.3(4)
N	C2	C3	C13	64.4(2)	C3	C13	C18	C17	176.1(2)
C1	C2	C3	C4	-53.6(3)	C14	C13	C18	C17	-0.7(4)
C1	C2	C3	C13	-177.11(19)	C13	C14	C15	C16	0.2(4)
C2	C3	C4	O3	-17.3(3)	C14	C15	C16	C17	-0.3(4)
C2	C3	C4	C19	163.6(2)	C15	C16	C17	C18	-0.2(4)
C13	C3	C4	O3	106.2(3)	C16	C17	C18	C13	0.7(4)
C13	C3	C4	C19	-73.0(3)	C4	C19	C20	C21	-179.7(3)
C2	C3	C13	C14	71.7(3)	C24	C19	C20	C21	0.5(4)
C2	C3	C13	C18	-105.1(2)	C4	C19	C24	C23	180.0(2)
C4	C3	C13	C14	-52.3(3)	C20	C19	C24	C23	-0.2(4)
C4	C3	C13	C18	130.9(2)	C19	C20	C21	C22	-0.3(5)
O3	C4	C19	C20	-7.8(4)	C20	C21	C22	C23	-0.1(5)
O3	C4	C19	C24	172.0(2)	C21	C22	C23	C24	0.5(5)
CC3	C4	C19	C20	171.3(2)	C22	C23	C24	C19	-0.3(4)

Table 6. Anisotropic Displacement Parameters (U_{ij}, Å^2)

Atom	U_{11}	U_{22}	U_{33}	U_{23}	U_{13}	U_{12}
O1	0.0397(12)	0.0421(13)	0.0831(15)	-0.0040(11)	0.0124(10)	0.0059(10)
O2	0.0509(13)	0.0598(15)	0.0686(14)	-0.0319(12)	0.0051(11)	-0.0070(11)
O3	0.0380(11)	0.0459(12)	0.0660(14)	0.0048(10)	0.0055(10)	-0.0107(10)
O4	0.0568(13)	0.0680(15)	0.0557(14)	0.0243(12)	-0.0023(11)	-0.0044(11)
N	0.0230(11)	0.0517(16)	0.0411(14)	0.0054(12)	0.0030(10)	-0.0040(11)
C1	0.0298(17)	0.045(2)	0.052(2)	-0.0082(17)	0.0157(14)	-0.0054(15)
C2	0.0262(14)	0.0347(16)	0.0396(17)	-0.0034(14)	0.0041(12)	-0.0002(13)
C3	0.0247(14)	0.0313(17)	0.0358(16)	0.0019(13)	0.0020(11)	-0.0005(12)
C4	0.0301(16)	0.0314(17)	0.052(2)	0.0024(14)	0.0103(13)	0.0051(13)
C5	0.076(2)	0.068(2)	0.112(3)	-0.055(2)	0.029(2)	-0.021(2)
C6	0.0319(16)	0.0343(16)	0.0297(15)	-0.0075(13)	0.0011(12)	-0.0040(13)
C7	0.0301(15)	0.0438(18)	0.0364(17)	-0.0085(15)	0.0039(13)	-0.0046(13)
C8	0.0420(18)	0.0427(18)	0.0355(18)	-0.0060(15)	0.0084(13)	-0.0130(14)
C9	0.0478(19)	0.0416(19)	0.0370(18)	0.0023(15)	-0.0021(14)	-0.0058(16)
C10	0.0315(17)	0.062(2)	0.056(2)	0.0134(18)	0.0006(14)	-0.0003(15)
C11	0.0344(17)	0.055(2)	0.0475(19)	0.0086(16)	0.0052(13)	-0.0028(15)
C12	0.084(3)	0.093(3)	0.049(2)	0.024(2)	0.0011(18)	-0.006(2)
C13	0.0320(15)	0.0322(16)	0.0308(15)	0.0024(13)	0.0023(11)	-0.0020(13)
C14	0.0308(16)	0.0355(17)	0.0441(17)	-0.0022(14)	0.0024(12)	-0.0016(13)
C15	0.0362(17)	0.0438(19)	0.051(2)	-0.0039(15)	0.0040(13)	0.0082(15)
C16	0.055(2)	0.0333(18)	0.049(2)	-0.0051(15)	0.0013(14)	0.0036(16)
C17	0.0428(18)	0.0361(19)	0.061(2)	-0.0031(15)	0.0033(14)	-0.0094(15)
C18	0.0302(15)	0.0387(18)	0.0493(18)	0.0040(15)	0.0038(13)	-0.0015(14)
C19	0.0400(17)	0.0316(16)	0.0393(18)	0.0072(14)	0.0095(14)	0.0038(14)
C20	0.069(2)	0.051(2)	0.053(2)	0.0119(17)	0.0132(17)	-0.0087(17)
C21	0.097(3)	0.064(2)	0.051(2)	0.0255(19)	0.017(2)	-0.006(2)
C22	0.084(3)	0.072(2)	0.047(2)	0.0150(19)	0.0030(19)	0.011(2)
C23	0.060(2)	0.078(2)	0.049(2)	0.0104(19)	-0.0046(17)	-0.0008(18)
C24	0.0464(18)	0.061(2)	0.0395(19)	0.0116(16)	0.0050(14)	0.0019(16)

The form of the anisotropic displacement parameter is:

$\exp[-2\pi^2(h^2a^{*2}U_{11} + k^2b^{*2}U_{22} + l^2c^{*2}U_{33} + 2klb^*c^*U_{23} + 2hla^*c^*U_{13} + 2hka^*b^*U_{12})]$

Table 7. Derived Atomic Coordinates and Displacement Parameters for Hydrogen Atoms

Atom	*x*	*y*	*z*	U_{eq}, Å^2
H1N	-0.0875	0.0865	-0.0740	0.046
H2	-0.3529	0.0511	-0.0419	0.040
H3	-0.1115	0.0564	0.0292	0.037
H5A	-0.3376	-0.1489	-0.1464	0.102
H5B	-0.2747	-0.1723	-0.0850	0.102
H5C	-0.1797	-0.1347	-0.1331	0.102
H7	-0.0485	0.1570	-0.1578	0.044
H8	-0.1287	0.2376	-0.2285	0.048
H10	-0.5106	0.2075	-0.1694	0.060
H11	-0.4311	0.1261	-0.0989	0.055
H12A	-0.3567	0.3431	-0.3129	0.091
H12B	-0.2635	0.2704	-0.3116	0.091
H12C	-0.2288	0.3388	-0.2699	0.091
H14	-0.4569	0.1218	0.0466	0.044
H15	-0.5180	0.2446	0.0644	0.052
H16	-0.3517	0.3362	0.0689	0.055
H17	-0.1238	0.3054	0.0561	0.056
H18	-0.0616	0.1826	0.0396	0.047
H20	-0.3678	-0.0641	0.1609	0.069
H21	-0.2856	-0.0711	0.2554	0.085
H22	-0.0876	-0.0096	0.2812	0.082
H23	0.0301	0.0594	0.2118	0.075
H24	-0.0526	0.0677	0.1172	0.059

University of Alberta Department of Chemistry
Structure Determination Laboratory

STRUCTURE REPORT

SDL Code: MAN9903
Date: 19 April 1999

Compound: 2-(*p*-Anisyl)amino-4-oxo-3-phenyl phenylpentanoic acid, methyl ester
Formula: $C_{25}H_{25}NO_4$

Supervisor: Philip Hultin, Department of Chemistry, University of Manitoba

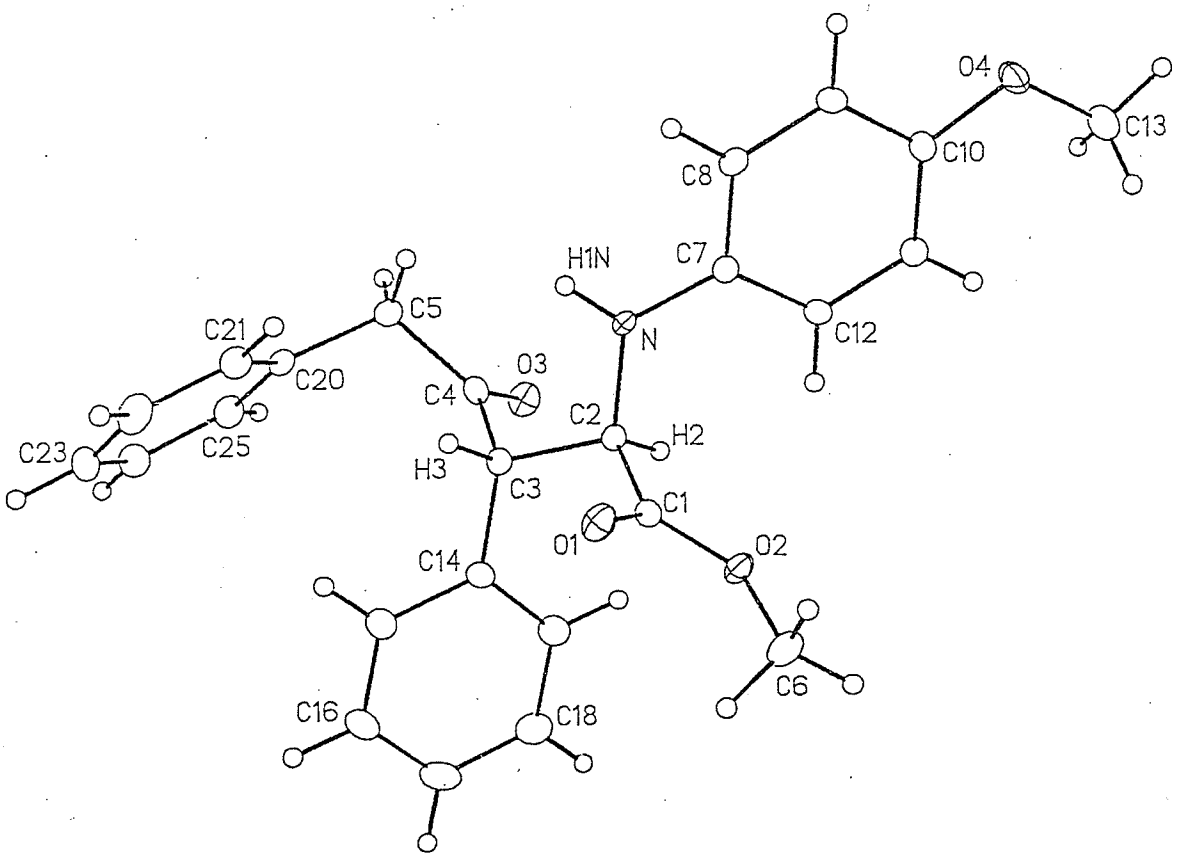

Table 1. Crystallographic Experimental Details

A. Crystal Data	
formula	$C_{25}H_{25}NO_4$
formula weight	403.46
crystal dimensions (mm)	$0.38 \times 0.11 \times 0.06$
crystal system	monoclinic
space group	$P2_1/c$ (No. 14)
unit cell parameters[a]	
a (Å)	7.6431 (9)
b (Å)	17.028 (2)
c (Å)	16.515 (2)
β (deg)	91.569 (2)
V (Å^3)	2148.6 (4)
Z	4
ρcalcd (g cm^{-3})	1.247
μ (mm^{-1})	0.084
B. Data Collection and Refinement Conditions	
diffractometer	Bruker P4/RA/SMART 1000 CCD[b]
radiation (λ [Å])	graphite-monochromated Mo Kα (0.71073)
temperature (°C)	–80
scan type	ϕ rotations (0.3°) / ω scans (0.3°) (20 s exposures)
data collection 2θ limit (deg)	51.40
total data collected	11361 ($-9 \le h \le 8$, $-20 \le k \le 19$, $-20 \le l \le 19$)
independent reflections	4076
number of observations (*NO*)	1891 [$F_o^2 \ge 2\sigma(F_o^2)$]
structure solution method	direct methods (*SHELXS–86*[c])
refinement method	full-matrix least-squares on F^2 (*SHELXL–93*[d])
absorption correction method	*SADABS*
range of transmission factors	0.9178–0.6629
data/restraints/parameters	4076 [$F_o^2 \ge -3\sigma(F_o^2)$] / 0 / 272
extinction coefficient (x)[e]	0.0041(6)
goodness-of-fit (S)[f]	0.831 [$F_o^2 \ge -3\sigma(F_o^2)$]
final R indices[g]	
R_1 [$F_o^2 \ge 2\sigma(F_o^2)$]	0.0503
wR_2 [$F_o^2 \ge -3\sigma(F_o^2)$]	0.1116
largest difference peak and hole	0.284 and –0.267 e Å^{-3}

[a]Obtained from least-squares refinement of 3158 centered reflections.

[b]Programs for diffractometer operation, data collection, data reduction and absorption correction were those supplied by Bruker.

Table 1. Crystallographic Experimental Details (continued)

[c]Sheldrick, G. M. *Acta Crystallogr.* **1990**, *A46*, 467–473.

[d]Sheldrick, G. M. *SHELXL-93*. Program for crystal structure determination. University of Göttingen, Germany, 1993. Refinement on F_o^2 for all reflections (all of these having $F_o^2 \geq -3\sigma(F_o^2)$). Weighted R-factors wR_2 and all goodnesses of fit S are based on F_o^2; conventional R-factors R_1 are based on F_o, with F_o set to zero for negative F_o^2. The observed criterion of $F_o^2 > 2\sigma(F_o^2)$ is used only for calculating R_1, and is not relevant to the choice of reflections for refinement. R-factors based on F_o^2 are statistically about twice as large as those based on F_o, and R-factors based on ALL data will be even larger.

[e]$F_c^* = kF_c[1 + x\{0.001F_c^2\lambda^3/\sin(2\theta)\}]^{-1/4}$ where k is the overall scale factor.

[f]$S = [\Sigma w(F_o^2 - F_c^2)^2/(n - p)]^{1/2}$ (n = number of data; p = number of parameters varied; $w = [\sigma^2(F_o^2) + (0.0413P)^2]^{-1}$ where $P = [\mathrm{Max}(F_o^2, 0) + 2F_c^2]/3$).

[g]$R_1 = \Sigma||F_o| - |F_c||/\Sigma|F_o|$; $wR_2 = [\Sigma w(F_o^2 - F_c^2)^2/\Sigma w(F_o^4)]^{1/2}$.

Table 2. Atomic Coordinates and Equivalent Isotropic Displacement Parameters

Atom	*x*	*y*	*z*	U_{eq}, Å2
O1	0.2272(2)	0.44151(11)	-0.02748(11)	0.0389(5)*
O2	0.24544(19)	0.34820(10)	-0.12274(10)	0.0342(5)*
O3	-0.2971(2)	0.25412(12)	-0.00424(11)	0.0420(5)*
O4	-0.3371(2)	0.49530(11)	-0.40564(10)	0.0479(6)*
N	-0.1481(2)	0.42389(12)	-0.08562(11)	0.0285(5)*
C1	0.1621(3)	0.38885(16)	-0.06648(15)	0.0266(6)*
C2	-0.0275(3)	0.36192(15)	-0.05940(14)	0.0255(6)*
C3	-0.0616(3)	0.34133(15)	0.02923(14)	0.0272(6)*
C4	-0.2519(3)	0.31245(17)	0.03287(15)	0.0298(7)*
C5	-0.3770(3)	0.35901(17)	0.08399(14)	0.0366(7)*
C6	0.4276(3)	0.36947(18)	-0.13476(16)	0.0462(8)*
C7	-0.1799(3)	0.44093(15)	-0.16809(15)	0.0255(6)*
C8	-0.2722(3)	0.50922(15)	-0.18836(15)	0.0300(7)*
C9	-0.3212(3)	0.52521(16)	-0.26766(15)	0.0339(7)*
C10	-0.2785(3)	0.47421(16)	-0.32917(15)	0.0320(7)*
C11	-0.1833(3)	0.40729(15)	-0.31069(15)	0.0312(7)*
C12	-0.1338(3)	0.39121(16)	-0.23092(15)	0.0292(7)*
C13	-0.2925(4)	0.44456(18)	-0.47058(16)	0.0517(9)*
C14	0.0617(3)	0.27902(15)	0.06403(15)	0.0281(6)*
C15	0.1143(3)	0.28313(17)	0.14525(16)	0.0368(7)*
C16	0.2225(3)	0.2256(2)	0.17906(18)	0.0475(8)*
C17	0.2814(4)	0.1647(2)	0.1324(2)	0.0524(9)*
C18	0.2313(4)	0.16036(18)	0.05191(19)	0.0500(8)*
C19	0.1221(3)	0.21716(16)	0.01796(17)	0.0416(8)*
C20	-0.3142(3)	0.36610(16)	0.17131(15)	0.0294(6)*
C21	-0.2293(3)	0.43265(17)	0.19977(16)	0.0381(7)*
C22	-0.1680(3)	0.43808(19)	0.27880(18)	0.0471(8)*
C23	-0.1916(4)	0.3758(2)	0.33103(18)	0.0504(9)*
C24	-0.2761(4)	0.30867(19)	0.30401(17)	0.0461(8)*
C25	-0.3355(3)	0.30382(17)	0.22427(16)	0.0378(7)*

Anisotropically-refined atoms are marked with an asterisk (*). The form of the anisotropic displacement parameter is: $\exp[-2\pi^2(h^2a^{*2}U_{11} + k^2b^{*2}U_{22} + l^2c^{*2}U_{33} + 2klb^*c^*U_{23} + 2hla^*c^*U_{13} + 2hka^*b^*U_{12})]$.

Table 3. Selected Interatomic Distances (Å)

Atom1	Atom2	Distance	Atom1	Atom2	Distance
O1	C1	1.204(3)	C8	C9	1.379(3)
O2	C1	1.334(3)	C9	C10	1.382(3)
O2	C6	1.457(3)	C10	C11	1.382(3)
O3	C4	1.212(3)	C11	C12	1.388(3)
O4	C10	1.376(3)	C14	C15	1.392(3)
O4	C13	1.426(3)	C14	C19	1.386(3)
N	C2	1.459(3)	C15	C16	1.390(4)
N	C7	1.407(3)	C16	C17	1.374(4)
C1	C2	1.528(3)	C17	C18	1.376(4)
C2	C3	1.535(3)	C18	C19	1.386(4)
C3	C4	1.538(3)	C20	C21	1.382(3)
C3	C14	1.522(3)	C20	C25	1.387(3)
C4	C5	1.517(3)	C21	C22	1.378(4)
C5	C20	1.512(3)	C22	C23	1.382(4)
C7	C8	1.396(3)	C23	C24	1.381(4)
C7	C12	1.392(3)	C24	C25	1.384(4)

Table 4. Selected Interatomic Angles (deg)

Atom1	Atom2	Atom3	Angle	Atom1	Atom2	Atom3	Angle
C1	O2	C6	116.2(2)	O4	C10	C9	115.7(2)
C10	O4	C13	117.0(2)	O4	C10	C11	125.0(2)
C2	N	C7	121.8(19)	C9	C10	C11	119.3(2)
O1	C1	O2	124.1(2)	C10	C11	C12	120.0(2)
O1	C1	C2	124.2(2)	C7	C12	C11	121.3(2)
O2	C1	C2	111.7(2)	C3	C14	C15	119.3(2)
N	C2	C1	110.7(2)	C3	C14	C19	122.3(2)
N	C2	C3	109.0(18)	C15	C14	C19	118.4(3)
C1	C2	C3	109.16(19)	C14	C15	C16	120.3(3)
C2	C3	C4	107.2(19)	C15	C16	C17	120.5(3)
C2	C3	C14	113.57(19)	C16	C17	C18	119.7(3)
C4	C3	C14	109.8(2)	C17	C18	C19	120.1(3)
O3	C4	C3	120.0(2)	C14	C19	C18	120.9(3)
O3	C4	C5	122.3(2)	C5	C20	C21	121.6(3)
C3	C4	C5	117.8(2)	C5	C20	C25	120.0(3)
C4	C5	C20	112.6(2)	C21	C20	C25	118.3(3)
N	C7	C8	118.5(2)	C20	C21	C22	121.4(3)
N	C7	C12	123.8(2)	C21	C22	C23	119.5(3)
C8	C7	C12	117.7(2)	C22	C23	C24	120.1(3)
C7	C8	C9	121.0(2)	C23	C24	C25	119.7(3)
C8	C9	C10	120.7(2)	C20	C25	C24	120.9(3)

Table 5. Torsional Angles (deg)

Atom1	Atom2	Atom3	Atom4	Angle	Atom1	Atom2	Atom3	Atom4	Angle
C6	O2	C1	O1	1.4(4)	C4	C5	C20	C25	-78.9(3)
C6	O2	C1	C2	179.7(2)	N	C7	C8	C9	-173.9(2)
C13	O4	C10	C9	178.9(2)	C12	C7	C8	C9	2.3(4)
C13	O4	C10	C11	-1.3(4)	N	C7	C12	C11	173.6(2)
C7	N	C2	C1	76.7(3)	C8	C7	C12	C11	-2.4(4)
C7	N	C2	C3	-163.3(2)	C7	C8	C9	C10	-0.6(4)
C2	N	C7	C8	-169.0(2)	C8	C9	C10	O4	178.7(2)
C2	N	C7	C12	15.1(3)	C8	C9	C10	C11	-1.1(4)
O1	C1	C2	N	64.8(3)	O4	C10	C11	C12	-178.8(2)
O1	C1	C2	C3	-55.2(3)	C9	C10	C11	C12	1.0(4)
O2	C1	C2	N	-113.6(2)	C10	C11	C12	C7	0.8(4)
O2	C1	C2	C3	126.4(2)	C3	C14	C15	C16	178.0(2)
N	C2	C3	C4	60.5(3)	C19	C14	C15	C16	-1.0(4)
N	C2	C3	C14	-177.9(19)	C3	C14	C19	C18	-178.6(2)
C1	C2	C3	C4	-178.4(2)	C15	C14	C19	C18	0.4(4)
C1	C2	C3	C14	-56.9(3)	C14	C15	C16	C17	1.2(4)
C2	C3	C4	O3	62.0(3)	C15	C16	C17	C18	-0.7(4)
C2	C3	C4	C5	-118.2(2)	C16	C17	C18	C19	0.1(4)
C14	C3	C4	O3	-61.9(3)	C17	C18	C19	C14	0.0(4)
C14	C3	C4	C5	117.9(2)	C5	C20	C21	C22	-178.2(2)
C2	C3	C14	C15	145.7(2)	C25	C20	C21	C22	-0.5(4)
C2	C3	C14	C19	-35.3(3)	C5	C20	C25	C24	178.8(2)
C4	C3	C14	C15	-94.3(3)	C21	C20	C25	C24	1.1(4)
C4	C3	C14	C19	84.7(3)	C20	C21	C22	C23	-0.1(4)
O3	C4	C5	C20	122.6(3)	C21	C22	C23	C24	0.0(4)
C3	C4	C5	C20	-57.2(3)	C22	C23	C24	C25	0.6(4)
C4	C5	C20	C21	98.8(3)	C23	C24	C25	C20	-1.2(4)

Table 6. Anisotropic Displacement Parameters (U_{ij}, Å^2)

Atom	U_{11}	U_{22}	U_{33}	U_{23}	U_{13}	U_{12}
O1	0.0384(10)	0.0349(13)	0.0437(12)	-0.0129(10)	0.0062(9)	-0.0059(10)
O2	0.0238(9)	0.0437(13)	0.0353(11)	-0.0113(10)	0.0045(8)	-0.0005(9)
O3	0.0407(11)	0.0391(13)	0.0463(13)	-0.0071(11)	0.0032(10)	-0.0088(10)
O4	0.0723(13)	0.0461(14)	0.0249(11)	-0.0013(10)	-0.0074(10)	0.0205(11)
N	0.0280(11)	0.0335(14)	0.0244(13)	0.0015(10)	0.0077(10)	0.0116(11)
C1	0.0327(15)	0.0235(17)	0.0234(15)	0.0020(13)	0.0013(13)	0.0041(13)
C2	0.0281(13)	0.0255(16)	0.0229(15)	-0.0020(12)	0.0021(11)	0.0032(12)
C3	0.0295(14)	0.0252(16)	0.0270(15)	-0.0015(13)	0.0010(12)	0.0004(12)
C4	0.0360(15)	0.0307(18)	0.0229(15)	0.0040(14)	0.0005(12)	0.0003(14)
C5	0.0305(15)	0.047(2)	0.0329(17)	0.0021(15)	0.0046(13)	0.0083(14)
C6	0.0265(15)	0.064(2)	0.0484(19)	-0.0140(17)	0.0056(13)	-0.0015(15)
C7	0.0231(13)	0.0272(17)	0.0264(15)	-0.0003(13)	0.0021(11)	-0.0021(12)
C8	0.0340(15)	0.0243(17)	0.0319(17)	-0.0060(13)	0.0027(13)	0.0047(13)
C9	0.0380(16)	0.0308(18)	0.0330(17)	0.0035(14)	0.0002(13)	0.0101(14)
C10	0.0371(15)	0.0341(18)	0.0246(16)	0.0004(14)	-0.0006(13)	0.0028(14)
C11	0.0408(16)	0.0244(17)	0.0284(16)	-0.0047(13)	0.0010(13)	0.0040(13)
C12	0.0326(15)	0.0255(17)	0.0294(16)	0.0019(13)	-0.0017(13)	0.0064(12)
C13	0.072(2)	0.054(2)	0.0291(17)	-0.0014(16)	-0.0066(16)	0.0144(18)
C14	0.0272(14)	0.0267(17)	0.0303(16)	0.0056(13)	-0.0001(12)	-0.0007(13)
C15	0.0316(15)	0.046(2)	0.0334(18)	0.0067(15)	0.0014(13)	-0.0033(14)
C16	0.0351(16)	0.068(2)	0.0391(19)	0.0177(18)	-0.0035(15)	0.0010(17)
C17	0.0425(18)	0.051(2)	0.064(2)	0.0217(19)	-0.0049(17)	0.0088(17)
C18	0.0532(19)	0.033(2)	0.064(2)	0.0001(17)	0.0011(17)	0.0124(16)
C19	0.0477(17)	0.0332(19)	0.0437(19)	0.0000(15)	-0.0034(15)	0.0075(15)
C20	0.0265(14)	0.0332(18)	0.0286(16)	0.0008(14)	0.0067(12)	0.0030(13)
C21	0.0438(17)	0.0331(19)	0.0377(18)	0.0048(15)	0.0067(14)	0.0024(15)
C22	0.0478(18)	0.041(2)	0.052(2)	-0.0159(18)	0.0047(16)	-0.0070(16)
C23	0.0494(19)	0.070(3)	0.0318(18)	-0.0083(18)	-0.0032(15)	0.0095(18)
C24	0.0522(18)	0.047(2)	0.040(2)	0.0085(17)	0.0071(16)	0.0040(17)
C25	0.0424(16)	0.0323(19)	0.0391(19)	-0.0012(15)	0.0058(14)	-0.0041(14)

The form of the anisotropic displacement parameter is:

$\exp[-2\pi^2(h^2a^{*2}U_{11} + k^2b^{*2}U_{22} + l^2c^{*2}U_{33} + 2klb^*c^*U_{23} + 2hla^*c^*U_{13} + 2hka^*b^*U_{12})]$

Table 7. Derived Atomic Coordinates and Displacement Parameters for Hydrogen Atoms

Atom	*x*	*y*	*z*	U_{eq}, Å^2
H1N	-0.2025	0.4514	-0.0488	0.034
H2	-0.0476	0.3143	-0.0939	0.031
H3	-0.0490	0.3901	0.0627	0.033
H5A	-0.3913	0.4123	0.0607	0.044
H5B	-0.4930	0.3331	0.0821	0.044
H6A	0.4760	0.3361	-0.1769	0.055
H6B	0.4950	0.3621	-0.0840	0.055
H6C	0.4342	0.4246	-0.1514	0.055
H8	-0.3017	0.5452	-0.1469	0.036
H9	-0.3849	0.5718	-0.2801	0.041
H11	-0.1517	0.3723	-0.3526	0.037
H12	-0.0671	0.3454	-0.2190	0.035
H13A	-0.3403	0.4658	-0.5217	0.062
H13B	-0.3416	0.3923	-0.4614	0.062
H13C	-0.1648	0.4408	-0.4733	0.062
H15	0.0761	0.3255	0.1778	0.044
H16	0.2560	0.2283	0.2348	0.057
H17	0.3564	0.1258	0.1557	0.063
H18	0.2716	0.1183	0.0195	0.060
H19	0.0881	0.2136	-0.0377	0.050
H21	-0.2130	0.4756	0.1641	0.046
H22	-0.1099	0.4843	0.2973	0.056
H23	-0.1496	0.3791	0.3856	0.060
H24	-0.2934	0.2660	0.3400	0.055
H25	-0.3917	0.2572	0.2055	0.045

University of Alberta Department of Chemistry
Structure Determination Laboratory

STRUCTURE REPORT

SDL Code: MAN9902
Date: 14 April 1999

Compound: 2-[1'-(N-*p*-anisyl)aminomethylaceto]-cyclohexan-1-one
Formula: $C_{16}H_{21}NO_4$

Supervisor: Philip Hultin, Department of Chemistry, University of Manitoba

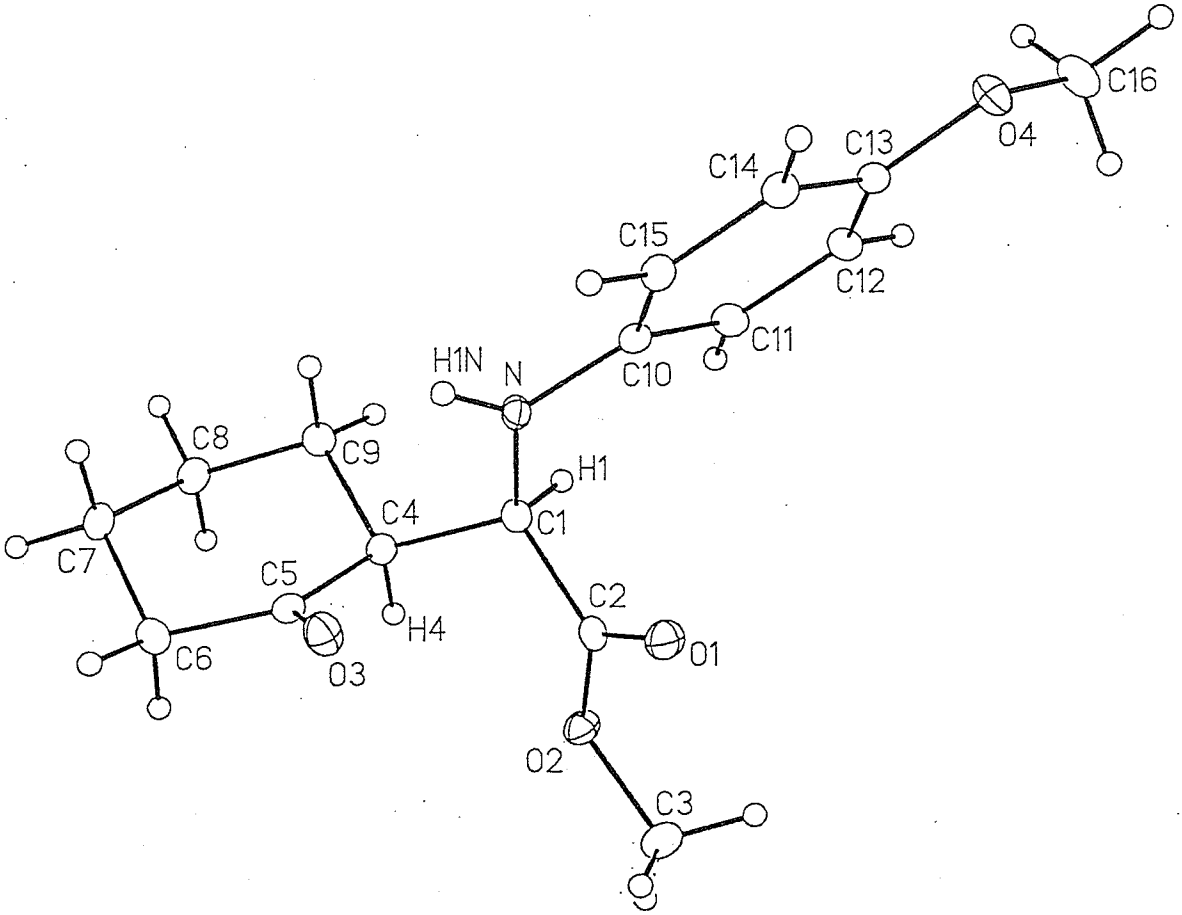

Table 1. Crystallographic Experimental Details

A. Crystal Data	
formula	$C_{16}H_{21}NO_4$
formula weight	291.34
crystal dimensions (mm)	$0.36 \times 0.34 \times 0.17$
crystal system	monoclinic
space group	$P2_1/c$ (No. 14)
unit cell parameters[a]	
a (Å)	12.326 (3)
b (Å)	7.812 (2)
c (Å)	15.903 (4)
β (deg)	104.374 (5)
V (Å^3)	1483.2 (7)
Z	4
ρcalcd (g cm^{-3})	1.305
μ (mm^{-1})	0.093
B. Data Collection and Refinement Conditions	
diffractometer	Bruker P4/RA/SMART 1000 CCD[b]
radiation (λ [Å])	graphite-monochromated Mo Kα (0.71073)
temperature (°C)	–80
scan type	ϕ rotations (0.3°) / ω scans (0.3°) (20 s exposures)
data collection 2θ limit (deg)	51.90
total data collected	8370 ($-14 \le h \le 15$, $-9 \le k \le 9$, $-19 \le l \le 19$)
independent reflections	2842
number of observations (*NO*)	2167 [$F_o^2 \ge 2\sigma(F_o^2)$]
structure solution method	direct methods (*SHELXS–86*[c])
refinement method	full-matrix least-squares on F^2 (*SHELXL–93*[d])
absorption correction method	*SADABS*
range of transmission factors	0.9803–0.6273
data/restraints/parameters	2842 [$F_o^2 \ge -3\sigma(F_o^2)$] / 0 / 190
goodness-of-fit (S)[e]	1.084 [$F_o^2 \ge -3\sigma(F_o^2)$]
final R indices[f]	
R_1 [$F_o^2 \ge 2\sigma(F_o^2)$]	0.0448
wR_2 [$F_o^2 \ge -3\sigma(F_o^2)$]	0.1329
largest difference peak and hole	0.539 and –0.519 e Å^{-3}

[a]Obtained from least-squares refinement of 5869 centered reflections.

[b]Programs for diffractometer operation, data collection, data reduction and absorption correction were those supplied by Bruker.

Table 1. Crystallographic Experimental Details (continued)

[c]Sheldrick, G. M. *Acta Crystallogr.* **1990**, *A46*, 467–473.

[d]Sheldrick, G. M. *SHELXL-93*. Program for crystal structure determination. University of Göttingen, Germany, 1993. Refinement on F_o^2 for all reflections (all of these having $F_o^2 \geq -3\sigma(F_o^2)$). Weighted R-factors wR_2 and all goodnesses of fit S are based on F_o^2; conventional R-factors R_1 are based on F_o, with F_o set to zero for negative F_o^2. The observed criterion of $F_o^2 > 2\sigma(F_o^2)$ is used only for calculating R_1, and is not relevant to the choice of reflections for refinement. R-factors based on F_o^2 are statistically about twice as large as those based on F_o, and R-factors based on ALL data will be even larger.

[e]$S = [\Sigma w(F_o^2 - F_c^2)^2/(n-p)]^{1/2}$ (n = number of data; p = number of parameters varied; $w = [\sigma^2(F_o^2) + (0.0730P)^2 + 0.1939P]^{-1}$ where $P = [\mathrm{Max}(F_o^2, 0) + 2F_c^2]/3$).

[f]$R_1 = \Sigma||F_o| - |F_c||/\Sigma|F_o|$; $wR_2 = [\Sigma w(F_o^2 - F_c^2)^2/\Sigma w(F_o^4)]^{1/2}$.

Table 2. Atomic Coordinates and Equivalent Isotropic Displacement Parameters

Atom	*x*	*y*	*z*	U_{eq}, Å^2
O1	0.14708(12)	0.11568(16)	0.07163(8)	0.0401(4)*
O2	0.17864(11)	-0.00184(15)	-0.04870(8)	0.0347(3)*
O3	0.03035(11)	0.38566(17)	-0.08920(8)	0.0404(4)*
O4	0.46626(11)	0.42369(16)	0.39761(8)	0.0360(3)*
N	0.24453(12)	0.42222(17)	0.04504(9)	0.0294(4)*
C1	0.24928(15)	0.2788(2)	-0.01247(10)	0.0277(4)*
C2	0.18441(14)	0.1253(2)	0.00906(11)	0.0281(4)*
C3	0.12702(18)	-0.1592(2)	-0.02928(13)	0.0414(5)*
C4	0.21372(14)	0.3322(2)	-0.10816(10)	0.0267(4)*
C5	0.09277(15)	0.3898(2)	-0.13735(11)	0.0292(4)*
C6	0.05574(16)	0.4506(2)	-0.22970(12)	0.0359(4)*
C7	0.13671(16)	0.5823(2)	-0.25109(12)	0.0328(4)*
C8	0.25587(16)	0.5150(2)	-0.22746(12)	0.0336(4)*
C9	0.29219(14)	0.4671(2)	-0.13177(11)	0.0306(4)*
C10	0.30453(14)	0.41440(19)	0.13288(10)	0.0256(4)*
C11	0.40315(15)	0.3222(2)	0.16300(11)	0.0295(4)*
C12	0.45955(14)	0.3225(2)	0.25066(11)	0.0290(4)*
C13	0.41822(14)	0.4166(2)	0.30928(11)	0.0271(4)*
C14	0.32068(15)	0.5112(2)	0.28003(11)	0.0286(4)*
C15	0.26442(15)	0.5095(2)	0.19341(11)	0.0281(4)*
C16	0.57058(17)	0.3389(3)	0.42844(13)	0.0436(5)*

Anisotropically-refined atoms are marked with an asterisk (*). The form of the anisotropic displacement parameter is: $\exp[-2\pi^2(h^2a^{*2}U_{11} + k^2b^{*2}U_{22} + l^2c^{*2}U_{33} + 2klb^*c^*U_{23} + 2hla^*c^*U_{13} + 2hka^*b^*U_{12})]$.

Table 3. Selected Interatomic Distances (Å)

Atom1	Atom2	Distance	Atom1	Atom2	Distance
O1	C2	1.198(2)	C4	C9	1.538(2)
O2	C2	1.343(2)	C5	C6	1.503(2)
O2	C3	1.453(2)	C6	C7	1.529(3)
O3	C5	1.213(2)	C7	C8	1.517(3)
O4	C13	1.383(2)	C8	C9	1.522(2)
O4	C16	1.421(2)	C10	C11	1.392(2)
N	C1	1.457(2)	C10	C15	1.400(2)
N	C10	1.410(2)	C11	C12	1.395(2)
C1	C2	1.526(2)	C12	C13	1.380(2)
C1	C4	1.533(2)	C13	C14	1.389(2)
C4	C5	1.515(2)	C14	C15	1.380(2)

Table 4. Selected Interatomic Angles (deg)

Atom1	Atom2	Atom3	Angle	Atom1	Atom2	Atom3	Angle
C2	O2	C3	115.62(14)	C5	C6	C7	111.91(15)
C13	O4	C16	117.02(13)	C6	C7	C8	110.92(14)
C1	N	C10	119.71(13)	C7	C8	C9	111.06(14)
N	C1	C2	111.00(13)	C4	C9	C8	111.45(14)
N	C1	C4	111.56(13)	N	C10	C11	124.17(15)
C2	C1	C4	113.58(14)	N	C10	C15	118.06(15)
O1	C2	O2	123.75(16)	C11	C10	C15	117.74(15)
O1	C2	C1	124.50(15)	C10	C11	C12	121.26(15)
O2	C2	C1	111.67(14)	C11	C12	C13	120.01(16)
C1	C4	C5	113.70(14)	O4	C13	C12	124.77(16)
C1	C4	C9	112.75(14)	O4	C13	C14	115.82(14)
C5	C4	C9	110.62(14)	C12	C13	C14	119.41(15)
O3	C5	C4	121.90(15)	C13	C14	C15	120.51(15)
O3	C5	C6	122.62(16)	C10	C15	C14	121.07(16)
C4	C5	C6	115.48(15)				

Table 5. Torsional Angles (deg)

Atom1	Atom2	Atom3	Atom4	Angle
C3	O2	C2	O1	-2.3(2)
C3	O2	C2	C1	174.8(14)
C16	O4	C13	C12	5.5(2)
C16	O4	C13	C14	-175.3(16)
C10	N	C1	C2	71.39(19)
C10	N	C1	C4	-160.8(14)
C1	N	C10	C11	29.0(2)
C1	N	C10	C15	153.0(15)
N	C1	C2	O1	-9.1(2)
N	C1	C2	O2	173.86(13)
C4	C1	C2	O1	- 135.7(17)
C4	C1	C2	O2	47.21(19)
N	C1	C4	C5	-63.98(18)
N	C1	C4	C9	62.97(19)
C2	C1	C4	C5	62.37(18)
C2	C1	C4	C9	-170.67(14)
C1	C4	C5	O3	-3.0(2)
C1	C4	C5	C6	177.49(14)
C9	C4	C5	O3	-131.08(17)
C9	C4	C5	C6	49.43(19)
C1	C4	C9	C8	178.97(13)
C5	C4	C9	C8	-52.45(19)
O3	C5	C6	C7	130.60(18)
C4	C5	C6	C7	-49.9(2)
C5	C6	C7	C8	52.7(2)
C6	C7	C8	C9	-57.39(19)
C7	C8	C9	C4	57.82(19)
N	C10	C11	C12	178.7(15)
C15	C10	C11	C12	0.8(2)
N	C10	C15	C14	-178.2(15)
C11	C10	C15	C14	-0.2(2)
C10	C11	C12	C13	-0.5(3)
C11	C12	C13	O4	178.83(15)
C11	C12	C13	C14	-0.4(3)
O4	C13	C14	C15	-178.3(14)
C12	C13	C14	C15	1.0(2)
C13	C14	C15	C10	-0.7(2)

Table 6. Anisotropic Displacement Parameters (U_{ij}, Å^2)

Atom	U_{11}	U_{22}	U_{33}	U_{23}	U_{13}	U_{12}
O1	0.0517(9)	0.0407(7)	0.0300(7)	0.0003(6)	0.0142(6)	-0.0077(6)
O2	0.0445(8)	0.0262(6)	0.0351(7)	-0.0020(5)	0.0129(6)	-0.0024(5)
O3	0.0329(7)	0.0541(9)	0.0342(7)	0.0063(6)	0.0085(6)	0.0001(6)
O4	0.0367(7)	0.0435(7)	0.0254(7)	-0.0052(5)	0.0033(5)	0.0046(6)
N	0.0383(9)	0.0236(7)	0.0236(8)	0.0006(5)	0.0027(6)	0.0057(6)
C1	0.0311(9)	0.0275(8)	0.0236(9)	-0.0008(7)	0.0049(7)	0.0029(7)
C2	0.0298(10)	0.0283(9)	0.0230(9)	0.0033(7)	0.0007(7)	0.0040(7)
C3	0.0484(12)	0.0282(9)	0.0484(12)	-0.0014(8)	0.0138(10)	-0.0052(8)
C4	0.0320(9)	0.0240(8)	0.0237(9)	-0.0002(6)	0.0058(7)	0.0005(7)
C5	0.0330(10)	0.0246(8)	0.0290(9)	0.0002(7)	0.0058(8)	-0.0054(7)
C6	0.0333(10)	0.0406(10)	0.0304(10)	0.0043(8)	0.0017(8)	-0.0027(8)
C7	0.0414(11)	0.0298(9)	0.0271(9)	0.0060(7)	0.0085(8)	0.0021(8)
C8	0.0408(11)	0.0316(9)	0.0317(10)	0.0030(7)	0.0153(8)	0.0014(8)
C9	0.0292(10)	0.0330(9)	0.0301(10)	0.0009(7)	0.0085(7)	0.0007(7)
C10	0.0292(9)	0.0224(8)	0.0256(9)	0.0003(6)	0.0075(7)	-0.0037(7)
C11	0.0315(10)	0.0301(9)	0.0279(9)	-0.0065(7)	0.0093(7)	0.0011(7)
C12	0.0234(9)	0.0317(9)	0.0302(9)	-0.0024(7)	0.0037(7)	-0.0003(7)
C13	0.0295(9)	0.0265(8)	0.0247(9)	-0.0006(7)	0.0058(7)	-0.0060(7)
C14	0.0342(10)	0.0262(8)	0.0277(9)	-0.0023(7)	0.0120(7)	0.0002(7)
C15	0.0298(9)	0.0253(8)	0.0295(10)	0.0019(7)	0.0081(7)	0.0031(7)
C16	0.0371(11)	0.0563(12)	0.0319(11)	-0.0062(9)	-0.0022(8)	0.0037(9)

The form of the anisotropic displacement parameter is:
$\exp[-2\pi^2(h^2a^{*2}U_{11} + k^2b^{*2}U_{22} + l^2c^{*2}U_{33} + 2klb^*c^*U_{23} + 2hla^*c^*U_{13} + 2hka^*b^*U_{12})]$

Table 7. Derived Atomic Coordinates and Displacement Parameters for Hydrogen Atoms

Atom	*x*	*y*	*z*	U_{eq}, Å^2
H1N	0.2044	0.5134	0.0251	0.035
H1	0.3296	0.2431	-0.0006	0.033
H3A	0.1265	-0.2436	-0.0750	0.050
H3B	0.0499	-0.1358	-0.0263	0.050
H3C	0.1698	-0.2045	0.0266	0.050
H4	0.2203	0.2277	-0.1428	0.032
H6A	-0.0197	0.5023	-0.2396	0.043
H6B	0.0505	0.3513	-0.2692	0.043
H7A	0.1144	0.6091	-0.3139	0.039
H7B	0.1328	0.6893	-0.2186	0.039
H8A	0.3069	0.6037	-0.2402	0.040
H8B	0.2610	0.4131	-0.2633	0.040
H9A	0.2923	0.5708	-0.0960	0.037
H9B	0.3695	0.4214	-0.1185	0.037
H11	0.4326	0.2577	0.1231	0.035
H12	0.5264	0.2580	0.2700	0.035
H14	0.2925	0.5776	0.3200	0.034
H15	0.1974	0.5738	0.1746	0.034
H16A	0.5962	0.3534	0.4915	0.052
H16B	0.6260	0.3880	0.4005	0.052
H16C	0.5615	0.2166	0.4146	0.052

APPENDIX 2

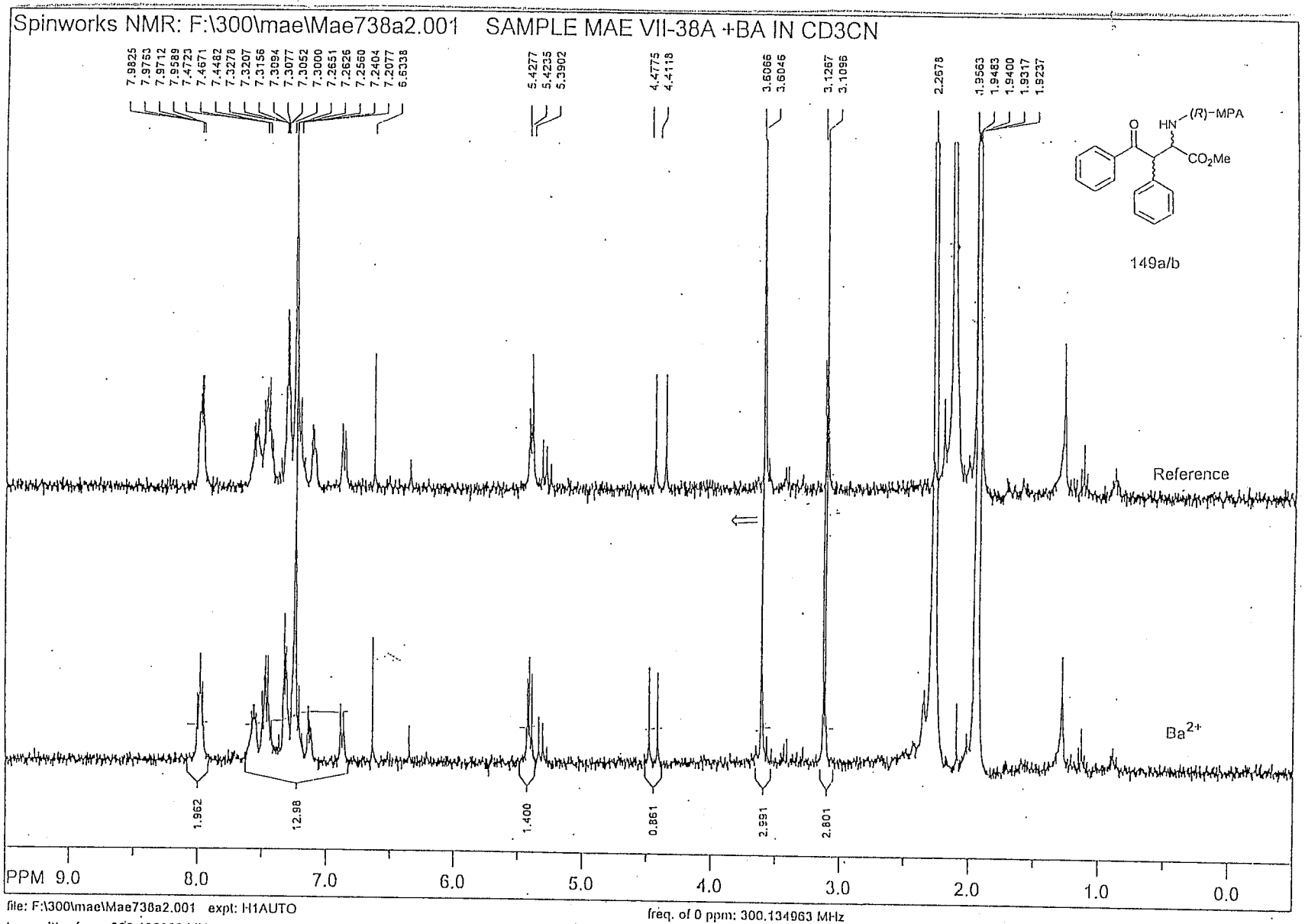

file: F:\300\mae\Mae738a2.001 expt: H1AUTO
transmitter freq.: 300.136800 MHz
time domain size: 32768 points
width: 5494.51 Hz = 18.306785 ppm = 0.167679 Hz/pt
number of scans: 32

freq. of 0 ppm: 300.134963 MHz
processed size: 16384 real points
LB: 0.335 GB: 0.0000
hz/cm: 120.054 ppm/cm: 0.40000

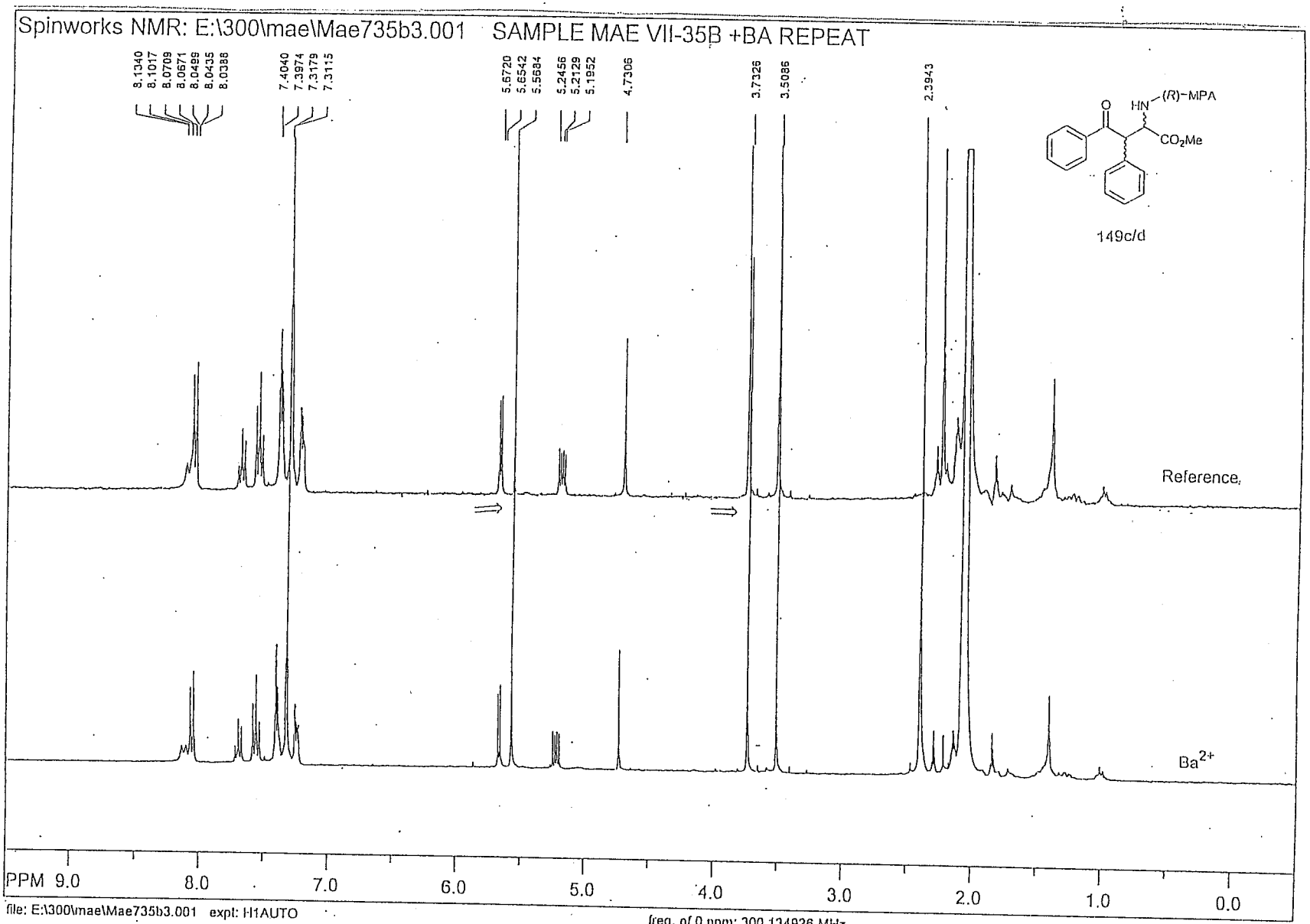

file: E:\300\mae\Mae735b3.001 expt: H1AUTO
transmitter freq.: 300.136800 MHz
time domain size: 32768 points
width: 5494.51 Hz = 18.306785 ppm = 0.167679 Hz/pt
number of scans: 32

freq. of 0 ppm: 300.134926 MHz
processed size: 16384 real points
LB: 0.335 GB: 0.0000
hz/cm: 120.054 ppm/cm: 0.40000

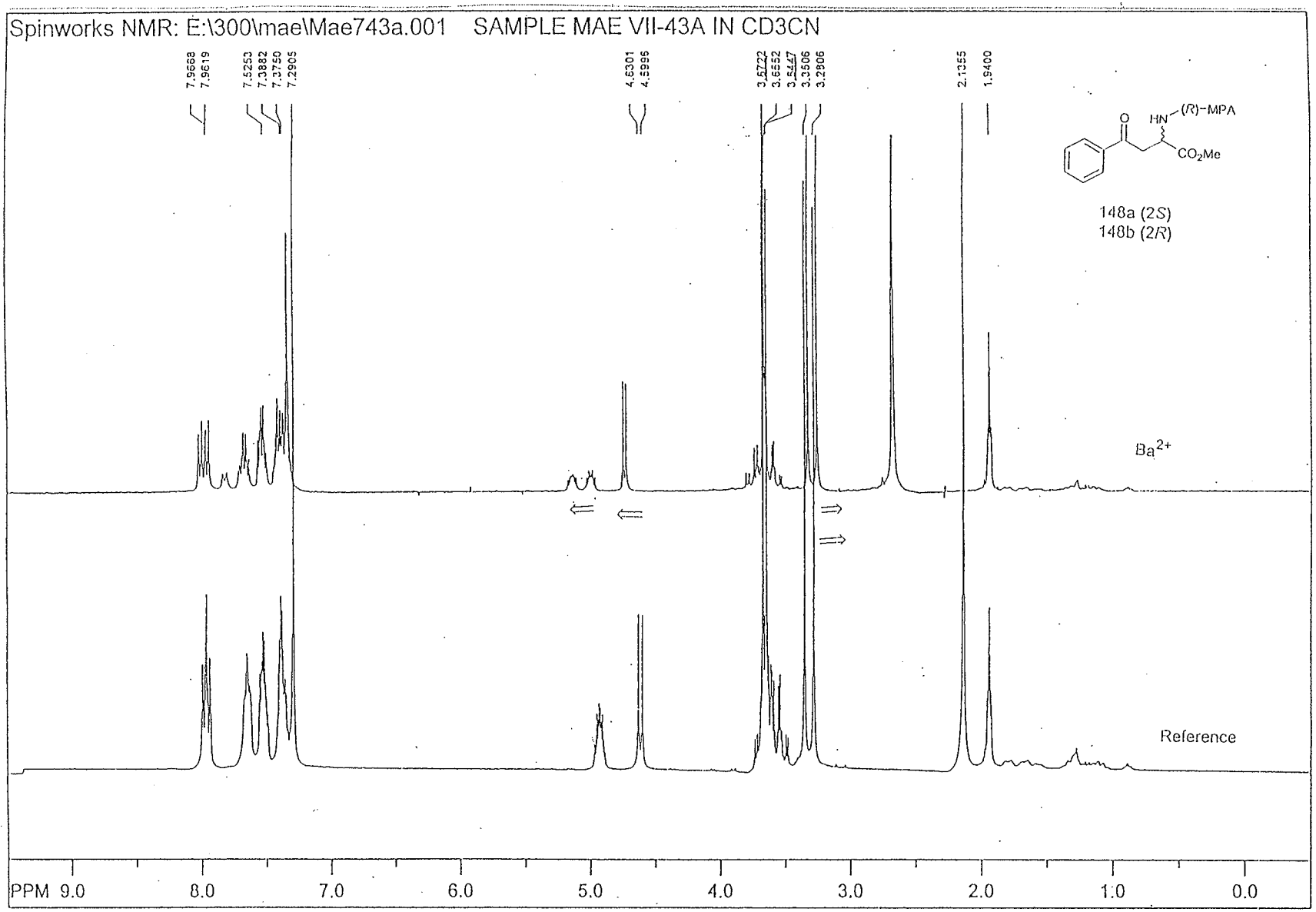

file: E:\300\mae\Mae743a.001 expt: H1AUTO
transmitter freq.: 300.136800 MHz
time domain size: 32768 points
width: 5494.51 Hz = 18.306785 ppm = 0.167679 Hz/pt
number of scans: 32

freq. of 0 ppm: 300.134963 MHz
processed size: 16384 real points
LB: 0.335 GB: 0.0000
hz/cm: 120.054 ppm/cm: 0.40000